

**DEPENDENCE MODELLING OF MARINE ENVIRONMENTAL VARIABLES AND
RESILIENCE ASSESSMENT OF OFFSHORE STRUCTURES OPERATING IN HARSH
ENVIRONMENTS**

by

© Adhitya Ryan Ramadhani

A thesis submitted to the
School of Graduate Studies
in partial fulfilment of the requirement for the degree of

Doctor of Philosophy
Faculty of Engineering & Applied Science
Memorial University of Newfoundland

February 2023

St. John's

Newfoundland and Labrador

Dedication

This thesis is dedicated to my beloved parents, who have always believed in me and loved me unconditionally, no matter what decisions I make in my life. I am truly blessed to call you my father and my mother.

This thesis is also dedicated to my grandmother, who passed away when I had just started my final year. I cannot fulfill my promise to take a picture with you in my graduation gown, but your memories and wisdom live forever in my heart.

ABSTRACT

With increasing global energy demand, energy-related offshore activities continue to increase. As part of this expansion, exploration and operations in harsh ocean environments are becoming more common. Harsh environments are characterized by low temperatures, strong winds, high waves, and ice. These harsher conditions apply increased structural loads and may increase the probability of accidents. Such environmental variables are usually interdependent. Failure to consider these dependencies, when modelling harsh environmental loads, leads to less accurate predictions of design loads and consequently less accurate predictions of offshore structures' capacity to withstand these loads.

This work addresses the dependence issue between environmental variables and seeks to improve predictions of environmental loads and offshore structural capacity. The benefits of considering dependence structures using copula functions are assessed for bivariate and vine-copulas are assessed for multivariate cases of the environmental variables. In each case this is followed by applications to assess offshore structure resilience. Two types of dependence structures are studied: symmetric and asymmetric. Environmental loads are estimated using copula functions to see how significantly the correlation influences the estimation. The copula functions are then applied to assess structural capacity in terms of resilience. A bivariate application case uses copula functions to model two influencing factors that determine the velocity of an iceberg. Results show that the resilience of the offshore structure is mainly dependent on absorptive capacity. Multivariate models are then constructed using Vine Copulas, and a total environmental load is estimated. This multivariate copula model is applied to assess the resilience of an offshore structure subjected to multiple environmental loads.

The study concludes that the accuracy of environmental load predictions can be improved using copula functions to model environmental factor dependencies. In addition, the concept of structural resilience provides a better means of considering the overall resistance of a structure subject to harsh and dependent multivariate environmental loads.

Applications of the proposed methodologies in this thesis help to develop a robust approach to deal with uncertainties related to dependence structures between marine environmental variables. In addition, this thesis helps to develop safer offshore structures operating in harsh environment by estimating the structure's capacity in term of resilience in the design stage.

ACKNOWLEDGEMENT

Firstly, I would like to thank the almighty Allah S.W.T for everything, especially for giving me the strength to finish this Ph.D. despite all the obstacles. I would also like to express my tremendous gratitude to my parents. Although they only graduated from elementary schools, they always taught me how important higher education is. Without them, I am not be who I am today.

I would also like to express my profound gratitude to my supervisor, Dr. Faisal Khan. Getting an acceptance letter from him to pursue my Ph.D. under his supervision still feels unreal as someone who had zero experience in research when I sent my first email to him. Thank you so much, Dr. Khan, for always believing in me and motivating me to explore all my potential. I also thank Dr. Khan for his valuable time, support, and advice. His time management skill is something that I have never seen before, and I will always admire them. I am truly blessed to call him my supervisor and my mentor. I wish we had more coffee time.

I also thank my co-supervisors, Dr. Salim Ahmed, Dr. Bruce Colbourne, and Dr. Mohammed Taleb-Berrouane. Their motivational feedback, ideas, and guidance are the key to shaping my mindset and attitude as a researcher. Thank you, Dr. Salim, for reminding me how important it is always to question everything that I present and always be critical. I only had one in-person meeting with him due to the pandemic, but it left a great impression on how detailed and directing Dr. Salim is as a co-supervisor. Thank you, Dr. Colbourne, for helping me understand the structural analysis and everything about icebergs and environmental load. As someone who has no experience in this expertise, his guidance is one of the primary keys for me to finish this thesis. Thank you, Dr. Mohammed, for always guiding me in writing my research manuscript. I could

finally produce my first research paper under his direction. I would say this is the best supervisory team I could ask for. Thank you again, Dr. Khan, for introducing me to this dream team.

I would also like to thank my best friend, my discussion partner, Waskito Pranowo. His excellent skills in programming helped me finish most of my problems in copula modelling. Thank you for your valuable time and input. To the Indonesian Student Association in Newfoundland, thank you for making it possible to have a work-life balance while finishing my degree and for introducing me to Newfoundland. I have also met some excellent and supportive colleagues in the Centre for Risk, Integrity, and Safety Engineering (C-Rise): Ulanni, Francis, Daniel, and Aghatise. Although the pandemic made it impossible for us to meet in person, your support and encouragement are precious.

I would also like to thank the Natural Science and Engineering Council of Canada (NSERC), the Canada Research Chair (CRC) Tier I Program in Offshore Safety and Risk Engineering, and the School of Graduate Studies (SGS) for providing the fund to complete my program.

I want to express my gratitude to the unanimous peers who reviewed the manuscripts and to all examiners for allocating their valuable time to examine this thesis.

TABLE OF CONTENTS

ABSTRACT.....	i
ACKNOWLEDGEMENT	iii
TABLE OF CONTENTS.....	v
LIST OF FIGURES.....	ix
LIST OF TABLES	xi
LIST OF ABBREVIATIONS.....	xiii
LIST OF SYMBOLS.....	xv
CHAPTER 1 INTRODUCTION	1
1.1 Background and Motivation.....	1
1.2 Thesis and Research Objectives	4
1.3 Novelties and Contributions.....	6
1.4 Outline of Thesis	8
1.5 Co-authorship Statement.....	10
References.....	11
CHAPTER 2 LITERATURE REVIEW	14
2.1 Joint Statistical Models.....	14
2.2 Resilience Assessment Framework.....	18
2.3 Research gaps	19
References.....	20
CHAPTER 3 ENVIRONMENTAL LOAD ESTIMATION FOR OFFSHORE STRUCTURES CONSIDERING PARAMETRIC DEPENDENCIES.....	25
Preface	25
Abstract.....	26
3.1 Introduction.....	26
3.2 Copula Theories.....	31
3.3 Proposed Methodology for Dynamic Environmental Load Estimation	33
3.3.1 Simulate the ocean parameters data	33
3.3.2 Transform observed data into pseudo-observations.....	33
3.3.3 Dependence measurements.....	36
3.3.4 Test for asymmetry	38
3.3.5 Construction of asymmetric copulas.....	39

3.3.6 Copula parameter estimation	41
3.4 Application of the Methodology: Load Estimation	43
3.4.1 Environmental load calculation	43
3.5 Synthetic Ocean Data Analysis	47
3.5.1 Dataset preparation using Hilbert Transform	48
3.6 The Case Study.....	55
3.7 Estimation of Probability of Occurrence.....	59
3.8 Conclusion.....	65
Conflict of Interest.....	66
Acknowledgements	66
References.....	66
Appendix 3A: Wave theories	71
Appendix 3B: Comparison between symmetric and asymmetric copulas	73
Appendix 3C: Detailed results	78
Appendix 3D: MATLAB code for Hilbert transform.....	83
CHAPTER 4 RESILIENCE ASSESSMENT OF OFFSHORE STRUCTURES SUBJECTED TO ICE LOAD CONSIDERING COMPLEX DEPENDENCIES.....	85
Preface	85
Abstract.....	86
4.1 Introduction.....	86
4.2 Research Methodology	93
4.2.1 Copula-based dependence model.....	94
4.2.2 Iceberg collision force.....	100
4.2.3 The concept of resilience assessment.....	105
4.3 Application of the Model	109
4.3.1 Copula modelling.....	113
4.4 Results and Discussion.....	114
4.4.1 Iceberg force	114
4.4.2 Resilience assessment	116
4.4.3 Model validation	124
4.5 Conclusion.....	125
Conflict of Interest.....	126
Acknowledgements	126

References.....	126
CHAPTER 5 A MULTIVARIATE MODEL TO ESTIMATE ENVIRONMENTAL LOAD ON AN OFFSHORE STRUCTURE.....	136
Preface	136
Abstract.....	137
5.1 Introduction	137
5.2 Proposed Methodology of the Multivariate Model.....	143
5.2.1 Copula theory.....	145
5.2.2 Construction of asymmetric copulas	145
5.2.3 Vine copula.....	146
5.2.4 Total environmental load.....	152
5.3 Application of the Multivariate Model	154
5.3.1 Vine copula modelling	157
5.4 Result and Discussion.....	161
5.4.1 Model verification.....	161
5.4.2 Estimation of the total environmental load.....	162
5.5 Conclusion.....	165
Conflict of Interest.....	167
Acknowledgements	167
References.....	167
Appendix 5A.....	172
CHAPTER 6 A COPULA-BASED PROBABILISTIC MODEL TO ASSESS THE RESILIENCE OF OFFSHORE STRUCTURES SUBJECTED TO MULTIPLE ENVIRONMENTAL LOADS.....	176
Preface	176
Abstract.....	177
6.1 Introduction	177
6.2 Methodologies.....	183
6.2.1 Copula theory.....	183
6.2.2 Modelling dependence structures using vine copulas	187
6.2.3 Resilience assessment	192
6.3 Marine environmental data modelling	196
6.4 Result and Discussion.....	203
6.4.1 Copula models verification.....	203
6.4.2 The estimation of the total environmental load	205

6.4.3 Structural reliability evaluation.....	208
6.4.4 Resilience assessment	211
6.5 Conclusion.....	216
Conflict of Interest.....	217
Acknowledgements	217
References.....	217
Appendix 6A.....	224
CHAPTER 7 SUMMARY, CONCLUSIONS, AND RECOMMENDATIONS	229
7.1 Summary	229
7.2 Conclusions	230
7.2.1 Development of bivariate copula models to estimate the total environmental loads	231
7.2.2 Development of a novel methodology to assess resilience considering a parametric dependence	231
7.2.3 Development of multivariate models to estimate total environmental loads using vine copulas	232
7.2.4 Development of a novel methodology to assess resilience subjected to multiple environmental loads.....	232
7.3 Recommendations.....	233
7.3.1 The use of a large met-ocean data set.....	233
7.3.2 Development of a multivariate model for risk analysis of offshore structures	233
7.3.3 Development of resilience assessment methodology considering managerial aspects	234
7.3.4 Development of more advanced modelling tools using neural networks.....	234

LIST OF FIGURES

Fig. 1.1. Research tasks	5
Fig. 1.2. Organization of the doctoral thesis	8
Fig. 3.1. Flowchart for the methodology	35
Fig. 3.2. Flowchart of linearized non-linear inversion method	42
Fig. 3.3. Hilbert transform flowchart.....	49
Fig. 3.4. Scatter plots for all synthetic ocean parameter pairs.....	52
Fig. 3.5. Empirical probability and scatter plots for synthetic ocean data in copula domain.....	52
Fig. 3.6. A vertical mounted cylindrical pile.	56
Fig. 3.7. Wave loads in time domain (second).....	57
Fig. 3.8. Total environmental load for best-fitted symmetric and asymmetric copula for (a) wind and wave, (b) wind and current, and (c) wave and current.	58
Fig. 3.9. Empirical data plotted against selected distribution functions for wind speed and wave height data	63
Fig. 4.1. General framework for copula-based resilience assessment	94
Fig. 4.2. Framework for copula modelling	99
Fig. 4.3. Sketch of iceberg-structure interaction geometry from (a) top view and (b) side view.....	102
Fig. 4.4. Sketch of dynamic equilibrium between iceberg and structure induced by wave and wind force	103
Fig. 4.5. Resilience metric in term of reliability	107
Fig. 4.6. Iceberg sighting (IIP).....	110
Fig. 4.7. Scatter plots between wind speed and wave height in (a) copula domain and (b) original domain	111
Fig. 4.8. Frequency distribution for iceberg drift velocity.....	114
Fig. 4.9. Estimated iceberg force.....	115
Fig. 4.10. Frequency distribution of time for iceberg to stop at maximum penetration	116
Fig. 4.11. Probability distribution of estimated iceberg loads with data taken as load in MN	117
Fig. 4.12. Resilience curve with Reliability at disrupted steady state (a) 0.99, (b) 0.95, (c) 0.90 and varied post-recovery reliability states	119
Fig. 4.13. Resilience curve with varied recovery times and reliability at disrupted steady state equal to 0.90.....	122
Fig. 4.14. Empirical data plotted against selected distribution functions for wind speed and wave height data	125
Fig. 5.1. Proposed methodology to develop a multivariate model to estimate the total environmental load	144
Fig. 5.2. A graphical model of C-Vine with three variables	149
Fig. 5.3. Scatter plots for all environmental variable pairs	155
Fig. 5.4. Probability distribution functions for (a) wind and wave data in Tree 1 (Table 5.26), (b) wind and current data in Tree 1, and (c) conditional environmental data in Tree 2 (Table 5.26) using symmetric copulas.....	158

Fig. 5.5. Probability distribution functions for (a) wind and wave data in Tree 1 (Table 5.27), (b) wind and current data in Tree 1, and (c) conditional environmental data in Tree 2 (Table 5.27) using asymmetric copulas.....	160
Fig. 5.6. Simulation flowchart to estimate the total environmental load	163
Fig. 5.7. Boxplots for the estimated total environmental loads.....	164
Fig. 6.1. Research framework to quantify structure’s resilience subjected to the total environmental load modelled using vine copulas	184
Fig. 6.2. Graphical model for (a) C-vine, and (b) D-vine Copulas	188
Fig. 6.3. Resilience metric in terms of reliability	194
Fig. 6.4. Scatter plots for all environmental variable pairs	196
Fig. 6.5. Probability distribution functions for (a) wind and wave data in Tree 1 (Table 4), (b) wind and current data in Tree 1, and (c) conditional environmental data in Tree 2 (Table 4) using symmetric copulas.....	200
Fig. 6.6. Probability distribution functions for (a) wind and wave data in Tree 1 (Table 5), (b) wind and current data in Tree 1 (Table ?), and (c) conditional environmental data in Tree 2 (Table 5) using asymmetric copulas	201
Fig. 6.7. Distribution fitting and error value calculations for all edges using the best fitted symmetric copulas (top), and asymmetric copulas (bottom)	204
Fig. 6.8. Boxplots for the estimated total environmental loads predicted using the simulated environmental data	206
Fig. 6.9. Probability of failure (left) and reliability index (right) in various return periods considering both asymmetric and symmetric C-vine copulas	210
Fig. 6.10. Resilience curves with Reliability at disrupted steady state (a) 0.99, (b) 0.95, (c) 0.90 and varied post-recovery reliability states	212

LIST OF TABLES

Table 3.1 Common Archimedean copulas (Zhang et al., 2018).....	33
Table 3.2. Archimedean copulas and their Kendall’s tau expressions.....	41
Table 3.3. The application of wave theories	45
Table 3.4. Factors of load combination.	46
Table 3.5. AIC values for all ocean parameters	49
Table 3.6. Distribution parameters statistics.....	51
Table 3.7. Dependence measures for simulated data.....	51
Table 3.8. Parameters estimates of wind speed and wave height.....	53
Table 3.9. Calculated wind loads.	55
Table 3.10. Design value with dominating factor Hmax and concomitant factor W or C.....	61
Table 3.11. Design value with dominating factor Wmax and concomitant factor H or C.....	62
Table 3.12. RMSE and mean absolute error between empirical data and fitted distribution functions.....	63
Table 4.1 Equations used in copula modelling	97
Table 4.2 Dependence Measurement.....	111
Table 4.3 Marginal distributions and statistical parameters for wind speed and wave height.....	112
Table 4.4 Copula parameters estimation.....	113
Table 4.5 Absorptive capacity of offshore structure subjected to ice load	119
Table 4.6 Adaptive capacity of offshore structure subjected to ice load	120
Table 4.7 Restorative capacity of offshore structure subjected to ice load for	120
Table 4.8 The estimated resilience with varied capacities and post-recovery states.....	120
Table 4.9 Resilience assessment with respect to different recovery times Tf-Tl2	122
Table 4.10 Resilience with different periods of stable disrupted operation.....	123
Table 5.1 Correlation and asymmetry measures for all pairs of environmental variables.....	155
Table 5.2. AIC values for all ocean parameters for environmental variables.....	156
Table 5.3. Best fitted distribution parameters statistics	156
Table 5.4. Best fitted symmetric copulas and their parameters for each tree.....	157
Table 5.5. Best fitted asymmetric copulas and their parameters for each tree	158
Table 5.6. Error values for each edge.....	161
Table 5.7. Error values for the Independent and Multivariate Gaussian method.....	164
Table 6.1. Common Archimedean copulas with their parameters	185
Table 6.2. Correlation coefficient (Kendall’s tau) between environmental variables	197
Table 6.3. Asymmetry measure between environmental variables.....	197
Table 6.4 AIC values for all environmental variables.....	198
Table 6.5 Statistical parameters for the best fitted marginal distribution	198
Table 6.6 Best fitted symmetric copulas and their parameters for each edge.....	200
Table 6.7 Best fitted asymmetric copulas and their parameters for each edge	201
Table 6.8 Error values for Independent and Multivariate Gaussian method	207
Table 6.9 Static reliability calculations using environmental variables data modelled with asymmetric and symmetric C-vine copulas	208

Table 6.10 Estimated wave height (m) and current velocity (mm/s) in various return periods (years)....	209
Table 6.11 Estimated resilience with varied capacities and post-recovery states	213
Table 6.12 Resilience assessment with respect to different recovery times T_f - T_{I2}	213
Table 6.13 Resilience with different periods of stable disrupted operation.....	214
Table 6.14 Allowable number of extreme events with different environmental variables data for various return periods	215

LIST OF ABBREVIATIONS

Ab	: Absorptive capacity
Ad	: Adaptive capacity
AIC	: Akaike Information Criterion
BNs	: Bayesian Networks
CAPP	: The Canadian Association of Petroleum Producers
CBN	: Copula Bayesian Network
CRC	: Canada Research Chair
C-vine	: Canonical Vine
D-vine	: Drawable Vine
FPSO	: Floating Production, Storage and Offloading systems
IIP	: International Ice Patrol
IRML	: Infrastructure Resilience-oriented Modelling Language
KC	: Keulegan-Carpenter
KS	: Kolmogorov-Smirnov
MaxEnt	: Maximum Entropy
MED	: Maximum Entropy Distribution
MLE	: Maximum Log-likelihood Estimation
MSCE	: Multivariate Spatial Conditional Extreme
NEVA	: Non-stationary Extreme Value Analysis
NSERC	: Natural Science and Engineering Research Council of Canada
PDF	: Probability Distribution Function

PM : Probabilistic Methods
Res : Restorative capacity
RMSE : Root mean square error
UMP : Unattended Machinery Plant

LIST OF SYMBOLS

A	:	Projected area
C	:	Copula Distribution Function
CoV	:	Covariance
d	:	Water depth
H	:	Wave height
h	:	Partial derivative of bivariate copula
K	:	Slope of the force-penetration relationship
L	:	Wavelength
T	:	Return period
U	:	Current velocity
V	:	Ice drift velocity
Var	:	Variance
\mathbf{W}	:	Hilbert transformation matrix
γ	:	Copula parameter
ρ	:	Pearson's correlation coefficient
τ	:	Kendall's tau
ρ_s	:	Spearman's rho
η	:	Asymmetry measurement
g_{ji}	:	Individual function
J_k	:	Jacobian matrix
F_{wind}	:	Wind force

F_{wave}	:	Wave force
$F_{current}$:	Current force
U_z	:	Wind velocity profile
F_I	:	Inertia force
F_D	:	Drag force
C_M	:	Inertia coefficient
C_D	:	Drag coefficient
u	:	Water wave particle velocity
\dot{u}	:	Water wave particle acceleration
ψ	:	Factor for load combination
ϕ	:	Phase rotation
$L(\theta)$:	Loglikelihood function
$Q(t)$:	Performance of system
$R(t)$:	Reliability function
R_0	:	Initial Reliability
R_f	:	Ideal recovered reliability
R'_f	:	Post-recovery reliability state

CHAPTER 1

INTRODUCTION

1.1 Background and Motivation

Oil and gas are still the dominating energy resources, although renewable energy keeps gaining more attention (Desilver, 2020). The Canadian Association of Petroleum Producers (CAPP) predicts that by 2040, global oil demand is projected to increase to 106.3 million barrels per day (CAPP, 2019). Energy-related offshore activities are also projected to increase by 2040, requiring regulators to be mindful of the offshore structures' operational and environmental performance (IEA, 2018). The increasing demand leads to energy exploration in harsh environments that are challenging conditions for humans, equipment, and infrastructure due mainly to extreme weather conditions (Khan et al., 2015). Freezing temperatures, strong winds, high waves, and icebergs are external factors commonly encountered in harsh environments (Necci et al., 2019; Shi and Duan, 2021). These environmental factors can cause severe impacts on offshore structures that may lead to major accidents.

Arctic and sub-arctic regions are considered the harshest environment due to their more extreme weather conditions and challenging locations (Fu et al., 2018; Necci et al., 2019). However, these areas remain favorable for oil and gas exploration despite these challenging factors due to their large recoverable hydrocarbon reserves; the melting of sea ice makes it even more attractive (Huntington, 2015; Necci et al., 2019). Even with these potentials, the risks from environmental factors remain. Deyab et al. (2018) state that the failure risk for offshore structures is strongly dependent on the harshness of the environmental conditions. Accidents caused by harsh environments are predicted to be more frequent in the Arctic compared to other areas (Tarantola et al., 2019). However, the recorded number of accidents in this area is minimal, making it more

challenging to develop data-based statistical models for this area. In addition, only a few studies have focused on offshore infrastructure in harsh environments (Necci et al., 2019; Zheng et al., 2016).

Studies on harsh marine environments are subject to data uncertainties and data scarcity. Another significant challenge is the existence of dependence among the environmental variables. API 2A-WSD mentions that relationships exist between environmental variables and should be considered carefully (American Petroleum Institute, 2002). Zhang et al. (2018) state that environmental variables may coincide and thus can cause more severe damage to offshore structures. Failure to capture this dependence will likely underpredict the probability of failures of offshore structures due to harsh environmental factors.

Generally, the typical environmental loads acting on offshore structures are wind, wave, and current loads (Chandrasekaran, 2015; Det Norske Veritas, 1996). These forces can, and regularly do, cause severe damage to offshore structures. Hurricane Katrina, Hurricane Rita, Hurricane Gustav, and Hurricane Ike are examples of extreme environmental conditions that destroyed offshore facilities (Cruz and Krausmann, 2008; Kaiser and Yu, 2010).

Modelling the degree of dependence between environmental variables is of crucial importance. In the API 2A-WSD standard, it is mentioned that wind speed/wave height, wave height/wave period, wave height/current speed, and wind speed/current speed usually show dependent relationships (American Petroleum Institute, 2002) that should be considered.

Several studies have been conducted to model the joint distributions between environmental variables in offshore engineering design. The traditional conditional joint probability model is the most recommended and widely used (Ernst and Seume, 2012; Zhang et al., 2018). However, these

standard conditional joint probability models assume that the environmental variables follow specific distribution models. It is assumed that wave height usually follows a Weibull distribution, while wave peak period follows a log-normal distribution (Zhang et al., 2018). Ewans and Jonathan (2014), Jonathan et al. (2010), and Jones et al. (2016) also utilized traditional conditional joint distribution models to identify the relationship between two ocean parameters. Using traditional conditional joint distribution models is convenient as they are already well-developed. However, one clear disadvantage of using this type of model is that the joint model only depends on one bivariate model that requires specific assumptions on the data distribution (Zhang et al., 2018). Thus, the marginal distribution of each environmental variable and their dependence structure is not captured properly.

Another method commonly used to construct multivariate models in marine engineering is the Nataf transformation. Sagrilo et al. (2011) and Sinsabvarodom et al. (2020) used the Nataf transformation to model bivariate ocean parameters and their dependence structure. But this transformation relies on normal data transformation, and its implementation can cause problems in some cases, for example, wave height data usually follow a Weibull distribution. The normal transformation will exclude outliers and it is better to understand why the data is distributed the way they are distributed. Thus, a more flexible model is needed to model dependence between environmental variables without assumptions about their marginal distributions.

An alternative method to model multivariate environmental variables is copula functions. A copula function is a model that combines two or more univariate marginal distributions and their dependence structure to form a multivariate function. The method has been widely used in hydrology, and environmental science related problems (Zhang et al., 2018). Guo et al. (2019) and Hashemi et al. (2015) used copula models to estimate risks in process industries. Zhang et al.

(2019) proposed a reliability assessment based on soil-structure interaction using copula models. In addition, Vanem (2016) and Zhang et al. (2018) developed joint statistical models using copula for ocean parameters. The applications of copula functions were mainly found in the financial, environmental science and hydrological industries. The use of copula functions to perform multivariate analysis for marine environmental variables is still limited. Hence, the motivation of this research is to investigate the applications of copula functions to perform multivariate analysis for offshore structures subjected to environmental variables. Copula functions are then used to estimate environmental loads acting on offshore structures to investigate the significance of copulas to the structures' safety.

1.2 Thesis and Research Objectives

The overall premise of this research is that better consideration of dependencies between environmental variables will improve predictions of environmental loads on offshore structures and that the use of Copula functions provides an improved way of modelling these dependencies that captures marginal dependencies and more complex dependency structures evident in environmental data, particularly the data from harsh environments. In order to investigate and assess this premise, a methodology for incorporating copula functions into offshore environmental load assessment is developed in four stages, listed below, and ultimately incorporates the concept of structural resilience as a better means of quantifying the resistance of offshore structures to more complex environmental load models.

- a. Understand the significance of copula functions to estimate environmental loads for the bivariate case
- b. Apply bivariate copula models to quantify the resilience of offshore structures subjected to ice load

- c. Develop copula models for multivariate cases
- d. Apply multivariate copula models to assess the resilience of offshore structures subjected to multiple natural hazards.

Fig. 1.1 outlines the tasks conducted to achieve the research objectives mentioned above.

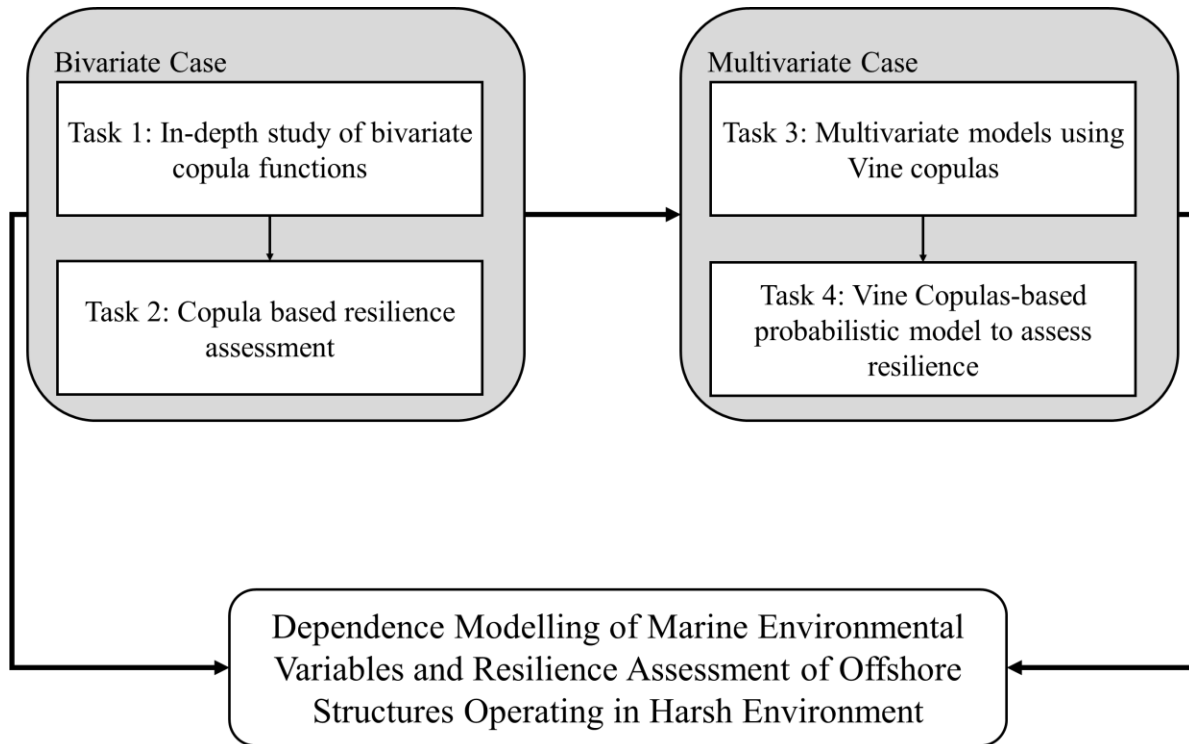


Fig. 1.1. Research tasks

Fig. 1.1 shows that two main cases are studied as two tasks to model marine environmental load for offshore structures: bivariate and multivariate cases. The first task is to compare symmetric and asymmetric copulas to model paired environmental variables to estimate the total environmental load in the bivariate case. Asymmetric copulas are constructed using the by-product rule with Archimedean copulas as the base copulas. This first task also aims to identify whether copula functions are well suited to model environmental variables. The second task in the bivariate case is to incorporate copula functions to assess the offshore structure’s capacity in terms of

resilience. Bivariate copula functions are used to model joint distribution between the influencing factors of the iceberg's velocity. Reliability-based resilience is estimated based on the calculated ice load considering complex dependencies.

In a multivariate case, after validating the construction of asymmetric copulas and implementing copula models in a bivariate case, modelling more than two variables is carried out. First, multivariate copula models are constructed using Vine copulas, where bivariate copulas are selected to model each pair of all selected environmental variables. After constructing multivariate copula models, the next task is to implement them to develop a probabilistic model using vine copulas to estimate total environmental loads for a structure subjected to multiple natural hazards.

1.3 Novelties and Contributions

This doctoral research's main novelties and contributions are highlighted as follows:

- a. An advanced probabilistic methodology is proposed for offshore system design considering complex dependencies for bivariate cases. The model is necessary to capture the dependence structure among ocean parameters and to have the flexibility in handling the statistical characteristics of ocean parameters. Copula functions are introduced to model the ocean parameters considering symmetric and asymmetric dependence. The probabilistic model estimates the total environmental load acting on an offshore structure. This contribution will help address the common assumption when modelling environmental variables that only consider symmetric dependence and independent cases to estimate the total environmental load. This scientific contribution is presented in Chapter 3 of this thesis.

- b. A novel framework is introduced to incorporate the probabilistic methodology using copula functions into assessing the resilience of offshore structures considering ice load. Independence between the influencing environmental parameters to estimate ice load was historically always assumed. In addition, the number of studies focused on the analysis of the capacities of offshore structures to resist ice load is still limited. This contribution aims to deal with this common assumption and investigate an offshore structure's response to an ice load considering all types of dependence structures between wind velocity and wave height. This scientific contribution is presented in Chapter 4 of this thesis.
- c. A novel advanced probabilistic methodology is introduced for offshore system design considering multiple natural hazards. Vine copulas are introduced to model more than two environmental variables considering both symmetric and asymmetric dependence. The application of the proposed methodology is demonstrated through its use in a real-life scenario. The methodology is helpful in the probabilistic structural analysis of offshore structures for design considering all types of dependence structures. This scientific contribution is presented in Chapter 5 of this thesis.
- d. A novel framework is introduced to assess the capacities of offshore structures to resist multiple environmental loads. The challenge of linearity and symmetric assumptions to define the relationship between environmental variables is addressed. The proposed methodology serves as a good tool for offshore structure design. The C-vine-based probabilistic methodology can reveal that symmetric and asymmetric copula functions can define the environmental variable in higher dimensions. This scientific contribution is presented in Chapter 6 of this thesis.

1.4 Outline of Thesis

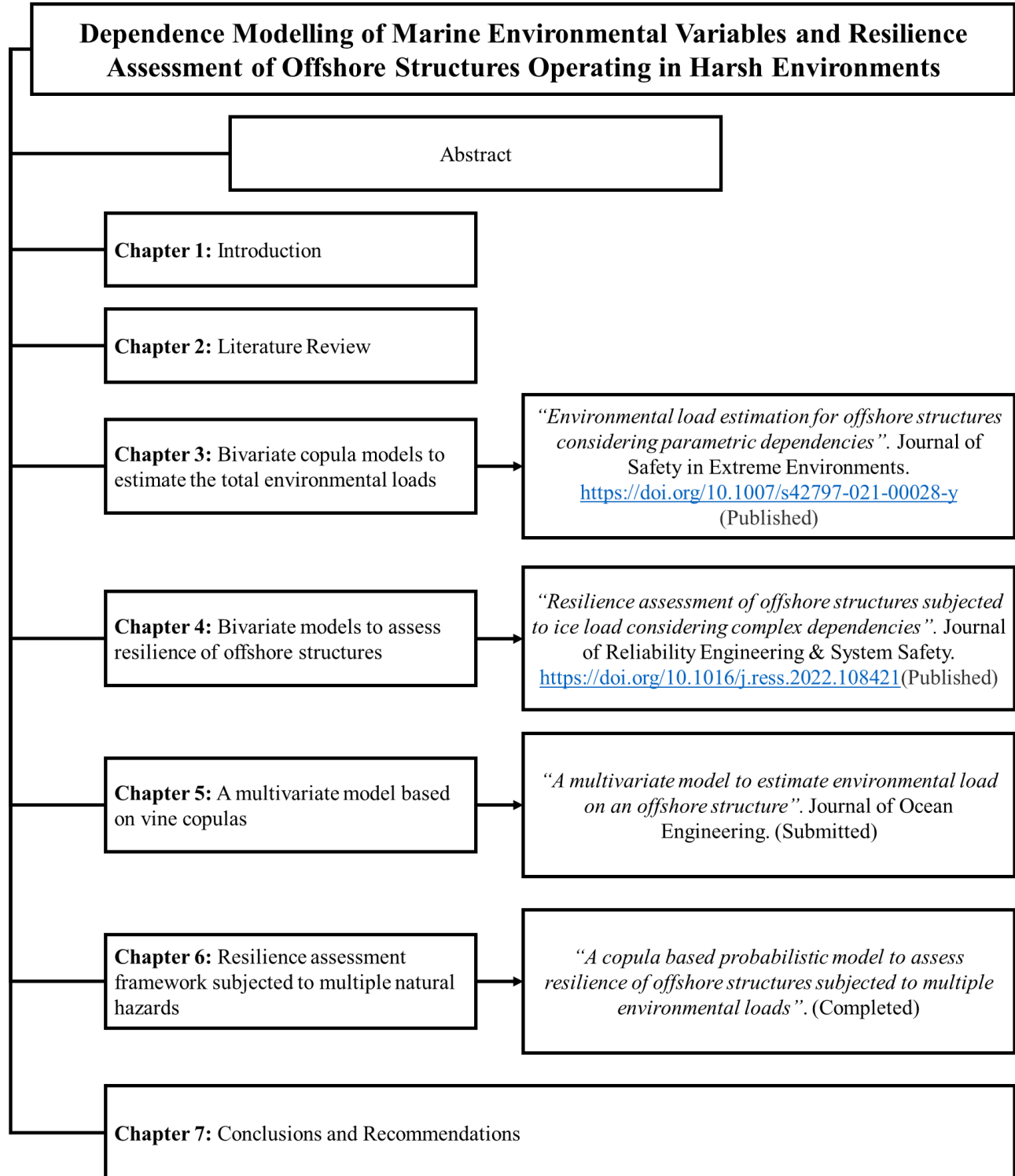


Fig. 1.2. Organization of the doctoral thesis

This doctoral thesis is written in a research manuscript-based format. Thus, the outcomes of the doctoral thesis are presented in four peer-reviewed journal articles. Fig. 1.2 illustrates the structures of this doctoral thesis. The introduction, literature review, and conclusions are presented in Chapters 1, 2, and 7. While Chapters 3 to 6 are written based on the submitted papers to the respective peer-reviewed journals.

Chapter 2 presents the literature review of relevant studies to address the research gaps in modelling the dependence between correlated variables.

Chapter 3 provided an in-depth study of bivariate copula models to estimate the total environmental loads on offshore structures. Symmetric and asymmetric copula models are used and compared to other models that include independent and traditional joint probabilistic models. This chapter is published in the *Journal of Safety in Extreme Environments*.

Chapter 4 proposed a copula-based methodology to assess the resilience of offshore structures considering bivariate dependence models between environmental variables. Symmetric and asymmetric copula functions are used to model the wind speed and wave height. The total ice load is estimated using the proposed methodology, and the capacities of offshore structures in terms of resilience are assessed. This chapter is published in the *Journal of Reliability Engineering & System Safety*.

Chapter 5 provided a further in-depth study to develop a probabilistic model in higher dimensions. Vine copulas are studied for both symmetric and asymmetric dependence. Multivariate models based on C-vine copulas are proposed to estimate the total environmental loads on offshore structures. The proposed methodology is compared to other methodologies to show the advantages

of using the copula-based probabilistic model when dealing with correlated variables in higher dimensions. This chapter is submitted to *Ocean Engineering*.

Chapter 6 proposed a framework for assessing the resilience of offshore structures subjected to multiple environmental loads. C-vine copula models proposed in the previous chapter are used to model the selected environmental variables. The results are used to assess the capacities of offshore structures to resist multiple environmental loads. This chapter is completed and ready for submission for publication.

Chapter 7 includes the summary of this thesis and the conclusions drawn through the technical works. Recommendations for future works are also presented in this chapter.

1.5 Co-authorship Statement

This doctoral thesis is the sole authorship of the candidate (Adhitya Ryan Ramadhani) under the supervisory committees comprising Dr. Faisal Khan, Dr. Salim Ahmed, Dr. Bruce Colbourne, and Dr. Mohammed Taleb-Berrouane. The detailed roles and contributions of the author and co-authors in the current research are presented below

Adhitya Ryan Ramadhani: Conceptualization and concept ideation, formulation and development of methodology, data processing, investigation and analysis, models testing and validation, writing the original draft, reviewing and editing the manuscripts in response to co-authors and journals' reviewers' feedback.

Dr. Faisal Khan: Supervision, research idea formulation, conceptualization, and review of the methodologies, formal analysis, reviewing and editing the copula-based models, reviewing and editing the manuscripts, project administration, and funding acquisition.

Dr. Salim Ahmed: Supervision, conceptualization, and reviewed the methodologies, and model validation, reviewed and edit of the manuscript and thesis.

Dr. Bruce Colbourne: Supervision, conceptualization, and review of the methodologies, models validation, review and edit of the manuscript and thesis.

Dr. Mohammed Taleb-Berrouane: Supervision, conceptualization and review of the methodologies, models validation, review and edit of the manuscript and thesis.

References

American Petroleum Institute, 2002. Recommended Practice for Planning, Designing and Constructing Fixed Offshore Platforms - Working Stress Design. Washington, D.C.

Chandrasekaran, S., 2015. Dynamic Analysis and Design of Offshore Structures, Ocean Engineering & Oceanography. Springer India, New Delhi. <https://doi.org/10.1007/978-81-322-2277-4>

Cruz, A.M., Krausmann, E., 2008. Damage to offshore oil and gas facilities following hurricanes Katrina and Rita: An overview. *J. Loss Prev. Process Ind.* 21, 620–626. <https://doi.org/10.1016/j.jlp.2008.04.008>

Desilver, D., 2020. Renewable energy is growing fast, but fossil fuels still dominate [WWW Document]. URL <https://www.pewresearch.org/fact-tank/2020/01/15/renewable-energy-is-growing-fast-in-the-u-s-but-fossil-fuels-still-dominate/>

Det Norske Veritas, 1996. Guideline for Offshore Structural Reliability Analysis: Application to Jacket Platforms.

Ernst, B., Seume, J.R., 2012. Investigation of Site-Specific Wind Field Parameters and Their Effect on Loads of Offshore Wind Turbines. *Energies* 5, 3835–3855. <https://doi.org/10.3390/en5103835>

Ewans, K., Jonathan, P., 2014. Evaluating environmental joint extremes for the offshore industry using the conditional extremes model. *J. Mar. Syst.* 130, 124–130. <https://doi.org/10.1016/j.jmarsys.2013.03.007>

Fu, S., Zhang, D., Montewka, J., Zio, E., Yan, X., 2018. A quantitative approach for risk assessment of a ship stuck in ice in Arctic waters. *Saf. Sci.* 107, 145–154. <https://doi.org/10.1016/j.ssci.2017.07.001>

Genest, C., Gendron, M., Bourdeau-Brien, M., 2009. The Advent of Copulas in Finance. *Eur. J. Financ.* 15, 609–618. <https://doi.org/10.1080/13518470802604457>

- Guo, C., Khan, F., Imtiaz, S., 2019. Copula-based Bayesian network model for process system risk assessment. *Process Saf. Environ. Prot.* 123, 317–326. <https://doi.org/10.1016/j.psep.2019.01.022>
- Hashemi, S.J., Ahmed, S., Khan, F.I., 2015. Correlation and Dependency in Multivariate Process Risk Assessment. *IFAC-PapersOnLine* 48, 1339–1344. <https://doi.org/10.1016/j.ifacol.2015.09.711>
- Huntington, H.P., 2015. Winter Is Still Harsh in the Arctic. *Environ. Sci. Policy Sustain. Dev.* 57, 26–32. <https://doi.org/10.1080/00139157.2015.983837>
- IEA, 2018. Special Report Offshore Energy Outlook. Paris.
- Jonathan, P., Flynn, J., Ewans, K., 2010. Joint modelling of wave spectral parameters for extreme sea states. *Ocean Eng.* 37, 1070–1080. <https://doi.org/10.1016/j.oceaneng.2010.04.004>
- Jones, M., Randell, D., Ewans, K., Jonathan, P., 2016. Statistics of extreme ocean environments: Non-stationary inference for directionality and other covariate effects. *Ocean Eng.* 119, 30–46. <https://doi.org/10.1016/j.oceaneng.2016.04.010>
- Kaiser, M.J., Yu, Y., 2010. The impact of Hurricanes Gustav and Ike on offshore oil and gas production in the Gulf of Mexico. *Appl. Energy* 87, 284–297. <https://doi.org/10.1016/j.apenergy.2009.07.014>
- Khan, F., Ahmed, S., Yang, M., Hashemi, S.J., Caines, S., Rathnayaka, S., Oldford, D., 2015. Safety challenges in harsh environments: Lessons learned. *Process Saf. Prog.* 34, 191–195. <https://doi.org/10.1002/prs.11704>
- Necci, A., Tarantola, S., Vamanu, B., Krausmann, E., Ponte, L., 2019. Lessons learned from offshore oil and gas incidents in the Arctic and other ice-prone seas. *Ocean Eng.* 185, 12–26. <https://doi.org/10.1016/j.oceaneng.2019.05.021>
- Nelsen, R., 2006. *An Introduction to Copulas*, Springer Series in Statistics. Springer New York, New York, NY. <https://doi.org/10.1007/0-387-28678-0>
- Sagrilo, L.V.S., Naess, A., Doria, A.S., 2011. On the long-term response of marine structures. *Appl. Ocean Res.* 33, 208–214. <https://doi.org/10.1016/j.apor.2011.02.005>
- Shi, K., Duan, X., 2021. A Review of Ice Protection Techniques for Structures in the Arctic and Offshore Harsh Environments. *J. Offshore Mech. Arct. Eng.* 143. <https://doi.org/10.1115/1.4050893>
- Sinsabvarodom, C., Chai, W., Leira, B.J., Høyland, K. V., Naess, A., 2020. Uncertainty assessments of structural loading due to first year ice based on the ISO standard by using Monte-Carlo simulation. *Ocean Eng.* 198, 106935. <https://doi.org/10.1016/j.oceaneng.2020.106935>
- Tarantola, S., Rossotti, A., Contini, P., Contini, S., 2019. guide to the equipment, methods and procedures for the prevention of risks, emergency response and mitigation of the consequences of accidents: Part I. Luxembourg. <https://doi.org/10.2760/204818>

- The Canadian Association of Petroleum Producers (CAPP), 2019. Crude Oil Forecast [WWW Document]. URL <https://www.capp.ca/resources/crude-oil-forecast/> (accessed 12.9.21).
- Vanem, E., 2016. Joint statistical models for significant wave height and wave period in a changing climate. *Mar. Struct.* 49, 180–205. <https://doi.org/10.1016/j.marstruc.2016.06.001>
- Zhang, Y., Gomes, A.T., Beer, M., Neumann, I., Nackenhurst, U., Kim, C.-W., 2019. Reliability analysis with consideration of asymmetrically dependent variables: Discussion and application to geotechnical examples. *Reliab. Eng. Syst. Saf.* 185, 261–277. <https://doi.org/10.1016/j.ress.2018.12.025>
- Zhang, Y., Kim, C.-W., Beer, M., Dai, H., Soares, C.G., 2018. Modelling multivariate ocean data using asymmetric copulas. *Coast. Eng.* 135, 91–111. <https://doi.org/10.1016/j.coastaleng.2018.01.008>
- Zheng, J., Chen, B., Thanyamanta, W., Hawboldt, K., Zhang, B., Liu, B., 2016. Offshore produced water management: A review of current practice and challenges in harsh/Arctic environments. *Mar. Pollut. Bull.* 104, 7–19. <https://doi.org/10.1016/j.marpolbul.2016.01.004>

CHAPTER 2

LITERATURE REVIEW

2.1 Joint Statistical Models

Offshore structures operating in harsh environments are prone to natural hazards. These natural hazards have significant interdependence. A multivariate joint probability model is required to model this dependence between correlated variables. There have been several past studies that focus on the development of joint statistical models. Stedinger (1983) developed a joint probability model using the logarithms of the peak flow values and probability-weighted moment estimators. The model was used to identify the dimensionless flood-flow frequency distribution. Hosking and Wallis (1988) used Monte Carlo simulation to assess flood frequency records' dependence on different sites. Kottegoda and Natale (1994) proposed a joint statistical model based on two-component log-normal distribution to represent the low natural flows. The maximum likelihood method was used to estimate the distribution parameters. However, most past studies assumed the joint probability models follow the multinormal distribution or its extensions (Salvadori and De Michele, 2010).

The most used model to study the joint statistical model for correlated variables is based on the conditional joint distribution model. Lucas and Guedes Soares (2015) modeled the bivariate distributions to describe the sea state conditions. A comparison was made to identify the performance between the conditional modelling approach, the Plackett model, and Box-Cox transformations. Morton and Bowers (1996) developed a multivariate point process model in extreme value analysis to assess the semi-submersible structure's response to the wind and waves. Muraleedharan et al. (2015) modeled the average conditional exceedance of wave peak periods using generalized Pareto and three-parameter Weibull models. Another popular joint statistical

model is the Nataf transformation. Sagrilo et al. (2011) and Sinsabvarodom et al. (2020) used the Nataf transformation to model bivariate ocean parameters and their dependence structure. Silva-González et al. (2013) used the Nataf transformation to model the environmental contours and examine the environmental variables' correlation coefficients. Xiao (2014) proposed a methodology to calculate the equivalent correlation coefficients for two correlated variables using the Nataf transformation. In addition, Lin et al. (2020) proposed a new approach for an efficient and accurate Nataf transformation. Although Nataf transformation and other traditional conditional joint probability models have been extensively used for multivariate analysis, these approaches only apply to a certain extent. A more flexible model is necessary to capture the dependence between environmental variables without requiring any assumptions about their marginal distributions.

A copula function is a powerful tool for multivariate analysis. Copula functions do not require the identification of univariate marginal distribution. The application of copula functions to model multivariate variables has been widely investigated. In the financial industry, Zhi et al. (2022) used copula functions to capture autocorrelations and dependencies for multiple collateral prices in inventory financing. The copula parameterization process was able to help identify the least risky and most predictable collateral unit. Fang and Madsen (2013) used the Gaussian copula to model dependencies on real-life insurance data and a finance data set. Copula functions were also used to capture the correlation between stock and cryptocurrency markets (Boako et al., 2019; Tiwari et al., 2019). The copula model could estimate the time-varying correlations between cryptocurrency and S&P index markets. In the process industry, Guo et al. (2019) and Li et al. (2022) proposed a Copula-Bayesian approach to risk assessment. The proposed model was able to be effective in estimating more reliable accident probabilities. In addition, Hashemi et al. (2015)

used the Archimedean copulas to work on multivariate process risk assessment and concluded that combining copula functions increased risk estimation accuracy. Copula functions have also been extensively used to model the multivariate analysis of hydrological variables such as rainfalls and flood events (Durante and Salvadori, 2009; Jiang et al., 2019; Salleh et al., 2016; Salvadori and De Michele, 2010). In these studies, copula functions captured the dependence structure among the investigated variables to provide better accuracy in estimating hydrological risk. De Michele et al. (2007) and Zhang et al. (2018) used Copula functions to model environmental variables and captured their dependency structures in the ocean and coastal engineering. However, most of these studies only considered a typical copula family to model the correlated variables. This copula family also assumes linearity when capturing the dependence structure. Marine environmental variables in ocean environments usually show nonlinear and asymmetric dependence structures. The asymmetric nature of dependence has not been duly considered in using copula functions to model marine environmental applications (Zhang et al., 2018). The inability to capture this type of dependence will result in a less accurate assessment with subsequent effects on the design of the offshore structures. Thus, asymmetric copulas are introduced in this research and will be used in all case studies in the following chapters. In addition, these past studies only focused on a bivariate case of environmental variables. An extreme marine weather event can involve more than two variables with interdependent relationships. Failure to capture this dependency may lead to unexpected load events.

Due to their flexibility in capturing all types of dependence structures, copula functions are beneficial in modelling marine environmental variables (De Michele et al., 2007; Dong et al., 2017; Ramadhani et al., 2021; Salleh et al., 2016; Zhang et al., 2018, 2015). Vine copulas are introduced to address the issue of modelling environmental variables in higher dimensions. Vine

copulas can provide much more flexibility based on a graphical model used to construct the multivariate joint statistical models from pair copulas (Bedford et al., 2016). Wei et al. (2021) proposed vine copula models to construct a trivariate joint probability model of typhoon-induced wind, waves, and the time lag between them. Heredia-Zavoni & Montes-Iturrizaga (2019) constructed directional environment contours using vine copulas. Amini et al. (2021) and Tang et al. (2020) applied vine copulas to estimate the reliability of physical structures. Bai et al. (2021) and Heredia-Zavoni & Montes-Iturrizaga (2019) proposed a joint model based on vine copulas to construct three-dimensional environmental contours. Dong et al. (2022) and Xu et al. (2020) investigated the multivariate analysis of loads on wind turbines using vine copulas. Nagler et al. (2022) investigated vine copulas to determine their ability to capture different types of dependence. It was concluded that copulas could capture both cross-sectional and serial dependency. Zhao et al. (2021) used a Gaussian copula model to estimate the characteristics of extreme response for a mooring system in a complex ocean environment. Vine copulas were also valuable in assessing the reliability of geotechnical structures. Vine copulas were used to model the dependence structure of multiple soil parameters (Lü et al., 2020; Tang et al., 2020; Xu and Zhou, 2018; Zhang et al., 2019). Copula functions could provide better results for the reliability-based geotechnical structure design (Lü et al., 2020). Vine copulas are also able to offer more flexible ways for geotechnical practitioners to model the cross-correlation among geotechnical random fields (Tang et al., 2020). From these studies, Vine copulas are shown to be able to fully define complex dependency structures between many observed variables. Vine copulas are also able to model dependency in higher dimensions, which traditional copulas cannot do. However, the multivariate copula models used in the vine copulas in these studies are mostly based on well-established copula functions that assume symmetric dependence. Hence, it is necessary to consider both symmetric

and asymmetric copulas to construct the multivariate joint distribution using C-Vine copulas when modelling marine environmental variables.

2.2 Resilience Assessment Framework

The concept of resilience was introduced. Resilience is the capacity of a system to survive the occurrence of unfavorable events and the capacity to recover the system's functionality (Genest et al., 2009; Hashemi et al., 2015; Vanem, 2016; Zarei et al., 2021). Offshore constructions are prone to various dangers and high degrees of functional unpredictability throughout their operational lifetimes since they are complex systems operating in challenging settings (Bucelli et al., 2018). Offshore structures must maintain high levels of structural reliability to withstand any disruption-causing dangers to keep operating. The ability of offshore safety to bounce back from extreme natural and human-made catastrophes is crucial for preventing disastrous results. The assessment of a structure's resilience has been the subject of various previous studies.

The process industry assessed pipeline systems' resilience against microbiologically-influenced corrosion using Petri-nets (Kamil et al., 2021; Taleb-Berrouane et al., 2020; Taleb Berrouane, 2020). A nuclear power plant resilience model was implemented in the power and energy field. A resilience framework in the nuclear industry was also researched to examine micro-events that occur during power plant operations. A resilience index was created for wind power plants as a diagnostic tool to evaluate potential risks (Afgan and Cvetinovic, 2010). To improve decision-making regarding asset integrity management, a novel resilience analysis of wind turbines was also presented (Qin and Faber, 2019). To determine priority in the ranking of choice alternatives, the resilience performance of a wind energy park was analyzed. Another probabilistic approach for predicting the robustness of offshore wind farms was created (Liu et al., 2022). The model illustrated the importance of current uncertainty in asset integrity management. The concept of

resilience is also common in the transportation industry. A minimum residual optimization model was used to explore the robustness of maritime transport systems (Dui et al., 2021). The Infrastructure Resilience-oriented Modelling Language (IRML), which was developed, served as the foundation for a framework to evaluate marine LNG offloading systems (Hu et al., 2021). A hybrid knowledge-based and data-driven strategy were presented to quantify railway system resilience (Yin et al., 2022). The model could show the quantitative relationship between the robustness of the railway system and various sorts of incidents. However, studies on the resilience of offshore structures to environmental loads, especially ice loads, have been minimal. Despite the vast body of application of resilience quantification in various fields, studies on the resilience of structures subjected to correlated multivariate environmental variables have not been reported in the open literature. Most assessments of resilience to natural disasters concentrate on the performance of bridges, homes, or commercial buildings under wind or seismic loads (N. Xu et al., 2020).

2.3 Research gaps

Based on literature reviews, some critical issues in modelling environmental loads for offshore platforms in harsh environments are as follows:

- a. Assumed marginal distributions to fit conditional joint distributions between environmental variables.
- b. Asymmetrical dependence is neglected when dealing with environmental variables
- c. Multivariate analyses (more than two variables) for marine environmental variables are still limited.
- d. An Independent case is usually assumed when estimating environmental loads on offshore structures.

- e. The resilience of offshore structures operating in a harsh environment subjected to correlated multivariate environmental variables, especially ice loads, has not been extensively investigated.

References

- Afgan, N., Cvetinovic, D., 2010. Wind power plant resilience. *Therm. Sci.* 14, 533–540. <https://doi.org/10.2298/TSCI1002533A>
- Amini, A., Abdollahi, A., Hariri-Ardebili, M.A., Lall, U., 2021. Copula-based reliability and sensitivity analysis of aging dams: Adaptive Kriging and polynomial chaos Kriging methods. *Appl. Soft Comput.* 109, 107524. <https://doi.org/10.1016/j.asoc.2021.107524>
- Bai, X., Jiang, H., Huang, X., Song, G., Ma, X., 2021. 3-Dimensional direct sampling-based environmental contours using a semi-parametric joint probability model. *Appl. Ocean Res.* 112, 102710. <https://doi.org/10.1016/j.apor.2021.102710>
- Bedford, T., Daneshkhah, A., Wilson, K.J., 2016. Approximate Uncertainty Modelling in Risk Analysis with Vine Copulas. *Risk Anal.* 36, 792–815. <https://doi.org/10.1111/risa.12471>
- Boako, G., Tiwari, A.K., Ibrahim, M., Ji, Q., 2019. Analysing dynamic dependence between gold and stock returns: Evidence using stochastic and full-range tail dependence copula models. *Financ. Res. Lett.* 31. <https://doi.org/10.1016/j.frl.2018.12.008>
- Bucelli, M., Landucci, G., Haugen, S., Paltrinieri, N., Cozzani, V., 2018. Assessment of safety barriers for the prevention of cascading events in oil and gas offshore installations operating in harsh environment. *Ocean Eng.* 158, 171–185. <https://doi.org/10.1016/j.oceaneng.2018.02.046>
- De Michele, C., Salvadori, G., Passoni, G., Vezzoli, R., 2007. A multivariate model of sea storms using copulas. *Coast. Eng.* 54, 734–751. <https://doi.org/10.1016/j.coastaleng.2007.05.007>
- Dong, S., Chen, C., Tao, S., 2017. Joint probability design of marine environmental elements for wind turbines. *Int. J. Hydrogen Energy* 42, 18595–18601. <https://doi.org/10.1016/j.ijhydene.2017.04.154>
- Dong, W., Sun, H., Tan, J., Li, Z., Zhang, J., Yang, H., 2022. Regional wind power probabilistic forecasting based on an improved kernel density estimation, regular vine copulas, and ensemble learning. *Energy* 238, 122045. <https://doi.org/10.1016/j.energy.2021.122045>
- Dui, H., Zheng, X., Wu, S., 2021. Resilience analysis of maritime transportation systems based on importance measures. *Reliab. Eng. Syst. Saf.* 209, 107461. <https://doi.org/10.1016/j.res.2021.107461>
- Durante, F., Salvadori, G., 2009. On the construction of multivariate extreme value models via copulas. *Environmetrics* n/a-n/a. <https://doi.org/10.1002/env.988>

- Fang, Y., Madsen, L., 2013. Modified Gaussian pseudo-copula: Applications in insurance and finance. *Insur. Math. Econ.* 53, 292–301. <https://doi.org/10.1016/j.insmatheco.2013.05.009>
- Genest, C., Gendron, M., Bourdeau-Brien, M., 2009. The Advent of Copulas in Finance. *Eur. J. Financ.* 15, 609–618. <https://doi.org/10.1080/13518470802604457>
- Guo, C., Khan, F., Imtiaz, S., 2019. Copula-based Bayesian network model for process system risk assessment. *Process Saf. Environ. Prot.* 123, 317–326. <https://doi.org/10.1016/j.psep.2019.01.022>
- Hashemi, S.J., Ahmed, S., Khan, F.I., 2015. Correlation and Dependency in Multivariate Process Risk Assessment. *IFAC-PapersOnLine* 48, 1339–1344. <https://doi.org/10.1016/j.ifacol.2015.09.711>
- Heredia-Zavoni, E., Montes-Iturrizaga, R., 2019. Modelling directional environmental contours using three dimensional vine copulas. *Ocean Eng.* 187, 106102. <https://doi.org/10.1016/j.oceaneng.2019.06.007>
- Hosking, J.R.M., Wallis, J.R., 1988. The effect of intersite dependence on regional flood frequency analysis. *Water Resour. Res.* 24, 588–600. <https://doi.org/10.1029/WR024i004p00588>
- Hu, J., Khan, F., Zhang, L., 2021. Dynamic resilience assessment of the Marine LNG offloading system. *Reliab. Eng. Syst. Saf.* 208, 107368. <https://doi.org/10.1016/j.ress.2020.107368>
- Jiang, C., Xiong, L., Yan, L., Dong, J., Xu, C.-Y., 2019. Multivariate hydrologic design methods under nonstationary conditions and application to engineering practice. *Hydrol. Earth Syst. Sci.* 23, 1683–1704. <https://doi.org/10.5194/hess-23-1683-2019>
- Kamil, M.Z., Taleb-Berrouane, M., Khan, F., Amyotte, P., 2021. Data-driven operational failure likelihood model for microbiologically influenced corrosion. *Process Saf. Environ. Prot.* 153, 472–485. <https://doi.org/10.1016/j.psep.2021.07.040>
- Kottegoda, N.T., Natale, L., 1994. Two-component log-normal distribution of irrigation-affected low flows. *J. Hydrol.* 158, 187–199. [https://doi.org/10.1016/0022-1694\(94\)90052-3](https://doi.org/10.1016/0022-1694(94)90052-3)
- Li, X., Liu, Y., Abbassi, R., Khan, F., Zhang, R., 2022. A Copula-Bayesian approach for risk assessment of decommissioning operation of aging subsea pipelines. *Process Saf. Environ. Prot.* 167, 412–422. <https://doi.org/10.1016/j.psep.2022.09.019>
- Lin, X., Jiang, Y., Peng, S., Chen, H., Tang, J., Li, W., 2020. An efficient Nataf transformation based probabilistic power flow for high-dimensional correlated uncertainty sources in operation. *Int. J. Electr. Power Energy Syst.* 116, 105543. <https://doi.org/10.1016/j.ijepes.2019.105543>
- Liu, M., Qin, J., Lu, D.-G., Zhang, W.-H., Zhu, J.-S., Faber, M.H., 2022. Towards resilience of offshore wind farms: A framework and application to asset integrity management. *Appl. Energy* 322, 119429. <https://doi.org/10.1016/j.apenergy.2022.119429>
- Lü, T.-J., Tang, X.-S., Li, D.-Q., Qi, X.-H., 2020. Modelling multivariate distribution of multiple soil parameters using vine copula model. *Comput. Geotech.* 118, 103340.

<https://doi.org/10.1016/j.compgeo.2019.103340>

- Lucas, C., Guedes Soares, C., 2015. Bivariate distributions of significant wave height and mean wave period of combined sea states. *Ocean Eng.* 106, 341–353. <https://doi.org/10.1016/j.oceaneng.2015.07.010>
- Morton, I.D., Bowers, J., 1996. Extreme value analysis in a multivariate offshore environment. *Appl. Ocean Res.* 18, 303–317. [https://doi.org/10.1016/S0141-1187\(97\)00007-2](https://doi.org/10.1016/S0141-1187(97)00007-2)
- Muraleedharan, G., Lucas, C., Martins, D., Guedes Soares, C., Kurup, P.G., 2015. On the distribution of significant wave height and associated peak periods. *Coast. Eng.* 103, 42–51. <https://doi.org/10.1016/j.coastaleng.2015.06.001>
- Nagler, T., Krüger, D., Min, A., 2022. Stationary vine copula models for multivariate time series. *J. Econom.* 227, 305–324. <https://doi.org/10.1016/j.jeconom.2021.11.015>
- Qin, J., Faber, M.H., 2019. Resilience Informed Integrity Management of Wind Turbine Parks. *Energies* 12, 2729. <https://doi.org/10.3390/en12142729>
- Ramadhani, A., Khan, F., Colbourne, B., Ahmed, S., Taleb-Berrouane, M., 2021. Environmental load estimation for offshore structures considering parametric dependencies. *Saf. Extrem. Environ.* <https://doi.org/10.1007/s42797-021-00028-y>
- Sagrilo, L.V.S., Naess, A., Doria, A.S., 2011. On the long-term response of marine structures. *Appl. Ocean Res.* 33, 208–214. <https://doi.org/10.1016/j.apor.2011.02.005>
- Salleh, N., Yusof, F., Yusop, Z., 2016. Bivariate copulas functions for flood frequency analysis. p. 060007. <https://doi.org/10.1063/1.4954612>
- Salvadori, G., De Michele, C., 2010. Multivariate multiparameter extreme value models and return periods: A copula approach. *Water Resour. Res.* 46, 2009WR009040. <https://doi.org/10.1029/2009WR009040>
- Silva-González, F., Heredia-Zavoni, E., Montes-Iturrizaga, R., 2013. Development of environmental contours using Nataf distribution model. *Ocean Eng.* 58, 27–34. <https://doi.org/10.1016/j.oceaneng.2012.08.008>
- Sinsabvarodom, C., Chai, W., Leira, B.J., Høyland, K. V., Naess, A., 2020. Uncertainty assessments of structural loading due to first year ice based on the ISO standard by using Monte-Carlo simulation. *Ocean Eng.* 198, 106935. <https://doi.org/10.1016/j.oceaneng.2020.106935>
- Stedinger, J.R., 1983. Estimating a regional flood frequency distribution. *Water Resour. Res.* 19, 503–510. <https://doi.org/10.1029/WR019i002p00503>
- Taleb-Berrouane, M., Khan, F., Amyotte, P., 2020. Bayesian Stochastic Petri Nets (BSPN) - A new modelling tool for dynamic safety and reliability analysis. *Reliab. Eng. Syst. Saf.* 193. <https://doi.org/10.1016/j.ress.2019.106587>
- Taleb Berrouane, M., 2020. Dynamic corrosion risk assessment in the oil and gas production and

processing facility (Doctoral dissertation, Memorial University of Newfoundland).

- Tang, X.-S., Wang, M.-X., Li, D.-Q., 2020. Modelling multivariate cross-correlated geotechnical random fields using vine copulas for slope reliability analysis. *Comput. Geotech.* 127, 103784. <https://doi.org/10.1016/j.compgeo.2020.103784>
- Tiwari, A.K., Raheem, I.D., Kang, S.H., 2019. Time-varying dynamic conditional correlation between stock and cryptocurrency markets using the copula-ADCC-EGARCH model. *Phys. A Stat. Mech. its Appl.* 535, 122295. <https://doi.org/10.1016/j.physa.2019.122295>
- Vanem, E., 2016. Joint statistical models for significant wave height and wave period in a changing climate. *Mar. Struct.* 49, 180–205. <https://doi.org/10.1016/j.marstruc.2016.06.001>
- Wei, K., Shen, Z., Ti, Z., Qin, S., 2021. Trivariate joint probability model of typhoon-induced wind, wave and their time lag based on the numerical simulation of historical typhoons. *Stoch. Environ. Res. Risk Assess.* 35, 325–344. <https://doi.org/10.1007/s00477-020-01922-w>
- Xiao, Q., 2014. Evaluating correlation coefficient for Nataf transformation. *Probabilistic Eng. Mech.* 37, 1–6. <https://doi.org/10.1016/j.probengmech.2014.03.010>
- Xu, N., Yuan, S., Liu, X., Ma, Y., Shi, W., Zhang, D., 2020. Risk assessment of sea ice disasters on fixed jacket platforms in Liaodong Bay. *Nat. Hazards Earth Syst. Sci.* 20, 1107–1121. <https://doi.org/10.5194/nhess-20-1107-2020>
- Xu, Q., Fan, Z., Jia, W., Jiang, C., 2020. Fault detection of wind turbines via multivariate process monitoring based on vine copulas. *Renew. Energy* 161, 939–955. <https://doi.org/10.1016/j.renene.2020.06.091>
- Xu, Z.-X., Zhou, X.-P., 2018. Three-dimensional reliability analysis of seismic slopes using the copula-based sampling method. *Eng. Geol.* 242, 81–91. <https://doi.org/10.1016/j.enggeo.2018.05.020>
- Yin, J., Ren, X., Liu, R., Tang, T., Su, S., 2022. Quantitative analysis for resilience-based urban rail systems: A hybrid knowledge-based and data-driven approach. *Reliab. Eng. Syst. Saf.* 219, 108183. <https://doi.org/10.1016/j.ress.2021.108183>
- Zarei, E., Ramavandi, B., Darabi, A.H., Omidvar, M., 2021. A framework for resilience assessment in process systems using a fuzzy hybrid MCDM model. *J. Loss Prev. Process Ind.* 69, 104375. <https://doi.org/10.1016/j.jlp.2020.104375>
- Zhang, Y., Beer, M., Quek, S.T., 2015. Long-term performance assessment and design of offshore structures. *Comput. Struct.* 154, 101–115. <https://doi.org/10.1016/j.compstruc.2015.02.029>
- Zhang, Y., Gomes, A.T., Beer, M., Neumann, I., Nackenhorst, U., Kim, C.-W., 2019. Modelling asymmetric dependences among multivariate soil data for the geotechnical analysis – The asymmetric copula approach. *Soils Found.* 59, 1960–1979. <https://doi.org/10.1016/j.sandf.2019.09.001>
- Zhang, Y., Kim, C.-W., Beer, M., Dai, H., Soares, C.G., 2018. Modelling multivariate ocean data using asymmetric copulas. *Coast. Eng.* 135, 91–111.

<https://doi.org/10.1016/j.coastaleng.2018.01.008>

Zhao, Y., Liao, Z., Dong, S., 2021. Estimation of characteristic extreme response for mooring system in a complex ocean environment. *Ocean Eng.* 225, 108809. <https://doi.org/10.1016/j.oceaneng.2021.108809>

Zhi, B., Wang, X., Xu, F., 2022. Managing inventory financing in a volatile market: A novel data-driven copula model. *Transp. Res. Part E Logist. Transp. Rev.* 165, 102854. <https://doi.org/10.1016/j.tre.2022.102854>

CHAPTER 3

ENVIRONMENTAL LOAD ESTIMATION FOR OFFSHORE STRUCTURES CONSIDERING PARAMETRIC DEPENDENCIES

Preface

A version of this chapter has been published in the Safety in Extreme Environments journal. As the primary author, I work with my co-authors: Dr. Faisal Khan, Dr. Salim Ahmed, Dr. Bruce Colbourne, and Dr. Mohammed Taleb-Berrouane. I conducted a literature review and developed the conceptual framework for modelling joint distributions for correlated marine environmental variables. I prepared the first manuscript draft and revised the manuscript based on the co-authors' and reviewers' feedback. Co-author Dr. Faisal Khan assisted in the idea formulation, development of the concept, and methodology design, reviewed and edited the manuscript draft, and acted as the corresponding author for the manuscript. Co-authors Dr. Salim Ahmed, Dr. Bruce Colbourne, and Dr. Mohammed Taleb-Berrouane provided valuable support and input in reviewing and revising the manuscript draft. These co-authors also assisted in validating, reviewing, and correcting the model and results.

Reference:

Ramadhani, A., Khan, F., Colbourne, B., Ahmed, S., & Taleb-Berrouane, M. (2021). Environmental load estimation for offshore structures considering parametric dependencies. *Safety in Extreme Environments*. <https://doi.org/10.1007/s42797-021-00028-y>

Abstract

Multivariate models to estimate environmental load on an offshore structure are an essential consideration. A reliable approach is necessary to capture the dependency among parameters and to be flexible in handling the statistical characteristics of ocean parameters. Previous studies on marine engineering usually assumed symmetric dependence when considering multivariate models. In this chapter, both symmetric and asymmetric copula functions are constructed for modelling ocean parameters and the estimation of total environmental load. Results are compared with the traditional joint probability approach to demonstrate the advantage of using copula functions. The results reveal that environmental loads strongly depend on the significance of dependence, which is defined as the copula function's correlation. The probability of failure, estimated using copula functions, is higher than the traditional joint probability estimate. In addition to this, Root-mean-square errors (RMSE) and the mean absolute errors using copula functions are lower than those of the traditional joint probability modelling. Thus, the use of copula functions provides a more conservative approach to safety. Therefore, the use of copula functions to capture both dependence types, while estimating ocean environmental loads provide a better understanding of the environmental load and its contribution to the failure probability.

Keywords: environmental load, copula functions, asymmetric copula functions

3.1 Introduction

Offshore structures are vulnerable to the harsh marine environments that they operate in. The design of offshore structures is dominated by environmental loads that can be categorized as wind, wave, current, marine ice, and temperature loads especially for steel offshore platforms (Wilson, 2002). However, environmental loads that are usually considered during structural analysis consist

of wind loads, wave loads and current loads during severe storms if these conditions are identified as having significant impact on the structure (Sigurdsson, 1996). The impact of natural hazards, such as hurricanes, on offshore structures can be enormous with 44 offshore oil and gas facilities destroyed and 21 others damaged during Katrina, and 69 destroyed installations and 32 severely damaged installations during Rita (Cruz and Krausmann, 2008). Hurricanes Gustav and Ike destroyed 60 platforms and damaged 31 in August and September 2008 (Kaiser and Yu, 2010). Thus, it is important to understand and assess the impact of marine environment variables on offshore structures.

The marine environment is a complex system subjected to various sources of data uncertainties. One of the main sources of uncertainties is the dependence among variables. From a practical perspective, due to their dependence, a combination of load variables can cause more severe damage to offshore structures than that predicted by applying the loads individually (Zhang et al., 2018). This dependence structure needs to be taken into account properly in the analysis of environmental loads. The commonly used assumption of linear dependence may not be able to adequately capture the dependence structure between ocean parameters as the parameters, by their nature, usually show a nonlinear dependence (Fazeres-Ferradosa et al., 2018). Also most of the previous studies assumed symmetric dependence for their modelling; this assumption may lead to more uncertainties when dealing with ocean parameters (Zhang et al., 2018). The main idea behind this research is to minimize uncertainty by capturing all possible dependence types between ocean variables.

There have been numerous published studies that deal with multivariate analysis. Performing multivariate analysis for marine environments requires consideration of the relationships between variables. API 2A-WSD specifies that environment data might have a specific type of relationship

that should be taken into account when using multivariate analysis (American Petroleum Institute, 2002). In this standard, the common marine environmental variables that have relationships are wind speed/wave height, wave height/wave period, wave height/current speed, and wind speed/current speed. These primary dependencies should be considered when performing multivariate analysis. The most common method used for multivariate analysis is the joint probability distribution. However, Fazeres-Ferradosa et al. (2018) concluded that the traditional joint probability distribution is not suitable for modelling the complex nature of a marine environment. de Waal and van Gelder (2005) used a probabilistic approach in multivariate analysis of the environmental loads on an offshore structure. They concluded that dependence between variables makes the analysis more complicated and a robust multivariate analysis method that can model all types of dependence is needed. One method that is quite popular to construct multivariate models in offshore engineering problems is the Nataf transformation. Sinsabvarodom et al. (2020) used the Nataf transformation to study uncertainties in modelling ice loads during ice - structure interaction. Sagrilo et al. (2011) also implemented this transformation method to construct a Nataf model that considered wave, wind and current parameters. However, the Nataf transformation depends on whether the transformed standard normal variables are close to multi-normal, so the implementation was criticized because the transformation procedure might be unnecessary for some cases (Bang Huseby et al., 2013).

An alternate method for conditional joint probability analysis is the use of copula models that are suited for multivariate analysis. Zhang et al. (2018) modeled multivariate ocean data using copula functions to capture the dependence of the data and model conditional joint distribution between ocean variables. De Michele et al. (2007) used copula functions in a multivariate analysis of sea storms variable. Hashemi et al. (2015) utilized copulas from the Archimedean family to work on

multivariate process risk assessment and concluded that the integration of copula functions for fault detection increased the accuracy of the risk estimation. Guo et al. (2019) incorporated copula functions into a Bayesian network in order to understand the influence of this integration on the calculation of probability of occurrence of an event for a process system. Taleb-Berrouane et al. (2020) proposed a combination of Petri-nets and Bayesian networks to present dependencies between influencing factors. In another work, Yang et al. (2020) also analyzed the dependency by integrating a conditional probability approach – the Bayesian network with a time-dependent scenario evolution approach (Abaei et al., 2022; Deyab et al., 2018; Kabir et al., 2019; Taleb-Berrouane et al., 2018), Stochastic Petri-nets (Kamil et al., 2019; Taleb-Berrouane et al., 2019; Taleb-Berrouane and Khan, 2019; Talebberrouane et al., 2016). Mahfoud and Massmann (2012) used copula functions in stock market analysis to model a relationship between two different stock indices; the German DAX-30 and French CAC-40. Thus, copula functions are powerful tools that can be used in multivariate analysis, especially in the ocean engineering field.

A Copula function in a multivariate analysis is a substitute for a traditional joint distribution. In a traditional joint distribution, marginal distributions should be identified and treated as belonging to the same family. In addition, a mathematical function for joint distribution becomes complicated for more than two variables. A Copula function does not require the identification of a univariate marginal distribution. The original data can be transformed into a copula domain that is uniformly distributed (Zhang et al., 2018). Hence, copula functions will be used in this work to perform the multivariate analysis for the environmental loads on an offshore structure.

The asymmetric nature of dependence has not been duly considered in the use of copula functions to model marine environmental applications. Zhang et al. (2019) constructed asymmetric copulas to capture the physical phenomena of soil parameters in a soil-structure loading analysis. They

concluded that ignorance of dependence structure may result in different estimation of structure response and lower quality of structural reliability analysis. Vanem (2016) mentions that much attention has been devoted to trying to capture asymmetric dependence, especially for ocean data. He also identifies several methods to construct asymmetric copulas. Wei and Kim (2018) constructed a copula-based regression to capture asymmetric dependence. Grimaldi and Serinaldi (2006) compared symmetric and asymmetric copulas and concluded that asymmetric copulas are more flexible. However, the effect of uncertainties in asymmetric dependence for ocean parameters has not been vastly investigated. Copulas from the Archimedean family are often used in the literature and in software packages due to their ease of use in capturing dependence between variables. Inability to capture this type of dependence will result in less accurate assessment with subsequent effects on the design and resilience of the offshore structures.

This work aims to fill the gaps in performing multivariate statistical modelling for ocean parameters considering all types of dependence. This work presents a copula-based environmental load estimation for an offshore structure. A comparative study between symmetric and asymmetric copulas to represent all possible dependencies between marine environment variables is also carried out. Several copula functions are compared to identify the best-fitted function in bivariate analysis. A comparison between the estimated probability of occurrence using traditional joint probability distribution and that derived from copulas is also presented to identify the benefits of the copula functions. Finally, various correlation coefficients from different copula functions are considered to identify the significance of these on the estimation of environment loads.

The remainder of this chapter is organized as follows. Section 3.2 presents basic theories in copula functions. The proposed methodology is presented in section 3.3 and the application of the proposed method in load estimation is presented in section 3.4. Data analysis for the synthetic data

used to illustrate symmetric and asymmetric copulas for a bivariate case is discussed in section 3.5. To understand the significant of copula application, a case study is described and discussed in section 3.6. Section 3.7 presents the two methods of estimation of probability of occurrence, to provide the comparison between copula functions and the traditional approach. The concluding remarks of this chapter are presented in section 3.8.

3.2 Copula Theories

A Copula is a function that joins or “couples” univariate marginal distributions to construct multivariate distribution (Nelsen, 2006). By using copulas, it is possible to construct a multivariate distribution from different univariate marginal distributions. This makes copula functions advantageous when dealing with conditional joint probability distributions. The definition of copula was first introduced in Sklar’s Theorem.

Let H be an n -dimensional distribution function with marginal distribution F_1, F_2, \dots, F_n , then there exists a copula C such that.

$$H(x_1, x_2, \dots, x_n) = C(F_1(x_1), F_2(x_2), \dots, F_n(x_n)) \quad (3.1)$$

The joint conditional probability distribution by taking into account the copula in the model can be estimated using

$$f_{x_2|x_1} = \frac{f_{x_1x_2}(x_1, x_2)}{f_{x_1}(x_1)} = C_{x_1x_2}(F_{x_1}(x_1), F_{x_2}(x_2)) \cdot f_{x_2}(x_2) \quad (3.2)$$

Based on Sklar’s Theorem, it can be seen that a copula model does not consider the characteristic of univariate marginal distribution in the multivariate model as the copula model is a multivariate

model for variables after being transformed into the cumulative distribution function with a uniform distribution function (Zhang et al., 2018). This is because the random variables $U_i = F_i(X_i)$ are uniformly distribution on $[0,1]$. Thus, the domain and range for an n-dimensional copula function can be seen as:

$$C: [0,1]^n \rightarrow [0,1] \quad (3.3)$$

In another form, a copula is a joint distribution function for an n-dimensional probability defined as

$$C(u_1, u_2, \dots, u_n) = P(U_1 \leq u_1, U_2 \leq u_2, \dots, U_n \leq u_n) \quad (3.4)$$

Due to this flexibility, this copula function is useful when modelling ocean parameters. There are many copula families that can be implemented on a single problem and one of these families, that has been widely used is the Archimedean families. Clayton, Gumbel and Frank copulas from the Archimedean family are used as the base copulas in this research. This Archimedean copula family is frequently applied as it is relatively easy to construct the copula functions compared to other copula families. An n-dimensional Archimedean copula can be constructed using a generating function $\phi(\cdot)$ (Nelsen, 2006)

$$C_{archimedean}(u_1, u_2, \dots, u_n; \theta) = \phi^{[-1]}(\phi(u_1; \theta) + \phi(u_2; \theta) + \dots + \phi(u_n; \theta); \theta) \quad (3.5)$$

where $\phi: [0,1] \times \theta \rightarrow$ is a monotone function with $\phi(1) = 0$ and θ is a parameter with the domain θ .

Three common families of Archimedean copula along with their parameters for bivariate distributions are presented in Table 3.1.

Table 3.1 Common Archimedean copulas (Zhang et al., 2018)

Copula	$C_\gamma(u_1, u_2)$	Generating function $\phi_\gamma(t)$	$\gamma \in$
Clayton	$(u_1^{-\gamma} + u_2^{-\gamma} - 1)^{\frac{-1}{\gamma}}$	$\frac{\gamma}{\gamma + 2}$	$(1, \infty)$
Gumbel	$\exp\left\{-\left[(-\ln u_1)^\gamma + (-\ln u_2)^\gamma\right]^{\frac{1}{\gamma}}\right\}$	$1 - \frac{1}{\gamma}$	$[1, \infty)$
Frank	$\frac{-1}{\gamma} \ln\left(1 + \frac{(e^{-u_1\gamma} - 1)(e^{-u_2\gamma} - 1)}{e^{-\gamma} - 1}\right)$	$1 - \frac{4}{\gamma}(1 - D_1(\gamma))$ Where $D_1(\gamma) = \frac{1}{\gamma} \int_0^\infty \frac{t dt}{\exp(t) - 1}$	$(-\infty, \infty)$

3.3 Proposed Methodology for Dynamic Environmental Load Estimation

The proposed methodology to estimate environmental load is schematically illustrated in Fig. 3.1. Dependency and asymmetry measurements are carried out after simulating the data sets. Different copula functions are then fitted to these data and used to estimate environmental loads.

3.3.1 Simulate the ocean parameters data

Three different ocean parameter data sets containing wind speed (m/s), wave height (m) and current speed (cm/s) are analyzed in order to identify whether any dependence occurs in one of the possible combinations of the three ocean parameters. Due to the limitation to obtain these data sets in any available resources, these data are simulated.

3.3.2 Transform observed data into pseudo-observations

One of the advantages of using copula is that it does not depend on the univariate marginal distribution of the variables, thus it is recommended to apply pseudo-observations to the observed data (Leontaris et al., 2016). These observed data (X_i); where i refers to random variables, can be

transformed into pseudo-observations using the ranks (R_i). Genest, et al defined pseudo-observations as (Genest et al., 2009)

$$U_i = \frac{R_i}{n+1} = \frac{n\hat{F}_i(X_i)}{n+1} \quad (3.6)$$

where n is the number of observations and \hat{F}_i is the empirical cumulative function defined as $\hat{F}_i(t) = \frac{1}{n} \sum_{i=1}^n 1(X_i \leq t)$.

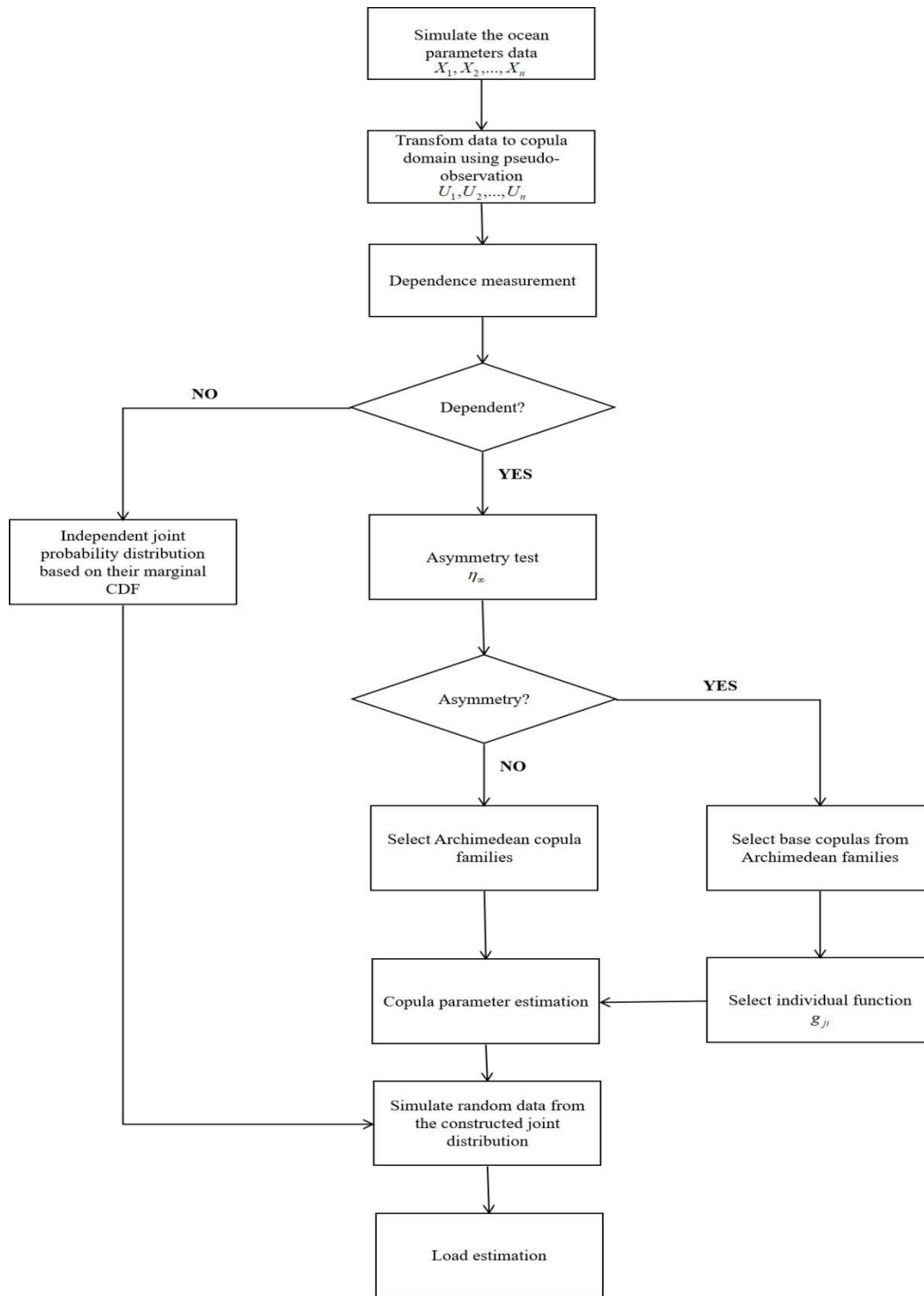


Fig. 3.1. Flowchart for the methodology

3.3.3 Dependence measurements

Dependence among variables is characterized by their correlation (Zhang et al., 2019). Correlation analysis is a method to evaluate the strength of the relationship between two random variables (Franzese and Iuliano, 2019). This analysis is carried out to identify if there is a connection between the two variables. If a correlation is found, a systematic change in one variable will influence a systematic change in the other variable. A positive correlation means if one variable increases, the other variable will also increase. Whereas a negative correlation means that if one variable increases, the other variable will decrease. Another type of correlation is the partial correlation. It measures the relationship between two variables by removing one or more related variables. Partial correlation is best used in multiple regression cases. In addition to this, partial correlation is used for data having an approximately normal distribution and a linear relationship between variables. In this chapter, attention is given to the measure of the relationship between two variables without controlling one or more of the other variables. As nonlinear relationships and marginal distributions, other than the normal distribution, are also considered. Bivariate correlation is then used to measure the relationship between two variables.

To identify the existence of dependence between ocean parameters, a concept of capturing and interpreting dependence is discussed in this section. There are two methods of measuring dependence between variables. The most common method is using Pearson's correlation, which is usually denoted by ρ . Suppose X and Y are two random variables and their linear correlation coefficient can be denoted as

$$\rho(X, Y) = \frac{CoV(X, Y)}{\sqrt{Var(X)}\sqrt{Var(Y)}} \quad (3.7)$$

where CoV is covariance and Var is variance (Zhang et al., 2018).

However, this Pearson's correlation has a distinctive weakness making it unsuitable for modelling ocean parameters. Pearson's correlation can only represent linear dependencies whereas ocean parameters show nonlinear dependencies (Zhang et al., 2018). Thus, a more robust method to measure dependence based on rank correlation is introduced here .

There are two measures based on rank correlation; Kendall's τ and Spearman's rho (ρ_s).

a) Spearman's rho (ρ_s)

Spearman's rho is a rank correlation that is proportional to the difference between the probabilities of concordance and dis-concordance of two vectors (Hashemi et al., 2015). If X and Y are continuous random variables whose copula is C then the Spearman's rho for X and Y is given as follows

$$\rho_s = 12 \iint uv dC(u, v) - 3 \quad (3.8)$$

b) Kendall's tau (τ)

Kendall's tau is the most widely used method to calculate dependence between random variables (Hashemi et al., 2015). Kendall's tau is defined by a concordance function between two continuous random variables with different joint distributions but common marginal distributions.

Nelsen stated that, for a bivariate random vector with copula C, Kendall's tau can be calculated by identifying the difference between the probabilities of concordance and dis-concordance of two independent observations (Nelsen, 2006).

$$\tau = 4 \int C(u, v) dC(u, v) - 1 \quad (3.9)$$

Zhang et al. (2018) mentioned that Kendall's τ and Spearman's ρ_s are able to minimize the influence of unequal variances, outliers and nonlinearity that cannot be solved using linear Person's correlation.

Another issue when applying copula to model environmental loads is that some copula families, especially Archimedean copulas, are only valid for symmetric data, while most ocean parameters show non-symmetric dependence. Thus, a way to identify whether a pair of ocean parameters is symmetric is also developed in this research.

3.3.4 Test for asymmetry

To understand how a copula is categorized as asymmetry, it is important to introduce the basic definition of symmetric copula. Genest and Nešlehová (2013) stated that a copula is said to be symmetrical when it satisfies these following properties

$$C(u_1, u_2) = C(u_2, u_1)$$

When the above condition is not satisfied for some $u_1, u_2 \in [0,1]$, a copula C is said to be asymmetric. This asymmetric dependence can occur in the present case as a result of causality relationships between selected ocean parameters.

In addition to this basic definition of symmetric dependence, Durante and Salvadori (2009) expressed a more general term to quantify the symmetry of a copula by the following equation

$$\eta_p(C) = 2 \left\{ \int_0^1 \int_0^1 |C(u_1, u_2) - C(u_2, u_1)|^p du_1 du_2 \right\}^{\frac{1}{p}} \quad (3.10)$$

Where p can be set to any value greater than or equal to 1. Eq. 3.10 can also be interpreted as this measure of asymmetry is the distance between copula C and its transposed copula C^T .

Zhang et al. (2019) also show a more general form to measure asymmetry for bivariate copulas by setting the value of p approaching infinity as seen in

$$\eta_{\infty}(C) = \sup_{(u_1, u_2) \in [0,1]^2} |C(u_1, u_2) - C(u_2, u_1)| \quad (3.11)$$

3.3.5 Construction of asymmetric copulas

There are several ways to construct asymmetric copulas and many involve intense mathematical modelling. Zhang, et al., on the other hand, proposed three methods for constructing asymmetric copulas that are practical and popular (Zhang et al., 2018). These methods are: 1) asymmetric copulas constructed by products, 2) asymmetric copulas constructed by linear convex combinations, and 3) skewed copula. These methods provide easy copula construction by utilizing base copulas such as the Archimedean copulas (Zhang et al., 2018). Zhang et al. (2019) state that the construction of asymmetric copula by product is the best tool to represent ocean parameters and more practical for implementation in a complex engineering system.

The construction of asymmetric copula by product was generally introduced by Liebscher through the following theorem (Liebscher, 2008)

Assume that C_1, \dots, C_k : are copulas. Let $g_{ji}: [0,1] \rightarrow [0,1]$ for $j = 1, \dots, k, i = 1, \dots, d$ be functions with the property that each of them is strictly increasing or identically equal to 1.

Then the general formula to construct asymmetric copula by product can be defined by

$$\tilde{C}(u_1, \dots, u_d) = \prod_{j=1}^k C_j(g_{j1}(u_1), \dots, g_{jd}(u_d)) \quad \text{for } u_i \in [0,1] \quad (3.12)$$

To satisfy the assumptions of the theorem, the function g_{ji} should have these following properties

- a) $g_{ji}(1) = 1$ and $g_{ji}(0) = 0$,
- b) g_{ji} is continuous on $(0,1]$,
- c) If there are at least two functions g_{j_1i}, g_{j_2i} with $1 \leq j_1, j_2 \leq k$ which are not identically equal to 1, then $g_{ji}(x) > x$ holds for $x \in (0,1), j = 1, \dots, k$

The introduction of function g_{ji} plays a significant role in constructing symmetric copulas into asymmetric copulas. Liebscher also introduced several functions g_{ji} that are usually applied to construct an asymmetric copula

- (I) $g_{ji}(v) = v^{\theta_{ji}}$ for $j = 1, \dots, k$, where $\theta_{ji} \in [0,1]$ and $\sum_{j=1}^k \theta_{ji} = 1$
- (II) $g_{ji}(v) = v^{\theta_{ji}} e^{(v-1)\alpha_{ji}}$ for $j = 1, \dots, k$, where $\sum_{j=1}^k \theta_{ji} = 1, \sum_{j=1}^k \alpha_{ji} = 0$ and $\theta_{ji} \in (0,1), \alpha_{ji} \in (-\infty, 1), \theta_{ji} \geq -\alpha_{ji}$
- (III) $g_{1i}(v) = \exp\left(\theta_i - \sqrt{|\ln v| + \theta_i^2}\right), g_{2i}(v) = v \exp\left(-\theta_i + \sqrt{|\ln v| + \theta_i^2}\right)$ for $\theta_i \geq \frac{1}{2}$

Zhang et al. (2019) also applied type-I function to construct asymmetric copula and obtained better results compared to other functions. The use of type I function in Eq. 3.12 is also known as constructing asymmetric copula by extra-parameterization and also satisfies a form of Khoudraji device when d is selected to be equal to 2 (Durante and Salvadori, 2009; Vanem, 2016). Type-I function are preferred by some researchers as the use of other functions might result in over-parameterized copula, as there are several new parameters introduced in the function in order to construct the asymmetry. Thus, in this work, asymmetric copula are constructed by product or extra-parameterization using Archimedean copulas as base copulas and type-1 function for the asymmetric dependence modelling. A simple illustration of constructing asymmetric copula using this technique can be seen in the following example.

Example: Constructing asymmetric copulas by product using a type-I function

Suppose $g_{j_1} = u^{\theta_{j_1}}$, and $g_{j_2} = u^{1-\theta_{j_2}}$, $C_1 =$ Clayton and $C_2 =$ Clayton.

Applying equation 13 and the type-I function

$\bar{C}(u_1, u_2) = \prod_{j=1}^k C_j(u^{\theta_{ji}}, u^{1-\theta_{ji}})$, with C_j follows Clayton family:

$$\bar{C}(u_1, u_2) = \left(1 + \sum_{i=1}^d (u_i^{\theta_{1i}})^{-\gamma_1} - 1 \right)^{\frac{-1}{\gamma_1}} \left(1 + \sum_{i=1}^d (u_i^{1-\theta_{2i}})^{-\gamma_2} - 1 \right)^{\frac{-1}{\gamma_2}}$$

For a bivariate problem, we set $d=2$, thus a constructed asymmetric copula based on two Clayton copula families and substituting a type-I function becomes

$$\bar{C}(u_1, u_2) = (u_1^{-\gamma_1\theta_{11}} + u_2^{-\gamma_1\theta_{12}} - 1)^{\frac{-1}{\gamma_1}} (u_1^{-\gamma_2(1-\theta_{21})} + u_2^{-\gamma_2(1-\theta_{22})} - 1)^{\frac{-1}{\gamma_2}}$$

3.3.6 Copula parameter estimation

The next step after applying the symmetric or asymmetric copula is to estimate the copula parameters. (Genest and MacKay, 1986) developed a method to estimate copula parameters by considering the relationship between a copula parameter and its Kendall's tau. Hashemi et al. (2015) estimated copula parameters using the relationships to Kendall's tau for the Archimedean copula families as follows in Table 3.2.

Table 3.2. Archimedean copulas and their Kendall's tau expressions.

Family	τ
Clayton	$\frac{\gamma}{\gamma + 2}$
Gumbel	$1 - \frac{1}{\gamma}$
Frank	$1 - \frac{4}{\gamma} + 4D_1(\gamma)/\gamma$

Linearized non-linear inversion can be implemented to estimate the parameters of copulas that have more than one parameter in their distribution function.

A flowchart of this method is presented in Fig. 3.2.

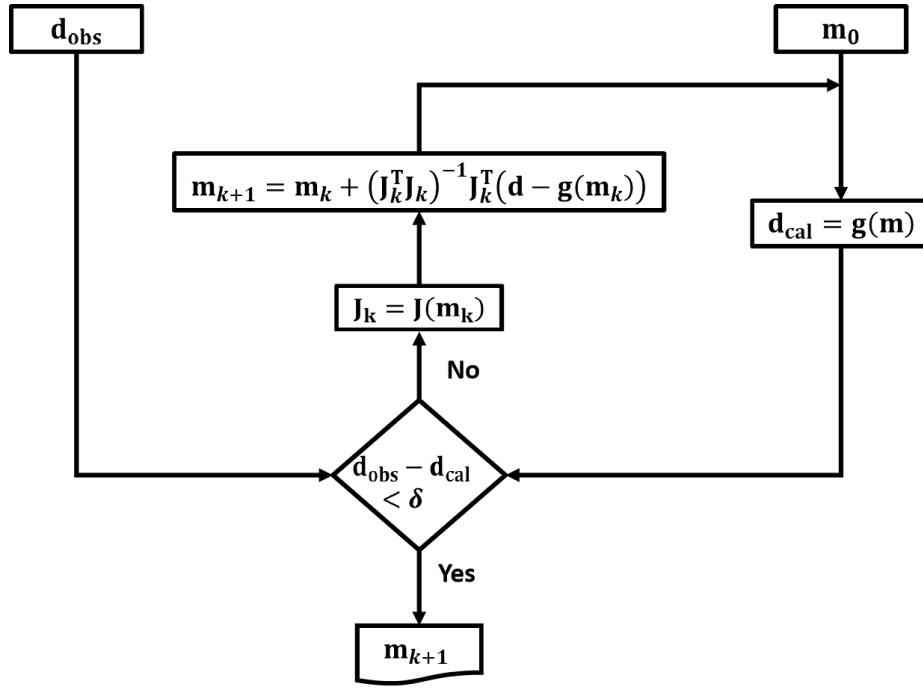


Fig. 3.2. Flowchart of linearized non-linear inversion method.

Step-1. Perform an iteration to develop an initial model (m_0) the relationship between the data and the model parameter can be defined as $d_{cal} = g(m)$.

Step-2. Identify the relation between the observed data (d_{obs}) and d_{cal} .

Step-3: Identify a Jacobian matrix. A Jacobian matrix (J_k), also known as a sensitivity matrix, is introduced when there is still significant difference between the observed and calculated data.

Step-4: Solve the inversion solution by applying Eq. 3.13 into any mathematical model of a problem.

$$m_{k+1} = m_k + (J_k^T J_k)^{-1} J_k^T (d - g(m_k)) \quad (3.13)$$

Copula parameters, including for asymmetric copulas, can then be estimated using Eq. 3.13.

3.4 Application of the Methodology: Load Estimation

Synthetic data from the constructed joint probability distribution and copula function are obtained for each ocean parameter to calculate the total load from the combined ocean parameters. Synthesized data from a constructed copula function is generated using a conditional distribution function. This conditional copula function is defined by using a partial derivative as shown in Eq. 3.14. Then, the synthetic data can be obtained by taking the inverse function of the conditional copula function.

$$F(U_2 \vee U_1; \gamma) = P(U_2 \leq u_2 \vee U_1 \leq u_1) = \frac{\partial C(u_1, u_2; \gamma)}{\partial(u_1)} \quad (3.14)$$

3.4.1 Environmental load calculation

Offshore marine structures are designed uniquely in order to withstand design loads arising from a specific location and environment. Loads that usually affect offshore marine structures are wind, wave, current, earthquake, and sometimes ice depending on the characteristic of the environment where the structures are to be located. In this research, the calculation of loads is limited to three environmental loads that most commonly affect marine structures; wind loads, wave loads and current loads (Nizamani et al., 2017).

Wind loads

Wind load on a structure arises from steady and fluctuating wind speed. The wind force can be calculated using several standards available for the design of offshore structures. In this research, the wind force, is calculated using a standard by DNV (DNV, 2010).

The wind force on a structural member or surface acting normal to the member axis can be calculated using the following equation

$$F_{wind} = CqA \sin \alpha \quad (3.15)$$

Where

C = shape coefficient

q = basic wind pressure or suction

A = projected area of the member normal to the direction of the wind velocity

α = angle between wind direction and the member axis

Basic wind pressure can be estimated using

$$q = \frac{1}{2} \rho_a U_z^2 \quad (3.16)$$

where, ρ_a is the mass density of air and assumed to be 1.226 kg/m³ and U_z is the wind velocity profile that can be estimated using

$$U_z = U_{z_0} \left(\frac{z}{z_0} \right)^{1/7} \quad (3.17)$$

where,

U_{z_0} = mean velocity at reference height

z_0 = reference height, usually taken as 10 m

z = height above mean sea level

Wave loads

There are several wave forces that can affect marine structure such as breaking wave loads, non-breaking wave loads and wave slam loads. A simple non-breaking wave load is used to illustrate the calculation of wave loads on a simple slender marine structure. The total wave force can be estimated by adding the drag force and inertia force (DNV, 2010).

The total wave force for a suitably slender structure, or element of a structure, can be estimated by using Morison's equation as follows (Bellad and Deshpande, 2018)

$$F_{T_{wave}} = F_I + F_D \quad (3.18)$$

$$F_{T_{wave}} = C_M \rho V \dot{u} + \frac{1}{2} C_D \rho A |u|u \quad (3.19)$$

where,

C_M and C_D are inertia and drag coefficient

ρ = water density

V = volume of the body

A = reference area

u = water wave particle velocity

\dot{u} = water wave particle acceleration

When calculating wave force on an offshore structure, it is also important to select the most appropriate wave theory as shown on Table 3.3. This wave theory selection can be based on (S. Zhang et al., 2015).

Table 3.3. The application of wave theories

Condition	Wave Theory
$\frac{d}{L} \geq 0.2, \frac{H}{L} \leq 0.2$	Airy wave theory
$0.1 < \frac{d}{L} < 0.2, \frac{H}{L} \geq 0.2$	Stokes wave theory
$0.04 < \frac{d}{L} < 0.1$	Solitary wave theory

where, d is water depth, L is wavelength, and H is wave height. Wave theories considered in this chapter can be seen in Appendix 3A.

Current loads

Current loads are also commonly taken into consideration in designing offshore structures. Chavito et al. (2014) provided an equation to calculate the force due to current load as a drag force

$$F_{Current} = \frac{1}{2} C_D \rho A U |U| \quad (3.20)$$

where,

C_D = drag coefficient

ρ = water density 1025 kg/m³

U = current velocity (m/s)

A = reference cross-sectional area (m²)

Total environmental loads

The total environmental load acting on a structure can then be estimated as

$$F_{Tot} = \sum \psi_i F_i \quad (3.21)$$

where, ψ_i are the factors for load combination. These factors can be taken as shown in Table 3.4 (Yu. Shmal et al., 2020).

Table 3.4. Factors of load combination.

Types of calculated loads	Combinations					
	I	II	III	IV	V	VI
Dead loads	1.0	1.0	0.9	1.0	1.0	1.0
Long-term live loads	0.95	—	0.8	1.0	0.95	0.95
Short-term live loads:						
• ice load (h = 0.8 m);	—	—	0.8	—	—	1.0
• wave load (repeated once in 100 years);	1.0	1.0	—	—	—	—
• wind load;	0.9	0.9	0.8	1.0	0.8	0.9

Types of calculated loads	Combinations					
	I	II	III	IV	V	VI
• current load	0.9	0.9	0.8	—	0.8	0.9
Special loads:						
• ice load (h = 2.5 m);	—	—	—	—	1.0	—
• seismic load	—	—	1.0	—	—	—

Using Table 3.4, the total environmental load in Eq. 3.21 is modified to $F_{tot} = F_{wave} + 0.9F_{wind} + 0.9F_{current}$

3.5 Synthetic Ocean Data Analysis

To demonstrate the effectiveness of the methodology in calculating environmental loads, a comparative study is presented here. It starts from the use of a general joint probability distribution, a symmetric copula, and an asymmetric copula for the combination of two ocean parameters analyzed in this research. The environmental data used to illustrate this proposed comparison were simulated using the Hilbert transform method.

As mentioned previously, asymmetric copulas are constructed to capture asymmetric phenomenon, usually found in ocean parameter data. These asymmetric copulas are constructed using a product rule method, also known as the extra-parameterization method, from selected base copulas. Although there are many copula families that can be set as base copulas, Archimedean copulas are used here as they have been commonly used in multivariate analysis. In addition, Archimedean copulas; Clayton, Gumbel, and Frank, can model tail dependencies, which might be suitable in constructing asymmetric copulas (Zhang et al., 2018). The possible combinations for constructing asymmetric copulas from the Archimedean copulas

are Clayton-Gumbel, Clayton-Frank, and Gumbel-Frank. These combinations provide a means to conduct multivariate analysis to estimate environmental loads.

3.5.1 Dataset preparation using Hilbert Transform

In this work, to capture the essence of real environmental data, wind speed is assumed to be the dominating factor. Wave height and current speed are the concomitant factors with a positive correlation with the dominating factor (i.e., wind speed and wave height). There is usually a delayed time between the occurrence of wind and wave. Wind speed will not immediately cause wave in the ocean. In this case, the Hilbert transform is found to be the most suitable method. It has been a common method in many aspects of science of technology especially in signal processing (Rusu et al., 2005). The Hilbert transform creates a function $H(u(t))$ from a given function $u(t)$ (Klingspor, 2015).

$$H(u(t)) = \lim_{\epsilon \rightarrow 0} \frac{1}{\pi} \int_{|s-t| > \epsilon} \frac{u(s)}{t-s} ds \quad (3.22)$$

Pranowo (2019) provided a general equation of this Hilbert transform as follows

$$\mathbf{W} \leftarrow \mathbf{W} \cos \phi + H(\mathbf{W}) \sin \phi \quad (3.23)$$

where $H(W)$ is the Hilbert transform of matrix W and ϕ is the phase rotation. This phase rotation can be varied to achieve a specific correlation coefficient between two ocean parameters. The phase rotation is ranging from 0 to $\pi/2$.

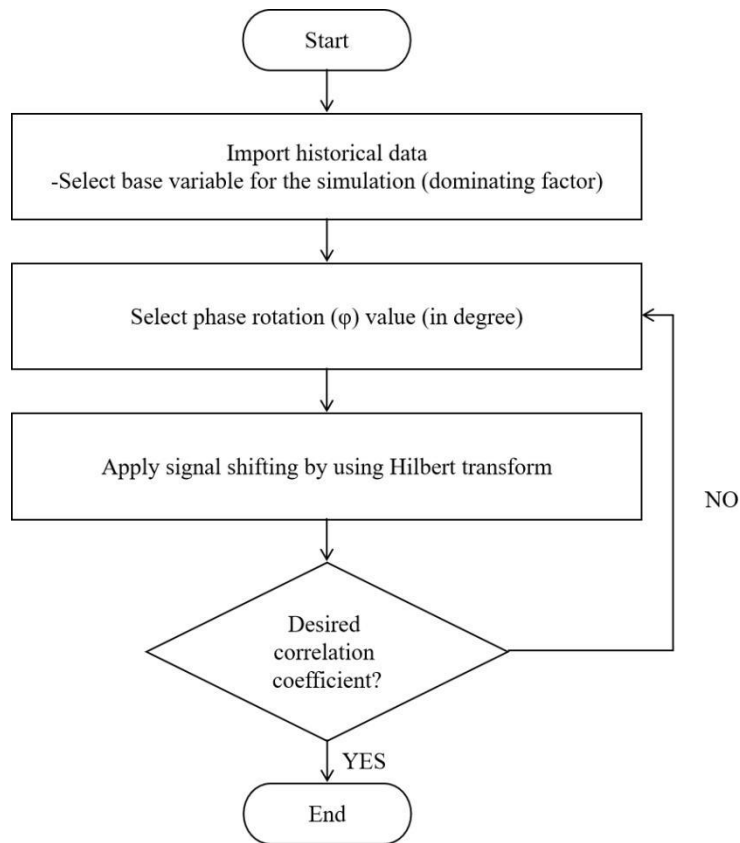


Fig. 3.3. Hilbert transform flowchart.

Fig. 3.3 shows the flowchart to perform Hilbert transform. Below is the procedure developed to implement the Hilbert transform to prepare the data sets used in the next section:

Select the data basis, in this case wind speed as the dominating factor.

1. Set the phase rotation. This value is ranging from $0 \leq \varphi \leq \frac{\pi}{2}$.
2. Apply Hilbert transform equation.
3. Transform the values to the original data statistics.

MATLAB codes for this Hilbert transform are presented in Appendix 3D.

Table 3.5. AIC values for all ocean parameters

	Weibull	Normal	Lognormal	Rayleigh	Extreme Value	Gamma
Wind	Inf.	23418*	Inf.	24177	25121	23637

Wave	13244	13677	13089	13546	15759	12985*
Current	45653*	45712	46953	46169	47310	46018

* Indicates the best model

Before continuing with joint probability analysis, marginal distributions for each ocean parameter are identified. The possible distributions fitted to the ocean parameters are Weibull, Normal, Lognormal, Rayleigh, Extreme Value and Gamma distribution. The Akaike Information Criterion (AIC) is utilized to select the best-fitted distribution among the possible distributions for the ocean parameters. AIC is a method based on using an in-sample fit to estimate the likelihood of a model (Mohammed et al., 2015). This method calculates the amount of information lost by a proposed model. AIC can be estimated using the following equation

$$AIC = -2 * \ln(L) + 2 * k \quad (3.24)$$

where, L is the value of maximum likelihood and k is the number of parameters.

The smallest value of AIC indicates the best distribution model for the data set as illustrated in Table 3.5. Table 3.5 shows the synthetic environmental data distribution fits after the Hilbert Transform process. This shows that the normal distribution is best-fitted to simulated wind data, Weibull is best-fitted to the simulated current data, while simulated wave height can be fitted by the gamma distribution. Kolmogorov-Smirnov (KS) tests are carried out to examine the goodness of fit of these distributions. P-Value from the KS test for wind, wave, and current data are 0.0398, 0.2398, and 0.0143 respectively. These P-values show that the fitted distribution is valid (fail to reject the null hypothesis) at a significance level of 1% for each ocean parameter. In terms of dependence measures, the synthetic ocean data show that the transform process introduces a much stronger dependence compared to the original data so that these data sets can be used to illustrate the comparison between symmetric and asymmetric copulas in the next section. Table 3.6 shows the distribution parameters for each variable.

Table 3.6. Distribution parameters statistics

	Mean	Variance	Shape	Scale
Wind	6.582	6.259		
Wave	2.159	0.892	5.226	0.413
Current	56.778	547.673	63.919	2.607

Fig. 3.4 illustrates that each pair of ocean parameter has positive dependence in the scatter plots. The value of the dependence for each pair are presented in Table 3.7.

Table 3.7. Dependence measures for simulated data.

	Pearson's linear correlation	Spearman's rho	Kendall's tau
Wind-Wave	0.8362	0.8097	0.6240
Wave-Current	0.7850	0.7693	0.5663
Wind-Current	0.7903	0.7596	0.5786

From Table 3.7, all dependence measures show that all pairs have positive dependence with wind speed and wave height having the strongest dependence. These synthetic data are utilized to construct asymmetric copulas using the Archimedean copulas as base copulas.

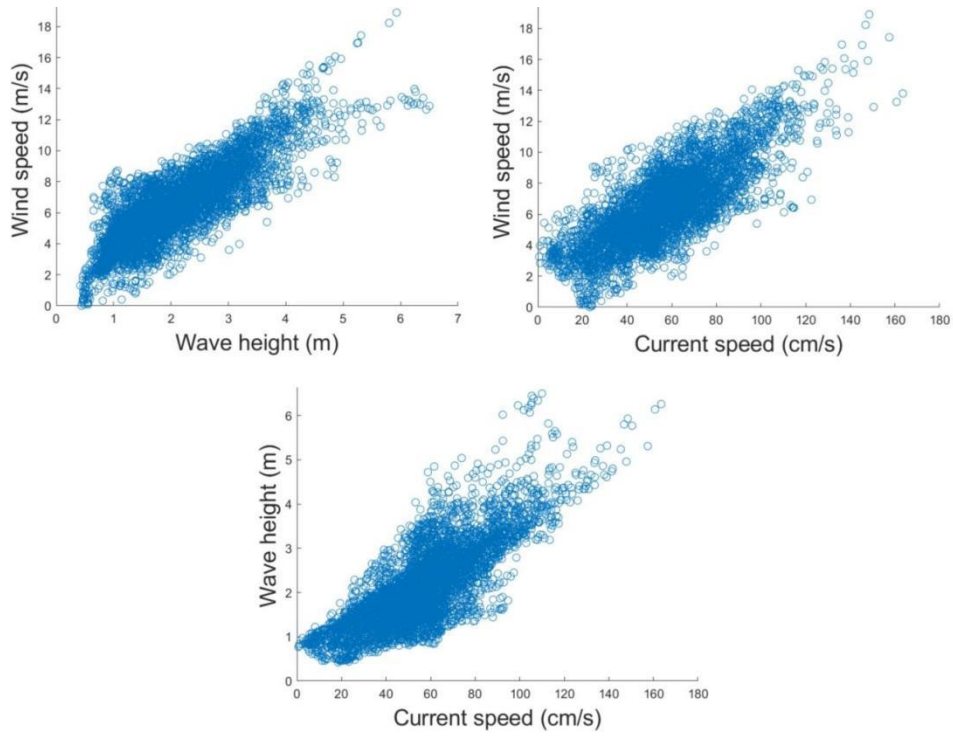


Fig. 3.4. Scatter plots for all synthetic ocean parameter pairs

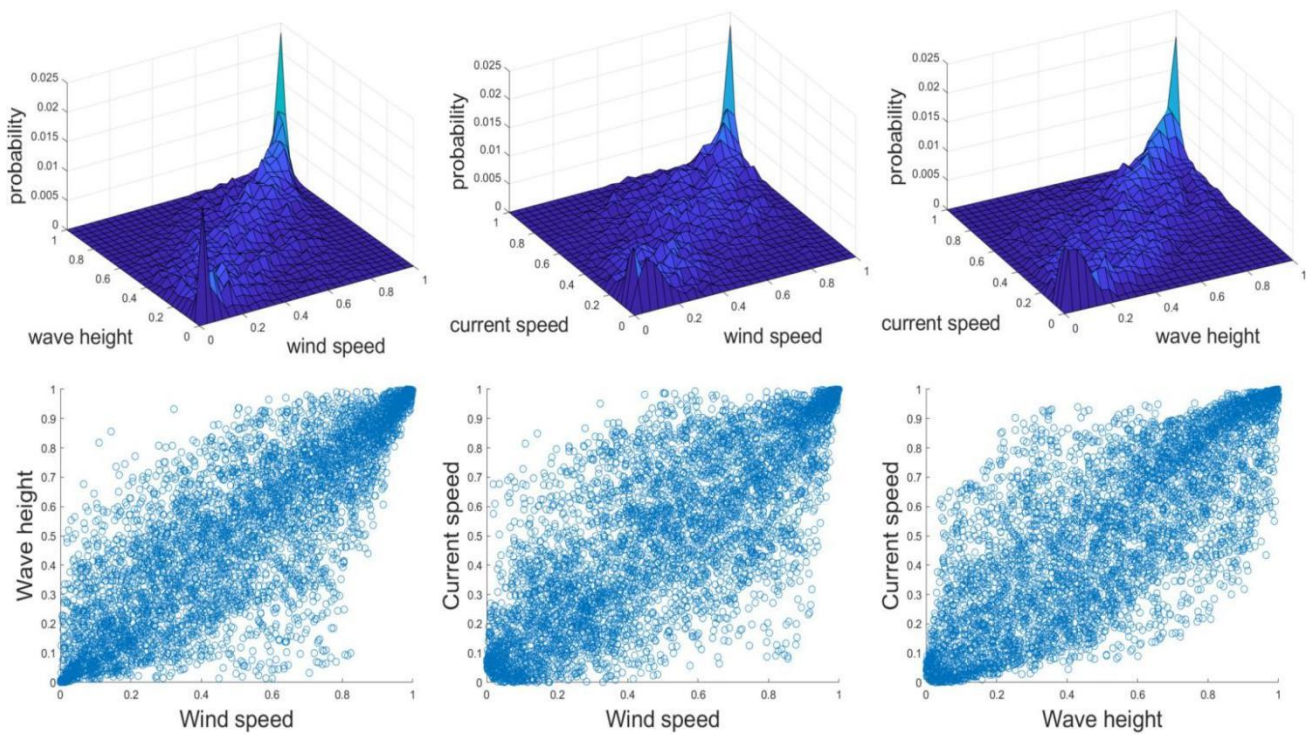


Fig. 3.5. Empirical probability and scatter plots for synthetic ocean data in copula domain.

Fig. 3.5 shows the empirical probability distribution function scatter plots for all pairs of ocean parameters in the copula domain. These synthetic data show a tail dependence in both upper and lower tails. The impact of this tail dependence can be further investigated by constructing asymmetric copulas.

Before constructing the asymmetric copulas, it is necessary to calculate the asymmetric value of each ocean parameter pair. By using Eq. 3.11, the measures of asymmetry of the wind-wave, wave-current, and wind-current pairs are 0.43 %, 0.58% and 0.43% respectively. Klement and Mesiar (2006) mentioned that a copula is symmetric only if $\eta_\infty = 0$ so that Eq. 3.11 will have values ranging from 0 to 1/3. Thus, the value η_p is greater than 0 if a pair of data sets is asymmetric. According to this, we may suspect that the synthetic ocean data pairs have a small degree of asymmetry so that the construction of asymmetric copulas will be necessary to fully capture this data characteristic. The comparison will be presented and discussed in the following section. As mentioned on the basic theories of constructing asymmetric copulas, the individual functions are developed from Type-1 functions by inserting $g_{ji} = u^{\theta_{ij}}$ and $g_{ji} = u^{1-\theta_{ij}}$ into the selected base copulas. For further details, all constructed asymmetric copulas using type-1 individual functions can be seen in Fig. 3C.1 in Appendix 3C.

The parameter estimates for all possible symmetric and asymmetric copulas for correlated wind speed and wave height are shown in Table 3.8. The values of parameter estimates are obtained using the concept of linearized non-linear inversion as explained previously. Parameters for other ocean parameter pairs can be seen in Table 3C.1 and Table 3C.2 in Appendix 3C.

Table 3.8. Parameters estimates of wind speed and wave height

Copula type	Copula function	Parameter estimate	Mean absolute error
One parameter copula	Clayton	$\gamma = 1.8918$	0.0132
	Gumbel	$\gamma = 2.5191$	0.0021

	Frank	$\gamma = 8.4663$	0.1253
Asymmetric copulas by product	Clayton-Gumbel Type-I	$\gamma_1 = 46.258$ $\gamma_2 = 3.0059$	0.0021
		$\theta_{11} = 0.1778\theta_{12}$ $= 0.3911$	
		$\theta_{21} = 0.8222\theta_{22}$ $= 0.6089$	
	Clayton-Frank Type-I	$\gamma_1 = 41.1615\gamma_2$ $= -11.2184$	0.0037
		$\theta_{11} = 0.2804\theta_{12}$ $= 0.0756$	
		$\theta_{21} = 0.7196\theta_{22}$ $= 0.9244$	
	Gumbel-Frank Type-I	$\gamma_1 = 2.6219\gamma_2$ $= -17.5714$	0.0024
		$\theta_{11} = 0.9002\theta_{12}$ $= 0.9343$	
		$\theta_{21} = 0.0998\theta_{22}$ $= 0.0657$	

From all of these asymmetric copula formulations using the synthetic data, the Gumbel-Frank Type-I seems to be the least appropriate fit to the wind-current and wave-current data, while Clayton-Frank Type-1 is the least fitted to the wind-wave data. The Gumbel copula is found to be the best fitted to model symmetrical dependence. This finding is also supported by a similar conclusion mentioned by Zhang et al that the Clayton-Frank combination cannot represent the data dependency very well (Zhang et al., 2018). The asymmetric copulas seem to represent the synthetic environmental data with smaller mean absolute errors compared to the symmetric copulas. Only the Gumbel copula has a similar mean absolute error value to the asymmetric copulas. Thus, considering asymmetric copulas when modelling environmental data, it is important to capture the real dependence type between environmental variables. This consideration can also be beneficial for further analysis. Appendix 3B contains further details and discussion on the comparison between symmetric and asymmetric copulas.

3.6 The Case Study

To illustrate the use of copula functions in estimating environmental loads, a simple offshore structure is selected. A mono-pile with a deck and a derrick on top are assumed.

Wind loads are calculated on the top side of the structure. There are two main structures subject to wind, a deck with dimensions of 15 x 15 x 4 for width, length, and height respectively and a cylindrical derrick with diameter equal to 3 m and height of 10 m. Shape coefficients, C , will be selected from available information on structure dimensions. Based on the DNV standard, the selected structures have shape coefficients of 0.5 and 0.9 for derrick and deck respectively (Sigurdsson, 1996). Wind loads will be calculated at different heights and the result can be seen in Table 3.9.

Table 3.9. Calculated wind loads.

Heights(m)	Fwind(N/m)	Reference Area
10	1433.63	Deck
12	1510.29	
14	1578.29	
16	455.46	Derrick
19	478.38	
24	511.40	

As can be seen, the wind load increases in accordance to the structure's height and depending on the dimensions of the reference area.

When calculating wave load, a single vertical cylindrical member is assumed (see Fig. 3.6). A steel pile with diameter of 1.32 m and length of 37.8 m is assumed. The immersed part of this steel pile is set to be 27.8 m.

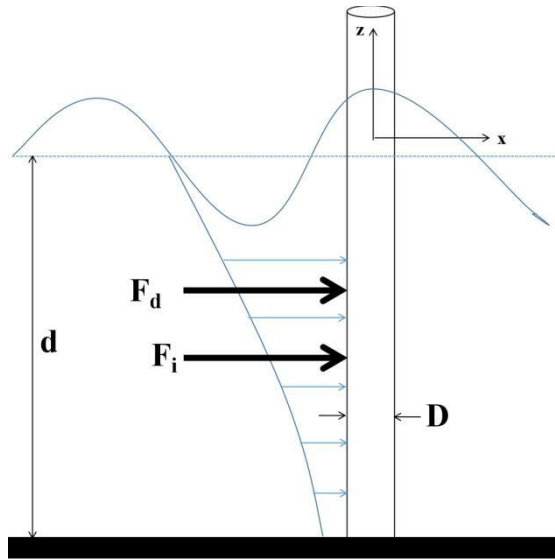


Fig. 3.6. A vertical mounted cylindrical pile.

There are two additional quantities that need to be estimated. The selection of drag and added mass coefficient will impact the calculated wave load. These two coefficients can be determined based on Reynold's number (Re) and Keulegan-Carpenter number (KC). KC can be obtained using Eq 25 (Haritos, 2007).

$$KC = \frac{u_{\max} T}{D} \quad (3.25)$$

where,

$$u_{\max} = \frac{\pi H}{T} \frac{1}{\tanh(kd)} \quad (3.26)$$

From these two equations, it is estimated that the drag and inertia coefficients are 1.25 and 1.5 respectively (Chakrabarti, 1994). These values are estimates, and values measured from real environment data, might differ according to the flow parameters and surface characteristics

To calculate wave loads, wavelength (L) of 85.29 m, wave period (T) of 7.54 second, wave height (H) of 3.26 m and angular frequency of 0.8333 were used to estimate wave loads in time domain and in the horizontal direction. The calculated wave load using Morison equation is illustrated in Fig. 3.7.

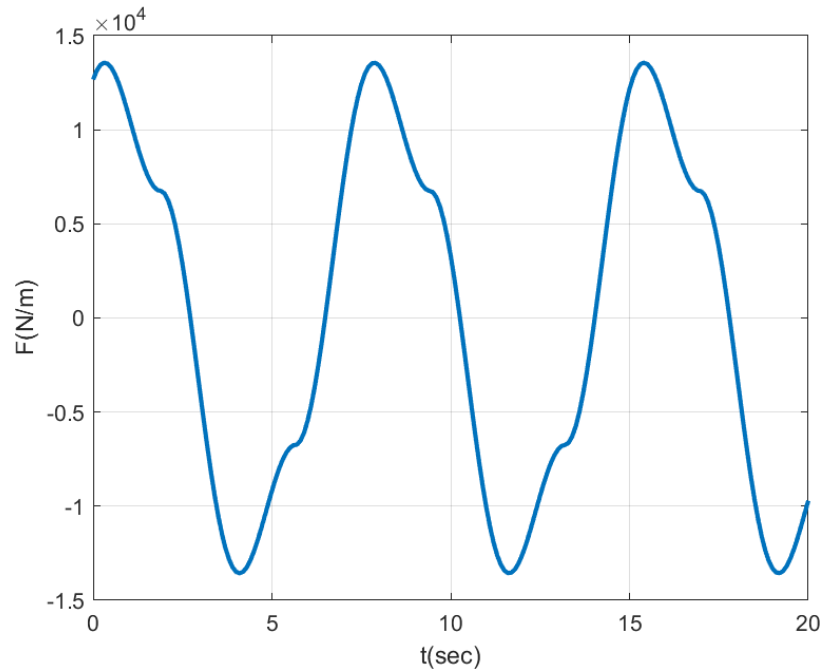


Fig. 3.7. Wave loads in time domain (second)

The current load is estimated to be 7614.57 N/m using the same pile dimensions and an average current speed from the data of 56.923 cm/s. Thus, the total environmental load acting on a structure can be estimated by adding these three different loads and applying the appropriate factor for load combination.

In order to compare the outcomes of applying three different symmetric copulas and three different constructed asymmetric copulas, random data is generated according to the selected copula function with various correlation coefficients (Kendall's tau). There are three possible pairs of correlated environmental variables that are compared here for the bivariate analysis. Significant wave height, average wind speed, and average current speed from each generated random data set are used to calculate the environmental loads acting on a structure.

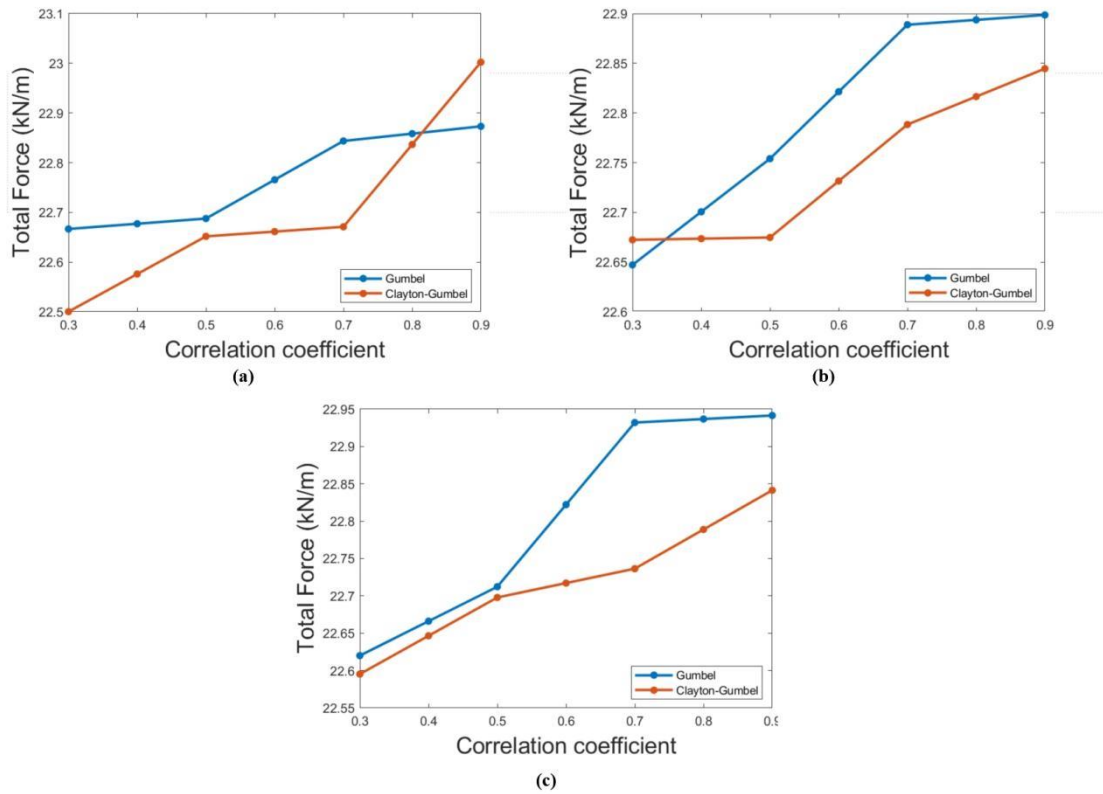


Fig. 3.8. Total environmental load for best-fitted symmetric and asymmetric copula for (a) wind and wave, (b) wind and current, and (c) wave and current.

From Fig. 3.8, it can also be seen that the asymmetric copula provides lower total environmental loads. However, the Gumbel copula provided better results in estimating total environmental loads with the selected data set. This is because the data set used to illustrate this comparison shows a very small asymmetry measurement and symmetric plot as seen in Fig. 3.5.

Estimation of total environmental loads using all copula functions can be seen in Fig. 3C.2 in Appendix 3C. This shows that each copula function shows different characteristics when it comes to environmental load estimation. Clayton shows decreasing value of total environmental loads when the correlation coefficient increases. This also shows that the Clayton copula has stronger dependence at lower values. The estimated environment load using

Gumbel shows increasing values with the increase in correlation coefficient. This is aligned with the characteristics of the Gumbel copula where a stronger dependence is found at higher values. On the other hand, the Frank copula shows fluctuating value when correlation is set to be 0.5 and 0.7. The Frank copula, in nature, does not show any stronger dependence at either tail. When using asymmetric copulas, a similar trend is found when Frank is used as the basis copula. Clayton-Frank and Gumbel-Frank also showed fluctuating estimated load when correlation is set to be 0.5 and 0.7. Clayton-Gumbel showed a similar trend to the Gumbel copula as the correlation coefficient increased. Asymmetric copula functions in this pair of environment variables are found to provide slightly lower total environmental load.

Another important aspect when modelling environmental loads is to be able to capture an accurate dependency type. This remains a challenge as it is a common problem to have data scarcity in real engineering practice. Thus, it is difficult to identify an appropriate copula function when the necessary information cannot be obtained. The use of symmetric copulas is often preferred. They can be easily applied and there have been several studies that have demonstrated application of these functions. However, in an engineering context, symmetrical dependence might not be an appropriate assumption, especially when dealing with environment variables. Ocean parameters usually show strong dependency at either one of the extremes. Thus, use of asymmetric copula can offer more accurate analysis in extreme cases.

3.7 Estimation of Probability of Occurrence

To illustrate the benefits of using copula functions, a comparison of probability of occurrence is estimated using the different methods. As mentioned previously wave, wind, and current loads were selected as they are the dominating loads on offshore structures. Offshore structures are normally designed to withstand extreme wind-wave-current conditions with low frequency

of occurrence and high severity. When dealing with this type of load, considering return period and the associated design values is important in estimating the probability occurrence for any combination of environmental loads. Dong et al. (2017) mentioned that when actual marine environmental data is used, selecting a conditional variable, which is commonly considered as dominating factor, is the initial step in trying to estimate the conditional probability of occurrence of the other factors. When a dominating factor (conditional variable) is given, the other variables then can be calculated, based on the selected return periods, that are usually selected from a design standard. Zhai et al. (2017) also concluded that when conditional probability density of a given variable reaches its maximum, the other two concomitant variables are likely to occur.

To illustrate this method, for a bivariate analysis, maximum wave height (H_{\max}) or maximum wind speed (W_{\max}) is selected as the dominating factor while one of the other two variables is considered the concomitant variable.

The conditional bivariate probability distribution can then be modeled using

$$f(y|x) = \frac{f(x,y)}{f(x)} = c(x,y).f(y) \quad (3.27)$$

With x as the dominating factor, $c(x,y)$ is the copula function between the two variables and $f(x,y)$ is the joint probability distribution.

Liu and Zhang (2016) explained a conditional correlation model that can describe the joint probability distribution based on copula function. The conditional probability distribution is written as follows

$$F(y_1 | X = x_1) = C(V \leq v_1 | U = u_1) = \frac{\partial C(u_1, v_1)}{\partial u_1} \quad (3.28)$$

And the conditional return period based on the copula function can be estimated using this equation

$$T(y_1 | X = x_1) = \frac{1}{1 - F(y_1 | X = x_1)} = \frac{1}{1 - \frac{\partial C(u_1, v_1)}{\partial u_1}} \quad (3.29)$$

Random variable X is denoted as the dominating factor, while random variable y is the selected concomitant factor.

In this work, a return period T (year) of 100 years is selected as recommended by the standard (American Petroleum Institute, 2002). The design value for the dominating factor (H_{\max} or W_{\max}) and the respected concomitant factor using different symmetric copulas can be seen in Table 3.10.

Table 3.10. Design value with dominating factor Hmax and concomitant factor W or C.

	Hmax with concomitant W or C					
	T = 100 years					
	H_{\max} (m)	W (m/s)	Prob.	H_{\max} (m)	C (cm/s)	Prob.
Clayton	12.97	14.371	4.26×10^{-6}	12.97	130.235	6.42×10^{-7}
Gumbel*		15.967	3.32×10^{-6}		146.38	5.79×10^{-7}
Frank		6.634	2.41×10^{-5}		62.158	2.00×10^{-6}
Clayton-Gumbel Type-1*		17.141	4.51×10^{-7}		152.103	1.46×10^{-7}
Clayton-Frank Type-1		18.124	3.20×10^{-8}		141.603	3.71×10^{-7}
Gumbel-Frank Type-1		15.479	6.35×10^{-6}		148.054	2.74×10^{-7}
Independent joint dist.		8.909	4.13×10^{-10}		83.631	3.35×10^{-11}

Conditional joint dist.		25.597	1.62×10^{-12}		113.507	3.59×10^{-13}
-------------------------	--	--------	------------------------	--	---------	------------------------

*Indicates the best-fitted copula

Table 3.11. Design value with dominating factor W_{max} and concomitant factor H or C

	W _{max} with concomitant H or C					
	T = 100 years					
	W _{max} (m/s)	H (m)	Prob.	W _{max} (m/s)	C (cm/s)	Prob.
Clayton	34.93	5.9798	1.01×10^{-5}	34.93	128.952	7.19×10^{-7}
Gumbel*		5.9158	7.61×10^{-5}		149.791	3.52×10^{-7}
Frank		2.1178	6.39×10^{-5}		62.905	1.92×10^{-6}
Clayton-Gumbel Type-1*		6.363	3.19×10^{-5}		145.189	5.46×10^{-7}
Clayton-Frank Type-1		6.319	1.39×10^{-5}		125.969	2.49×10^{-6}
Gumbel-Frank Type-1		6.184	4.63×10^{-5}		147.514	3.79×10^{-7}
Independent joint dist.		0.732	2.07×10^{-29}		35.033	1.34×10^{-30}
Conditional joint dist.		18.249	2.07×10^{-26}		141.125	2.28×10^{-28}

*Indicates the best-fitted copula

A detailed consideration is given to the best fitted symmetric and asymmetric copula, along with traditional joint distribution approaches. Probabilities of occurrence of a concomitant factor given a dominating factor are found to be greater when estimated using copula functions. The Root-Mean-Square error (RMSE) and the mean absolute error values are used to select the best model fitted to the synthetic data. RMSE is calculated between empirical data and the selected distribution functions compared in this chapter. In general, RMSE can be estimated using

$$RMSE = \sqrt{\frac{\sum_{i=1}^n (\hat{y}_i - y_i)^2}{n}} \quad (\text{STYLER1})$$

Where, y_i is the actual data, \hat{y}_i is the predicted data, and n is the number of data. RMSE values from the best-fit symmetric and asymmetric copula, traditional joint independent and conditional functions are compared below.

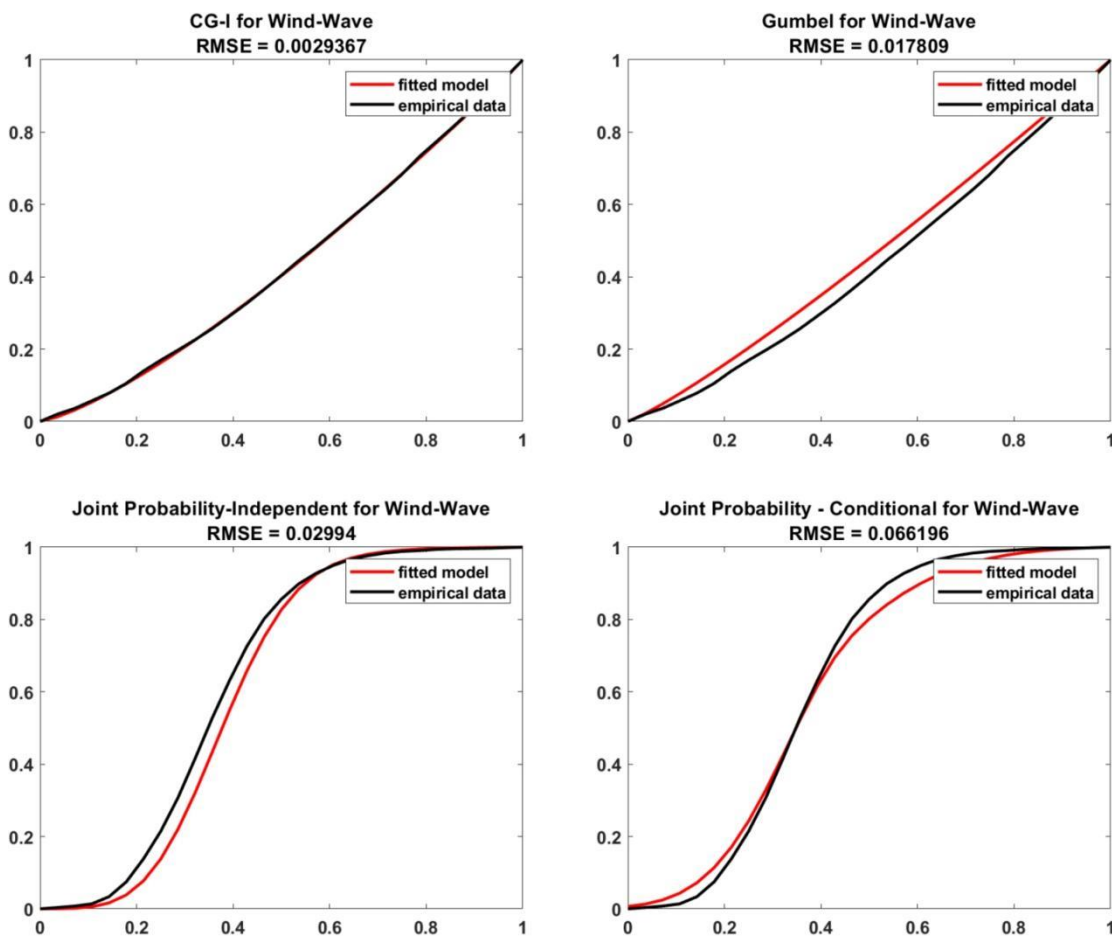


Fig. 3.9. Empirical data plotted against selected distribution functions for wind speed and wave height data

Table 3.12. RMSE and mean absolute error between empirical data and fitted distribution functions

Ocean parameter	Gumbel		Clayton-Gumbel Type-1		Traditional joint independent function		Traditional joint conditional function	
	RMSE	Absolute Error	RMSE	Absolute Error	RMSE	Absolute Error	RMSE	Absolute Error
Wind-wave	0.0178	0.0021	0.0029	0.0021	0.0299	0.0299	0.0662	0.0481
Wind-current	0.0232	0.0052	0.0053	0.0033	0.0305	0.0209	0.0797	0.0497
Wave-current	0.0228	0.0038	0.0039	0.0027	0.0313	0.0216	0.0995	0.0775

Fig. 3.9 and Table 3.12 show that the Gumbel and the Clayton-Gumbel type-1 have lower RMSE and mean absolute error than the traditional joint distribution approaches. For the Gumbel function, mean absolute error values are lower than RMSE. This is because RMSE has higher sensitivity to outliers in the data set. This shows that the synthetic environmental data are better modeled using the copula functions. It also supports the results showing the probabilities of occurrence in Table 3.10 and Table 3.11. In this illustration, Gumbel and Clayton-Gumbel type-1 are found to provide a better inherent safety when designing a structure. This finding supports some of the work conducted by other researchers. Salleh et al. (2016) demonstrated that the copula method is effective for bivariate analysis of flood risks while preserving the dependence structure of the flood characteristics. Zhang et al. (2015) compared the conditional approach to model offshore environment parameters using the Nataf transformation and copula functions. They concluded that the copula-based approach provides more flexibility and a better description of the nonlinear dependencies between ocean parameters. The copula was also used for marine environmental analysis (Dong et al., 2022). They concluded that conditional probability using the copula function could better present a joint design value of significant wave height and the corresponding wind and current speed. Thus, from the findings of this research and other relevant works, it can be concluded that the

use of copula functions to analyze marine environmental variables will result in a better approach and interpretation compared to the traditional joint probability approach and the Nataf transformation. In addition to this, the predicted concomitant factor from the dominating factor in both Gumbel and Clayton-Gumbel Type-1 show similar results. However, the Gumbel copula provided higher probability compared to Clayton-Gumbel Type-1. It also supported a finding on the estimated total environmental load where the Gumbel copula resulted in higher loads. As mentioned before, the data set used to illustrate this copula application shows symmetrical dependence from the beginning with a relatively small asymmetric measurement. Although mean average errors estimated using all asymmetric copulas show lower values than symmetric copulas, the Gumbel copula seems to be the best-fitted function in this case. Therefore, the total environmental load estimated using this copula will give better design values for further analysis. However, this symmetric dependence in environment parameters is unlikely to be found in other data sets, and thus a consideration of asymmetric copulas remains necessary in this case.

3.8 Conclusion

In this chapter, the influence of different copula functions used to estimate environmental loads on an offshore structure is analyzed and interpreted. The Gumbel and Clayton-Gumbel type-1 Copula functions were concluded to provide lower RMSE values and higher probability of occurrence compared to the traditional joint distribution function approaches. This improves the inherent safety when designing a fixed offshore platform. The generated data set was scattered symmetrically in copula domain and was shown to have relatively small asymmetry measurement. Thus, a symmetrical copula, in this case the Gumbel copula, was best fitted to the data set to estimate the environment load and probability of occurrence.

The case study shows that there are two main factors that can lead to different results from the application of asymmetric copulas. Firstly, the selection of new individual functions to construct asymmetric copulas is important. Different individual functions will result in different models. Secondly, varying dependency level or correlation coefficient in asymmetric copulas is also uncertain. Unlike symmetric copula, this process can be done by assuming the same parameter to vary the desired dependence level. However, the ignorance in considering asymmetric dependence when dealing with environment variables may also result in errors when estimating total environmental loads. The application of asymmetric copula to perform multivariate analysis for offshore structures are concluded to be beneficial to capture all possible dependency levels that ocean parameters data might have.

In a future work, a large met-ocean data set will be used to improve the reliability of the environmental load estimation for offshore structures. A copula-based multivariate analysis will also be potential future research when dealing with marine environment.

Conflict of Interest

The authors declare that they have no known competing financial interests or personal relationships that could have appeared to influence the work reported in this chapter.

Acknowledgements

The authors would like to express their gratitude to the financial assistance provided by the Natural Science and Engineering Council of Canada (NSERC) and the Canada Research Chair (CRC) Tier I Program in Offshore Safety and Risk Engineering.

References

Abaei, M.M., Hekkenberg, R., BahooToroody, A., Banda, O.V., van Gelder, P., 2022. A probabilistic model to evaluate the resilience of unattended machinery plants in

- autonomous ships. *Reliab. Eng. Syst. Saf.* 219, 108176. <https://doi.org/10.1016/j.ress.2021.108176>
- American Petroleum Institute, 2002. Recommended Practice for Planning, Designing and Constructing Fixed Offshore Platforms - Working Stress Design. Washington, D.C.
- Bang Huseby, A., Vanem, E., Natvig, B., 2013. A new approach to environmental contours for ocean engineering applications based on direct Monte Carlo simulations. *Ocean Eng.* 60, 124–135. <https://doi.org/10.1016/j.oceaneng.2012.12.034>
- Bellad, A., Deshpande, R., 2018. Estimation of wave loads and their effect on piled structures. *Int. J. Res. Appl. Sci. Eng. Technol.* 6, 136–142.
- Chakrabarti, S., 1994. Hydrodynamics of offshore structures. Offshore Structure Analysis Inc.
- Chavito, R., Kougioumtzoglou, M., Sanchez, N., 2014. Jacket substructures for offshore wind turbines and pre-piled grouted connections [WWW Document]. URL http://www.esru.strath.ac.uk/EandE/Web_sites/13-14/Jacket_Substructures/jackets/waveawind.html
- Cruz, A.M., Krausmann, E., 2008. Damage to offshore oil and gas facilities following hurricanes Katrina and Rita: An overview. *J. Loss Prev. Process Ind.* 21, 620–626. <https://doi.org/10.1016/j.jlp.2008.04.008>
- De Michele, C., Salvadori, G., Passoni, G., Vezzoli, R., 2007. A multivariate model of sea storms using copulas. *Coast. Eng.* 54, 734–751. <https://doi.org/10.1016/j.coastaleng.2007.05.007>
- de Waal, D.J., van Gelder, P.H.A.J.M., 2005. Modelling of extreme wave heights and periods through copulas. *Extremes* 8, 345–356. <https://doi.org/10.1007/s10687-006-0006-y>
- Deyab, S.M., Taleb-berrouane, M., Khan, F., Yang, M., 2018. Failure analysis of the offshore process component considering causation dependence. *Process Saf. Environ. Prot.* 113, 220–232. <https://doi.org/10.1016/j.psep.2017.10.010>
- DNV, 2010. Environmental conditions and environmental loads. Recommended Practice DNV-RP-C205.
- Dong, S., Chen, C., Tao, S., 2017. Joint probability design of marine environmental elements for wind turbines. *Int. J. Hydrogen Energy* 42, 18595–18601. <https://doi.org/10.1016/j.ijhydene.2017.04.154>
- Dong, W., Sun, H., Tan, J., Li, Z., Zhang, J., Yang, H., 2022. Regional wind power probabilistic forecasting based on an improved kernel density estimation, regular vine copulas, and ensemble learning. *Energy* 238, 122045. <https://doi.org/10.1016/j.energy.2021.122045>
- Durante, F., Salvadori, G., 2009. On the construction of multivariate extreme value models via

- copulas. *Environmetrics* n/a-n/a. <https://doi.org/10.1002/env.988>
- Fazerer-Ferradosa, T., Taveira-Pinto, F., Vanem, E., Reis, M.T., Neves, L. das, 2018. Asymmetric copula-based distribution models for met-ocean data in offshore wind engineering applications. *Wind Eng.* 42, 304–334. <https://doi.org/10.1177/0309524X18777323>
- Franzese, M., Iuliano, A., 2019. Correlation Analysis, in: *Encyclopedia of Bioinformatics and Computational Biology*. Elsevier, pp. 706–721. <https://doi.org/10.1016/B978-0-12-809633-8.20358-0>
- Genest, C., MacKay, J., 1986. The Joy of Copulas: Bivariate Distributions with Uniform Marginals. *Am. Stat.* 40, 280. <https://doi.org/10.2307/2684602>
- Genest, C., Nešlehová, J.G., 2013. Assessing and Modelling Asymmetry in Bivariate Continuous Data. pp. 91–114. https://doi.org/10.1007/978-3-642-35407-6_5
- Genest, C., Rémillard, B., Beaudoin, D., 2009. Goodness-of-fit tests for copulas: A review and a power study. *Insur. Math. Econ.* 44, 199–213. <https://doi.org/10.1016/j.insmatheco.2007.10.005>
- Grimaldi, S., Serinaldi, F., 2006. Asymmetric copula in multivariate flood frequency analysis. *Adv. Water Resour.* 29, 1155–1167. <https://doi.org/10.1016/j.advwatres.2005.09.005>
- Guo, C., Khan, F., Imtiaz, S., 2019. Copula-based Bayesian network model for process system risk assessment. *Process Saf. Environ. Prot.* 123, 317–326. <https://doi.org/10.1016/j.psep.2019.01.022>
- Haritos, N., 2007. Introduction to the Analysis and Design of Offshore Structures– An Overview. *Electron. J. Struct. Eng.* 55–65. <https://doi.org/10.56748/ejse.651>
- Hashemi, S.J., Ahmed, S., Khan, F.I., 2015. Correlation and Dependency in Multivariate Process Risk Assessment. *IFAC-PapersOnLine* 48, 1339–1344. <https://doi.org/10.1016/j.ifacol.2015.09.711>
- Kabir, S., Taleb-Berrouane, M., Papadopoulos, Y., 2019. Dynamic reliability assessment of flare systems by combining fault tree analysis and Bayesian networks. *Energy Sources, Part A Recover. Util. Environ. Eff.* <https://doi.org/10.1080/15567036.2019.1670287>
- Kaiser, M.J., Yu, Y., 2010. The impact of Hurricanes Gustav and Ike on offshore oil and gas production in the Gulf of Mexico. *Appl. Energy* 87, 284–297. <https://doi.org/10.1016/j.apenergy.2009.07.014>
- Kamil, M.Z., Taleb-Berrouane, M., Khan, F., Ahmed, S., 2019. Dynamic domino effect risk assessment using Petri-nets. *Process Saf. Environ. Prot.* 124, 308–316. <https://doi.org/10.1016/j.psep.2019.02.019>

- Klement, E.P., Mesiar, R., 2006. How non-symmetric can a copula be? *Comment. Math. Univ. Carolinae* 47, 141–148.
- Klingspor, M., 2015. Hilbert transform: mathematical theory and applications to signal processing. Linköping University.
- Leontaris, G., Morales-Nápoles, O., Wolfert, A.R.M. (Rogier.), 2016. Probabilistic scheduling of offshore operations using copula based environmental time series – An application for cable installation management for offshore wind farms. *Ocean Eng.* 125, 328–341. <https://doi.org/10.1016/j.oceaneng.2016.08.029>
- Liebscher, E., 2008. Construction of asymmetric multivariate copulas. *J. Multivar. Anal.* 99, 2234–2250. <https://doi.org/10.1016/j.jmva.2008.02.025>
- Liu, X., Zhang, Q., 2016. Analysis of the return period and correlation between the reservoir-induced seismic frequency and the water level based on a copula: A case study of the Three Gorges reservoir in China. *Phys. Earth Planet. Inter.* 260, 32–43. <https://doi.org/10.1016/j.pepi.2016.09.001>
- Mahfoud, M., Massmann, M., 2012. Bivariate archimedean copulas: an application to two stock market indices.
- Mohammed, E.A., Naugler, C., Far, B.H., 2015. Emerging Business Intelligence Framework for a Clinical Laboratory Through Big Data Analytics, in: *Emerging Trends in Computational Biology, Bioinformatics, and Systems Biology*. Elsevier, pp. 577–602. <https://doi.org/10.1016/B978-0-12-802508-6.00032-6>
- Nelsen, R.B., 2006. *An introduction to copulas*, 2nd ed. Springer.
- Nizamani, Z., Woan Yih, L., Wahab, M.M., Mustaffa, Z., 2017. Determination of Correlation for Extreme Metocean Variables. *MATEC Web Conf.* 103, 04013. <https://doi.org/10.1051/mateconf/201710304013>
- Pranowo, W., 2019. Time-varying wavelet estimation and its applications in deconvolution and seismic inversion. *J. Pet. Explor. Prod. Technol.* 9, 2583–2590. <https://doi.org/10.1007/s13202-019-00748-9>
- Rusu, C., Kuosmanen, P., Astola, J., 2005. Hilbert transform of discrete data: a brief review, in: *Proceeding of the International TICSOS Workshop on Spectral Methods and Multivariate Signal Processing*.
- Sagrilo, L.V.S., Naess, A., Doria, A.S., 2011. On the long-term response of marine structures. *Appl. Ocean Res.* 33, 208–214. <https://doi.org/10.1016/j.apor.2011.02.005>
- Salleh, N., Yusof, F., Yusop, Z., 2016. Bivariate copulas functions for flood frequency analysis. p. 060007. <https://doi.org/10.1063/1.4954612>

- Sigurdsson, G., 1996. Guideline for offshore structural reliability analysis-application to jacket platforms.
- Sinsabvarodom, C., Chai, W., Leira, B.J., Høyland, K. V., Naess, A., 2020. Uncertainty assessments of structural loading due to first year ice based on the ISO standard by using Monte-Carlo simulation. *Ocean Eng.* 198, 106935. <https://doi.org/10.1016/j.oceaneng.2020.106935>
- Taleb-Berrouane, M., Khan, F., 2019. Dynamic Resilience Modelling of Process Systems. *Chem. Eng. Trans.* 77, 313–318. <https://doi.org/10.3303/CET1977053>
- Taleb-Berrouane, M., Khan, F., Amyotte, P., 2020. Bayesian Stochastic Petri Nets (BSPN) - A new modelling tool for dynamic safety and reliability analysis. *Reliab. Eng. Syst. Saf.* 193. <https://doi.org/10.1016/j.ress.2019.106587>
- Taleb-berrouane, M., Khan, F., Hawboldt, K., Eckert, R., Skovhus, T.L., 2018. Model for microbiologically influenced corrosion potential assessment for the oil and gas industry and gas industry. *Corros. Eng. Sci. Technol.* 53, 378–392. <https://doi.org/10.1080/1478422X.2018.1483221>
- Taleb-Berrouane, M., Khan, F., Kamil, M.Z., 2019. Dynamic RAMS analysis using advanced probabilistic approach. *Chem. Eng. Trans.* 77. <https://doi.org/10.3303/CET1977041>
- Talebberrouane, M., Khan, F., Lounis, Z., 2016. Availability analysis of safety critical systems using advanced fault tree and stochastic Petri net formalisms. *J. Loss Prev. Process Ind.* 44, 193–203. <https://doi.org/10.1016/j.jlp.2016.09.007>
- Vanem, E., 2016. Joint statistical models for significant wave height and wave period in a changing climate. *Mar. Struct.* 49, 180–205. <https://doi.org/10.1016/j.marstruc.2016.06.001>
- Wei, Z., Kim, D., 2018. On multivariate asymmetric dependence using multivariate skew-normal copula-based regression. *Int. J. Approx. Reason.* 92, 376–391. <https://doi.org/10.1016/j.ijar.2017.10.016>
- Wilson, J., 2002. *Dynamic Offshore Structure*. John Wiley & Sons, New Jersey.
- Yang, R., Khan, F., Taleb-Berrouane, M., Kong, D., 2020. A time-dependent probabilistic model for fire accident analysis. *Fire Saf. J.* 111. <https://doi.org/10.1016/j.firesaf.2019.102891>
- Yu. Shmal, G., A. Nadein, V., A. Makhutov, N., A. Truskov, P., I. Osipov, V., 2020. Hybrid Modelling of Offshore Platforms' Stress-Deformed and Limit States Taking into Account Probabilistic Parameters, in: *Probability, Combinatorics and Control*. IntechOpen. <https://doi.org/10.5772/intechopen.88894>

- Zhai, J., Yin, Q., Dong, S., 2017. Metocean design parameter estimation for fixed platform based on copula functions. *J. Ocean Univ. China* 16, 635–648. <https://doi.org/10.1007/s11802-017-3327-3>
- Zhang, S., Chen, C., Zhang, Q., Zhang, D., Zhang, F., 2015. Wave Loads Computation for Offshore Floating Hose Based on Partially Immersed Cylinder Model of Improved Morison Formula. *Open Pet. Eng. J.* 8, 130–137. <https://doi.org/10.2174/1874834101508010130>
- Zhang, Y., Beer, M., Quek, S.T., 2015. Long-term performance assessment and design of offshore structures. *Comput. Struct.* 154, 101–115. <https://doi.org/10.1016/j.compstruc.2015.02.029>
- Zhang, Y., Gomes, A.T., Beer, M., Neumann, I., Nackenhorst, U., Kim, C.-W., 2019. Reliability analysis with consideration of asymmetrically dependent variables: Discussion and application to geotechnical examples. *Reliab. Eng. Syst. Saf.* 185, 261–277. <https://doi.org/10.1016/j.ress.2018.12.025>
- Zhang, Y., Kim, C.-W., Beer, M., Dai, H., Soares, C.G., 2018. Modelling multivariate ocean data using asymmetric copulas. *Coast. Eng.* 135, 91–111. <https://doi.org/10.1016/j.coastaleng.2018.01.008>

Appendix 3A: Wave theories

There are three possible methods to calculate wave load in this chapter.

1. Airy Wave Theory

In this theory, water particle velocity and acceleration in the horizontal direction can be estimated by

$$\left. \begin{aligned} u_x &= \frac{Hgk \cosh(k(z+d))}{2\omega \cosh(kd)} \cos(kx - \omega t) \\ \dot{u}_x &= \frac{2\pi^2 H \cosh(k(z+d))}{T^2 \sinh(kd)} \sin(kx - \omega t) \end{aligned} \right\} (3A.1)$$

g = standard gravity

H = wave height

k = wave number that is calculated using this equation

$$k = \frac{2\pi}{L} \quad (3A.2)$$

While in the vertical direction

$$\left. \begin{aligned} u_z &= \frac{Hgk \sinh(k(z+d))}{2\omega \cosh(kd)} \sin(kx - \omega t) \\ \dot{u}_z &= -\frac{2\pi^2 H \sinh(k(z+d))}{T^2 \sinh(kd)} \cos(kx - \omega t) \end{aligned} \right\} \quad (3A.3)$$

2. Stokes Wave Theory

The horizontal water particle velocity and acceleration should satisfy this following equation

$$\left. \begin{aligned} u_x &= \frac{H\pi \cosh(k(z+d))}{T \sinh(kd)} \cos(kx - \omega t) + \frac{3}{4} \left(\frac{H\pi}{T}\right) \left(\frac{H\pi}{L}\right) \frac{\cosh(2k(z+d))}{\sinh^4(kd)} \cos 2(kx - \omega t) \\ \dot{u}_x &= 2 \left(\frac{\pi^2 H}{T^2}\right) \frac{\cosh(k(z+d))}{\sinh(kd)} \sin(kx - \omega t) + 3 \left(\frac{H\pi^2}{T^2}\right) \left(\frac{H\pi}{L}\right) \frac{\cosh(2k(z+d))}{\sinh^4(kd)} \sin 2(kx - \omega t) \end{aligned} \right\} \quad (3A.4)$$

While equation 3A.5 is used to estimate water particle velocity and acceleration in the vertical direction

$$\left. \begin{aligned} u_z &= \frac{H\pi \sinh(k(z+d))}{T \sinh(kd)} \sin(kx - \omega t) + \frac{3}{4} \left(\frac{H\pi}{T}\right) \left(\frac{H\pi}{L}\right) \frac{\sinh(2k(z+d))}{\sinh^4(kd)} \sin 2(kx - \omega t) \\ \dot{u}_z &= -2 \left(\frac{\pi^2 H}{T^2}\right) \frac{\sinh(k(z+d))}{\sinh(kd)} \cos(kx - \omega t) - 3 \left(\frac{H\pi^2}{T^2}\right) \left(\frac{H\pi}{L}\right) \frac{\sinh(2k(z+d))}{\sinh^4(kd)} \cos 2(kx - \omega t) \end{aligned} \right\} \quad (3A.5)$$

3. Solitary Wave Theory

Water particle velocity and acceleration can be approached by Equation 3A.6

$$\left. \begin{aligned} u &= \frac{CN \left[1 + \cos \left(M \left[\frac{z+d}{d} \right] \right) \cdot \cos \left(M \frac{x}{d} \right) \right]}{\left\{ \cos \left(M \left[\frac{z+d}{d} \right] \right) + \cosh \left(M \frac{x}{d} \right) \right\}^2} \\ \dot{u} &= \frac{CN \left[\sin \left(M \left[\frac{z+d}{d} \right] \right) \cdot \sinh \left(M \frac{x}{d} \right) \right]}{\left\{ \cos \left(M \left[\frac{z+d}{d} \right] \right) + \cosh \left(M \frac{x}{d} \right) \right\}^2} \end{aligned} \right\} \quad (3A.6)$$

Where M,N are functions of H/d and

C is speed of solitary wave that can be estimated using

$$C = \sqrt{2g(H + d)} \quad (3A.7)$$

Appendix 3B: Comparison between symmetric and asymmetric copulas

In order to give a full comparison between symmetric and asymmetric copulas, the dependence level between two environmental variables will be varied. For Archimedean copulas used as symmetric copulas, it is very straightforward to be able to specify the desired dependence level as there is a relationship between Kendall's tau and the copula parameter as seen in Table 3.1.

Fig. 3B.1 shows the constructed scatter plots for Clayton copula with different dependence levels. Clayton with $\tau = 0.3$ is very scattered as the dependence level is weak, while specifying $\tau = 0.9$ will result in a more centered scatter plot that shows very strong dependence between two variables.

In order to show the dependence characteristic among symmetric copulas, scatter plots will be constructed by specifying the same dependence level, taken $\tau = 0.7$, for each copula. Fig. 3B.2 shows that Clayton copula will be best used to capture data set exhibiting strong low values dependencies. Gumbel on the other hand, will be best-fitted to characterise strong dependency at high values, while Frank is best used to describe the characteristics of data that possess weak

dependency on both tails. In addition to this, all the Archimedean copulas can be seen to be distributed symmetrically along the diagonal line thus they are appropriate to capture symmetrical dependence among variables. Furthermore, selecting the best-fitted copula for the environmental variable is then very crucial in order to be able to capture the true dependency characteristic for the data pairs.

However, when the pair of the environmental variables shows asymmetric dependence, varying dependence level will not be as easy as on the symmetric case. Unlike symmetric copulas, the constructed asymmetric copulas does not have any exact or explicit relationship between their parameters and the Kendall's tau. There are additional parameters introduced to construct the asymmetric copulas in this chapter. Varying the dependence level (Kendall's tau) will result in changes in all these new introduced parameters. In this chapter, limitation will be made in order to illustrate the impact of varying this dependence level. γ_1 and γ_2 will be set constant so that the variation of Kendall's tau will only impact on the values of θ_{11} and θ_{12} .

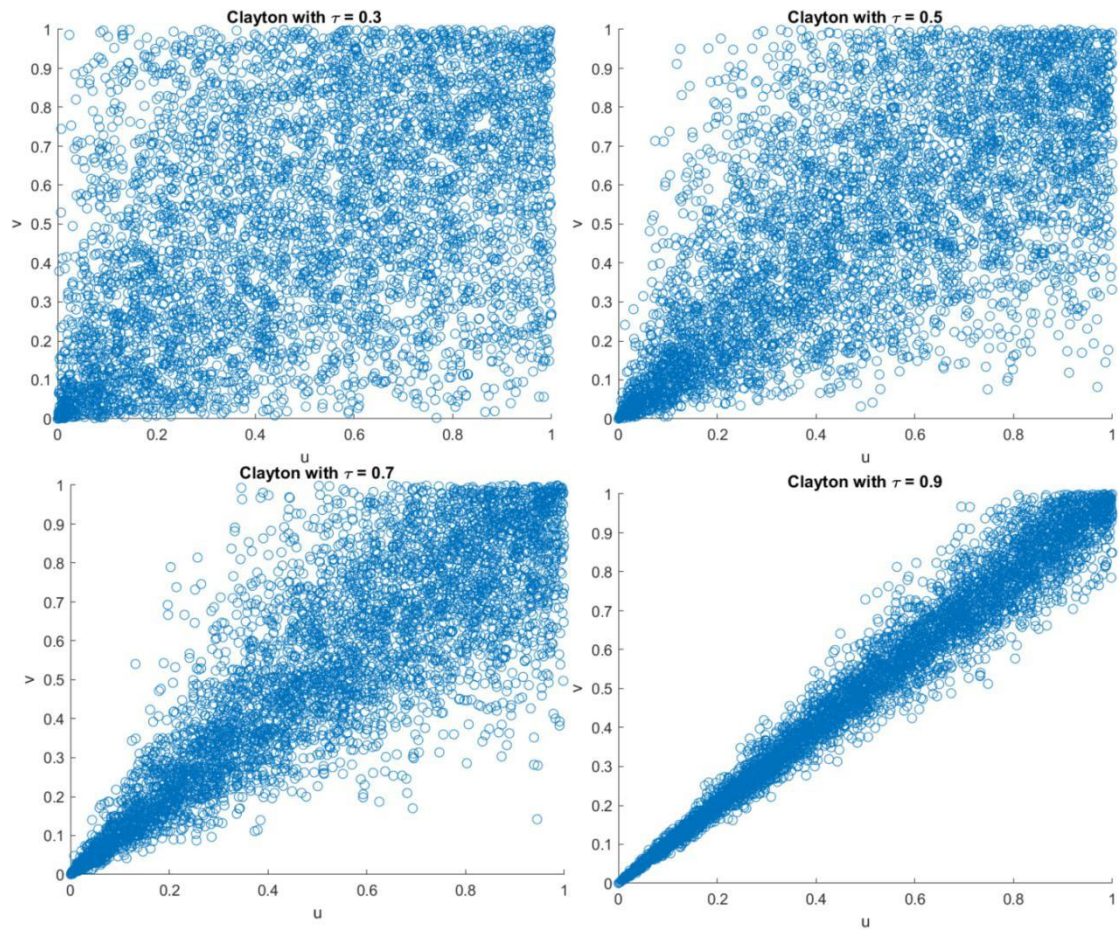


Fig. 3B.1. Clayton copula with various dependence levels

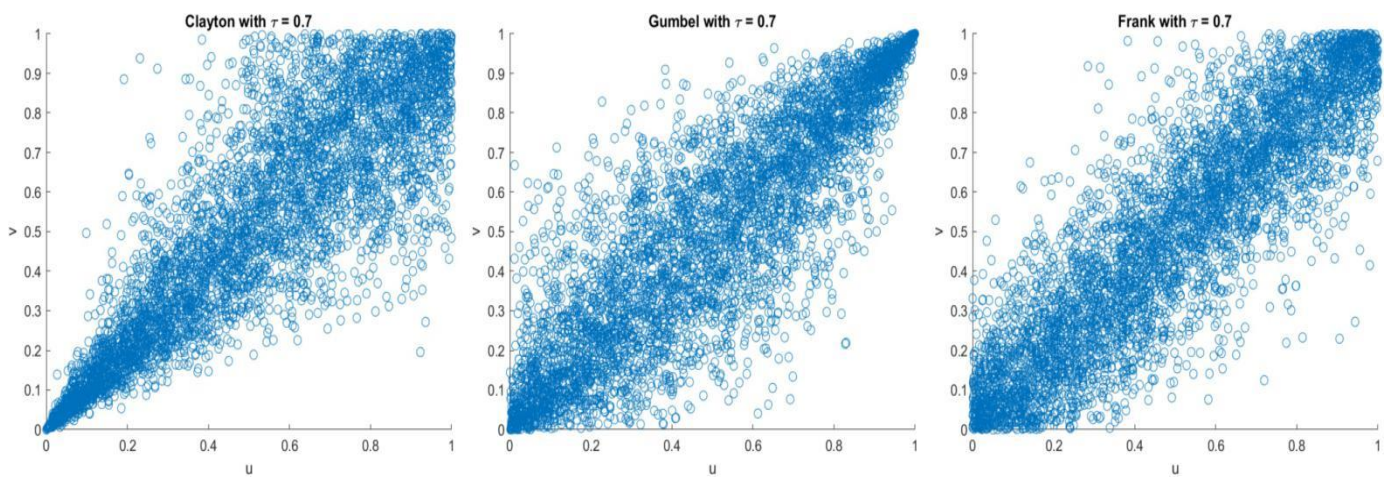


Fig. 3B.2. Symmetric copulas with $\tau = 0.7$

For illustration purpose, asymmetric copulas for wave height and wind speed will be selected to know the relations between the value of Kendall's tau and copula parameter θ_{11} and θ_{12} .

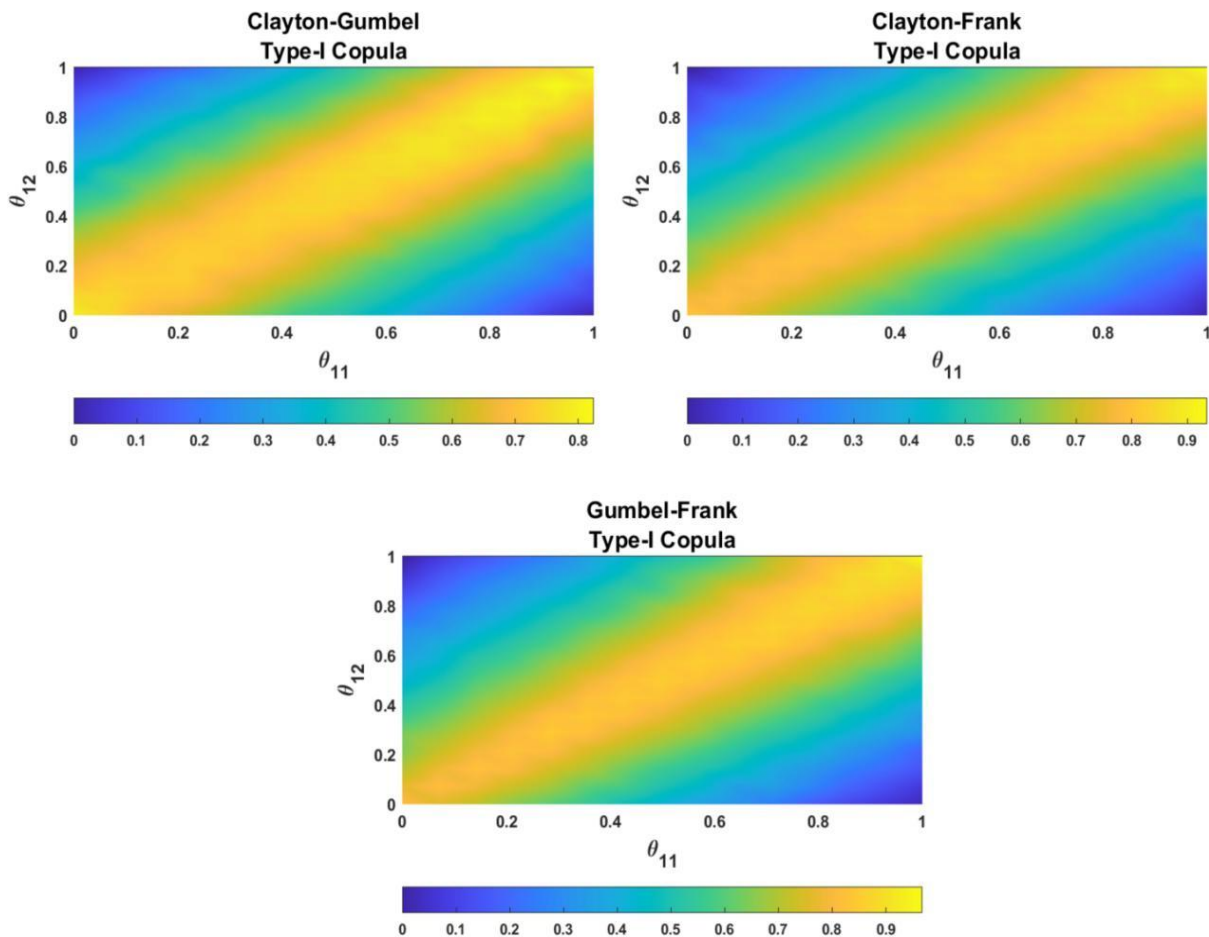


Fig. 3B.3. Plots of the value of Kendall's tau by changing θ_{11} and θ_{12} for a specified data set

Fig. 3B.3 shows that by varying θ_{11} and θ_{12} from 0 to 1, the value of Kendall's tau for this data set applied for wind speed and wave height will change from 0 to around 0.9. These values will change differently according to the assumed γ_1 and γ_2 used in the construction of this Kendall's tau simulation. The maximum kendall's tau value will be obtained if $\theta_{11} = \theta_{12}$. Whereas, dependence between two variables can be neglected if $\theta_{11} = 1$ and $\theta_{12} = 0$, and vice versa. From this simulation, it can be seen that the degree of freedom in the dependence modelling for asymmetric copulas really depends on the characteristic of the data set and the additional copula parameters introduced. The newer copula parameters introduced in the function, the

process to vary dependence level will become more complicated. The comparison of all asymmetric copula functions with a selected Kendall's tau used in this chapter will be illustrated on Fig. 3B.4.

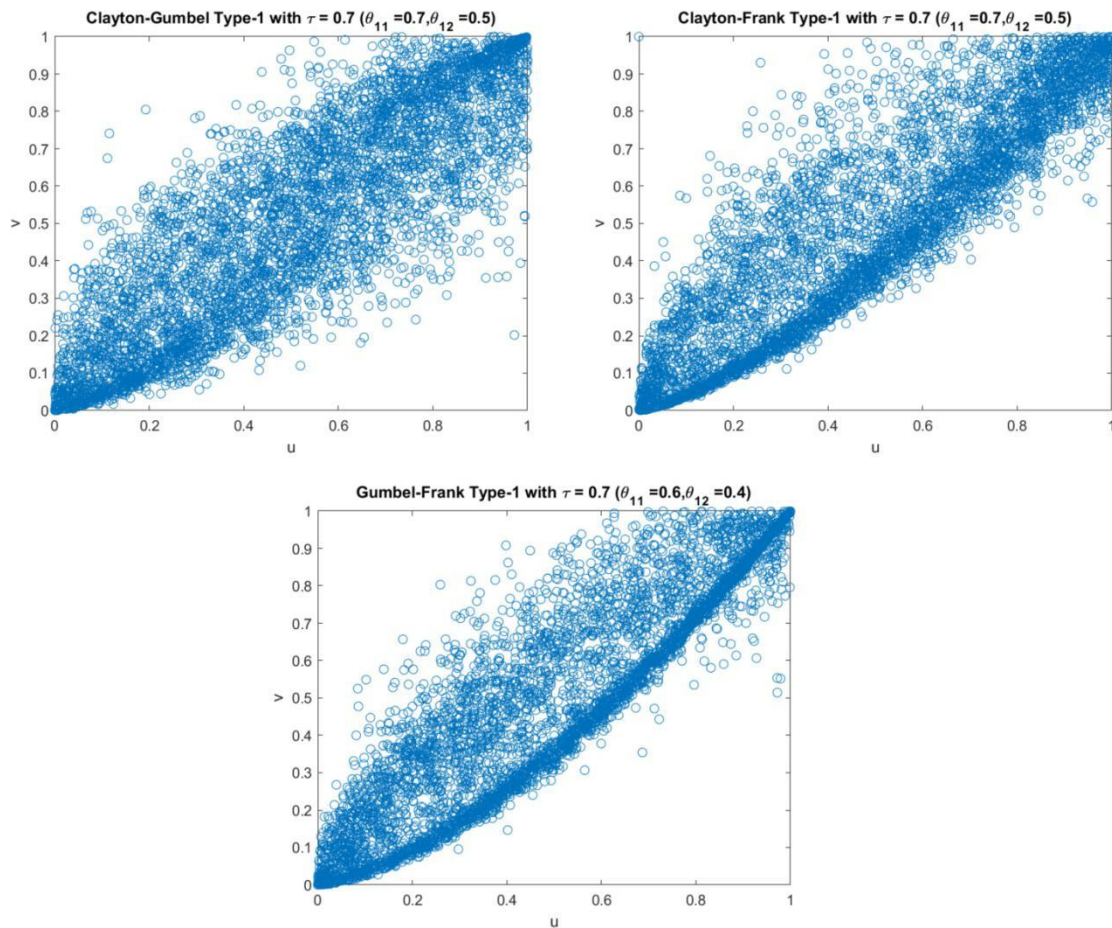


Fig. 3B.4. Asymmetric copulas with $\tau = 0.7$

Compared to Fig. 3B.2, Fig. 3B.4 shows more asymmetrical dependence with the same Kendall's tau value. Thus, by applying some assumptions mentioned previously, the constructed asymmetric copulas can still be used to generate various dependence levels by changing the values of θ_{11} and θ_{12} . However, there has not been any universal guidance on how to really conclude that two variables possess asymmetrical dependence, as also discussed earlier. In addition to this, another uncertainty rises when it comes to the selection of best-fitted

copula for a data set to perform further analysis. All in all, considering asymmetric copula functions in dealing with environmental data has been found very important to capture all possible dependence types. Thus, with these concerns, a simple case study to estimate environmental loads for an offshore installation will be provided using various types of copulas function, both symmetric and asymmetric. This is to give a complete comparison how the selection of a copula function can impact on the estimated environmental load with various dependence levels.

Appendix 3C: Detailed results

The constructed asymmetric copulas for the synthetic data can be seen as follows

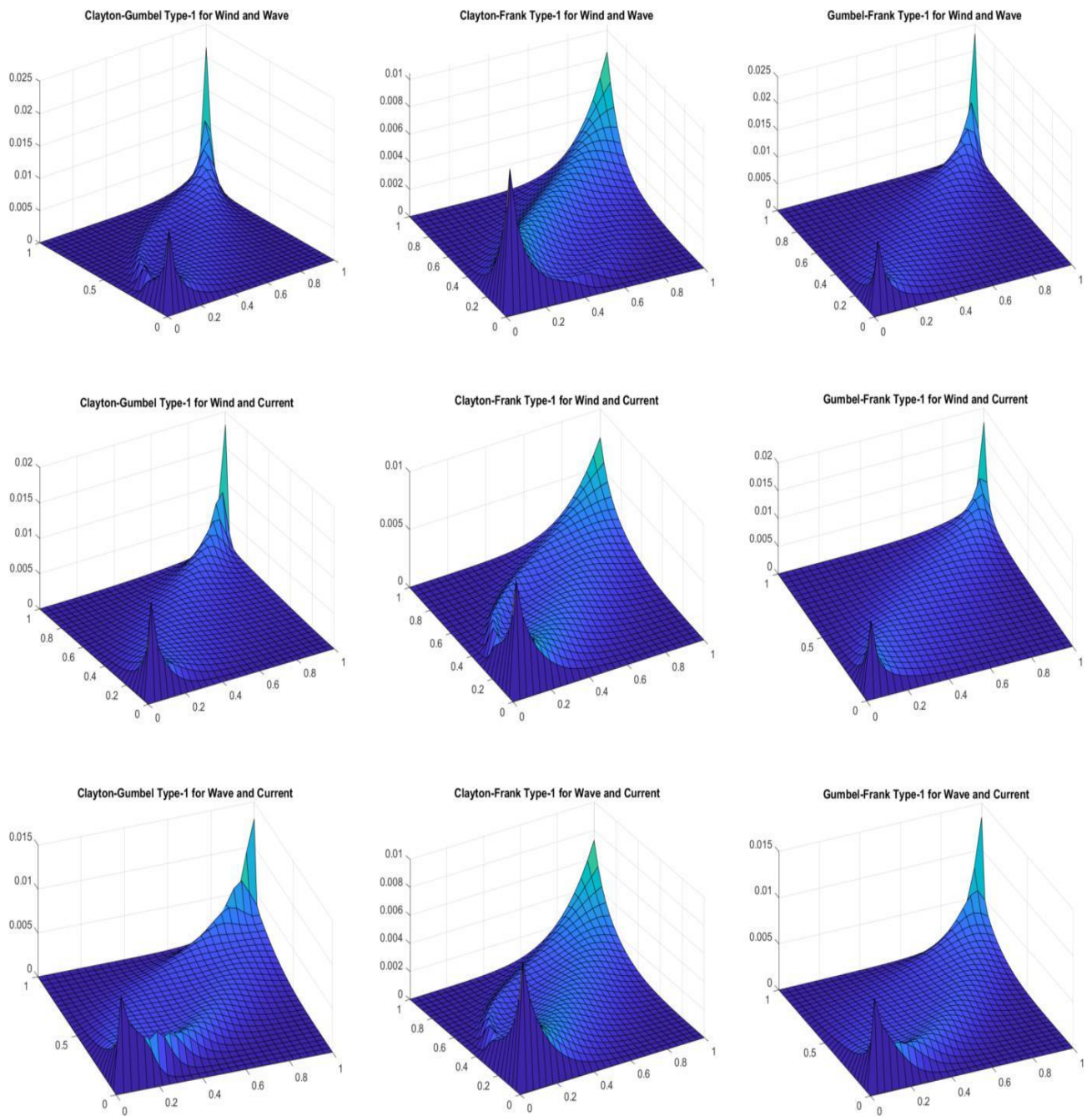


Fig. 3C.1. Probability distribution function of asymmetric copulas for synthetic environment data

While copula parameters for the wind-current and wave-current data pair can be seen on Table 3C.1 and Table 3C.2.

Table 3C.1 Parameters estimates of wind speed and current speed

Copula type	Copula function	Parameter estimate	Mean absolute error
One parameter copula	Clayton	$\gamma = 1.4035$	0.013
	Gumbel	$\gamma = 2.1656$	0.0052
	Frank	$\gamma = 7.0566$	0.118
Asymmetric copulas by product	Clayton-Gumbel Type-I	$\gamma_1 = 6.2068$ $\gamma_2 = 3.155$	0.0033
		$\theta_{11} = 0.449\theta_{12}$ $= 0.2405$	
		$\theta_{21} = 0.551\theta_{22}$ $= 0.7595$	
	Clayton-Frank Type-I	$\gamma_1 = 48.7659\gamma_2$ $= -8.4883$	0.0036
		$\theta_{11} = 0.149\theta_{12}$ $= 0.3747$	
		$\theta_{21} = 0.851\theta_{22}$ $= 0.6253$	
	Gumbel-Frank Type-I	$\gamma_1 = 2.3593\gamma_2$ $= -17.7482$	0.0038
		$\theta_{11} = 0.7011\theta_{12}$ $= 0.5656$	
		$\theta_{21} = 0.2989\theta_{22}$ $= 0.4344$	

Table 3C.2 Parameters estimates of wave height and current speed

Copula type	Copula function	Parameter estimate	Mean absolute error
One parameter copula	Clayton	$\gamma = 1.4734$	0.0138
	Gumbel	$\gamma = 2.1930$	0.0038
	Frank	$\gamma = 7.2175$	0.1186
Asymmetric copulas by product	Clayton-Gumbel Type-I	$\gamma_1 = 10.4446\gamma_2$ $= 3.3543$ $\theta_{11} = 0.7267\theta_{12}$ $= 0.3746$	0.0027

		$\theta_{21} = 0.2733\theta_{22}$ $= 0.6254$	
Clayton-Frank Type-I		$\gamma_1 = 53.8552\gamma_2$ $= -8.3465$	0.0034
		$\theta_{11} = 0.1097\theta_{12}$ $= 0.3431$	
		$\theta_{21} = 0.8903\theta_{22}$ $= 0.6569$	
Gumbel-Frank Type-I		$\gamma_1 = 2.2252\gamma_2$ $= -15.868$	0.0037
		$\theta_{11} = 0.3064\theta_{12}$ $= 0.6266$	
		$\theta_{21} = 0.6936\theta_{22}$ $= 0.3734$	

Total environmental loads estimated using all copula functions are depicted as follows

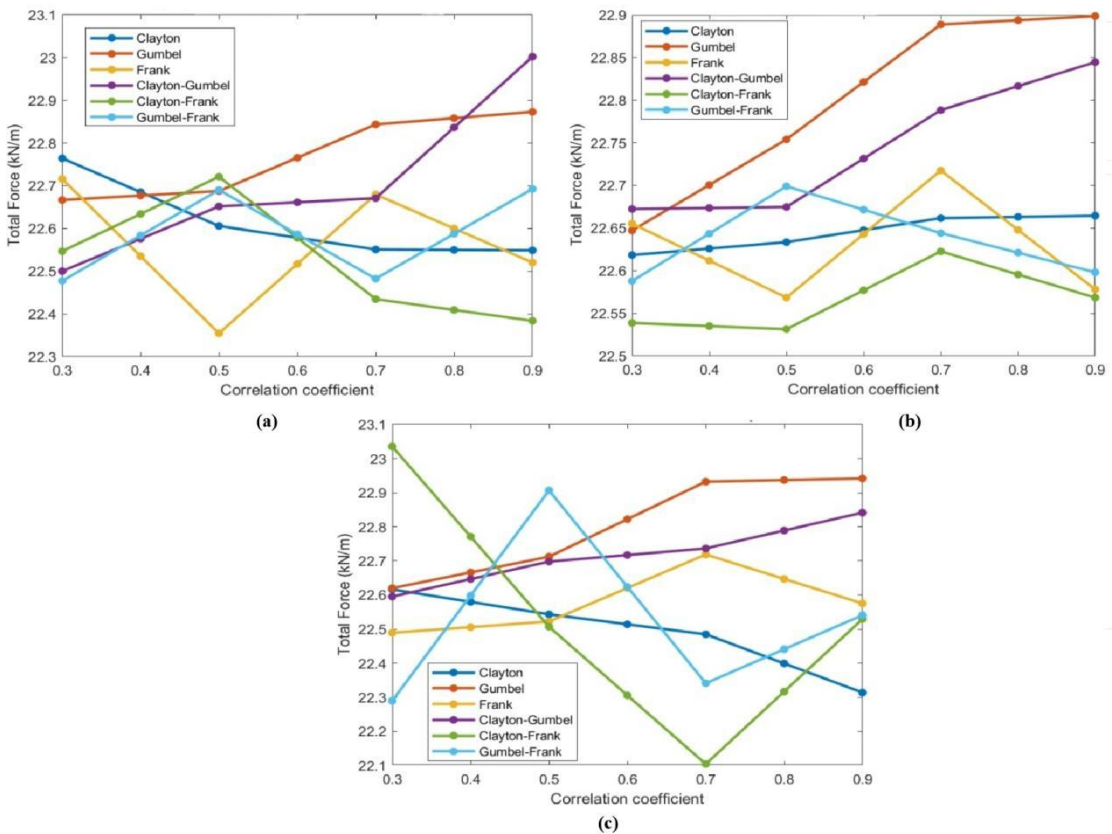


Fig. 3C.2. Total environmental load for (a) wind and wave, (b) wind and current, and (c) wave and current

Table 3C.3 Total loads (kN/m) for correlated wind and wave

Correlation	Clayton	Gumbel	Frank	Clayton-Gumbel	Clayton-Frank	Gumbel-Frank
0.3	22.764	22.667	22.716	22.500	22.547	22.477
0.4	22.685	22.677	22.535	22.576	22.634	22.584
0.5	22.606	22.688	22.355	22.652	22.721	22.690
0.6	22.578	22.766	22.517	22.661	22.578	22.586
0.7	22.551	22.844	22.680	22.671	22.435	22.483
0.8	22.550	22.858	22.600	22.837	22.409	22.588
0.9	22.549	22.873	22.520	23.002	22.384	22.693

Table 3C.4 Total loads (kN/m) for correlated wind and current

Correlation	Clayton	Gumbel	Frank	Clayton-Gumbel	Clayton-Frank	Gumbel-Frank
0.3	22.618	22.647	22.655	22.672	22.539	22.588
0.4	22.626	22.701	22.612	22.674	22.535	22.643
0.5	22.634	22.754	22.568	22.675	22.532	22.699
0.6	22.648	22.821	22.643	22.732	22.577	22.672
0.7	22.662	22.889	22.717	22.788	22.623	22.644
0.8	22.663	22.894	22.648	22.816	22.596	22.621
0.9	22.665	22.899	22.578	22.845	22.568	22.598

Table 3C.5 Total loads (kN/m) for correlated wave and current

Correlation	Clayton	Gumbel	Frank	Clayton-Gumbel	Clayton-Frank	Gumbel-Frank
-------------	---------	--------	-------	----------------	---------------	--------------

0.3	22.616	22.620	22.489	22.595	23.035	22.290
0.4	22.580	22.666	22.506	22.647	22.771	22.598
0.5	22.543	22.712	22.522	22.698	22.507	22.907
0.6	22.514	22.822	22.620	22.717	22.306	22.624
0.7	22.485	22.932	22.719	22.736	22.104	22.341
0.8	22.399	22.937	22.647	22.789	22.317	22.441
0.9	22.314	22.942	22.575	22.841	22.529	22.541

Appendix 3D: MATLAB code for Hilbert transform

```
clear, clc, close all
```

```
data = load('new ori data.txt');
```

```
wind = data(:,1);
```

```
wave = data(:,2);
```

```
curr = data(:,3);
```

```
r = 30; % phase rotation
```

```
r = deg2rad(r);
```

```
wave2 = wind*cos(r) + imag(hilbert(wind))*sin(r);
```

```
wave2 = (wave2 - min(wave2))/(max(wave2) - min(wave2))*(max(wave) - min(wave)) + min(wave);
```

```
corr(wind, wave2)
```

```
r = 70; % phase rotation
```

```
r = deg2rad(r);
```

```
curr2 = wind*cos(r) + imag(hilbert(wind))*sin(r);
```

```
curr2 = (curr2 - min(curr2))/(max(curr2) - min(curr2))*(max(curr) - min(curr)) + min(curr);
```

```
corr(wave2, curr2)
```

```
corr(wind, curr2)
```

```
figure
```

```
plot(wind, wave2, '!')
```

```
figure
```

```
plot(wave2, curr2, '!')
```

```
figure
```

```
subplot(3,1,1)
```

```
plot(wind)
```

```
subplot(3,1,2)
```

```
plot(wave2)
```

```
subplot(3,1,3)
```

```
plot(curr2)
```

CHAPTER 4

RESILIENCE ASSESSMENT OF OFFSHORE STRUCTURES SUBJECTED TO ICE LOAD CONSIDERING COMPLEX DEPENDENCIES

Preface

A version of this chapter has been published in the Reliability Engineering & System Safety journal. As the primary author, I work with my co-authors: Dr. Faisal Khan, Dr. Salim Ahmed, Dr. Bruce Colbourne, and Dr. Mohammed Taleb-Berrouane. I conducted a literature review and developed the conceptual framework for a resilience assessment considering parametric dependence for two correlated variables. I prepared the first manuscript draft and revised the manuscript based on the co-authors' and reviewers' feedback. Co-author Dr. Faisal Khan assisted in the idea formulation, development of the concept, and methodology design, reviewed and edited the manuscript draft, and acted as the corresponding author for the manuscript. Co-authors Dr. Salim Ahmed, Dr. Bruce Colbourne, and Dr. Mohammed Taleb-Berrouane provided valuable support and input in reviewing and revising the manuscript draft. These co-authors also assisted in validating, reviewing, and correcting the model and results.

References:

Ramadhani, A., Khan, F., Colbourne, B., Ahmed, S., Taleb-Berrouane, M., 2022. Resilience assessment of offshore structures subjected to ice load considering complex dependencies. Reliab. Eng. Syst. Saf. 222, 108421. <https://doi.org/10.1016/j.ress.2022.108421>

Abstract

Offshore structures in arctic and subarctic regions are subjected to various natural hazards. These structures need to be designed to withstand these natural hazards and to recover quickly after an undesirable event occurs. Ice load is a significant natural hazard for structures in these regions. The magnitude of ice load depends on the ice drifting velocity, which is influenced by other environmental conditions such as wind speed and wave activity. Most studies in literature assume independence among these influencing environmental parameters, although they have significant dependence. In addition, there are a limited number of studies focused on analyzing the capacities of offshore structures to resist ice loads. This chapter investigates an offshore structure's response to an ice load, using the concept of resilience. Resilience is quantified by considering absorptive, adaptive, and restorative capacities. Dependence between wind velocity and wave height is considered in the analysis; the Gumbel-Frank Type-1 Copula function is used to model relationships between these influencing variables. The study highlights that a mono-pile vertical structure shows resilience in terms of absorptive capacity. An offshore structure in arctic conditions needs to be designed considering both absorptive and adaptive capacities.

Keywords: Offshore structure; resilience assessment; copula functions; iceberg load; absorptive capacity; absorptive capacity

4.1 Introduction

Climate change has made offshore structures suffer more frequently from extreme natural hazards. These extreme environmental events can cause catastrophic failures if offshore structures are not designed to withstand such events (Stochino et al., 2019). In addition, a number of offshore structures in Canada have been built and operated in arctic and sub-arctic

regions (Ning et al., 2019). These structures are subject to increased natural hazards, particularly from sea ice. Sea ice damage is a significant threat to the safety of offshore structures and can cause severe consequences (Xu et al., 2020). In practice, these consequences can vary from ice-induced vibration that can lead to fatigue, to bending failures of local structural elements, to total structure collapse. These undesired events can cause losses if they are not considered as part of both design and operation (Taleb-Berrouane & Khan, 2018; Taleb-Berrouane & Lounis, 2016; Zarei, Khan, et al., 2021). Thus, considering the effects of natural hazards to ensure safety of people and to avoid losses in the offshore industry is important. A robust approach is required to design safe structures that are able to resist failures and able to recover quickly if unwanted events occur (Deyab et al., 2018; Sarwar et al., 2018; Taleb-berrouane et al., 2018).

Modelling sea ice loads has been found to be more complex compared to modelling other environmental effects (Ning et al., 2019). This is due to the combined influence of complex environmental conditions and sea ice physical properties. The most common ice hazard is drifting sea ice. This drifting ice is influenced by the combination of wind and wave forces acting on the ice itself (Sinsabvarodom et al., 2020). Furthermore, there are different ice types such as pack ice, bergy bits, and icebergs, classified depending on their shapes, masses and dimensions (Colbourne, 2000; Zhou et al., 2019). Despite these general classifications, specific data on sea ice parameters are not publicly available; this is another challenge for research seeking to quantify ice loads.

There are two main ice failure mechanisms arising from structural interactions; crushing mode and flexural mode (Sinsabvarodom et al., 2020). Crushing mode is dominantly found in interactions with vertical structures, while flexural mode is induced in sheet ice by interactions with sloping structures.

There are several uncertainties that exist when dealing with modelling ice load for offshore structures. In practice, engineering models are affected by two types of uncertainties: aleatory and epistemic (Cheng et al., 2019; De Michele et al., 2007; McKeand et al., 2021; Reilly et al., 2021; Tabandeh et al., 2022; Zhang et al., 2018). Aleatory uncertainties are the inherent randomness in a system's properties, while epistemic uncertainties are caused by lack of knowledge about a system (Chen et al., 2021). Castaldo et al., (2019) also mention that providing better estimation in considering uncertainties can result in a better accuracy in estimation of structural behaviors. These two uncertainties usually exist simultaneously in engineering applications. Epistemic uncertainties can be reduced by updating and collecting more information about a system, while aleatory uncertainties cannot be treated by just gathering more information. The epistemic uncertainty that is most commonly neglected is the existence of dependence among the investigated variables (Kiureghian & Ditlevsen, 2009). The assumption of independence between environmental conditions has been identified as a factor that should be eliminated (Li et al., 2020). As an illustrative example, ice drift is caused by both wind and wave load acting on the sea ice. This drifting ice then induces dynamic loading on a structure (Shi et al., 2016). The relationship between wind and wave is also normally that the wave height is dependent on the wind (Zhang et al., 2018, 2019). In this example, assuming independence in load estimation will generally result in less accurate predictions of loads experienced in the field.

In this study two types of dependence, symmetrical and asymmetrical, will be assessed. Copula functions are introduced to model both types of dependence. Copula functions are proven to be suitable for modelling the effects of natural hazards on infrastructure in both offshore (Dong et al., 2017; Ramadhani et al., 2021; Zhang et al., 2015, 2018) and onshore structures (Bai et al., 2016; Desilver, 2020; Fang et al., 2020; Li et al., 2021; Taleb-Berrouane et al., 2019; Zhang & Lam, 2015).

The example interaction scenario used in this research is a single vertical steel pile interacting with an iceberg. This provides a relatively simple ice-structure interaction that is used to demonstrate the analysis. Mechanical response of the system is usually used as a basis for assessing structural safety. Mechanical properties of the selected structure contribute to the existence of aleatory uncertainties. Probability theories are usually used to model aleatory uncertainties (Zarghami & Dumrak, 2021). To consider the aleatory uncertainties on the mechanical properties of the structural system, different safety formats should be investigated to estimate the capacities of the system (Castaldo et al., 2019). Different safety formats can have different material properties values. Probabilistic methods (PM) should also be considered as they are able to capture variations in the mechanical behaviors of the structural system. A combination of material properties can be assessed in the model so that aleatory uncertainties are taken into account (Castaldo et al., 2019).

The concept of resilience is introduced, where resilience is the ability of a system to withstand the occurrence of unwanted events and the ability to restore the system function (Genest, Gendron, et al., 2009; Hashemi et al., 2015; Vanem, 2016; Zarei, Ramavandi, et al., 2021). As complex systems operating in harsh environments, offshore structures are vulnerable to various hazards and high levels of functional unpredictability during their operation lifetimes (Bucelli et al., 2018). To maintain their operability, offshore structures need to maintain high levels of structural reliability to withstand hazards that can cause disruption. Resilience in offshore safety then plays an important role in avoiding catastrophic outcomes due to both natural and man-made extreme events. Resilience also ensures offshore structures maintain their performance after a disruptive event. Impact from a drifting iceberg will affect the resilience of a structure. There have been several past studies on resilience assessment of structures. However, studies on the resilience of structures subjected to ice load have not been publicly reported. Most resilience assessment for natural hazards is focused on bridges, houses or

commercial buildings under wind, or seismic loads (Xu et al., 2020). Cai et al. (2021) developed a novel resilience evaluation methodology that combined a Markov model and dynamic Bayesian networks. They concluded that the assessment of a system's ability to absorb external disruptive events was improved. Cheng et al. (2021) and Kammouh et al. (2020) used Bayesian Networks to develop a resilience model. Kammouh et al. (2020) concluded that a Bayesian network can handle both static and dynamic systems and assist in evaluating resilience. While Cheng et al. (2021) concluded that the model was effective for multi hazards scenario. Francis & Bekera (2014) provided a resilience framework and literature review for civil infrastructure. They introduced management activities and socio-ecological aspects in their framework. Stochino et al. (2019) assessed resilience of a bridge subject to earthquake load. They studied absorptive, restorative and adaptive capacities using structural-based approaches and evaluated system performance. Qeshta et al. (2019) provided a resilience assessment of bridges under wave forces. They concluded that their existing model for assessing resilience can be expanded to account for more hazards. Poulin & Kane (2021) developed infrastructure resilience curves by providing a common vocabulary for both practitioners and researchers to design and assess infrastructure resilience. Zhang et al. (2021) divided resilience evaluation into degradation process and recovery process. The assessment methodology for resilience was a combination of a finite element method and a dynamic Bayesian network. The quantification of resilience in energy systems was also attempted in many recent publications. Examples include Chen et al., (2021); Senkel et al., (2021); Zeng et al., (2021).

Ning et al. (2019) and Xu et al. (2020) developed a matrix-based resilience quantification for offshore platforms considering many types of structural failure mechanisms. Resilience assessment has also been studied in the nuclear industry. Carvalho et al. (2008) proposed a framework to analyze micro incidents during nuclear power plant operations. The framework

provides a mechanism for systemic and critical analysis to assess resilience of socio-technical critical systems. Kim et al. (2018) proposed a resilience model for nuclear power plant based on the Model of Resilience in Situation. Statistical analysis was performed to examine the relations in the resilience models and to validate the developed quantitative model. The method provided a new approach for safety assessment of nuclear power plants. Bhattacharya & Goda (2016) considered the addition of an offshore wind farm to increase seismic resilience of nuclear power plants. Based on their brief study, the existence of a wind farm can provide emergency backup power to a nuclear power plant so that it can avoid catastrophic consequences. For wind power plants, Afgan & Cvetinovic (2010) developed a resilience index that can be used as a diagnostic tool to assess potential hazards. Qin & Faber (2019) proposed a novel resilience analysis of wind turbine parks to optimize the decisions on asset integrity management. Resilience performance characteristics of a wind energy park were quantified to help identify priority in the ranking of decision alternatives. Dui et al. (2021) investigated resilience of maritime transport systems based on the minimum residual optimization model. This model could provide valuable information to guide the recovery process. Hu et al. (2021) developed a framework to assess marine LNG offloading systems based on an Infrastructure Resilience-oriented Modelling Language (IRML). Abaei et al. (2022) developed a machine learning-based model to assess resilience of an unattended machinery plant (UMP). The framework provides important information to evaluate uncertainties and predict events that cause increased risk in marine engine rooms.

Zhang et al. (2018) quantified resilience of a large and complex metro network by calculating a vulnerability and recovery rate using unifying metrics and model. Yin et al. (2022) developed a hybrid knowledge-based and data-driven approach to quantify resilience of urban rail systems. This approach was able to prioritize a maintenance task that could eventually improve the system's resilience. Yodo & Wang (2016) developed a general framework to quantify

resilience based on Bayesian Networks (BNs). This framework was implemented for an electric motor supply chain system and concluded that the BN (Kabir et al., 2019; Taleb-Berrouane et al., 2017; Zarei et al., 2022) contributed to better prediction of the overall resilience of a system. Taleb-Berrouane and Khan, 2019 (Dawuda et al., 2021; Taleb-Berrouane, Khan, Eckert, et al., 2019; Taleb-Berrouane et al., 2021; Taleb-berrrouane, 2019) (Kamil et al., 2019; M. Taleb-Berrouane, Khan, & Kamil, 2019; Talebberrouane et al., 2016) assessed the resilience of pipeline systems against microbiologically-influenced corrosion using Petri-nets. Yang et al. (2020) and Taleb-Berrouane et al. (2020) proposed a combination of Petri-nets and Bayesian networks present dependencies between influencing factors Joyce et al. (2018) assessed the resilience of bridges under combinations of loads caused by flooding. In this work, risk was defined as the product of hazard and vulnerability, where vulnerability is defined as the product of exposure, sensitivity, and resilience. In addition to this, time-variant reliability of a structure is incorporated into the resilience model. Qian et al. (2021) developed a time-variant reliability method based on a multiple response Gaussian process and subset simulation for a small failure probability problem. This method was effective for both low and high dimensional problems. Bhardwaj et al. (2022) used a Bayesian network probabilistic approach to quantify reliability of two conceptual subsea processing systems. Yang et al. (2022) developed a novel reliability approach based on a Gamma stochastic resistance degradation model. The method combined a spatial degradation and a non-stationary degradation process for an aging structure. Cao et al. (2022) and Wang et al. (2021) used a single-loop reliability analysis approach based on the Kriging model to deal with time-dependent reliability problems. Castaldo et al. (2017) implemented a computational probabilistic approach to estimate the time-variant reliability and expected lifetime of a deteriorating reinforced concrete bridge subjected to chloride-induced corrosion. This approach was able to provide optimal time intervals for maintenance activities to extend the bridge's lifetime. Structural reliability of offshore structures subjected to time

varying environments were also studied and the work demonstrated that the time-variant reliability approach provided better understanding in capturing the failure probability of the structures (Bai et al., 2016; Idris et al., 2017; Kim et al., 2014; Wang et al., 2022; X.-Y. Zhang et al., 2021; Zhang & Lam, 2015; Zuniga et al., 2021). Furthermore, in order to consider dependence between variables, (Guo et al., 2019; Joyce et al., 2018; Li & Zhang, 2020; Liu & Chen, 2020; Lü et al., 2020; Wang et al., 2018; Yoo & Cho, 2018) incorporated copula functions in their resilience quantification. However, the quantification of resilience of an offshore structure subjected to ice loading remains a challenging and less explored research topic.

This chapter provides an implementation of a more robust approach to assess resilience of a structure subject to an iceberg load. As a data-driven approach, it relies on recorded historical data to represent environmental condition from a field (Seghier et al., 2021; Kamil et al., 2021). Correlated wind and wave data are generated using copula functions to eliminate the independence assumption in the estimate of the drifting velocity of an iceberg.

The remainder of this chapter is organized as follows. Section 4.2 presents the proposed methodology and the basic theories used in developing the methodology. Application of copula models is discussed in Section 4.3. Results and discussion from the estimation of iceberg load and structural resilience quantification are presented in Section 4.4. The concluding remarks of this chapter are presented in Section 4.5.

4.2 Research Methodology

The methodology used to assess the resilience of an offshore structure subject to iceberg collision is illustrated in Fig. 4.1. Correlated environmental parameters are generated using Copula functions. The iceberg collision force is estimated by assuming wind speed and wave height are dependent.

4.2.1 Copula-based dependence model

A copula is used to construct multivariate distribution by joining or ‘coupling’ univariate marginal distributions. A copula is advantageous as it is possible to construct a multivariate distribution from different marginal distributions. The definition of copula was introduced in Sklar’s Theorem (Nelsen, 2006).

Let H be an n -dimensional distribution function with marginal distribution F_1, F_2, \dots, F_n , then there exists a copula C such that.

$$H(x_1, x_2, \dots, x_n) = C(F_1(x_1), F_2(x_2), \dots, F_n(x_n)) \quad (4.1)$$

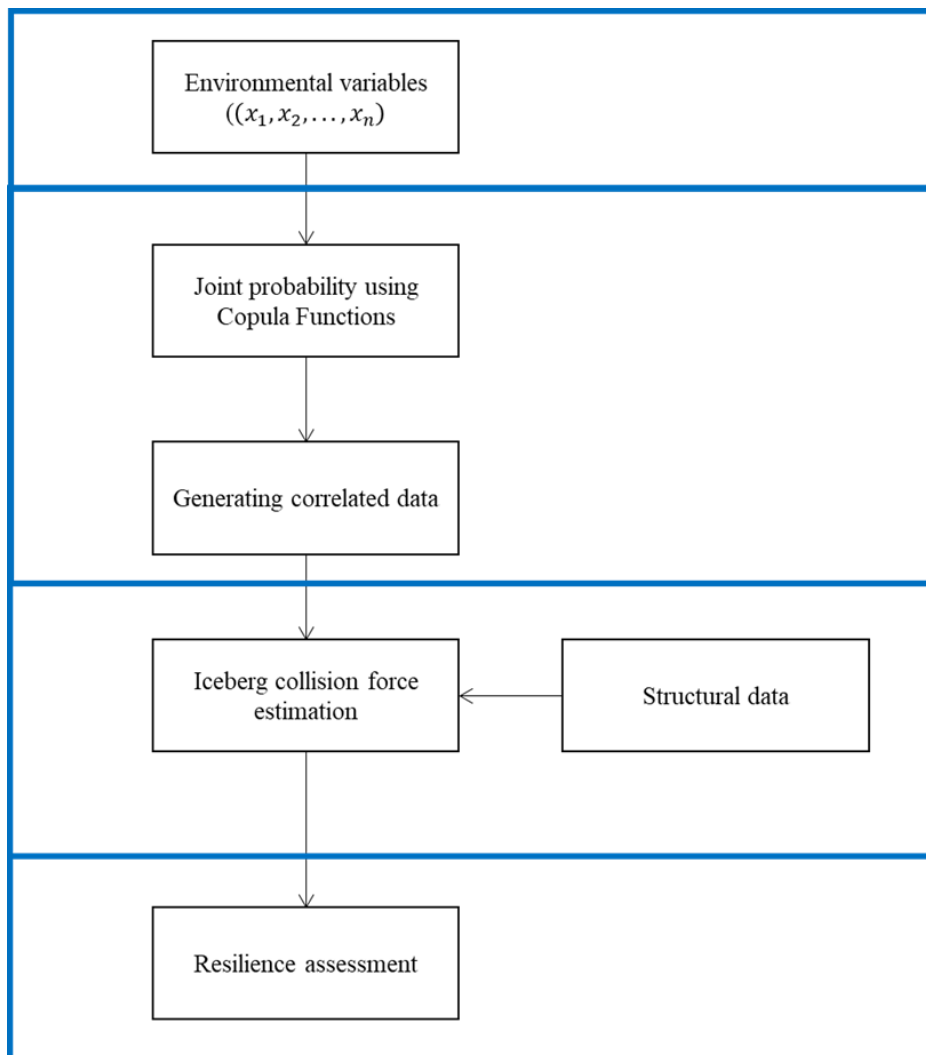


Fig. 4.1. General framework for copula-based resilience assessment

Based on Sklar's Theorem, it can be seen that a copula model does not consider the characteristic of the univariate marginal distributions in the multivariate model, as the copula model is a multivariate model for the original variables, after being transformed into a cumulative distribution function with a uniform distribution function (Zhang et al., 2018). A marine environment is a complex system with many natural factors arising from the ocean and atmosphere. Ocean parameters have uncertainties due to their complex dependencies. One of the most challenging tasks when modelling these systems is to understand the nonlinear and asymmetric dependencies that exist between ocean parameters. These complex dependencies between ocean parameters need to be captured, especially when used to assess the performance of an offshore structure. Zhang et al. (2015) provided a comparison of approaches to conditional joint probability to model ocean parameters using the Nataf transformation and copula functions. Copula functions were shown to better describe the nonlinear dependencies between ocean parameters. Dong et al. (2017) also mentioned that copula functions were able to better present a joint design value between two ocean parameters. Considering these findings, the use of copula functions to model ocean parameters should provide a better approach and interpretation. Copula functions are also able to be incorporated into other modelling tools as mentioned in the previous section.

In this chapter, the Archimedean copula family and asymmetric copula functions were used to model the environmental parameters. Ramadhani et al., (2021) discussed the advantages of copula functions for modelling environmental parameters and the construction of asymmetric copula functions. Asymmetric copulas are constructed by applying the product rule. This rule is implemented by introducing individual functions and the selection of base copulas. In this work Archimedean copulas are selected, as discussed in our previous work (Ramadhani et al., 2021). Fig. 4.2 shows the overall framework used to identify a joint probability distribution

between two environmental parameters using copula functions. Table 4.1 shows the equations needed to perform copula modelling.

Table 4.1 Equations used in copula modelling

Method	Equation	Parameter description	References
Data transformation	$U_i = \frac{R_i}{n+1} = \frac{nF_i(X_i)}{n+1} \quad (4.2)$ <p>where,</p> $\hat{F}_i(t) = \sum_{i=1}^n \frac{1}{n} (X_i \leq t) \quad (4.3)$	<p>n : the number of data X_i: observed data R_i: ranking of the data</p>	(Genest, Rémillard, et al., 2009)
Dependence measurement	<p>Linear Pearson correlation:</p> $\rho(X, Y) = \frac{Cov(X, Y)}{\sqrt{Var(X)}\sqrt{Var(Y)}} \quad (4.4)$ <p>Spearman's rho (ρ_s)</p> $\rho_s = 12 \iint uv dC(u, v) - 3 \quad (4.5)$ <p>Kendall's tau (τ)</p> $\tau = 4 \int C(u, v) dC(u, v) - 1 \quad (4.6)$	<p>X, Y: Observed data u, v: transformed data in copula domain</p>	<p>(Yi Zhang et al., 2018)</p> <p>(Hashemi et al., 2015)</p> <p>(Nelsen, 2006)</p>
Asymmetry test	$\eta_\infty(C) = \sup_{(u_1, u_2) \in [0, 1]^2} C(u_1, u_2) - C(u_2, u_1) \quad (4.7)$		(Bang Huseby et al., 2013; Durante & Salvadori, 2009; D.

Method	Equation	Parameter description	References
			Zhang et al., 2018; Yi Zhang et al., 2019)
Individual function	$g_{ji}(v) = v^{\theta_{ji}} \text{ for } j = 1, \dots, k, \quad (4.8)$	$\theta_{ji} \in [0,1]$ $\sum_{j=1}^k \theta_{ji} = 1$	(Liebscher, 2008)
Loglikelihood estimation	$L(\theta) = \sum_{i=1}^N \text{ln}c(u_1, u_2; \theta) \quad (4.9)$	θ : estimated parameter $L(\theta)$: loglikelihood function	(Lü et al., 2020)
	$\hat{\theta} = \text{argmax}L(\theta) \quad (4.10)$		
Akaike Information Criterion (AIC)	$AIC = -2L(\hat{\theta}) + 2k = -2 \sum_{i=1}^N \text{ln}c(u_{1i}, u_{2i}; \hat{\theta}) + 2k \quad (4.11)$	k: the number of estimated parameter	(D. Li & Tang, 2014; Lü et al., 2020)

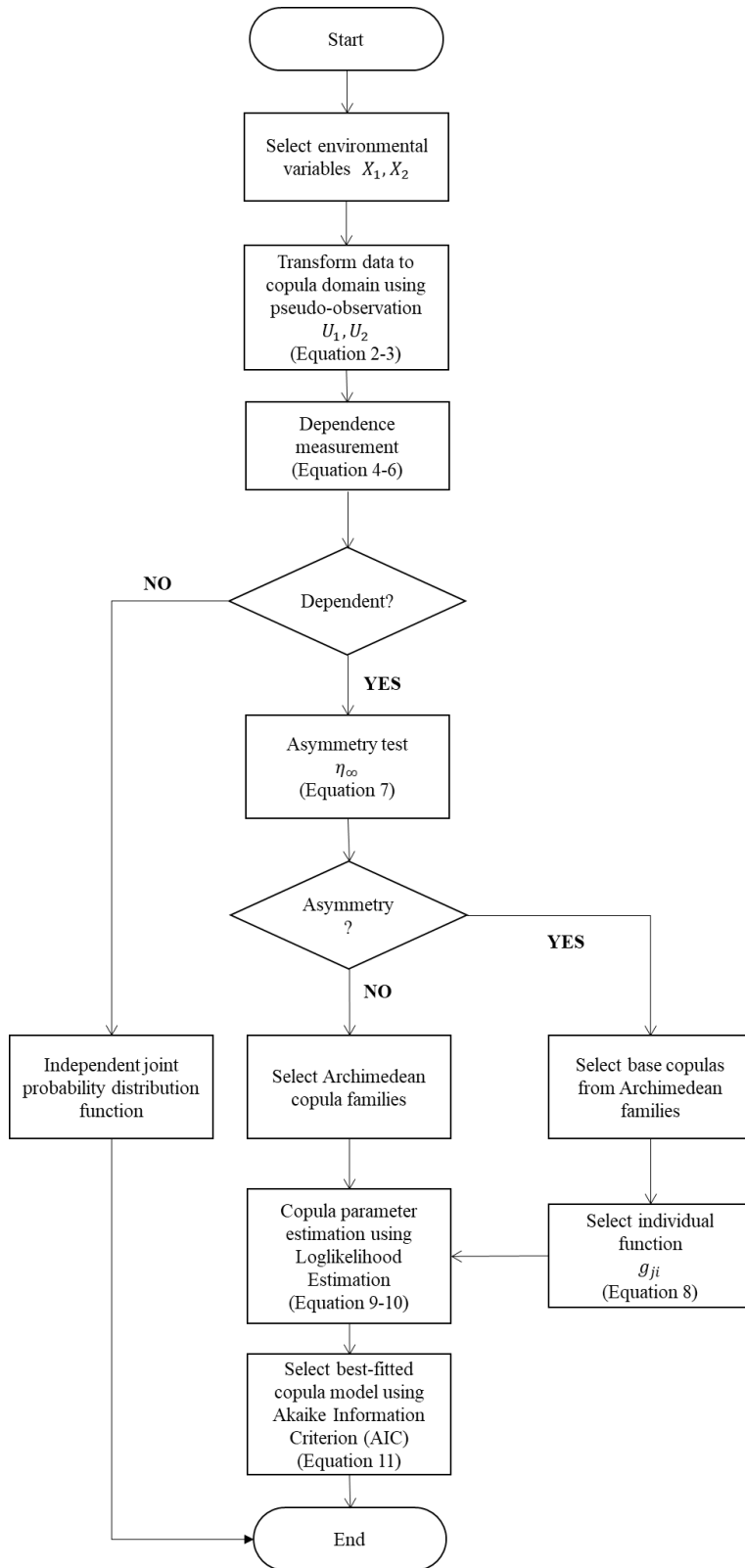


Fig. 4.2. Framework for copula modelling

4.2.2 Iceberg collision force

Ice load is usually the most significant uncertainty for structural design in arctic regions. The main challenge is in identifying appropriate ice conditions such as ice concentration, ice thickness, ice drift, ridges, etc. for pack ice or berg occurrence and berg size for icebergs. In either case ice strength properties also need to be estimated. Structural performance under ice load is usually estimated for several possible ice failure mechanisms such as ice crushing, bending and buckling. The interaction between the failing ice and the structure is then analyzed. Modelling the dynamic interaction between moving ice and a stationary structure is a complex process. Ice load for crushing scenarios is estimated by multiplying a nominal contact area and the nominal ice-induced pressure (Thijssen et al., 2014). In this chapter, an iceberg collision leading to a pure ice crushing failure scenario is taken as the example case.

In cases where the ice is a continuous sheet, and the interaction occurs over an extended period of time, a fundamental mode of vibration is usually assumed as the basic response of a structure. Specifically, there are three different ways for a vertical structure to respond against the advancing crushing ice: intermittent crushing, frequency lock-in and continuous brittle crushing (Hoek, 2021). Intermittent crushing is developed when low ice velocities are present and causes structure to possibly vibrate around its equilibrium position. If ice velocities are slightly higher, frequency lock-in can be developed that causes structural vibrations limited only by the damping in the system. This response can cause structural fatigue due to many repetitions that can occur. Continuous brittle crushing is developed under higher ice velocities that can result in induced forces on the structure that are relatively low.

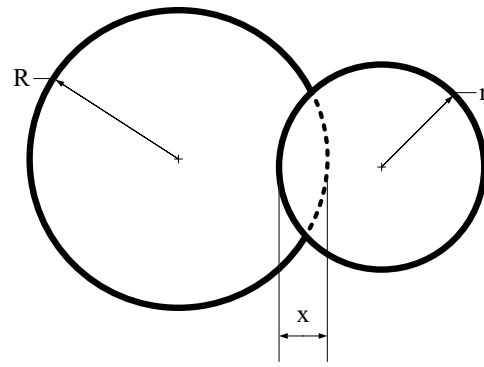
Since a single-impact iceberg interaction is assumed in this chapter, iceberg drift velocity is expected to be low and there is no potential for continuous structural vibration. The ice force acting on the structure is assumed to vary linearly and elastically along with the deformation of the ice until it stops (Venturella et al., 2011).

Iceberg load on a structure is estimated using an energy balance where the initial kinetic energy of the iceberg is equated to the energy dissipated through ice failure (Foschi et al., 1996). The iceberg will stop when its kinetic energy is dissipated through ice crushing and structural deformation. The iceberg in this chapter is assumed to be circular in plane and ellipsoidal in elevation as shown in Fig. 4.3. Although iceberg shape in real life is complex, iceberg characterization is generally represented by the water line length, L . This variable is commonly cited in the literature (Fuglem et al., 1996). The offshore structure here is also assumed to have a simple shape, represented by a single vertical cylindrical member.

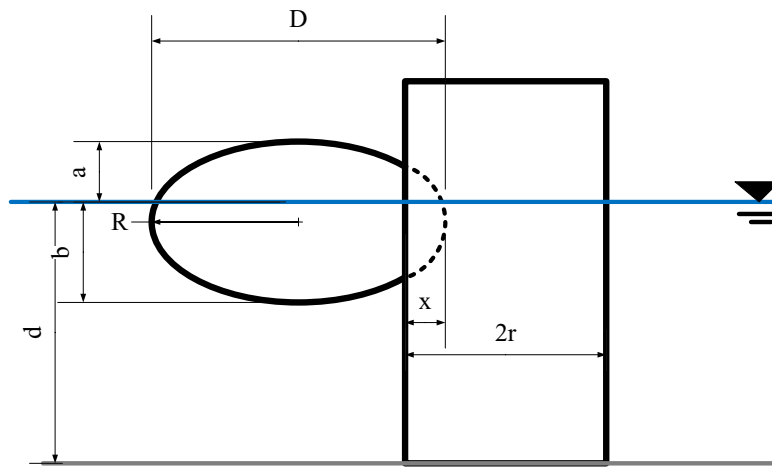
The iceberg collision force acting on the structure is estimated by considering the presence of wind and waves. The iceberg force on the structure, $F(x)$ can be estimated using a linearized equation, assuming iceberg will be stopped at a value of x .

$$F(x) = Kx \quad (4.12)$$

Where K is the slope of the force-penetration relationship (Foschi et al., 1996)



(a)



(b)

Fig. 4.3. Sketch of iceberg-structure interaction geometry from (a) top view and (b) side view

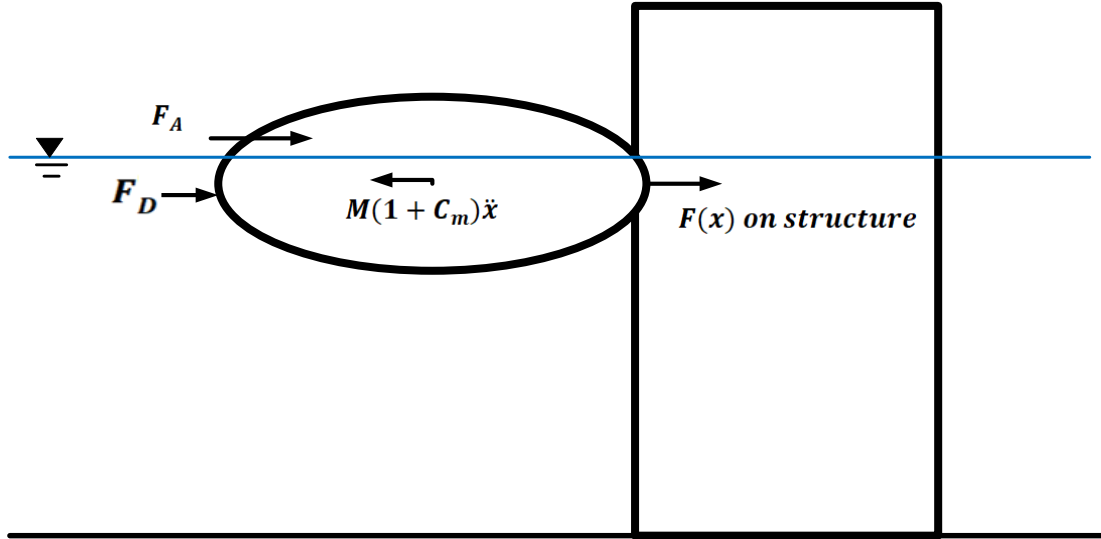


Fig. 4.4. Sketch of dynamic equilibrium between iceberg and structure induced by wave and wind force

Penetration of the iceberg can be estimated using the dynamic equilibrium of the iceberg as shown in Fig. 4.4, where iceberg drift is assumed to be influenced by wave and wind forces (Foschi et al., 1996).

$$M(1 + C_m)\ddot{x} = -F(x) + F_D + F_A \quad (4.13)$$

Where F_A is the wind force, and M is the mass of the iceberg. Equation 4.13 is set with initial conditions when $x = 0$ and $\dot{x} = V$ at $t = 0$. V is the drift velocity of the iceberg induced by the wind and wave drift forces. Wave drift force is then estimated using (Fuglem et al., 1996)

$$F_D = \frac{1}{2} C_D \rho_w g D_1 H^2 \quad (4.14)$$

Where,

C_D is the wave drift coefficient for the given iceberg shape

ρ_w is the density of water (kg/m^3)

g is the acceleration due to gravity (m/s^2)

D_1 is a characteristic dimension of the iceberg (m)

H is the regular wave height (m)

When applying the wave drift model, a spherical iceberg shape is assumed so D_1 is set to be the water line length L .

Ice drift velocity (V) is affected by the combination of wind, wave and current. First, the combined wind and wave force on the iceberg is investigated. Then the velocity of the iceberg relative to the current speed is estimated so that the water drag force is in equilibrium with the wind and wave drift force.

To calculate the velocity of water (U_w), it assumed that wind drag force (F_A) and wave force (F_D) act in the same direction. The drift velocity of the iceberg is the sum of U_w and the current velocity (U_C)

$$V_i = U_w + U_C \quad (4.15)$$

U_w can be calculated by setting the water drag force ($F_w = F_A + F_D$) (Fuglem et al., 1996)

The wind drag force was calculated as (Fuglem et al., 1996)

$$F_A = \frac{1}{2} C_A \rho_A A_A U_A^2 \quad (4.16)$$

Where,

C_A is the wind drag coefficient for the given iceberg shape

ρ_A is the density of air (kg/m^3)

A_A is the projected area of the iceberg perpendicular to the wind direction (m^2)

U_A is the wind velocity (m/s)

A_A can be estimated as the mean above water projected area ($0.115 L^2$); L is the water line length, and C_A can be taken as 1.0.

The water drag force is calculated using (Fuglem et al., 1996)

$$F_w = \frac{1}{2} C_w \rho_w A_B U_w^2 \quad (4.17)$$

Where,

C_w is the water drag coefficient for the given iceberg shape (assumed to be 1)

ρ_w is the density of water (kg/m^3)

A_B is the below water projected area (m^2) of the iceberg perpendicular to its direction of movement relative to the water. It is usually taken as $0.612L^2$

U_w is the velocity of the water relative to the iceberg (m/s)

4.2.3 The concept of resilience assessment

Resilience has been defined in various ways. It is the ability of a system to withstand adverse conditions and to recover quickly (Sarwar et al., 2018). (Yodo & Wang, 2016) defined resilience as a systems' ability to autonomously recover from a disruptive event or adjust easily to changes. (Aven, 2011; Ayyub, 2015) provided a general definition; resilience is the ability of a system to prepare and adapt to changing conditions and to withstand and recover from disruptive events. From this definition, (M Taleb-Berrouane & Khan, 2019) then defined resilience of a process system as its ability to cope with disruptive events and avoid failures. (Yarveisy et al., 2020) concluded resilience is the ability of a system to absorb disruptive events, continue its operation

under a degraded state and recover to previous or a new state. From all these definitions, there are three main capacities when assessing resilience of a system:

1. *Absorptive capacity*: The ability of a system to withstand a given stress or demand through adaptive mechanisms.
2. *Adaptive capacity*: The effect of control actions that will level off the performance of a system and allow restoration process to a new stable level.
3. *Restorative capacity*: Corrective actions taken to bring back the system to the previous or new states.

To quantify resilience, the following equation shows the general approach (Ayyub, 2015; Bonstrom & Corotis, 2016; M Taleb-Berrouane & Khan, 2019)

$$Resilience(R) = \int_{T_0}^{T_R} \frac{Q(t)}{T_R} dt \quad (4.18)$$

Where $Q(t)$ is the performance of a system, T_0 is the time when the disruptive event occurs, and T_{RE} is the time to complete restoration of system performance.

However, to assess resilience of an offshore structure subjected to iceberg load, a more robust approach is needed to define system performance on a resilience metric.

(Yarveisy et al., 2020) developed a simple yet robust approach to assess resilience in term of reliability.

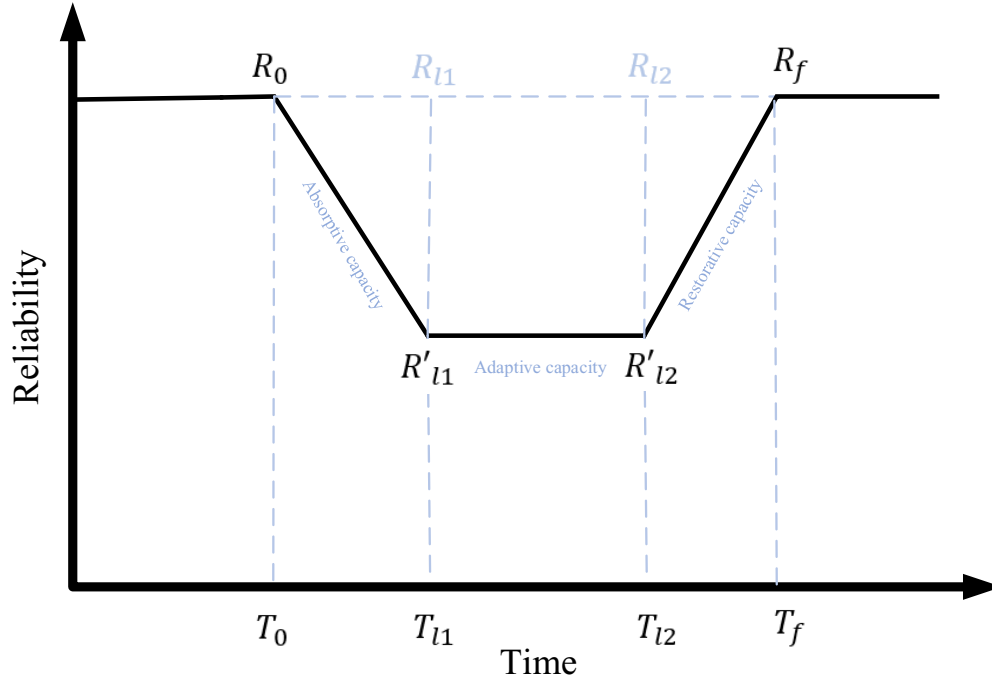


Fig. 4.5. Resilience metric in term of reliability

Fig. 4.5 shows initial and final reliability denoted by R_0 and R_f at their respective times T_0 and T_f . R'_{11} and R'_{12} represent the disrupted steady state reliability at times T_{11} and T_{12} . While, reliability levels in the absence of disruption are denoted by R_{11} and R_{12} . (Yarveisy et al., 2020) then developed an equation to quantify resilience as follows

$$Resilience = Ab + Ad * Res - Ab * Ad * Res \quad (4.19)$$

Where,

- a. The Absorptive Capacity (Ab): Defined as the ratio of residual reliability to the initial reliability at the time of the disruptive event (Bougofa et al., 2021; Mohammed Taleb-Berrouane et al., 2019). It can be estimated as (Yarveisy et al., 2020)

$$Ab = \left(\frac{R'_{l1}}{R_0} \right) * \left(1 + \left(\frac{R_0 - R_{l1}}{R_0} \right) \right) \quad (4.20)$$

Where $\left(1 + \left(\frac{R_0 - R_{l1}}{R_0} \right) \right)$ is applied to account for the aging effect and associated reliability loss during the failure phase.

- b. The Adaptive Capacity (Ad): Defined by the ratio of operation duration in the disrupted state to the total period from disruption to a new stable state condition. This capacity can be estimated using (Yarveisy et al., 2020)

$$Ad = 1 - \left(\frac{T_{l2} - T_{l1}}{T_f - T_0} \right) \quad (4.21)$$

- c. The Restorative Capacity (Res): Defined as the slope of the recovery and estimated using (Yarveisy et al., 2020)

$$Res = \frac{\arctan \left[\frac{R'_f - R'_{l2}}{\left(\frac{T_f - T_{l2}}{T_f - T_0} \right)} \right]}{90} * \left(\frac{R'_f}{R_f} \right) * \left(\frac{T_{l2} - T_0}{T_f - T_0} \right) \quad (4.22)$$

The main feature of this approach is the estimation of reliability of the structure, which is generally assumed to follow a Poisson process (Rózsás & Mogyorósi, 2017). Loads are applied at random and thus the number of loads per unit time follows the Poisson process and the probability of n loads occurring during time, t , can be estimated using

$$P_n(t) = \frac{(\alpha t)^n e^{(-\alpha t)}}{n!}, n = 0,1,2, \dots \quad (4.23)$$

Where α is the mean number of loads per unit of time. Thus the reliability can be calculated as follows (Ebeling, 2004)

$$R(t) = e^{-(1-R)\alpha t} \quad (4.24)$$

Static reliability (R) can be estimated using a limit state assuming random stress and constant strength for the structure. (Ebeling, 2004; X. Li & Zhang, 2020; Wei et al., 2015)

4.3 Application of the Model

To demonstrate the estimation of an iceberg collision load, considering correlated wave and wind variables, ocean data was retrieved from the Smart Atlantic website (ERDDAP, n.d.). The data were collected at the mouth of Placentia Bay, Newfoundland and Labrador (58.4160N 041.7168W) which has a water depth of 230 m. The data used in this chapter were extracted between January 1st 2010 and December, 31st 2020 and were recorded hourly. API 2A-WSD specifies that environment data might have a specific type of relationship that should be considered (American Petroleum Institute, 2002). According to this standard, the common marine environmental variables that have relationships are wind speed/wave height, wave height/wave period, wave height/current speed, and wind speed/current speed. Thus, four ocean parameters were selected: wave height (meter), wave period (second), wind speed (meter per second), and current speed (millimeter per second). Three of these ocean parameters: wave heights, wind speed and current speed, also play important roles in estimating the drifting velocity of an iceberg (Foschi et al., 1996).

In order to select representative months including iceberg existence, data recorded by the International Ice Patrol (IIP) were also extracted. The data were extracted from January 2017 to December 2020 (International Ice Patrol, 2020)

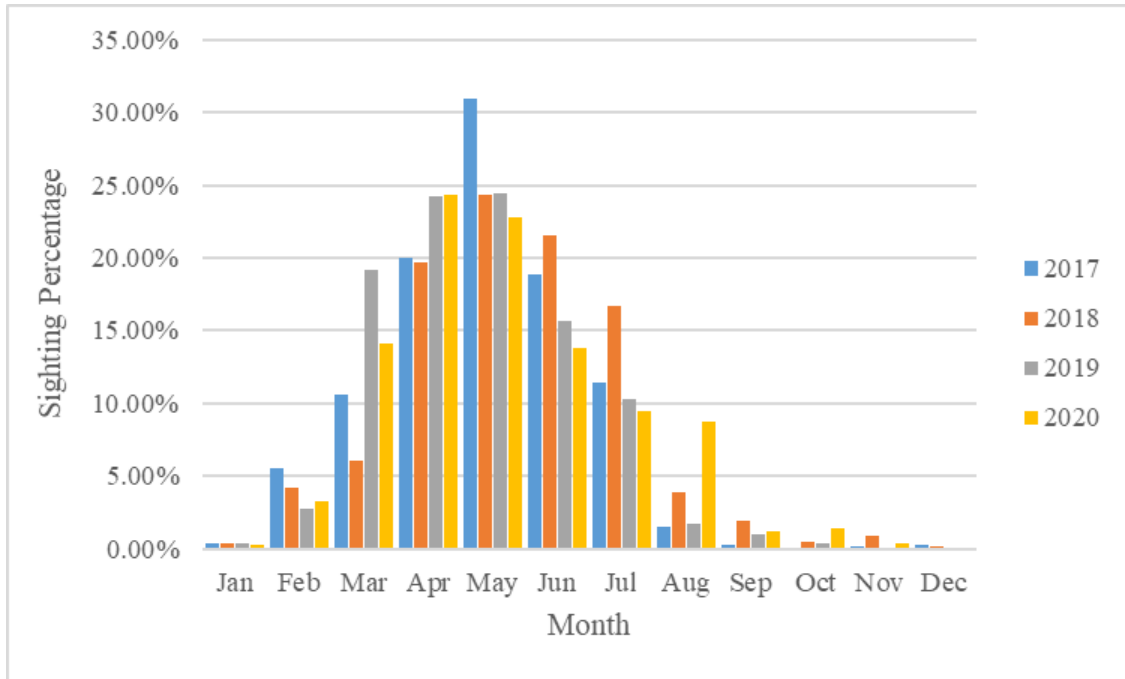


Fig. 4.6. Iceberg sighting (IIP)

Fig. 4.6 shows that iceberg season is effectively from March to July each year with April or May the peak of iceberg sightings. Thus, environmental variables from March to July were used to correspond with the iceberg season. Scatter plots for the observed data sets can be seen in Fig. 4.7.

To model the selected environmental variables using copulas, the dependence between wind speed and wave height is investigated. The dependence measurements considered in this chapter include the linear Pearson coefficient, Spearman's rho and Kendall's tau. A measure of asymmetry is also presented in Table 4.2.

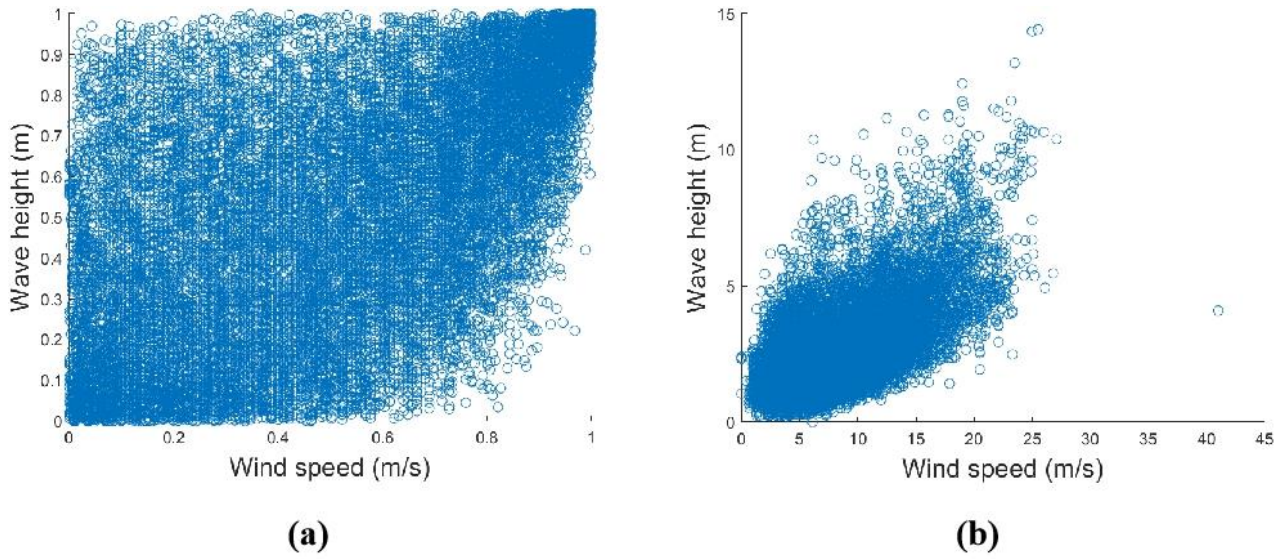


Fig. 4.7. Scatter plots between wind speed and wave height in (a) copula domain and (b) original domain

Table 4.2 Dependence Measurement

Correlated Variables	Pearson coefficient	Spearman's rho	Kendall's tau	Measure of asymmetry
Wind speed - Wave height	0.6156	0.5599	0.3994	0.0133

From Table 4.2, wind speed and wave height from the data sets are correlated. Thus, copula functions will be advantageous in considering the dependence between these environmental variables.

Before proceeding to copula modelling, the marginal distribution for each ocean parameter is also investigated. A group of probability distributions is selected to determine the best-fit model for each data stream. These distributions include Weibull, Normal, Lognormal, Rayleigh, Extreme

Value, Exponential and Gamma. The Akaike Information Criterion (AIC) is used to select the best-fitted model. The lowest AIC score indicates the best model.

Table 4.3 Marginal distributions and statistical parameters for wind speed and wave height

	Wind Speed	Wave Height
AIC Values		
Weibull	Inf	Inf
Normal	104,759	66,681
Lognormal	Inf	Inf
Rayleigh	102,322	61,718
Extreme Value	112,824	79,873
Exponential	114,566	70,668
Gamma	101,831*	58,599*
Statistical Parameters		
	(m/s)	(m)
Mean	8.3677	2.5274
Std. Deviation	4.2121	1.4911
Shape	3.9465**	2.8732**
Scale	2.1203**	0.8797**

*Indicates the best-fit marginal distribution

**Obtained from the best-fit marginal distribution

Table 4.3 shows AIC values for all selected marginal distribution functions for wind speed and wave height along with their statistical parameters. Both wind speed and wave height are best fitted by the Gamma distribution.

4.3.1 Copula modelling

The parameter estimates for all possible symmetric and asymmetric copulas for correlated wind speed and wave height are shown in Table 4.4. The values of the parameter estimates are obtained using the Maximum Log-Likelihood Estimation (MLE)

Table 4.4 Copula parameters estimation

Copula type	Copula function	Parameter estimate	AIC
Symmetric copula	Clayton	$\gamma = 1.0049$	95433
	Gumbel	$\gamma = 1.6254$	95903
	Frank	$\gamma = 4.0046$	95548
Asymmetric copulas	Clayton-Gumbel Type-I	$\gamma_1 = 1.7933$ $\gamma_2 = 1.4285$	78521
		$\theta_{11} = 0.9953\theta_{12} =$ 0.8232	
		$\theta_{21} = 0.0047\theta_{22} =$ 0.1768	
	Clayton-Frank Type-I	$\gamma_1 = 9.0047\gamma_2 = 8.4484$	78579
		$\theta_{11} = 0.0470\theta_{12} =$ 0.4790	
		$\theta_{21} = 0.9530\theta_{22} =$ 0.5210	
	Gumbel-Frank Type-I	$\gamma_1 = 1.9869\gamma_2 =$ 19.1918	78504
		$\theta_{11} = 0.9776\theta_{12} =$ 0.6297	
		$\theta_{21} = 0.0224\theta_{22} =$ 0.3703	

Table 4.4 shows that Gumbel-Frank Type-I is the best fitted copula to model wind speed and wave height with the lowest AIC score. Thus, in order to estimate the iceberg load on the structure and

the resilience, correlated wind and wave data are generated using the Gumbel-Frank Type-I copula to best capture the wind-wave dependence.

4.4 Results and Discussion

4.4.1 Iceberg force

A cylindrical structure with diameter of 100 m is used in this example calculation of iceberg force, considering a water depth of 200 m. It remains a challenge to know the exact dimension of an iceberg. Thus, in this chapter, a key variable for water length line, L , is set to be 100 m with the iceberg mass of 1 million tons. The immersed part of the structure is set to be 200 m. Iceberg collision force is then calculated using the equations in previous sections. Firstly, drift velocity is estimated from the generated correlated wind speed and wave height. Below are the estimated values for iceberg drift velocity.

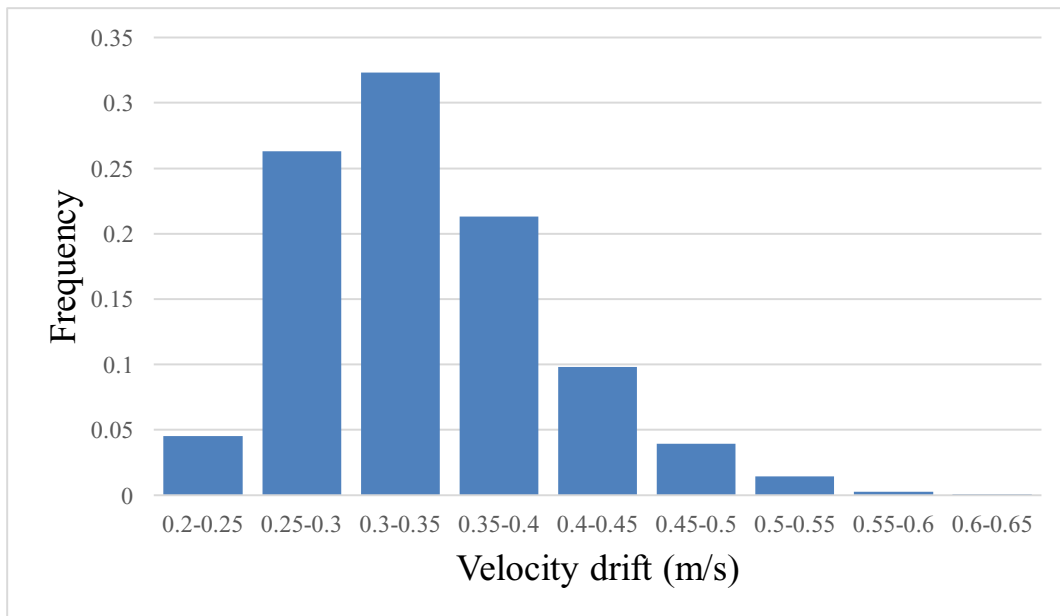


Fig. 4.8. Frequency distribution for iceberg drift velocity

Fig. 4.8 shows that the estimated drift velocity of the iceberg ranges between 0.3 to 0.35 m/s with an average of 0.34 m/s. This result is expected as only smaller bergs may have significant influence on their drift velocity induced by wave and wind action. But in larger bergs, high velocity is unlikely to be found (Colbourne, 2000). While the iceberg force calculated from these initial values as follows

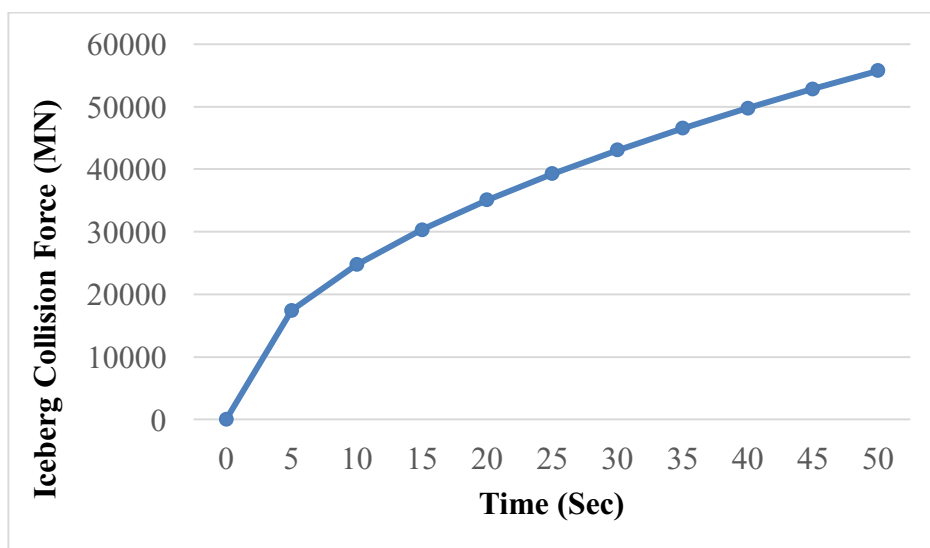


Fig. 4.9. Estimated iceberg force

Fig. 4.9 shows that the estimated iceberg force is increasing with the increase in time. (Foschi et al., 1996) states that an iceberg will be stopped after few meters of penetration. Fig. 4.10 shows the summary of the calculated time for an iceberg to stop after reaching its maximum penetration. It is found that the average time for an iceberg to stop is 38.86 seconds from the generated correlated wind speed and wave height.

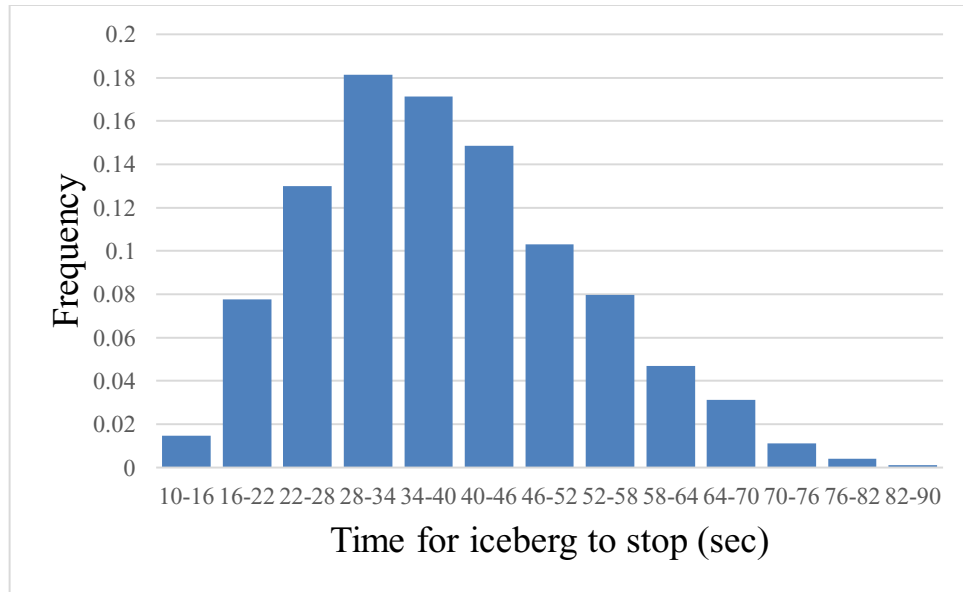


Fig. 4.10. Frequency distribution of time for iceberg to stop at maximum penetration

4.4.2 Resilience assessment

As mentioned in the previous section, resilience is assessed in terms of reliability of the structure. To calculate reliability, the strength capacity is taken as the yield strength of a steel jacket leg and typically assumed to be 700 MPa (Health and Safety Executive UK, 2003). Whereas the demand on the structure is taken as a function of the iceberg load. The function of iceberg load is derived by considering a 100-year return period of correlated wave height and wind speed data modeled using copula functions. From the simulation, the estimated iceberg load follows a general extreme value probability distribution as shown in Fig. 4.11 below

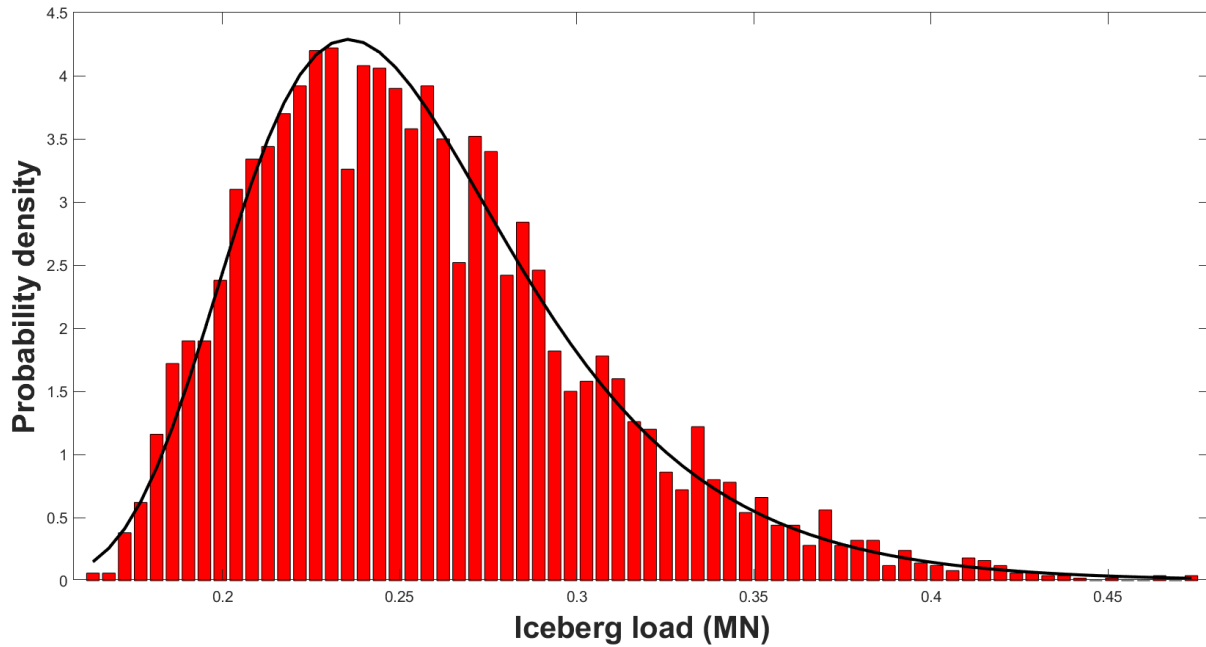
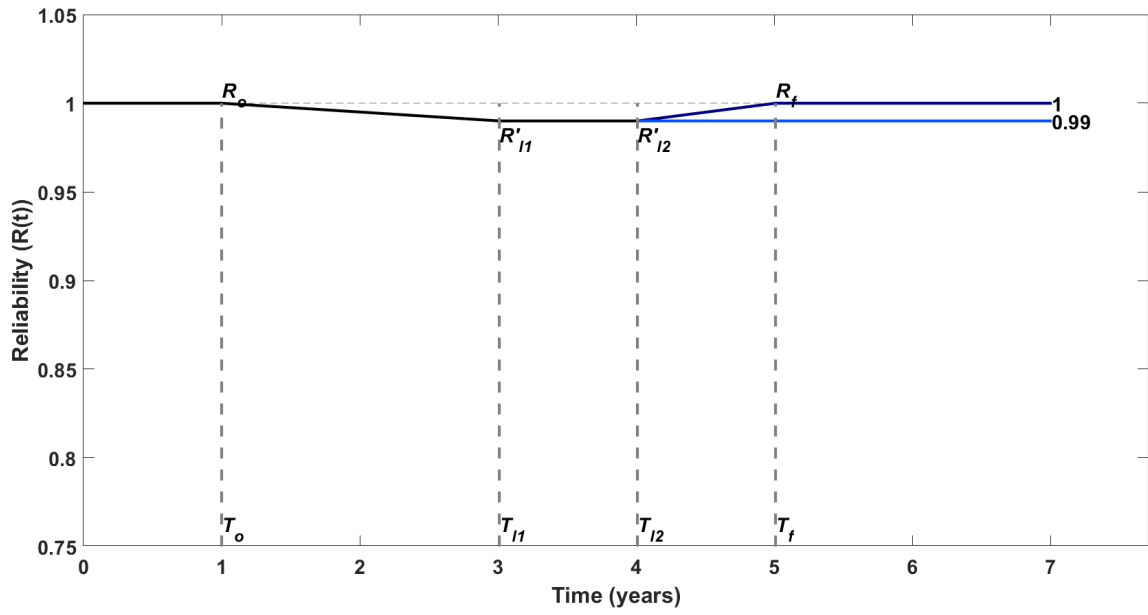
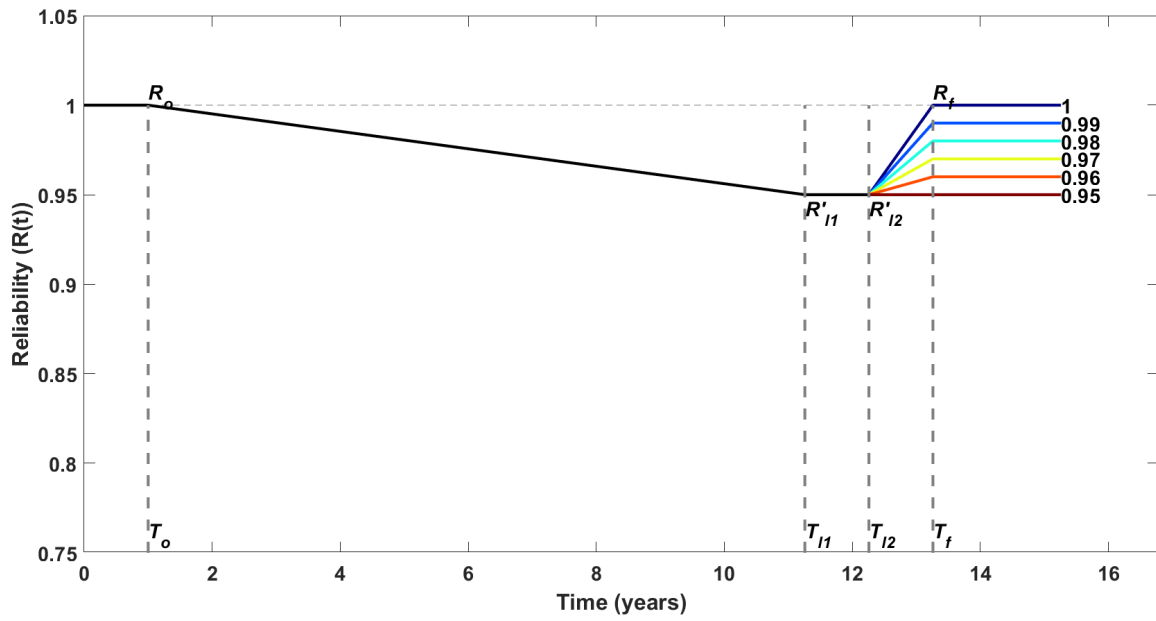


Fig. 4.11. Probability distribution of estimated iceberg loads with data taken as load in MN

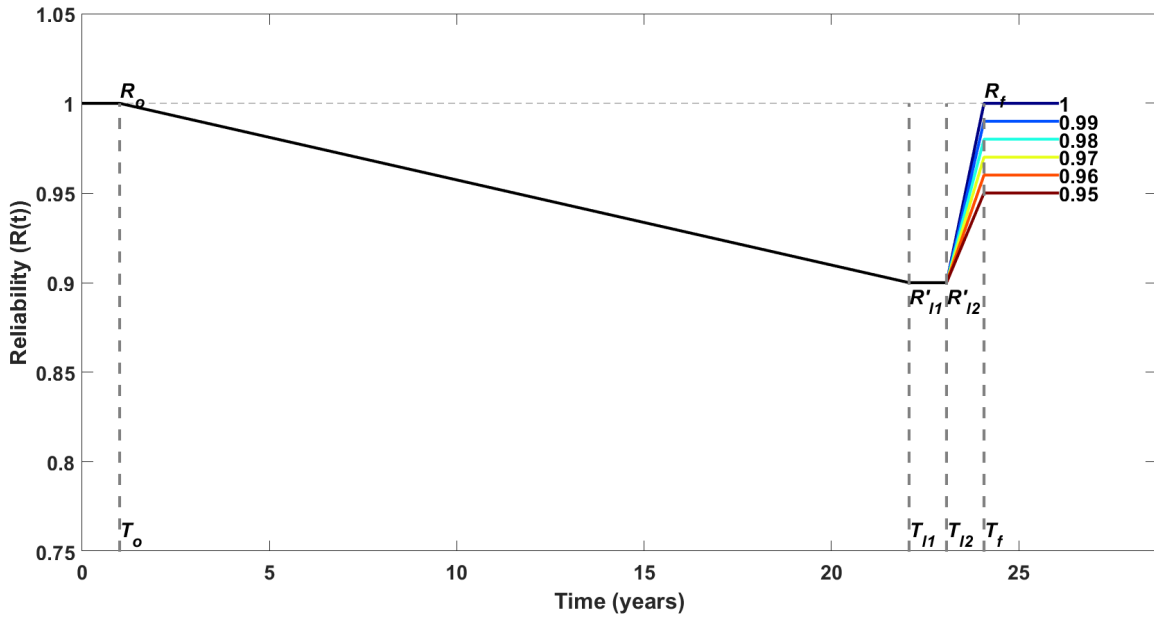
Several scenarios are developed to illustrate the quantification of resilience. Initial reliability R_0 is taken as 1, assuming there is no iceberg-structure interaction during the first year. Then, five iceberg-structure interactions per year are assumed to simulate the reliability of the structure. Three different values for reliability at a disrupted steady state are also selected, 0.99, 0.95 and 0.90. Ideal recovered reliability, R_f , is set to be equal to the initial reliability. Different new post-recovery reliability states (R'_f) are also chosen to simulate the impacts on the estimated resilience assessment. For recovery period, $T_f - T_{l2}$, the completion of this overall mitigation process is assumed to take approximately 1 year. A resilience curve for the reliability level at three different disrupted steady states is shown in Fig. 4.12.



(a)



(b)



(c)

Fig. 4.12. Resilience curve with Reliability at disrupted steady state (a) 0.99, (b) 0.95, (c) 0.90 and varied post-recovery reliability states

The values of Absorptive capacities for different reliability levels at the disrupted event are presented in Table 4.5.

Table 4.5 Absorptive capacity of offshore structure subjected to ice load

No	R_0	R_{11}	R'_{11}	Ab
1.	1.000	0.999	0.990	0.991
2.	1.000	0.999	0.950	0.951
3.	1.000	0.999	0.900	0.901

Where the adaptive capacity values at different reliability levels at the disrupted event are also presented in Table 4.6.

Table 4.6 Adaptive capacity of offshore structure subjected to ice load

No	T_0 (year)	$T_{l2} - T_{l1}$ (year)	$T_f - T_{l2}$ (year)	Ad
1.	1.000	1.000	1.000	0.751
2.	1.000	1.000	1.000	0.918
3.	1.000	1.000	1.000	0.957

Table 4.7 shows the estimated restorative capacity values for different post-recovery reliability target with reliability level at disrupted event equal to 0.9.

Table 4.7 Restorative capacity of offshore structure subjected to ice load for

No	R_0	R'_{l2}	R_f	R'_f	T_0 (year)	T_{l2} (years)	T_f (years)	Res
1	1.000	0.900	1.000	1.000	1.000	23.072	24.072	0.013
2	1.000	0.900	1.000	0.990	1.000	23.072	24.072	0.012
3	1.000	0.900	1.000	0.980	1.000	23.072	24.072	0.011
4	1.000	0.900	1.000	0.970	1.000	23.072	24.072	0.011
5	1.000	0.900	1.000	0.960	1.000	23.072	24.072	0.009
6	1.000	0.900	1.000	0.950	1.000	23.072	24.072	0.008

Thus, the estimated resilience for different scenarios is presented in Table 4.8.

Table 4.8 The estimated resilience with varied capacities and post-recovery states

No	R'_{l1}	R'_f	Ab	Ad	Res	Resilience
1.	0.990	1.000	0.991	0.751	0.013	0.991
2.		0.990			0.012	
3.	0.950	1.000	0.951	0.918	0.013	0.952
4.		0.990			0.012	
5.		0.980			0.011	

6.		0.970			0.011	0.951
7.		0.960			0.009	0.950
8.	0.900	1.000	0.901	0.957	0.013	0.902
9.		0.990			0.012	0.902
10.		0.980			0.011	0.902
11.		0.970			0.011	0.901
12.		0.960			0.009	0.901
13.		0.950			0.008	0.901

Fig. 4.13 shows different scenarios to assess resilience of the monopile structure. Three different reliability levels at the disrupted steady state are selected. The reliability of the system is restored to better steady states, R_f , or at least the same level as their R'_{l1} for scenario 0.95 and 0.99. From Table 4.5, it is shown that the value of Absorptive capacity is not significantly different from the value of reliability at the disrupted steady state R'_{l1} . During the stable disrupted operation, $R'_{l2} - R'_{l1}$, the adaptive capacity of the system is higher when R'_{l1} gets smaller as seen in Table 4.6. Table 4.7 shows that with the same level of R'_{l1} , the higher target recovered reliability R_f , restorative capacity is also higher. For a comparison, with $R_f = R_0 = 1$, where the system is restored to the initial reliability, the estimated resilience will become higher when the value of reliability at the disrupted steady state, R'_{l1} , is higher. This shows that the resilience metric used in this chapter significantly depends on the value of absorptive capacity. To validate this result, different recovery times from 2-5 years are selected to illustrate their impact on the resilience quantification. Fig. 4.13 shows resilience curves for different recovery times with the same post-recovery reliability target and the same reliability level at the disrupted steady state.

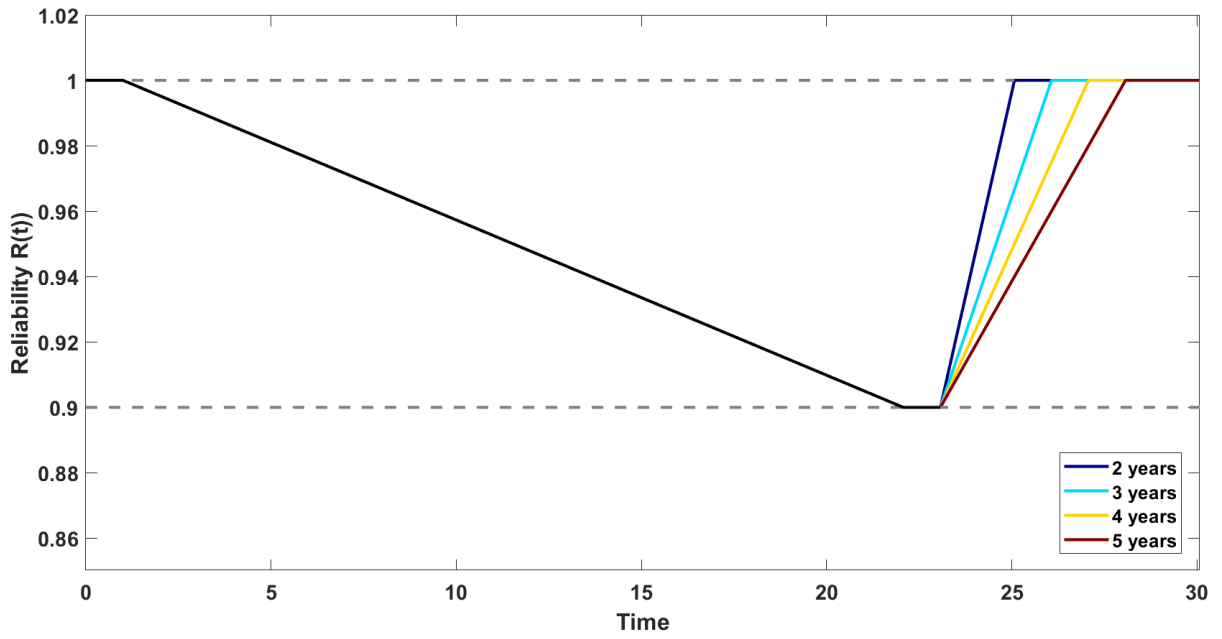


Fig. 4.13. Resilience curve with varied recovery times and reliability at disrupted steady state equal to 0.90

Table 4.9 Resilience assessment with respect to different recovery times ($T_f - T_{l2}$)

No	R'_{l1}	$T_f - T_{l2}$ (years)	Ab	Ad	Res	Resilience
1.	0.9000	2.0000	0.9009	0.9585	0.0045	0.9017
2.		3.0000	0.9009	0.9601		0.9015
3.		4.0000	0.9009	0.9616		0.9014
4.		5.0000	0.9009	0.9631		0.9013
5.	0.9500	2.0000	0.9509	0.9246	0.0012	0.9511
6.		3.0000	0.9509	0.9299		0.9510
7.		4.0000	0.9509	0.9345		0.9510
8.		5.0000	0.9509	0.9385		0.9510
9.	0.9900	2.0000	0.9910	0.8004	0.0001	0.9910
10.		3.0000	0.9910	0.8336		0.9910
11.		4.0000	0.9910	0.8573		0.9910

12.		5.0000	0.9910	0.8752		0.9910
-----	--	--------	--------	--------	--	--------

From Table 4.9 and Fig. 4.13, it is shown that even though different recovery times are selected for different reliability levels at the disrupted steady state, the value of resilience does not differ significantly from its absorptive capacity. Eq. 4.19 shows that restorative capacity is dependent on both absorptive and adaptive capacity. Another comparison is presented with respect to different periods during stable disrupted operation, $T_{l2} - T_{l1}$.

Table 4.10 Resilience with different periods of stable disrupted operation

No.	R'_{l1}	R'_f	$T_{l2} - T_{l1}$ (year)	Ad	Resilience
1.	0.9900	1.0000	2.0000	0.6008	0.9910
2.			4.0000	0.4294	0.9910
3.			6.0000	0.3341	0.9910
1.	0.9500	1.0000	2.0000	0.8492	0.9512
2.			4.0000	0.7379	0.9512
3.			6.0000	0.6524	0.9512
1.	0.900	1.0000	2.0000	0.9169	0.9020
2.			4.0000	0.8466	0.9019
3.			6.0000	0.7863	0.9019

Table 4.10 shows that the adaptive capacity of the system decreases when the period of disrupted operation gets longer. However, this does not impact on the assessment of resilience. Its values do not differ significantly from the absorptive capacity. This also validates Eq. 4.19 such that adaptive capacity also depends on absorptive capacity. Thus, absorptive capacity in this resilience metric is found to be the only independent resilience capacity. This absorptive capacity reflects on the inherent design of the system or structure to withstand disruptive events, in this case iceberg load.

This capacity is influenced by the safety design and physical characteristics of the structure. If reliability at a disrupted steady state can be maintained close to the initial reliability, the ability of the system to withstand the disruptive events and restore its functionality will be high too. Higher absorptive capacity means less effort and resources are necessary to perform restoration on the structure. This finding also supports arguments presented by (Yarveisy et al., 2020).

4.4.3 Model validation

The Root-Mean-Square error (RMSE) and the mean absolute error values are used to compare the performance of the models based on copula models and the model assuming independent joint probability. RMSE calculated between empirical data and the selected distribution functions are compared in this work.

Fig. 4.14 shows that the Gumbel-Frank copula has lower RMSE and mean absolute error compared to the independent joint distribution approaches. This validates that the ocean parameters are better modeled using the copula functions. Copula functions can capture complex dependencies among ocean parameters, and it is reflected in the small error values compared to the independent case.

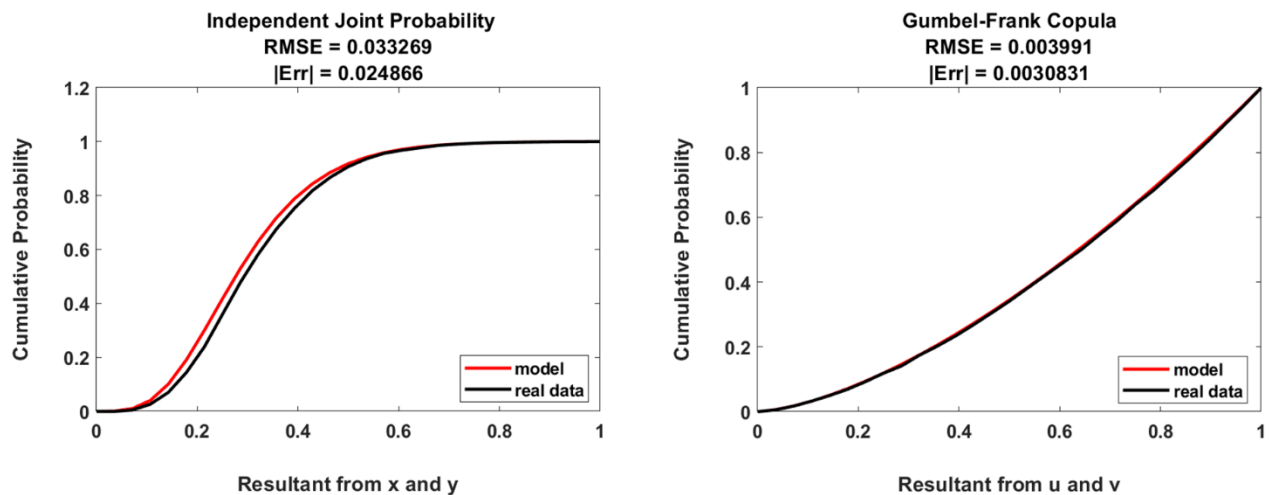


Fig. 4.14. Empirical data plotted against selected distribution functions for wind speed and wave height data

4.5 Conclusion

This chapter presents an implementation of a robust approach to quantify resilience. A simple demonstration case study is selected as an offshore structure subjected to iceberg load. The iceberg collision force is influenced by both ice parameters and meteorological factors. From the meteorological perspective, wave and wind load influence the drift velocity of the iceberg. These ocean parameters are found to be correlated and show a slight asymmetrical dependence. Assuming independence in evaluating icebergs, drift velocity is thus not recommended. Copula functions were applied to model this dependence between wave and wind data. Out of the commonly used copula functions, the Gumbel-Frank Type-I was found to best fit the bivariate model.

Resilience is quantified based on a reliability assessment of the structure subjected to the iceberg load. Quantification of resilience was found largely dependent on the absorptive capacity. This is the only capacity in the resilience metric that is independent compared to the other two capacities. Absorptive capacity is critical in a system as a higher level of residual reliability will result in better ability to withstand disruptive events and restore functionality. This capacity is the inherent physical characteristic of the structure that enables it to withstand disruptive events. Thus, system design plays an important role in achieving a high resilience metric.

The main challenge in this resilience quantification is the assumption of iceberg parameters required to estimate ice load and structural reliability in order to estimate all resilience capacities. In addition to this, an acceptable level of reliability at the disrupted steady state should also be

better quantified. This identification will require involvement from all stakeholders in an organization to provide more practical and realistic assumptions. Future work will involve managerial aspects in quantifying the resilience of an offshore structure. In addition, broader analysis of multi-hazards acting on a structure should be considered.

Conflict of Interest

The authors declare that they have no known competing financial interests or personal relationships that could have appeared to influence the work reported in this chapter.

Acknowledgements

The authors would like to express their gratitude to the financial assistance provided by the Natural Science and Engineering Council of Canada (NSERC) and the Canada Research Chair (CRC) Tier I Program in Offshore Safety and Risk Engineering.

References

- Abaei, M. M., Hekkenberg, R., BahooToroodi, A., Banda, O. V., & van Gelder, P. (2022). A probabilistic model to evaluate the resilience of unattended machinery plants in autonomous ships. *Reliability Engineering & System Safety*, 219, 108176. <https://doi.org/10.1016/j.ress.2021.108176>
- Afgan, N., & Cvetinovic, D. (2010). Wind power plant resilience. *Thermal Science*, 14(2), 533–540. <https://doi.org/10.2298/TSC11002533A>
- American Petroleum Institute. (2002). *Recommended Practice for Planning, Designing and Constructing Fixed Offshore Platforms - Working Stress Design*.
- Aven, T. (2011). On Some Recent Definitions and Analysis Frameworks for Risk, Vulnerability, and Resilience. *Risk Analysis*, 31(4), 515–522. <https://doi.org/10.1111/j.1539-6924.2010.01528.x>
- Ayyub, B. M. (2015). Practical Resilience Metrics for Planning, Design, and Decision Making. *ASCE-ASME Journal of Risk and Uncertainty in Engineering Systems, Part A: Civil Engineering*, 1(3), 04015008. <https://doi.org/10.1061/AJRUA6.0000826>
- Bai, Y., Yan, H., Cao, Y., Kim, Y., Yang, Y., & Jiang, H. (2016). Time-dependent reliability assessment of offshore jacket platforms. *Ships and Offshore Structures*, 11(6), 591–602.

<https://doi.org/10.1080/17445302.2015.1038869>

- Bang Huseby, A., Vanem, E., & Natvig, B. (2013). A new approach to environmental contours for ocean engineering applications based on direct Monte Carlo simulations. *Ocean Engineering*, *60*, 124–135. <https://doi.org/10.1016/j.oceaneng.2012.12.034>
- Ben Seghier, M. E. A., Keshtegar, B., Taleb-Berrouane, M., Abbassi, R., & Trung, N.-T. (2021). Advanced intelligence frameworks for predicting maximum pitting corrosion depth in oil and gas pipelines. *Process Safety and Environmental Protection*, *147*, 818–833. <https://doi.org/10.1016/j.psep.2021.01.008>
- Bhardwaj, U., Teixeira, A. P., & Guedes Soares, C. (2022). Bayesian framework for reliability prediction of subsea processing systems accounting for influencing factors uncertainty. *Reliability Engineering & System Safety*, *218*, 108143. <https://doi.org/10.1016/j.res.2021.108143>
- Bhattacharya, S., & Goda, K. (2016). Use of offshore wind farms to increase seismic resilience of Nuclear Power Plants. *Soil Dynamics and Earthquake Engineering*, *80*, 65–68. <https://doi.org/10.1016/j.soildyn.2015.10.001>
- Bonstrom, H., & Corotis, R. B. (2016). First-Order Reliability Approach to Quantify and Improve Building Portfolio Resilience. *Journal of Structural Engineering*, *142*(8). [https://doi.org/10.1061/\(ASCE\)ST.1943-541X.0001213](https://doi.org/10.1061/(ASCE)ST.1943-541X.0001213)
- Bougofa, M., Taleb-Berrouane, M., Bouafia, A., Baziz, A., Kharzi, R., & Bellaouar, A. (2021). Dynamic availability analysis using dynamic Bayesian and evidential networks. *Process Safety and Environmental Protection*, *153*, 486–499. <https://doi.org/10.1016/j.psep.2021.07.003>
- Bucelli, M., Landucci, G., Haugen, S., Paltrinieri, N., & Cozzani, V. (2018). Assessment of safety barriers for the prevention of cascading events in oil and gas offshore installations operating in harsh environment. *Ocean Engineering*, *158*, 171–185. <https://doi.org/10.1016/j.oceaneng.2018.02.046>
- Cai, B., Zhang, Y., Wang, H., Liu, Y., Ji, R., Gao, C., Kong, X., & Liu, J. (2021). Resilience evaluation methodology of engineering systems with dynamic-Bayesian-network-based degradation and maintenance. *Reliability Engineering & System Safety*, *209*, 107464. <https://doi.org/10.1016/j.res.2021.107464>
- Cao, R., Sun, Z., Wang, J., & Guo, F. (2022). A single-loop reliability analysis strategy for time-dependent problems with small failure probability. *Reliability Engineering & System Safety*, *219*, 108230. <https://doi.org/10.1016/j.res.2021.108230>
- Carvalho, P. V. R., dos Santos, I. L., Gomes, J. O., & Borges, M. R. S. (2008). Micro incident analysis framework to assess safety and resilience in the operation of safe critical systems: A case study in a nuclear power plant. *Journal of Loss Prevention in the Process Industries*, *21*(3), 277–286. <https://doi.org/10.1016/j.jlp.2007.04.005>
- Castaldo, P., Palazzo, B., & Mariniello, A. (2017). Effects of the axial force eccentricity on the

- time-variant structural reliability of aging r.c. cross-sections subjected to chloride-induced corrosion. *Engineering Structures*, 130, 261–274. <https://doi.org/10.1016/j.engstruct.2016.10.053>
- Castaldo, Paolo, Gino, D., & Mancini, G. (2019). Safety formats for non-linear finite element analysis of reinforced concrete structures: discussion, comparison and proposals. *Engineering Structures*, 193, 136–153. <https://doi.org/10.1016/j.engstruct.2019.05.029>
- Chen, C., Yang, M., & Reniers, G. (2021). A dynamic stochastic methodology for quantifying HAZMAT storage resilience. *Reliability Engineering & System Safety*, 215, 107909. <https://doi.org/10.1016/j.ress.2021.107909>
- Chen, Y., Li, S., & Kang, R. (2021). Epistemic uncertainty quantification via uncertainty theory in the reliability evaluation of a system with failure Trigger effect. *Reliability Engineering & System Safety*, 215, 107896. <https://doi.org/10.1016/j.ress.2021.107896>
- Cheng, Y., Elsayed, E. A., & Chen, X. (2021). Random Multi Hazard Resilience Modelling of Engineered Systems and Critical Infrastructure. *Reliability Engineering & System Safety*, 209, 107453. <https://doi.org/10.1016/j.ress.2021.107453>
- Cheng, Z., Svangstu, E., Moan, T., & Gao, Z. (2019). Long-term joint distribution of environmental conditions in a Norwegian fjord for design of floating bridges. *Ocean Engineering*, 191, 106472. <https://doi.org/10.1016/j.oceaneng.2019.106472>
- Colbourne, D. B. (2000). Scaling pack ice and iceberg loads on moored shiped shapes. *Oceanic Engineering*, 4(1), 39–45. <https://nrc-publications.canada.ca/eng/view/object/?id=7997b255-3f2c-4147-8e8b-0a15863849ce>
- Dawuda, A.-W., Taleb-berrouane, M., & Khan, F. (2021). A probabilistic model to estimate microbiologically influenced corrosion rate. *Process Safety and Environmental Protection*. <https://doi.org/10.1016/j.psep.2021.02.006>
- De Michele, C., Salvadori, G., Passoni, G., & Vezzoli, R. (2007). A multivariate model of sea storms using copulas. *Coastal Engineering*, 54(10), 734–751. <https://doi.org/10.1016/j.coastaleng.2007.05.007>
- Desilver, D. (2020). *Renewable energy is growing fast, but fossil fuels still dominate*. <https://www.pewresearch.org/fact-tank/2020/01/15/renewable-energy-is-growing-fast-in-the-u-s-but-fossil-fuels-still-dominate/>
- Deyab, S. M., Taleb-berrouane, M., Khan, F., & Yang, M. (2018). Failure analysis of the offshore process component considering causation dependence. *Process Safety and Environmental Protection*, 1(8), 220–232. <https://doi.org/10.1016/j.psep.2017.10.010>
- Dong, S., Chen, C., & Tao, S. (2017). Joint probability design of marine environmental elements for wind turbines. *International Journal of Hydrogen Energy*, 42(29), 18595–18601. <https://doi.org/10.1016/j.ijhydene.2017.04.154>
- Dui, H., Zheng, X., & Wu, S. (2021). Resilience analysis of maritime transportation systems based on importance measures. *Reliability Engineering & System Safety*, 209, 107461.

<https://doi.org/10.1016/j.res.2021.107461>

- Durante, F., & Salvadori, G. (2009). On the construction of multivariate extreme value models via copulas. *Environmetrics*, n/a-n/a. <https://doi.org/10.1002/env.988>
- Ebeling, C. E. (2004). *An introduction to reliability and maintainability engineering*. McGraw-Hill Education.
- ERDDAP. (n.d.). *Mouth of Placentia Bay Buoy*. Retrieved August 28, 2021, from https://www.smartatlantic.ca/erddap/tabledap/SMA_MouthofPlacentiaBayBuoy.html
- Fang, G., Pan, R., & Hong, Y. (2020). Copula-based reliability analysis of degrading systems with dependent failures. *Reliability Engineering & System Safety*, 193, 106618. <https://doi.org/10.1016/j.res.2019.106618>
- Foschi, R., Isaacson, M., Allyn, N., & Yee, S. (1996). Combined wave – iceberg loading on offshore structures. *Canadian Journal of Civil Engineering*, 23(5), 1099–1110. <https://doi.org/10.1139/196-917>
- Francis, R., & Bekera, B. (2014). A metric and frameworks for resilience analysis of engineered and infrastructure systems. *Reliability Engineering & System Safety*, 121, 90–103. <https://doi.org/10.1016/j.res.2013.07.004>
- Fuglem, M., Jordaan, I., Crocker, G., Cammaert, G., & Berry, B. (1996). Environmental factors in iceberg collision risks for floating systems. *Cold Regions Science and Technology*, 24(3), 251–261. [https://doi.org/10.1016/0165-232X\(95\)00013-2](https://doi.org/10.1016/0165-232X(95)00013-2)
- Genest, C., Gendron, M., & Bourdeau-Brien, M. (2009). The Advent of Copulas in Finance. *The European Journal of Finance*, 15(7–8), 609–618. <https://doi.org/10.1080/13518470802604457>
- Genest, C., Rémillard, B., & Beaudoin, D. (2009). Goodness-of-fit tests for copulas: A review and a power study. *Insurance: Mathematics and Economics*, 44(2), 199–213. <https://doi.org/10.1016/j.insmatheco.2007.10.005>
- Guo, Y., Huang, S., Huang, Q., Wang, H., Wang, L., & Fang, W. (2019). Copulas-based bivariate socioeconomic drought dynamic risk assessment in a changing environment. *Journal of Hydrology*, 575, 1052–1064. <https://doi.org/10.1016/j.jhydrol.2019.06.010>
- Hashemi, S. J., Ahmed, S., & Khan, F. I. (2015). Correlation and Dependency in Multivariate Process Risk Assessment. *IFAC-PapersOnLine*, 48(21), 1339–1344. <https://doi.org/10.1016/j.ifacol.2015.09.711>
- Health and Safety Executive UK. (2003). *Review of the performance of high strength steels used offshore*. <https://www.hse.gov.uk/research/rrpdf/rr105.pdf>
- Hoek, J. (2021). *Dynamic ice-structure interaction for jacket substructures*. Delft University of Technology.
- Hu, J., Khan, F., & Zhang, L. (2021). Dynamic resilience assessment of the Marine LNG

- offloading system. *Reliability Engineering & System Safety*, 208, 107368. <https://doi.org/10.1016/j.ress.2020.107368>
- Idris, A., Harahap, I. S. H., & Ali, M. O. A. (2017). An approach for time-dependent reliability analysis of Jackup structures. *Cogent Engineering*, 4(1), 1409932. <https://doi.org/10.1080/23311916.2017.1409932>
- International Ice Patrol. (2020). *National Snow and Ice Data Center*. <https://nsidc.org/data/G00807/versions/1>
- Joyce, J., Chang, N.-B., Harji, R., & Ruppert, T. (2018). Coupling infrastructure resilience and flood risk assessment via copulas analyses for a coastal green-grey-blue drainage system under extreme weather events. *Environmental Modelling & Software*, 100, 82–103. <https://doi.org/10.1016/j.envsoft.2017.11.008>
- Kabir, S., Taleb-Berrouane, M., & Papadopoulos, Y. (2019). Dynamic reliability assessment of flare systems by combining fault tree analysis and Bayesian networks. *Energy Sources, Part A: Recovery, Utilization and Environmental Effects*. <https://doi.org/10.1080/15567036.2019.1670287>
- Kamil, M. Z., Taleb-Berrouane, M., Khan, F., & Ahmed, S. (2019). Dynamic domino effect risk assessment using Petri-nets. *Process Safety and Environmental Protection*, 124, 308–316. <https://doi.org/10.1016/j.psep.2019.02.019>
- Kamil, M. Z., Taleb-Berrouane, M., Khan, F., & Amyotte, P. (2021). Data-driven operational failure likelihood model for microbiologically influenced corrosion. *Process Safety and Environmental Protection*, 153, 472–485. <https://doi.org/10.1016/j.psep.2021.07.040>
- Kammouh, O., Gardoni, P., & Cimellaro, G. P. (2020). Probabilistic framework to evaluate the resilience of engineering systems using Bayesian and dynamic Bayesian networks. *Reliability Engineering & System Safety*, 198, 106813. <https://doi.org/10.1016/j.ress.2020.106813>
- Kim, D. K., Liew, M. S., Youssef, S. A. M., Mohd, M. H., Kim, H. B., & Paik, J. K. (2014). Time-Dependent Ultimate Strength Performance of Corroded FPSOs. *Arabian Journal for Science and Engineering*, 39(11), 7673–7690. <https://doi.org/10.1007/s13369-014-1364-4>
- Kim, J. T., Park, J., Kim, J., & Seong, P. H. (2018). Development of a quantitative resilience model for nuclear power plants. *Annals of Nuclear Energy*, 122, 175–184. <https://doi.org/10.1016/j.anucene.2018.08.042>
- Kiureghian, A. Der, & Ditlevsen, O. (2009). Aleatory or epistemic? Does it matter? *Structural Safety*, 31(2), 105–112. <https://doi.org/10.1016/j.strusafe.2008.06.020>
- Li, D., & Tang, X. (2014). Modelling and simulation of bivariate distribution of shear strength parameters using copulas. In *Risk and Reliability in Geotechnical Engineering* (pp. 77–128). CRC Press.
- Li, H., Wang, P., Huang, X., Zhang, Z., Zhou, C., & Yue, Z. (2021). Vine copula-based parametric sensitivity analysis of failure probability-based importance measure in the presence of multidimensional dependencies. *Reliability Engineering & System Safety*, 215, 107898.

<https://doi.org/10.1016/j.res.2021.107898>

- Li, X., & Zhang, W. (2020). Long-term assessment of a floating offshore wind turbine under environmental conditions with multivariate dependence structures. *Renewable Energy*, *147*, 764–775. <https://doi.org/10.1016/j.renene.2019.09.076>
- Li, Y., Dong, Y., & Zhu, D. (2020). Copula-Based Vulnerability Analysis of Civil Infrastructure Subjected to Hurricanes. *Frontiers in Built Environment*, *6*. <https://doi.org/10.3389/fbuil.2020.571911>
- Liebscher, E. (2008). Construction of asymmetric multivariate copulas. *Journal of Multivariate Analysis*, *99*(10), 2234–2250. <https://doi.org/10.1016/j.jmva.2008.02.025>
- Liu, X., & Chen, Z. (2020). An Integrated Risk and Resilience Assessment of Sea Ice Disasters on Port Operation. *Risk Analysis*, *risa.13660*. <https://doi.org/10.1111/risa.13660>
- Lü, T.-J., Tang, X.-S., Li, D.-Q., & Qi, X.-H. (2020). Modelling multivariate distribution of multiple soil parameters using vine copula model. *Computers and Geotechnics*, *118*, 103340. <https://doi.org/10.1016/j.compgeo.2019.103340>
- McKeand, A. M., Gorgularslan, R. M., & Choi, S.-K. (2021). Stochastic analysis and validation under aleatory and epistemic uncertainties. *Reliability Engineering & System Safety*, *205*, 107258. <https://doi.org/10.1016/j.res.2020.107258>
- Nelsen, R. B. (2006). *An introduction to copulas* (2nd ed.). Springer.
- Ning, X., Xueqin, L., Shuai, Y., Yuxian, M., Wenqi, S., & Weibin, C. (2019). Sea ice disaster risk assessment index system based on the life cycle of marine engineering. *Natural Hazards*, *95*(3), 445–462. <https://doi.org/10.1007/s11069-018-3463-0>
- Poulin, C., & Kane, M. B. (2021). Infrastructure resilience curves: Performance measures and summary metrics. *Reliability Engineering & System Safety*, *216*, 107926. <https://doi.org/10.1016/j.res.2021.107926>
- Qeshta, I. M. I., Hashemi, M. J., Gravina, R., & Setunge, S. (2019). Review of resilience assessment of coastal bridges to extreme wave-induced loads. *Engineering Structures*, *185*, 332–352. <https://doi.org/10.1016/j.engstruct.2019.01.101>
- Qian, H.-M., Li, Y.-F., & Huang, H.-Z. (2021). Time-variant system reliability analysis method for a small failure probability problem. *Reliability Engineering & System Safety*, *205*, 107261. <https://doi.org/10.1016/j.res.2020.107261>
- Qin, J., & Faber, M. H. (2019). Resilience Informed Integrity Management of Wind Turbine Parks. *Energies*, *12*(14), 2729. <https://doi.org/10.3390/en12142729>
- Ramadhani, A., Khan, F., Colbourne, B., Ahmed, S., & Taleb-Berrouane, M. (2021). Environmental load estimation for offshore structures considering parametric dependencies. *Safety in Extreme Environments*. <https://doi.org/10.1007/s42797-021-00028-y>
- Reilly, A. C., Baroud, H., Flage, R., & Gerst, M. D. (2021). Sources of uncertainty in

- interdependent infrastructure and their implications. *Reliability Engineering & System Safety*, 213, 107756. <https://doi.org/10.1016/j.res.2021.107756>
- Rózsás, Á., & Mogyorósi, Z. (2017). The effect of copulas on time-variant reliability involving time-continuous stochastic processes. *Structural Safety*, 66, 94–105. <https://doi.org/10.1016/j.strusafe.2017.02.004>
- Sarwar, A., Khan, F., Abimbola, M., & James, L. (2018). Resilience Analysis of a Remote Offshore Oil and Gas Facility for a Potential Hydrocarbon Release. *Risk Analysis*, 38(8), 1601–1617. <https://doi.org/10.1111/risa.12974>
- Senkel, A., Bode, C., & Schmitz, G. (2021). Quantification of the resilience of integrated energy systems using dynamic simulation. *Reliability Engineering & System Safety*, 209, 107447. <https://doi.org/10.1016/j.res.2021.107447>
- Shi, W., Tan, X., Gao, Z., & Moan, T. (2016). Numerical study of ice-induced loads and responses of a monopile-type offshore wind turbine in parked and operating conditions. *Cold Regions Science and Technology*, 123, 121–139. <https://doi.org/10.1016/j.coldregions.2015.12.007>
- Sinsabvarodom, C., Chai, W., Leira, B. J., Høyland, K. V., & Naess, A. (2020). Uncertainty assessments of structural loading due to first year ice based on the ISO standard by using Monte-Carlo simulation. *Ocean Engineering*, 198, 106935. <https://doi.org/10.1016/j.oceaneng.2020.106935>
- Stochino, F., Bedon, C., Sagaseta, J., & Honfi, D. (2019). Robustness and Resilience of Structures under Extreme Loads. *Advances in Civil Engineering*, 2019, 1–14. <https://doi.org/10.1155/2019/4291703>
- Tabandeh, A., Sharma, N., & Gardoni, P. (2022). Uncertainty propagation in risk and resilience analysis of hierarchical systems. *Reliability Engineering & System Safety*, 219, 108208. <https://doi.org/10.1016/j.res.2021.108208>
- Taleb-Berrouane, M., Khan, F., Eckert, R. B., & Skovhus, T. L. (2019). Predicting Sessile Microorganism Populations in Oil and Gas Gathering and Transmission Facilities- Preliminary Results. *7th International Symposium on Applied Microbiology and Molecular Biology in Oil Systems (ISMOS 7)*.
- Taleb-berrouane, M., Khan, F., Hawboldt, K., Eckert, R., & Skovhus, T. L. (2018). Model for microbiologically influenced corrosion potential assessment for the oil and gas industry and gas industry. *Corrosion Engineering, Science and Technology*, 53(5), 378–392. <https://doi.org/10.1080/1478422X.2018.1483221>
- Taleb-Berrouane, M., Khan, F., & Kamil, M. Z. (2019). Dynamic RAMS analysis using advanced probabilistic approach. *Chemical Engineering Transactions*, 77. <https://doi.org/10.3303/CET1977041>
- Taleb-Berrouane, M., & Khan, F. (2019). Dynamic Resilience Modelling of Process Systems. *Chemical Engineering Transaction*, 77, 313–318. <https://doi.org/https://doi.org/10.3303/CET1977053>

- Taleb-Berrouane, Mohammed, & Khan, F. (2018). Development of MIC Risk Index for Process Operations. *C-RISE & Geno-MIC Workshop & Symposium*.
- Taleb-Berrouane, Mohammed, Khan, F., & Amyotte, P. (2020). Bayesian Stochastic Petri Nets (BSPN) - A new modelling tool for dynamic safety and reliability analysis. *Reliability Engineering and System Safety*, 193. <https://doi.org/10.1016/j.res.2019.106587>
- Taleb-Berrouane, Mohammed, Khan, F., & Hawboldt, K. (2021). Corrosion risk assessment using adaptive bow-tie (ABT) analysis. *Reliability Engineering & System Safety*, 214(May), 107731. <https://doi.org/10.1016/j.res.2021.107731>
- Taleb-Berrouane, Mohammed, Khan, F., & Kamil, M. Z. (2019). Dynamic RAMS Analysis Using Advanced Probabilistic Approach. *Chemical Engineering Transaction*, 77, 241–246. <https://doi.org/https://doi.org/10.3303/CET1977041>
- Taleb-Berrouane, Mohammed, & Lounis, Z. (2016). Safety Assessment of Flare System by Fault Tree Analysis. *Journal of Chemical Technology and Metallurgy*, 51(2), 229–234.
- Taleb-Berrouane, Mohammed, Sterrahmane, A., Mehdaoui, D., & Lounis., Z. (2017). Emergency Response Plan Assessment Using Bayesian Belief Networks. *3rd Workshop and Symposium on Safety and Integrity Management of Operations in Harsh Environments (C-RISE3)*.
- Taleb-berrrouane, M. (2019). *Dynamic Corrosion Risk Assessment in the Oil and Gas Production and Processing Facility* (Issue October). Memorial University of Newfoundland.
- Talebberrouane, M., Khan, F., & Lounis, Z. (2016). Availability analysis of safety critical systems using advanced fault tree and stochastic Petri net formalisms. *Journal of Loss Prevention in the Process Industries*, 44, 193–203. <https://doi.org/10.1016/j.jlp.2016.09.007>
- Thijssen, J., Fuglem, M., Richard, M., & King, T. (2014). Implementation of ISO 19906 for probabilistic assessment of global sea ice loads on offshore structures encountering first-year sea ice. *2014 Oceans - St. John's*, 1–8. <https://doi.org/10.1109/OCEANS.2014.7003190>
- Vanem, E. (2016). Joint statistical models for significant wave height and wave period in a changing climate. *Marine Structures*, 49, 180–205. <https://doi.org/10.1016/j.marstruc.2016.06.001>
- Venturella, M. A., Patil, M. J., & McCue, L. S. (2011). Modal Analysis of the Ice-Structure Interaction Problem. *Journal of Offshore Mechanics and Arctic Engineering*, 133(4). <https://doi.org/10.1115/1.4003388>
- Wang, D., Qiu, H., Gao, L., & Jiang, C. (2021). A single-loop Kriging coupled with subset simulation for time-dependent reliability analysis. *Reliability Engineering & System Safety*, 216, 107931. <https://doi.org/10.1016/j.res.2021.107931>
- Wang, L., Liu, Y., & Li, M. (2022). Time-dependent reliability-based optimization for structural-topological configuration design under convex-bounded uncertain modelling. *Reliability Engineering & System Safety*, 221, 108361. <https://doi.org/10.1016/j.res.2022.108361>
- Wang, Y., Liu, G., Guo, E., & Yun, X. (2018). Quantitative Agricultural Flood Risk Assessment

- Using Vulnerability Surface and Copula Functions. *Water*, 10(9), 1229. <https://doi.org/10.3390/w10091229>
- Wei, K., Arwade, S. R., Myers, A. T., Hallowell, S., Hajjar, J. F., & Hines, E. M. (2015). Performance Levels and Fragility for Offshore Wind Turbine Support Structures during Extreme Events. *Structures Congress 2015*, 1891–1902. <https://doi.org/10.1061/9780784479117.163>
- Xu, N., Yuan, S., Liu, X., Ma, Y., Shi, W., & Zhang, D. (2020). Risk assessment of sea ice disasters on fixed jacket platforms in Liaodong Bay. *Natural Hazards and Earth System Sciences*, 20(4), 1107–1121. <https://doi.org/10.5194/nhess-20-1107-2020>
- Yang, R., Khan, F., Taleb-Berrouane, M., & Kong, D. (2020). A time-dependent probabilistic model for fire accident analysis. *Fire Safety Journal*, 111. <https://doi.org/10.1016/j.firesaf.2019.102891>
- Yang, Y., Peng, J., Cai, C. S., Zhou, Y., Wang, L., & Zhang, J. (2022). Time-dependent reliability assessment of aging structures considering stochastic resistance degradation process. *Reliability Engineering & System Safety*, 217, 108105. <https://doi.org/10.1016/j.ress.2021.108105>
- Yarveisy, R., Gao, C., & Khan, F. (2020). A simple yet robust resilience assessment metrics. *Reliability Engineering & System Safety*, 197, 106810. <https://doi.org/10.1016/j.ress.2020.106810>
- Yin, J., Ren, X., Liu, R., Tang, T., & Su, S. (2022). Quantitative analysis for resilience-based urban rail systems: A hybrid knowledge-based and data-driven approach. *Reliability Engineering & System Safety*, 219, 108183. <https://doi.org/10.1016/j.ress.2021.108183>
- Yodo, N., & Wang, P. (2016). Resilience Modelling and Quantification for Engineered Systems Using Bayesian Networks. *Journal of Mechanical Design*, 138(3). <https://doi.org/10.1115/1.4032399>
- Yoo, C., & Cho, E. (2018). Vulnerability Assessment of Dam Water Supply Capacity Based on Bivariate Frequency Analysis Using Copula. *Water*, 10(9), 1113. <https://doi.org/10.3390/w10091113>
- Zarei, E., Gholamizadeh, K., Khan, F., & Khakzad, N. (2022). A dynamic domino effect risk analysis model for rail transport of hazardous material. *Journal of Loss Prevention in the Process Industries*, 74, 104666. <https://doi.org/10.1016/j.jlp.2021.104666>
- Zarei, E., Khan, F., & Yazdi, M. (2021). A dynamic risk model to analyze hydrogen infrastructure. *International Journal of Hydrogen Energy*, 46(5), 4626–4643. <https://doi.org/10.1016/j.ijhydene.2020.10.191>
- Zarei, E., Ramavandi, B., Darabi, A. H., & Omidvar, M. (2021). A framework for resilience assessment in process systems using a fuzzy hybrid MCDM model. *Journal of Loss Prevention in the Process Industries*, 69, 104375. <https://doi.org/10.1016/j.jlp.2020.104375>
- Zarghami, S. A., & Dumrak, J. (2021). Aleatory uncertainty quantification of project resources

- and its application to project scheduling. *Reliability Engineering & System Safety*, 211, 107637. <https://doi.org/10.1016/j.res.2021.107637>
- Zeng, Z., Fang, Y.-P., Zhai, Q., & Du, S. (2021). A Markov reward process-based framework for resilience analysis of multistate energy systems under the threat of extreme events. *Reliability Engineering & System Safety*, 209, 107443. <https://doi.org/10.1016/j.res.2021.107443>
- Zhang, D., Du, F., Huang, H., Zhang, F., Ayyub, B. M., & Beer, M. (2018). Resiliency assessment of urban rail transit networks: Shanghai metro as an example. *Safety Science*, 106, 230–243. <https://doi.org/10.1016/j.ssci.2018.03.023>
- Zhang, X.-Y., Lu, Z.-H., Wu, S.-Y., & Zhao, Y.-G. (2021). An Efficient Method for Time-Variant Reliability including Finite Element Analysis. *Reliability Engineering & System Safety*, 210, 107534. <https://doi.org/10.1016/j.res.2021.107534>
- Zhang, Yanping, Cai, B., Liu, Y., Jiang, Q., Li, W., Feng, Q., Liu, Y., & Liu, G. (2021). Resilience assessment approach of mechanical structure combining finite element models and dynamic Bayesian networks. *Reliability Engineering & System Safety*, 216, 108043. <https://doi.org/10.1016/j.res.2021.108043>
- Zhang, Yi, Beer, M., & Quek, S. T. (2015). Long-term performance assessment and design of offshore structures. *Computers & Structures*, 154, 101–115. <https://doi.org/10.1016/j.compstruc.2015.02.029>
- Zhang, Yi, Gomes, A. T., Beer, M., Neumann, I., Nackenhorst, U., & Kim, C.-W. (2019). Reliability analysis with consideration of asymmetrically dependent variables: Discussion and application to geotechnical examples. *Reliability Engineering & System Safety*, 185, 261–277. <https://doi.org/10.1016/j.res.2018.12.025>
- Zhang, Yi, Kim, C.-W., Beer, M., Dai, H., & Soares, C. G. (2018). Modelling multivariate ocean data using asymmetric copulas. *Coastal Engineering*, 135, 91–111. <https://doi.org/10.1016/j.coastaleng.2018.01.008>
- Zhang, Yi, & Lam, J. S. L. (2015). Reliability analysis of offshore structures within a time varying environment. *Stochastic Environmental Research and Risk Assessment*, 29(6), 1615–1636. <https://doi.org/10.1007/s00477-015-1084-7>
- Zhou, L., Gao, J., & Li, D. (2019). An engineering method for simulating dynamic interaction of moored ship with first-year ice ridge. *Ocean Engineering*, 171, 417–428. <https://doi.org/10.1016/j.oceaneng.2018.11.027>
- Zuniga, M. M., Murangira, A., & Perdrizet, T. (2021). Structural reliability assessment through surrogate based importance sampling with dimension reduction. *Reliability Engineering & System Safety*, 207, 107289. <https://doi.org/10.1016/j.res.2020.107289>

CHAPTER 5

A MULTIVARIATE MODEL TO ESTIMATE ENVIRONMENTAL LOAD ON AN OFFSHORE STRUCTURE

Preface

A version of this chapter has been submitted to the journal of *Ocean Engineering*. As the primary author, I work with my co-authors: Dr. Faisal Khan, Dr. Salim Ahmed, Dr. Bruce Colbourne, and Dr. Mohammed Taleb-Berrouane. I conducted a literature review and developed the conceptual framework for the multivariate model considering correlated marine environmental variables in higher dimensions. I prepared the first manuscript draft and revised the manuscript based on the co-authors' and reviewers' feedback. Co-author Dr. Faisal Khan assisted in the idea formulation, development of the concept, and methodology design, reviewed and edited the manuscript draft, and acted as the corresponding author for the manuscript. Co-authors Dr. Salim Ahmed, Dr. Bruce Colbourne, and Dr. Mohammed Taleb-Berrouane provided valuable support and input in reviewing and revising the manuscript draft. These co-authors also assisted in validating, reviewing, and correcting the model and results.

Abstract

Offshore structures such as oil platforms are subjected to significant environmental loads caused by wind, waves, and current. The complexity of offshore environment requires robust and reliable models to capture dependencies among environmental variables. A vine copula is a powerful tool that can be used to construct multivariate models by decomposing the complex structure into a series of simple pair copulas. Previous studies have shown that simple and symmetric copulas can be used as building blocks to construct vine copula models. In this study, symmetric and asymmetric copula functions are considered building blocks to capture all possible dependency structures. The c-vine model is then used to estimate the total environmental load on an offshore structure. Estimated loads are compared with those using the traditional independent variable approach and a multi-Gaussian distribution function-based method. The results reveal that both symmetric and asymmetric copula functions can be fitted to build c-vine copula models for the trivariate case. C-vine copulas, constructed using asymmetric copulas, provide a better estimation of the total environmental load than the independent and multivariate Gaussian methods. The result of this study is useful in probabilistic structural analysis of offshore structures for design and resilience analysis.

Keywords: vine copula, environmental load, complex dependency structure, multivariate analysis

5.1 Introduction

Offshore structures such as oil platforms, drill-ships, and Floating Production, Storage and Offloading systems (FPSO) are designed to operate in harsh marine environments. The design of offshore structures requires comprehensive knowledge of environmental variables during their construction and lifetime (Fazeres-Ferradosa et al., 2018). These structures also operate for long

periods of time and this makes them vulnerable to extreme environmental loads (Zhao and Dong, 2020) and degradation processes (Taleb-Berrouane et al., 2021), which can cause severe damage (Yang et al., 2020). Failure of offshore structures can also be caused by the occurrence of a combination of environmental variables in a single disruptive event (Deyab et al., 2018; Salvadori and De Michele, 2010; Shooter et al., 2022). Environmental loads are estimated based on a selection of design criteria; thus, offshore structures' design and operation require a detailed analysis of expected environmental parameters.

Marine environmental variables are interdependent, and their interactions should be included in any analysis. A robust and accurate multivariate model can capture the interdependence of the marine environmental variables (Ma and Zhang, 2022; Montes-Iturrizaga and Heredia-Zavoni, 2016; Sadegh et al., 2017). Although the probability of extreme marine events is low, such events can cause severe consequences to the structures. In the past, wind and wave loads were assumed to be two independent variables and univariate distributions were used (Wei et al., 2021) in their analysis. However, this assumption does not reflect real-life conditions. Marine natural hazards may involve several environmental variables. Their occurrence is also interdependent. Some current codes and standards, such as DNV-RP-C203, API-RP-2FPS and API-RP-2A-WSD, require consideration of the combined effects of wind, wave, and current acting on an offshore structure (Ma and Zhang, 2022). This simultaneous occurrence of marine environmental variables should be considered by obtaining accurate information and developing representative models of their interdependent relationship. Thus, a multivariate joint probability distribution should better capture the true characteristics of marine environmental variables.

There have been several studies dealing with the modelling of environmental variables. Modelling extreme environmental variables has also attracted much research attention recently (Lin-Ye et al.,

2017; Mazas, 2019). Cheng et al. (2019) proposed a long-term joint probability distribution for environmental conditions in Norway, which was modeled in terms of wind speed, significant wave height and wave period. Sandvik et al. (2019) evaluated three long-term wave models for their effects on a ship and marine structures. They showed that the models were able to describe design performance but unable to represent the physical process completely. Horn et al. (2018) modeled a joint distribution for environmental variables suitable for the long-term probabilistic design of offshore wind turbines and other stationary structures. Lian et al. (2013) utilized the Gumbel copula to model the joint probability of rainfall and tidal level in regions of China subject to typhoons. De Michele et al. (2007) and Zhang et al. (2018) used Copula functions to model environmental variables and captured their dependency structures. In the geotechnical area, bivariate copulas were used to model the dependence structure of shear strength parameters and to evaluate the reliability of geotechnical structures (Li et al., 2015; Wang and Li, 2019; Wu, 2015). However, these studies only focused on a bivariate case of environmental variables. In practice, an extreme marine weather event involves more than two variables whose occurrences are correlated between one another. Failure to capture this dependency may lead to non-conservative designs and/or unexpected load events. Traditional copulas are not sufficiently flexible to capture complex dependencies in high-dimensional modelling (Li and Zhang, 2020; Xu et al., 2020). In addition, previous studies on the impact of multiple loads acting on a structure mainly focus on bivariate distribution models (Zhao and Dong, 2020). Currently available standards such as ISO-19901, DNVGL-RP-C205, DNVGL-RP-C203 and DNVGL-RP-210 do not provide adequate information for multivariate models of marine environmental variables (S. Zhang et al., 2019). Thus, a joint probability distribution that fits three or more variables is necessary in this area.

Several researchers have contributed to multivariate statistical analysis of marine environmental conditions. Mackay & Johanning (2018) proposed a multivariate model for ocean parameters using a generalized extreme value model. Petrov et al. (2013) compared maximum entropy (MaxEnt) to provide a framework for extreme value theory. The model was able to predict extreme values of significant wave heights and concluded that MaxEnt was more stable with changes in different thresholds. De Leo et al. (2021) developed a multivariate model for sea states based on Non-stationary Extreme Value Analysis (NEVA) by considering trends in time series data. However, the proposed model required an assumption of linearity for the selected variables. Shooter et al. (2022) proposed a multivariate model using multivariate spatial conditional extreme (MSCE). This model was based on non-linear regression analysis and the marginal distributions were required to follow normal distribution. Agarwal et al. (2022) proposed a trivariate model using a cubic spine model in time, representing it as a linear combination function. The proposed model was able to highlight the non-convex features of the joint distribution. Dong et al. (2015) developed trivariate maximum entropy distribution (MED) of significant wave height, wind speed and relative direction. The model provided a good fit for available environmental data. However, the model was based on the Nataf transformation, and the Nataf transformation is only appropriate for data showing linearity and marginal distributions that are assumed to follow Gaussian distribution (Li and Zhang, 2020). From these studies, the standard and commonly used joint statistical methods to model multivariate data are not generally sufficient for the more complex relationships evident in marine environmental variables. Therefore, a more robust and advanced statistical method is needed to model multivariate ocean data. Copula theories have gained attention as a means to address this issue. Ganguli and Reddy (2013) proposed a copula-based methodology for assessing flood risks and evaluated the performance of trivariate copulas in capturing the dependency

structure of flood variables. Bezak et al. (2014) studied trivariate frequency analyses of peak discharge, hydrocarbon volume and suspended sediment concentration using copula functions and concluded that copula functions are a useful mathematical tool. Due to their flexibility in capturing dependency structures, copula functions are beneficial in modelling marine environmental variables (De Michele et al., 2007; Dong et al., 2017; Ramadhani et al., 2021; Salleh et al., 2016; Y. Zhang et al., 2015; Zhang et al., 2018). Copula functions can also be integrated with other techniques to build hybrid models, such as the Copula Bayesian Network (CBN) (Elidan, 2010). The latter combines the modelling capabilities of complex dependencies provided by the Copula function and the conditional probability distribution provided by Bayesian network (Taleb-berrouane et al., 2018; Taleb-Berrouane et al., 2017; Taleb Berrouane, 2020).

To model more than two variables, the vine copula is introduced. This allows much more flexibility based on a graphical model used to construct multivariate models from pair copulas (Bedford et al., 2016). Wei et al. (2021) used vine copulas to construct a trivariate joint probability model of typhoon-induced wind, waves, and the time lag between them. Heredia-Zavoni & Montes-Iturrizaga (2019) constructed directional environment contours using vine copulas. They noted that the vine copula is advantageous in modelling multivariate distributions using bivariate copulas that capture pairwise dependencies between environmental parameters. Amini et al. (2021) and Tang et al. (2020) utilized vine copulas to estimate the reliability of physical structures. Bai et al. (2021) and Heredia-Zavoni & Montes-Iturrizaga (2019) used a vine copula to construct three-dimensional environmental contours. Dong et al. (2022) and Xu et al. (2020) modeled the multivariate analysis of loads on wind turbines using vine copulas. They concluded that vine copulas were able to capture the dependency among multiple variables in wind turbine analysis. Nagler et al. (2022) investigated vine copulas to determine their ability to capture different types

of dependency. It was concluded that copulas were able to capture both cross-sectional and serial dependency. Qian and Dong (2022) incorporated copula functions to assess surrogate-assisted seismic performance. A vine copula model was able to characterize the complete non-linear dependency structure of the investigated variables. Tao et al. (2021) predicted daily water temperatures of the Yangtze River using a vine copula model and concluded that the proposed model could perform better than a logarithmic model. Zhao et al. (2021) used a Gaussian copula model to estimate the characteristics of extreme response for a mooring system in a complex ocean environment. Vine copulas were also used in assessing reliability of geotechnical structures. Vine copulas were used to model the dependence structure of multiple soil parameters (Lü et al., 2020; Tang et al., 2020; Xu and Zhou, 2018; Y. Zhang et al., 2019). Copula functions were found to provide better results for reliability-based design of geotechnical structure (Lü et al., 2020). Vine copulas are also able to provide more flexible ways for geotechnical practitioners to model the cross-correlation among geotechnical random fields (Tang et al., 2020). From these studies, Vine copulas are shown to be able to fully define complex dependency structures between many observed variables. Vine copulas are also able to model dependency in higher dimensions, which traditional copulas cannot do. However, the multivariate copula models used in the vine copulas in these studies are mostly based on well-established copula functions. These copula functions are usually simple and symmetrical one-parameter copulas such as the Archimedean copula family (Jiang et al., 2021; Yang and Qian, 2019).

This work presents copula-based trivariate environmental load estimation for offshore structures. Vine copulas are used to model the multivariate analysis. Symmetric and asymmetric copula functions for use within the vine copula structure are compared to identify the best-fitted functions in trivariate analysis. The objectives of this study are as follows: (1) to construct a trivariate joint

distribution model of significant wave height, wind speed, and current velocity using symmetrical and asymmetrical vine copulas, and (2) to compare the estimated environmental load obtained from vine copulas and other traditional methods in a case study.

The remainder of this chapter is organized as follows. Section 5.2 presents the methodology and the basic theories used in developing the multivariate model. The application of the multivariate copula models is discussed in Section 5.3. Results and discussions from the estimation of total environmental load are presented in Section 5.4. The concluding remarks of this chapter are presented in Section 5.5.

5.2 Proposed Methodology of the Multivariate Model

The proposed method used to construct the multivariate model of environmental variables is illustrated in Fig. 5.1. Environmental variables are collected from a historical data set. Dependency measures are carried out to estimate the correlation coefficient between variables. C-vine copula with wind speed as the dominating factor is then generated and the best copula function for each edge is identified. Environmental variables data are generated using vine copulas constructed from different copula functions. Total environmental load is estimated to assess the effectiveness of the multivariate model using vine copulas.

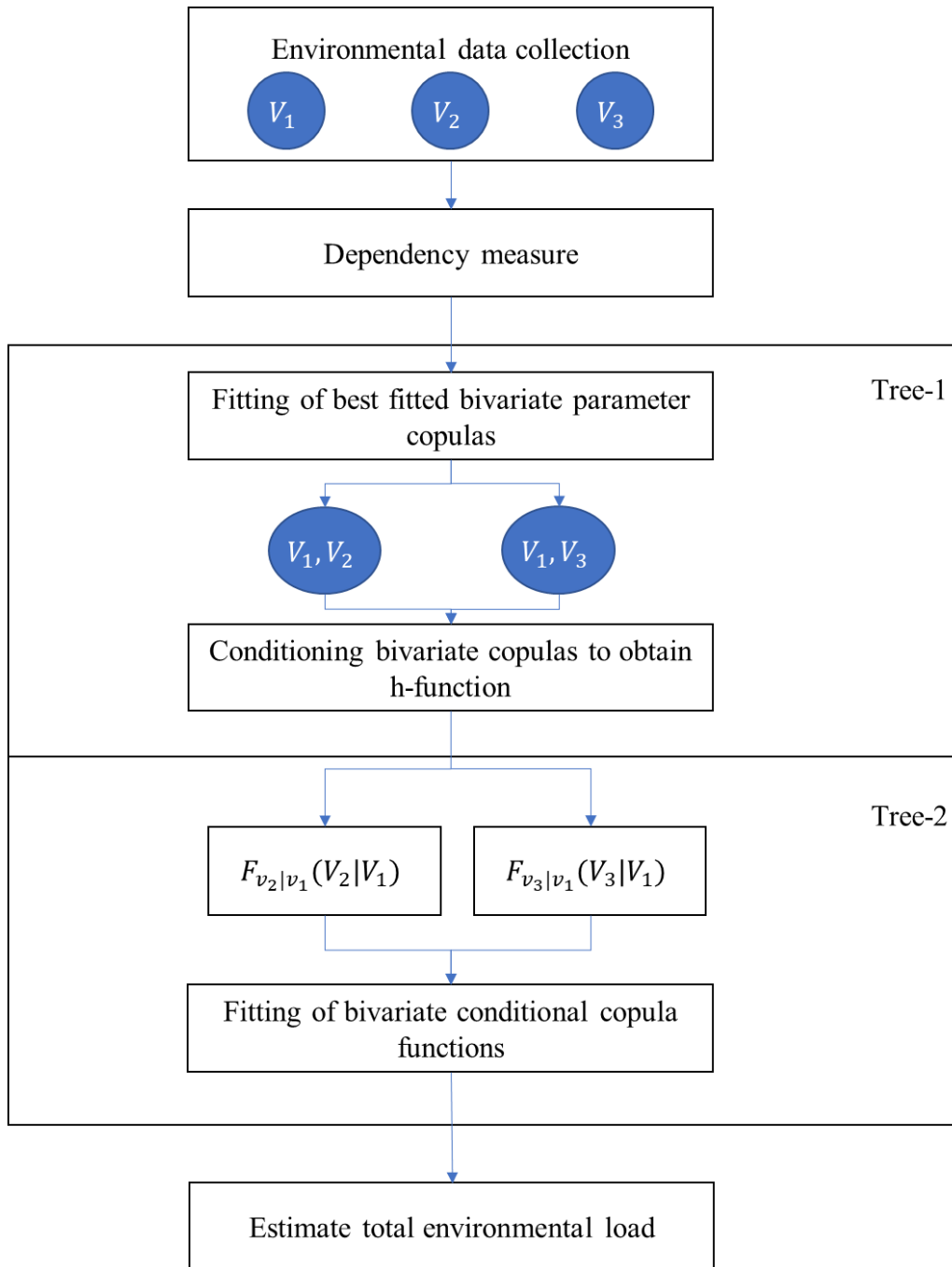


Fig. 5.1. Proposed methodology to develop a multivariate model to estimate the total environmental load

5.2.1 Copula theory

Copula functions are used here to model multivariate ocean parameters. Uni-variate marginal distributions are “coupled” or “joined” to construct multivariate distributions. The formal definition of a copula was firstly introduced in Sklar’s Theorem (Nelsen, 2006). Let H be an n -dimensional distribution function with marginal distribution F_1, F_2, \dots, F_n , then there exists a copula C such that.

$$H(x_1, x_2, \dots, x_n) = C(F_1(x_1), F_2(x_2), \dots, F_n(x_n)) \quad (5.1)$$

Based on this theorem, when used to construct multivariate models, copula models do not consider the character of the univariate marginal distributions. Detailed studies on copula functions and their application to bivariate cases were carried out previously (Ramadhani et al., 2022, 2021). In this chapter, multivariate models constructed using vine copulas are studied.

5.2.2 Construction of asymmetric copulas

There are various ways to construct asymmetric copulas, such as 1) asymmetric copulas constructed by product, 2) asymmetric copulas constructed by linear convex combination, and 3) skewed copulas (Zhang et al., 2018). The construction of asymmetric copulas using by product rule was concluded to be the best to represent ocean parameters and more practical for a complex engineering system (Zhang et al., 2018). Liebscher (2008) first introduced this by product rule through the following theorem

“Assume that C_1, \dots, C_k : are copulas. Let $g_{ji}: [0,1] \rightarrow [0,1]$ for $j = 1, \dots, k, i = 1, \dots, d$ be functions with the property that each of them is strictly increasing or identically equal to 1.”

Then the general equation to construct asymmetric copulas by product is defined by

$$\bar{C}(u_1, \dots, u_d) = \prod_{j=1}^k C_j(g_{j1}(u_1), \dots, g_{jd}(u_d)) \quad \text{for } u_i \in [0,1] \quad (5.2)$$

To satisfy the assumptions of the theorem, the function g_{ji} should have these following properties

- d) $g_{ji}(1) = 1$ and $g_{ji}(0) = 0$,
- e) g_{ji} is continuous on $(0,1]$,
- f) If there are at least two functions g_{j_1i}, g_{j_2i} with $1 \leq j_1, j_2 \leq k$ which are not identically equal to 1, then $g_{ji}(x) > x$ holds for $x \in (0,1), j = 1, \dots, k$

The function g_{ji} plays a significant role in constructing symmetric copulas into asymmetric copulas.

In this chapter, Type-1 individual function g_{ji} , is used, where

$$(IV) \quad g_{ji}(v) = v^{\theta_{ji}} \text{ for } j = 1, \dots, k, \text{ where } \theta_{ji} \in [0,1] \text{ and } \sum_{j=1}^k \theta_{ji} = 1 \quad (5.3)$$

Archimedean copulas are used as the basis copula functions to construct asymmetric copulas.

5.2.3 Vine copula

The vine copula is used to model multiple random variables. The idea is to decompose a joint probability distribution function of multivariate random variables into a product of its marginal distribution, and unconditional pair and a conditional pair. For example, let X_1, X_2, \dots, X_n denote random variables with their joint probability density function (PDF) $f(x_1, x_2, \dots, x_n)$. This joint PDF can be decomposed to

$$f(x_1, x_2, \dots, x_n) = f_n(x_n) \cdot f(x_{n-1} \vee x_n) \cdot f(x_{n-2} \vee x_{n-1}, x_n) \dots f(x_1 \vee x_2, \dots, x_n) \quad (5.4)$$

Where the conditional PDF can be expressed by (Tang et al., 2020)

$$f(x \vee v) = c(F(x \vee v_{-m}), F(v_m \vee v_{-m}); \theta_{x, v_m \vee v_{-m}}) f(x \vee v_{-m}) \quad (5.5)$$

Where $c(\cdot, \cdot; \theta)$ is the bivariate copula density function, v_m is an arbitrarily selected component from vector \mathbf{v} , and v_{-m} is the vector \mathbf{v} excluding v_m .

The conditional cumulative distribution function (CDF) can then be expressed as

$$F(x \vee v) = \frac{\partial C(F(x \vee v_{-m}), F(v_m \vee v_{-m}); \theta_{x, v_m \vee v_{-m}})}{\partial F(v_m \vee v_{-m})} \quad (5.6)$$

This partial derivative of the copula function is also called the h-function $h(F(x \vee v_{-m}), F(v_m \vee v_{-m}); \theta_{x, v_m \vee v_{-m}})$.

When modelling multiple random variables using a vine copula, a graphical model is used to help with the complexity of modelling in a high-dimensional distribution. This graphical model is called a regular vine (Aas et al., 2009). In general, a d-dimensional vine copula is a pair-copula consisting of $d(d-1)/2$ unconditional and conditional bivariate copulas, where the structure can be expressed as a set of linked trees T_1, T_2, \dots, T_{d-1} that also satisfies (Kraus and Czado, 2017)

1. $T_1 = (V_1, E_1)$ is Tree 1 with nodes $V_1 = \{1, 2, \dots, d\}$ and edges E_1 .
2. For $m = 2, \dots, d - 1$, tree T_m has nodes $V_m = E_{m-1}$ and edges E_m .
3. For $m = 2, \dots, d - 1$, two nodes of T_m can be linked by an edge if these nodes have a shared node with the corresponding edges of T_{m-1} .

Canonical vine (C-vine) and Drawable vine (D-vine) copulas are two additional types of regular vine. In C-vine, each node has a unique node connected to other nodes, whereas, in D-vine, each node is only connected to one or two other nodes and each tree is a path.

Generally, a joint PDF of d-dimensional random variables can be decomposed using a C-vine that satisfies the following equation (Czado, 2019)

$$f(x_1, \dots, x_d) = \left[\prod_{j=1}^{d-1} \prod_{i=1}^{d-j} c_{j, j+i; 1, \dots, j-1} \right] \times \left[\prod_{k=1}^d f_k(x_k) \right] \quad (5.7)$$

While decomposition using a D-vine can be expressed using the equation below (Czado, 2019)

$$f(x_1, \dots, x_d) = \left[\prod_{j=1}^{d-1} \prod_{i=1}^{d-j} c_{i, (i+j); (i+1), \dots, (i+j-1)} \right] \times \left[\prod_{k=1}^d f_k(x_k) \right] \quad (5.8)$$

When there is one variable known to be a dominating factor, the C-vine will be advantageous as data interaction is considered. C-vine copulas are thus more suitable for environmental variables with one dominating factor. The construction of a C-vine for three variables will be shown in this chapter. The bivariate copulas considered in this chapter are Archimedean copulas (Clayton, Gumbel and Frank) and the constructed asymmetric copulas (Clayton-Gumbel Type-1, Clayton-Frank Type-1 and Gumbel-Frank Type-1). Fig. 5.2 shows a graphical model of three variables with one dominating factor as follows

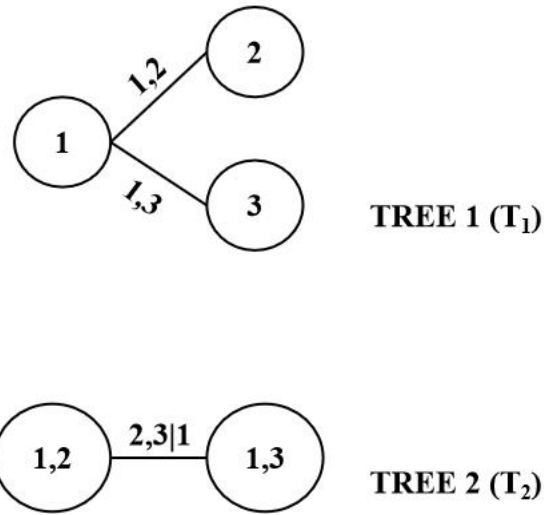


Fig. 5.2. A graphical model of C-Vine with three variables

Steps to construct C-vine copula for three variables with one dominating factor are as follows (Lü et al., 2020)

1. Determine the marginal PDF of each variable.
2. Identify the best-fit bivariate copula for Tree 1
 - a) Original data are transformed into the copula domain

$$U_i = \frac{R_i}{n+1} = \frac{n\hat{F}_i(X_i)}{n+1} \tag{5.9}$$

where n is the number of observations and \hat{F}_i is the empirical cumulative function defined as

$$\hat{F}_i(t) = \frac{1}{n} \sum_{i=1}^n 1(X_i \leq t).$$

- b) Copula parameter estimation using Maximum Log-likelihood Estimation (MLE). The log-likelihood function $L(\theta)$ of a copula function can be expressed as (Lü et al., 2020)

$$L(\theta) = \sum_{i=1}^N \ln c(u_1, u_2; \theta) \quad (5.10)$$

The estimated $\hat{\theta}$ using MLE can be obtained by maximizing $L(\theta)$ (Lü et al., 2020)

$$\hat{\theta} = \operatorname{argmax} L(\theta) \quad (5.11)$$

- c) Select the best-fit copula using AIC scores. (Lü et al., 2020)

$$AIC = -2L(\hat{\theta}) + 2k = -2 \sum_{i=1}^N \ln c(u_{1i}, u_{2i}; \hat{\theta}) \quad (5.12)$$

Where k is the unknown parameter estimated using MLE. The best-fit copula is indicated by the lowest AIC score.

2. Identify the best-fit bivariate copula for the next tree (Tree 2)

Tree 2 consists of $f(x_2, x_3 \vee x_1) = C_{2,3 \vee 1}(F_{2 \vee 1}(x_2 \vee x_1), F_{3 \vee 1}(x_3 \vee x_1); \theta)$

- a) Data $\{F_2(x_{2i}), F_1(x_{1i}), i = 1, 2, \dots, N\}$ are transformed into data $\{F_{2 \vee 1}(x_{2i} \vee x_{1i}), i = 1, 2, \dots, N\}$ using h function (a partial derivative of bivariate copula with respect to the given variable), where (Lü et al., 2020)

$$h(u_2 \vee u_1; \theta) = \frac{\partial C(u_1, u_2; \theta)}{\partial u_1} \quad (5.13)$$

So, $\{F_{2v1}(x_{2i} \vee x_{1i}) = h_{1,2}(F_2(x_{2i}), F_1(x_{1i}); \theta), i = 1, 2, \dots, N\}$

- b) Data $\{F_3(x_{3i}), F_1(x_{1i}), i = 1, 2, \dots, N\}$ are also transformed to data $\{F_{3v1}(x_{3i} \vee x_{1i}), i = 1, 2, \dots, N\}$ using its h function, resulting in $\{F_{3v1}(x_{3i} \vee x_{1i}) = h_{1,3}(F_3(x_{3i}), F_1(x_{1i}); \theta), i = 1, 2, \dots, N\}$
- c) Based on $\{F_{2v1}(x_{2i} \vee x_{1i}), F_{3v1}(x_{3i} \vee x_{1i})\}$, select the best-fit copula for $C_{2,3|1}$.

3. Perform the same procedure if there are more trees

4. Obtain the joint PDF. For trivariate analysis, the joint PDF will be decomposed as follows

$$f(x_1, x_2, x_3) = f(x_1) \cdot f(x_2) \cdot f(x_3) \cdot C_{1,2}\{F(x_1), F(x_2)\} \cdot C_{1,3}\{F(x_1), F(x_3)\} \cdot C_{2,3v1}\{F(x_2 \vee x_1), F(x_3 \vee x_1)\}$$

5.2.3.1 Data simulation using vine copula

To generate simulated samples from the constructed probability distribution function (PDF) $f_{1,2,\dots,n}(y_1, y_2, \dots, y_n)$, random sampling can be performed. Let (y_1, y_2, \dots, y_n) denote a simulated data sample from $f_{1,2,\dots,n}(y_1, y_2, \dots, y_n)$ and (r_1, r_2, \dots, r_n) is a sample independent standard, uniform on $[0,1]$. A Rosenblatt transformation is then used to generate (y_1, y_2, \dots, y_n) based on (r_1, r_2, \dots, r_n) (Lü et al., 2020):

- 1) Solving y_1 . Let $r_1 = F_1(y_1)$. Then, $y_1 = F_1^{-1}(r_1)$ is obtained.
- 2) Solving y_2 . Let $r_2 = F_{2v1}(y_2|y_1) = h_{2,1}(F_2(y_2), F_1(y_1); \theta)$. Then, $y_2 = F_2^{-1}\left(h_{2v1}^{-1}(r_2, F_1(y_1); \theta)\right)$ is obtained.
- 3) Solving y_3 . Let $r_3 = F_{3v1,2}(y_3|y_1, y_2) = h_{3,1v2}(F_{3v2}(y_3|y_2), F_{1v2}(y_1|y_2); \theta) = h_{3,1v2}(h_{3v2}(F_3(y_3), F_2(y_2); \theta), h_{1v2}(F_1(y_1), F_2(y_2); \theta); \theta)$. Then, $y_3 = F_3^{-1}\left(h_{3,2}^{-1}\left(h_{3,1v2}^{-1}(r_3, h_{1,2}(F_1(y_1), F_2(y_2); \theta); \theta), F_2(y_2); \theta)\right)\right)$ is obtained.

5.2.4 Total environmental load

The total environmental load acting on a structure is estimated using

$$F_{Tot} = \sum \psi_i F_i \quad (5.14)$$

where, ψ_i are the factors for load combination (Yu. Shmal et al., 2020). Three environmental loads considered here are wind, wave, and current loads

The wind force on a structural member or surface acting normal to the member axis is calculated using (Jacomet et al., 2021)

$$F_{wind} = CqA \sin \alpha \quad (5.15)$$

where

C = shape coefficient

q = basic wind pressure or suction

A = projected area of the member normal to the direction of the wind velocity

α = angle between wind direction and the member axis

Basic wind pressure can be estimated using

$$q = \frac{1}{2} \rho_a U_z^2 \quad (5.16)$$

where, ρ_a is the mass density of air and U_z is the wind velocity profile estimated using the following equation

$$U_z = U_{z_0} \left(\frac{z}{z_0} \right)^{1/7} \quad (5.17)$$

where,

U_{z_0} = mean velocity at a reference height (m/s)

z_0 = reference height (m)

z = height above mean sea level (m)

The total wave force for a suitably slender structure, or element of a structure, is then estimated using Morison's equation (Jacomet et al., 2021; Zhang et al., 2015)

$$F_{T_{wave}} = F_I + F_D \quad (5.18)$$

$$F_{T_{wave}} = C_M \rho V \dot{u} + \frac{1}{2} C_D \rho A |u| u \quad (5.19)$$

where,

C_M and C_D are inertia and drag coefficient

ρ = water density (kg/m³)

V = volume of the body (m³)

A = reference area (m²)

u = water wave particle velocity (m/s)

\dot{u} = water wave particle acceleration (m/s²)

When calculating wave force on an offshore structure, it is also important to select the most appropriate wave theory. Water wave particle velocity and acceleration are calculated using these wave theories. Wave theories considered in this chapter can be seen in Appendix 5A.

Current loads are also commonly taken into consideration in designing offshore structures and are estimated using (Yu. Shmal et al., 2020)

$$F_{Current} = \frac{1}{2} C_D \rho A U |U| \quad (5.20)$$

where,

C_D = drag coefficient

ρ = water density

U = current velocity (m/s)

A = reference cross-sectional area

5.3 Application of the Multivariate Model

Ocean data was collected from the Smart Atlantic website (ERDDAP, 2022). Environmental data were collected from the mouth of Placentia Bay in the province of Newfoundland and Labrador (58.4160N 041.7168W) – Canada. The data were recorded hourly between January 1st 2010 and December, 31st 2020. It consists of wave height, wind speed and current velocity as specified by API 2A-WSD (American Petroleum Institute, 2002). According to this standard, the selected three ocean variables have a specific type of relationship that should be considered.

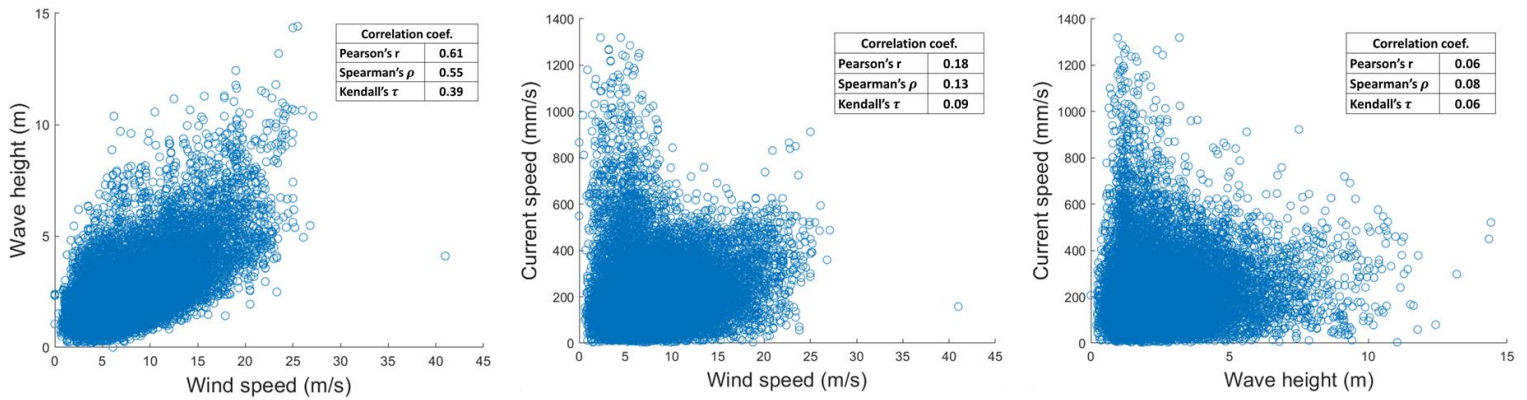


Fig. 5.3. Scatter plots for all environmental variable pairs

Table 5.1 Correlation and asymmetry measures for all pairs of environmental variables

	Pearson's linear correlation	Spearman's rho	Kendall's tau	Asymmetry Measure
Wind speed- Wave height	0.61	0.55	0.39	0.01
Wind speed- Current velocity	0.18	0.13	0.09	0.23
Wave height – Current velocity	0.06	0.08	0.06	0.24

Fig. 5.3 illustrates that each pair of ocean parameters has a positive correlation in the scatter plots. The value of the correlation for each pair is presented in Table 5.1. From this table, wind speed and wave height have a strong correlation, while wind speed - current velocity and wave height – current velocity have a weak correlation. However, although their correlations are weak, the asymmetry level for these pairs is much higher than wind-wave pair data. In this case, asymmetric copulas play an important role in modelling this measure, as pointed out in previous studies (Ramadhani et al., 2022, 2021).

Before continuing with the multivariate models, marginal distributions for each individual environmental variable are identified. The Akaike Information Criterion (AIC) parameter is used to select the best-fitted distribution among the possible distributions selected in this chapter. Table 5.2 shows the AIC values for each distribution, and Table 5.3 shows the parameter statistics for the best-fitted distribution for each environmental variable.

Table 5.2. AIC values for all ocean parameters for environmental variables

	Weibull	Normal	Lognormal	Rayleigh	Extreme Value	Exponential	Gamma
Wind speed	Inf.	104,759	Inf	102,322	112,824	114,566	101,831 ^a
Wave height	Inf	66,681	Inf	61,718	79,873	70,668	58,599 ^a
Current velocity	228,042	235,574	227,975	231,076	227,221	232,762	227,183 ^a

^aIndicates the best-fit marginal distribution

Table 5.3. Best fitted distribution parameters statistics

	Mean	Variance	Shape	Scale
Wind speed	8.36 m/s	4.21 m/s	3.94	2.12
Wave height	2.52 m	1.49 m	2.87	0.87
Current velocity	210.36 mm/s	149.38 mm/s	2.24	93.65

The smallest value of AIC indicates the best distribution model for the data set as illustrated in Table 5.2. The Gamma distribution is best fitted to all environmental variables. Kolmogorov-Smirnov (KS) tests are carried out to examine the goodness of fit of gamma distribution for all

environmental variables. The test statistic values from the KS test for wind, wave, and current data are 0.0129, 0.0062, and 0.011, respectively. These statistics show that the fitted distribution is valid (fail to reject the null hypothesis) at a significance level of 5% (critical value for KS-test is 0.0135) for each environmental variable.

5.3.1 Vine copula modelling

As mentioned previously, C-vine copulas for three variables are constructed for this model. Firstly, Archimedean family copulas are used to construct vine copulas for three environmental variables.

Table 5.4 shows the best-fitted copula function for each tree and its parameters.

Table 5.4. Best fitted symmetric copulas and their parameters for each tree

Tree	Edge	Copula	Copula Parameter	$L(\theta)$ ($\times 10^5$)	AIC ($\times 10^5$)
1	X_1, X_2	Clayton	$\gamma = 1.0165$	-4.7946	9.5891
		Gumbel	$\gamma = 1.6327$	-4.7709	9.5417 *
		Frank	$\gamma = 40795$	-4.7766	9.5532
	X_1, X_3	Clayton	$\gamma = 1.0115$	-4.8418	9.6836
		Gumbel	$\gamma = 1.0810$	-4.8094	9.6188
		Frank	$\gamma = 0.8698$	-4.8092	9.6184 *
2	$X_2, X_3 X_1$	Clayton	$\gamma = 1.0004$	-4.8561	9.7122
		Gumbel	$\gamma = 1.0021$	-4.8109	9.6218
		Frank	$\gamma = -0.2008$	-4.8108	9.6216 *

*Lowest AIC score indicates the best-fit copula

The Gumbel copula is best fitted to pair wind and wave data in the first tree, while the Frank copula is best fitted to model wind and current data, and the conditional probability, in the second tree.

Their probability distribution functions are shown in Fig. 5.4.

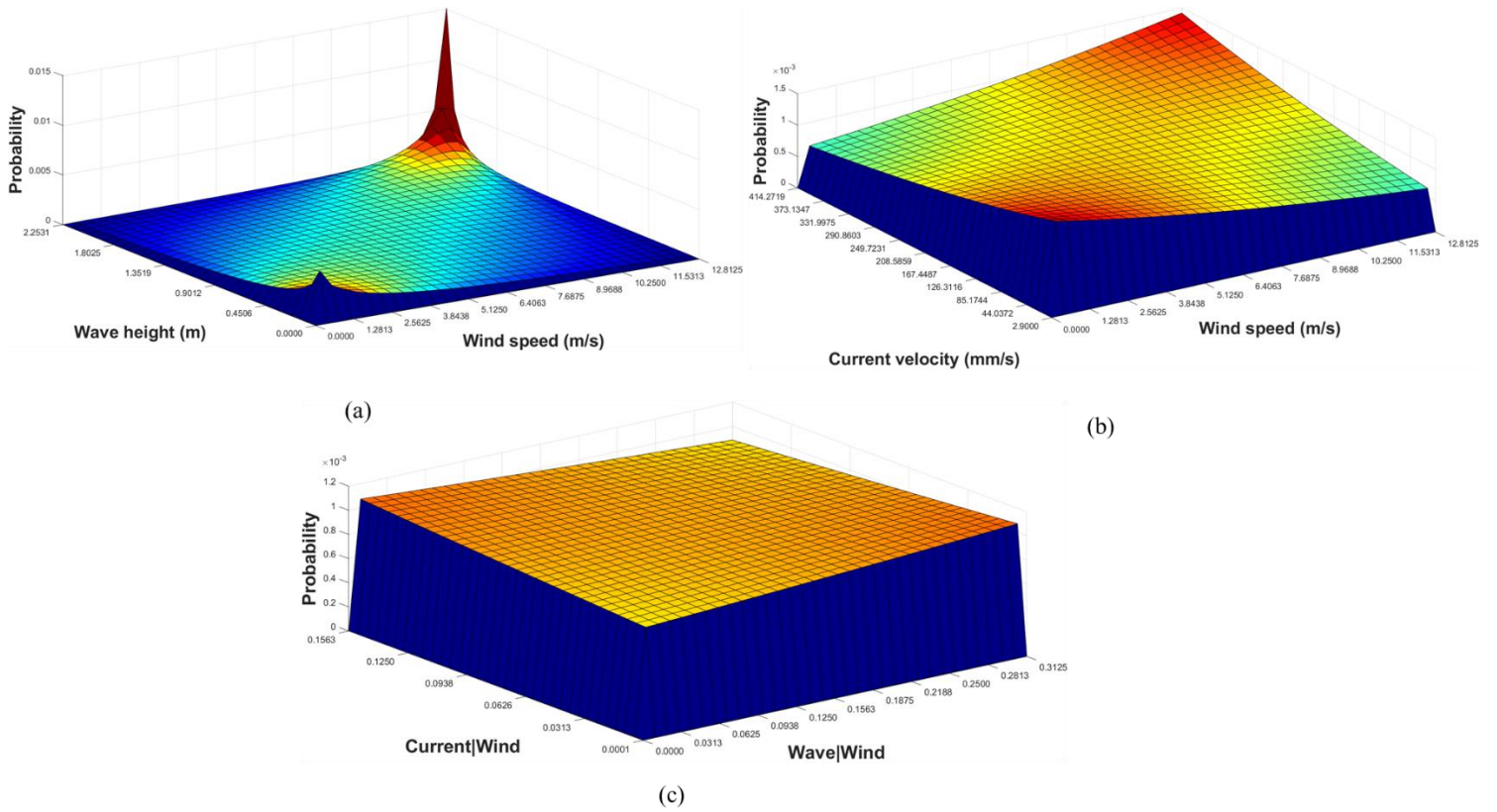


Fig. 5.4. Probability distribution functions for (a) wind and wave data in Tree 1 (Table 5.4), (b) wind and current data in Tree 1, and (c) conditional environmental data in Tree 2 (Table 5.4) using symmetric copulas

Using asymmetric copulas, the best-fitted copula function for each tree and their parameters are shown in Table 5.5.

Table 5.5. Best fitted asymmetric copulas and their parameters for each tree

Tree	Edge	Copula	Copula Parameter	$L(\theta)$ ($\times 10^5$)	AIC ($\times 10^5$)
1	X_1, X_2	Clayton-Gumbel Type-1	$\gamma_1 = 1.8032$ $\gamma_2 = 5.5582$ $\theta_{11} = 0.8976, \theta_{12} = 0.6996$ $\theta_{21} = 0.1024, \theta_{22} = 0.3004$	-3.9261	7.8522 *
		Clayton-Frank	$\gamma_1 = 2.5252$	-3.9296	7.8583

		Type-1	$\gamma_2 = 10.0215$ $\theta_{11} = 0.1216, \theta_{12} = 0.5965$ $\theta_{21} = 0.8784, \theta_{22} = 0.4035$		
		Gumbel-Frank Type-1	$\gamma_1 = 2.5754$ $\gamma_2 = 13.5428$ $\theta_{11} = 0.9478, \theta_{12} = 0.4516$ $\theta_{21} = 0.0522, \theta_{22} = 0.5484$	-3.9263	7.8527
	X_1, X_3	Clayton-Gumbel Type-1	$\gamma_1 = 1.5395$ $\gamma_2 = 1.7458$ $\theta_{11} = 0.9956, \theta_{12} = 0.1193$ $\theta_{21} = 0.0044, \theta_{22} = 0.8807$	-3.9625	7.9251
		Clayton-Frank Type-1	$\gamma_1 = 6.7539$ $\gamma_2 = -14.7535$ $\theta_{11} = 0.9545, \theta_{12} = 0.1623$ $\theta_{21} = 0.0455, \theta_{22} = 0.8377$	-3.9633	7.9267
		Gumbel-Frank Type-1	$\gamma_1 = 1.5959$ $\gamma_2 = 0.7605$ $\theta_{11} = 0.9296, \theta_{12} = 0.2078$ $\theta_{21} = 0.0704, \theta_{22} = 0.7922$	-3.9625	7.9251 *
2	$X_2, X_3 \vee X_1$	Clayton-Gumbel Type-1	$\gamma_1 = 1.1496$ $\gamma_2 = 5.2962$ $\theta_{11} = 0.6725, \theta_{12} = 0.5885$ $\theta_{21} = 0.3275, \theta_{22} = 0.4115$	-3.2710	6.5422
		Clayton-Frank Type-1	$\gamma_1 = 2.8401$ $\gamma_2 = -4.3100$ $\theta_{11} = 0.7521, \theta_{12} = 0.6344$ $\theta_{21} = 0.2479, \theta_{22} = 0.3656$	-3.2403	6.4807 *
		Gumbel-Frank Type-1	$\gamma_1 = 1.0833$ $\gamma_2 = 2.2394$ $\theta_{11} = 0.2439, \theta_{12} = 0.0118$ $\theta_{21} = 0.7561, \theta_{22} = 0.9882$	-3.2516	6.5034

*Lowest AIC score indicates the best-fit copula

The Clayton-Gumbel copula is best fitted to pair wind and wave data in the first tree, while the Gumbel-Frank copula is best fitted to model wind and current data and the Clayton-Frank copula

is best fitted for the conditional probability in the second tree. Their probability distribution functions are shown in Fig. 5.5.

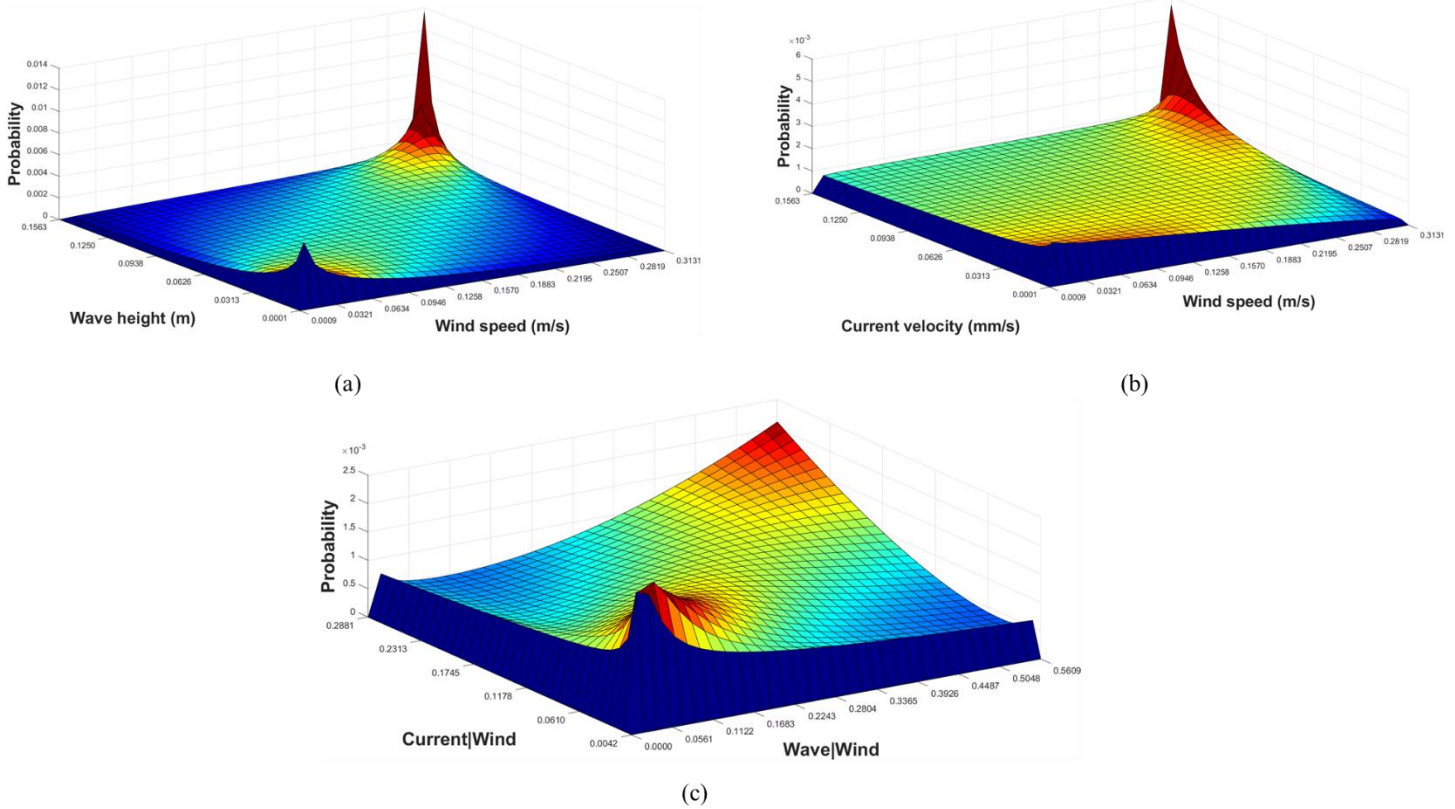


Fig. 5.5. Probability distribution functions for (a) wind and wave data in Tree 1 (Table 5.5), (b) wind and current data in Tree 1, and (c) conditional environmental data in Tree 2 (Table 5.5) using asymmetric copulas

After obtaining the parameters for the best-fitted copulas on each node, correlated data can be generated to estimate total environmental variables.

5.4 Result and Discussion

5.4.1 Model verification

In order to determine if these C-vine copulas are fit to model multivariate data, error values between real data and the copula models are calculated. Root mean square error (RMSE) and mean absolute errors are used to compare the calculation.

Table 5.6. Error values for each edge

Symmetric copulas						
Edge	Clayton		Gumbel		Frank	
	RMSE	Mean Absolute Error	RMSE	Mean Absolute Error	RMSE	Mean Absolute Error
X_1, X_2	0.0189	0.0409	0.0070	0.0248	0.0115	0.0303
X_1, X_3	0.0369	0.0415	0.0091	0.0264	0.0091	0.0261
$X_2, X_3 X_1$	0.1003	0.1676	0.1305	0.1629	0.1334	0.1696
Asymmetric copulas						
Edge	Clayton-Gumbel		Clayton-Frank		Gumbel-Frank	
	RMSE	Mean Absolute Error	RMSE	Mean Absolute Error	RMSE	Mean Absolute Error
X_1, X_2	0.0069	0.0053	0.0085	0.0061	0.0032	0.0023
X_1, X_3	0.0065	0.0046	0.0060	0.0040	0.0084	0.0064
$X_2, X_3 X_1$	0.1055	0.0798	0.1075	0.0815	0.1089	0.0834

From Table 5.6, C-vine copulas are fitted to model the multivariate data. It shows that both symmetric and asymmetric copulas can model multivariate environmental variables for each edge in all trees.

The C-vine copula was used to model the dependency structures among marine environmental variables and build trivariate joint probability distributions of these variables using bivariate copulas as the building blocks. Wind speed was selected as the dominating factor because its occurrence influenced the other two variables. Wind speed can influence both wave height and current velocity in the ocean. The results obtained in Table 5.6 are also supported by similar results in other studies. Bai et al. (2021) mentioned that the joint probability model using the vine copula is well suited to build multivariate joint models of ocean environmental parameters. Vine copulas were also able to model the statistical characteristics and complex dependency structures in higher dimensions. Lin & Dong (2019) also pointed out that their proposed model using a vine copula fits the multivariate distribution and can be used to represent wave climate. Thus, the application of vine copulas in marine environmental analysis is able to address the issue of interdependent relationships between variables in higher dimensions. The multivariate model constructed from the vine copula can also be used for further analysis.

5.4.2 Estimation of the total environmental load

To determine the significance and benefits of vine copula modelling in the multivariate case, a case study is presented in this section. A monopile steel structure with a diameter of 8 m is used as a simple structural example. The immersed part of this pile is assumed to be 30 m. The wind force is calculated at the height of 15 m above the water surface with a drag coefficient of 0.7, according to recommended practice for marine operations (Det Norske Veritas, 2011). While for wave load, inertia coefficient and drag coefficient are set to be 2 and 1, respectively (Bai, Y & Bai, Q, 2005).

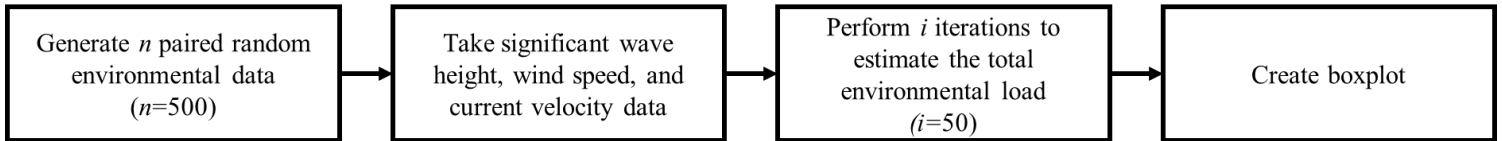


Fig. 5.6. Simulation flowchart to estimate the total environmental load

To get the total environmental load, Eq. 5.14 is used. The factors for load combination, ψ_i , for wave, wind and current load are set to be 1.0, 0.9, and 0.9 respectively. Eq. 5.15 is used to calculate the total wind forcing acting on a structure. Wind force is assumed to be perpendicular to the structure. To get the total wind force, basic wind pressure is estimated using Eq. 5.16 – 5.17, where the mass density of air, ρ_a , is assumed to be 1.226 kg/m^3 and the reference height is taken as 10 m. The total wave force is estimated using Eq. 5.18 – 5.19, where water density, ρ , is taken to be 1025 kg/m^3 . Water wave particle velocity and acceleration are estimated using the appropriate wave theory presented in Appendix 5A. Eq. 5.20 is then used to estimate the current load.

A simulation is carried out to estimate the total environmental load acting on the structure. In addition to the C-vine copula models using symmetric and asymmetric copulas, two other common methods are selected for comparison. An independent case is illustrated using marginal distribution functions for each environmental variable. The remaining method selected is commonly used for multivariate cases, a multi-gaussian distribution function. For each method, n random data are generated and iterated i times. After each simulation to generate random data, significant wave height, wind speed and current velocity are computed. This data are then used to estimate the total estimated environmental load using Eq. 5.14 – 5.20. This process is then repeated 50 times and the summary of the simulation is presented in Fig. 5.7. This simulation process is also presented in Fig. 5.6.

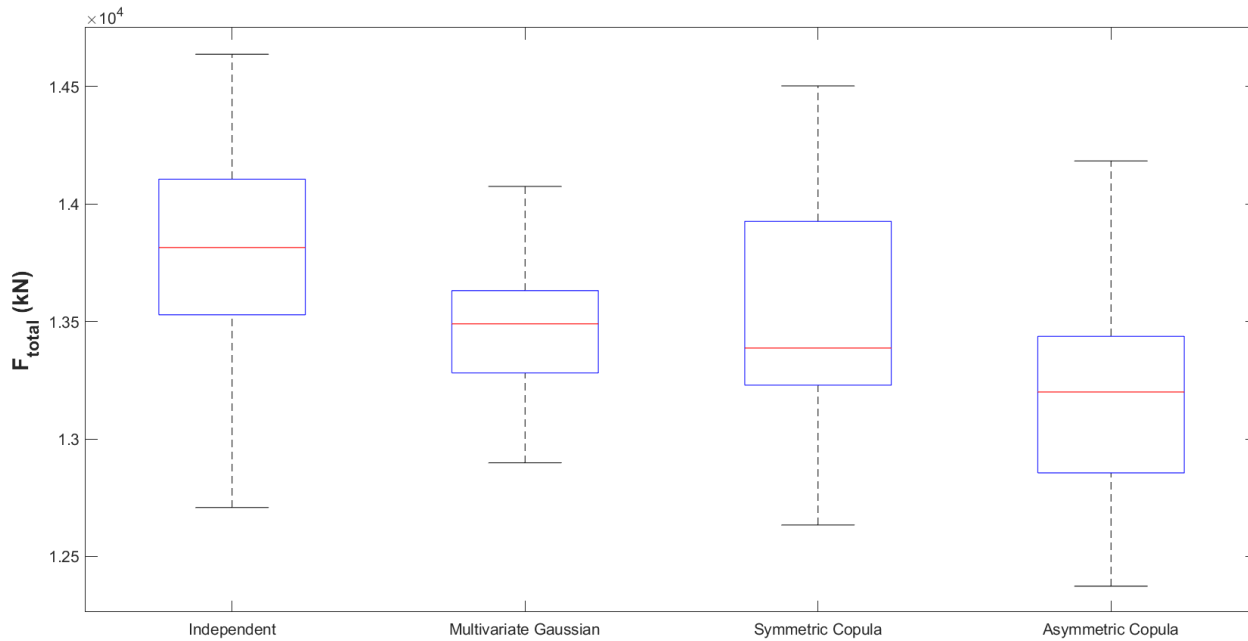


Fig. 5.7. Boxplots for the estimated total environmental loads

Table 5.7. Error values for the Independent and Multivariate Gaussian method

	RMSE	Mean Absolute Error
Independent method	0.2249	0.1520
Multivariate Gaussian method	0.2235	0.1505

Fig. 5.7 shows that, on average, multivariate Gaussian models provided a lower median than the independent model in estimating total environmental load. While c-vine copula models based on symmetry copulas resulted in a slightly lower estimation compared to the independent and multivariate Gaussian model. C-vine copula models constructed using asymmetry copulas have the lowest median of total environmental load. This low estimation is also a result of the characteristic of the Clayton copula used in Tree 2. The conditional distribution function on this edge is fitted to Clayton-Frank Type-1. Clayton copulas can characterize data showing strong low value dependencies. While in the symmetric case, the Frank copula is best fitted to model the conditional distribution function of Tree 2. Frank copulas are appropriate to model data that show

weak dependencies in both tails. This result supports the statement made by Zhang et al. (2018) that a failure to capture the real dependency structure of environmental variables can lead to an overestimation of the safety of offshore structures. Vine copula using asymmetric copulas as the building blocks have smaller error values compared to the symmetric ones and provide a lower estimation of total environmental loads. Table 5.7 also shows that error values when using the independent and multivariate gaussian are higher to model the environmental variables compared to the asymmetric copula in Table 5.6. Jiang et al. (2021) also showed that their proposed multivariate model using vine copulas with asymmetric copulas as the building blocks resulted in more realistic values describing the complex dependency structures between ocean variables. Vine copulas constructed using asymmetric copulas were also found to be more appropriate for trivariate joint probability analysis. Thus, from this study, and supported by the conclusions of other research, vine copulas involving pair-copula decomposition are found to be flexible models with different copula functions as the building blocks.

The result obtained from the estimation of total environmental load using trivariate models can be used for further analysis. The total environmental load can be used as an input to estimate the resilience of an offshore structure (Taleb-Berrouane et al., 2019; Yazdi et al., 2022). Detailed work on estimating the resilience of an offshore structure was performed in a previous study (Ramadhani et al., 2022) and the bivariate model in the previous study can be replaced by the trivariate model developed in this chapter.

5.5 Conclusion

In this chapter, a vine copula-based framework is proposed to estimate the total environmental load on an offshore installation in a higher dimension. Firstly, the correlations between wind speed,

wave height and current velocity were investigated. Then, the joint distribution for trivariate analysis, with wind speed as the dominating factor, was constructed using the c-vine model. Both symmetric and asymmetric copulas were used as building blocks. After fitting the model, a simulation to estimate the total environmental load was carried out based on the developed multivariate model. These results were compared with the other known methods, independent load case and multi-gaussian distribution function.

The estimation of the total environmental load was found dependent on the copula function fitted in the final edge of the tree. The Clayton copula was able to generate data that show strong dependency on the lower tail, while the Gumbel copula is appropriate for data having a stronger dependency on the higher tail. It is concluded that vine copulas are well suited to model multivariate environmental variables and provide more realistic models of interdependent environmental effects. The C-vine copula, constructed using asymmetric copulas as the building blocks, provided a lower estimation of total environmental load compared to results from the calculation of each environmental variable individually. The results obtained from c-vine using asymmetric copula are also lower compared to the ones obtained from the multi-gaussian distribution function. Error values from fitting the environmental variables to c-vine with asymmetric copula are also lower. Marine environmental variables usually show complex interdependence structures that a Gaussian distribution is unable to capture. Furthermore, identifying wind speed as the dominating variable made it possible to derive and generate correlated data of the other two variables.

This study provides a new perspective on the application of vine copulas to model marine environmental variables with complex dependency structures in higher dimensions. The result from this study is also potentially useful in further probabilistic structural analysis of offshore

structures, such as resilience analysis using the multivariate model. Further studies will focus on a more detailed application of the multivariate model for risk and resilience analysis of offshore structures.

Conflict of Interest

The authors declare that they have no known competing financial interests or personal relationships that could have appeared to influence the work reported in this chapter.

Acknowledgements

The authors would like to express their gratitude to the financial assistance provided by the Natural Science and Engineering Council of Canada (NSERC) and the Canada Research Chair (CRC) Tier I Program in Offshore Safety and Risk Engineering.

References

- Aas, K., Czado, C., Frigessi, A., Bakken, H., 2009. Pair-copula constructions of multiple dependence. *Insur. Math. Econ.* 44, 182–198. <https://doi.org/10.1016/j.insmatheco.2007.02.001>
- Agarwal, G., Tu, W., Sun, Y., Kong, L., 2022. Flexible quantile contour estimation for multivariate functional data: Beyond convexity. *Comput. Stat. Data Anal.* 168, 107400. <https://doi.org/10.1016/j.csda.2021.107400>
- American Petroleum Institute, 2002. Recommended Practice for Planning, Designing and Constructing Fixed Offshore Platforms - Working Stress Design. Washington, D.C.
- Amini, A., Abdollahi, A., Hariri-Ardebili, M.A., Lall, U., 2021. Copula-based reliability and sensitivity analysis of aging dams: Adaptive Kriging and polynomial chaos Kriging methods. *Appl. Soft Comput.* 109, 107524. <https://doi.org/10.1016/j.asoc.2021.107524>
- Bai, X., Jiang, H., Huang, X., Song, G., Ma, X., 2021. 3-Dimensional direct sampling-based environmental contours using a semi-parametric joint probability model. *Appl. Ocean Res.* 112, 102710. <https://doi.org/10.1016/j.apor.2021.102710>
- Bai, Y., Bai, Q., 2005. *Subsea Pipelines and Risers*. Elsevier BV: Amsterdam.
- Bedford, T., Daneshkhah, A., Wilson, K.J., 2016. Approximate Uncertainty Modelling in Risk Analysis with Vine Copulas. *Risk Anal.* 36, 792–815. <https://doi.org/10.1111/risa.12471>

- Bezak, N., Mikoš, M., Šraj, M., 2014. Trivariate Frequency Analyses of Peak Discharge, Hydrograph Volume and Suspended Sediment Concentration Data Using Copulas. *Water Resour. Manag.* 28, 2195–2212. <https://doi.org/10.1007/s11269-014-0606-2>
- Cheng, Z., Svangstu, E., Moan, T., Gao, Z., 2019. Long-term joint distribution of environmental conditions in a Norwegian fjord for design of floating bridges. *Ocean Eng.* 191, 106472. <https://doi.org/10.1016/j.oceaneng.2019.106472>
- Czado, C., 2019. *Analyzing Dependent Data with Vine Copulas, Lecture Notes in Statistics.* Springer International Publishing, Cham. <https://doi.org/10.1007/978-3-030-13785-4>
- De Leo, F., Besio, G., Briganti, R., Vanem, E., 2021. Non-stationary extreme value analysis of sea states based on linear trends. Analysis of annual maxima series of significant wave height and peak period in the Mediterranean Sea. *Coast. Eng.* 167, 103896. <https://doi.org/10.1016/j.coastaleng.2021.103896>
- De Michele, C., Salvadori, G., Passoni, G., Vezzoli, R., 2007. A multivariate model of sea storms using copulas. *Coast. Eng.* 54, 734–751. <https://doi.org/10.1016/j.coastaleng.2007.05.007>
- Det Norske Veritas, 2011. Modelling and analysis of marine operations. Recommended Practice: DNV-RP-H103.
- Deyab, S.M., Taleb-berrouane, M., Khan, F., Yang, M., 2018. Failure analysis of the offshore process component considering causation dependence. *Process Saf. Environ. Prot.* 1, 220–232. <https://doi.org/10.1016/j.psep.2017.10.010>
- Dong, S., Chen, C., Tao, S., 2017. Joint probability design of marine environmental elements for wind turbines. *Int. J. Hydrogen Energy* 42, 18595–18601. <https://doi.org/10.1016/j.ijhydene.2017.04.154>
- Dong, S., Tao, S., Li, X., Soares, C.G., 2015. Trivariate maximum entropy distribution of significant wave height, wind speed and relative direction. *Renew. Energy* 78, 538–549. <https://doi.org/10.1016/j.renene.2015.01.027>
- Dong, W., Sun, H., Tan, J., Li, Z., Zhang, J., Yang, H., 2022. Regional wind power probabilistic forecasting based on an improved kernel density estimation, regular vine copulas, and ensemble learning. *Energy* 238, 122045. <https://doi.org/10.1016/j.energy.2021.122045>
- Elidan, G., 2010. Copula bayesian networks. *Adv. neural Inf. Process.* ... 1–9.
- ERDDAP, 2022. Mouth of Placentia Bay Buoy [WWW Document]. URL https://www.smartatlantic.ca/erddap/tabledap/SMA_MouthofPlacentiaBayBuoy.html (accessed 8.28.21).
- Fazeres-Ferradosa, T., Taveira-Pinto, F., Vanem, E., Reis, M.T., Neves, L. das, 2018. Asymmetric copula-based distribution models for met-ocean data in offshore wind engineering applications. *Wind Eng.* 42, 304–334. <https://doi.org/10.1177/0309524X18777323>
- Ganguli, P., Reddy, M.J., 2013. Probabilistic assessment of flood risks using trivariate copulas. *Theor. Appl. Climatol.* 111, 341–360. <https://doi.org/10.1007/s00704-012-0664-4>

- Heredia-Zavoni, E., Montes-Iturrizaga, R., 2019. Modelling directional environmental contours using three dimensional vine copulas. *Ocean Eng.* 187, 106102. <https://doi.org/10.1016/j.oceaneng.2019.06.007>
- Horn, J.-T., Bitner-Gregersen, E., Krokstad, J.R., Leira, B.J., Amdahl, J., 2018. A new combination of conditional environmental distributions. *Appl. Ocean Res.* 73, 17–26. <https://doi.org/10.1016/j.apor.2018.01.010>
- Jacomet, A., Khosravifardshirazi, A., Sahafnejad-Mohammadi, I., Dibaj, M., Javadi, A.A., Akrami, M., 2021. Analysing the Influential Parameters on the Monopile Foundation of an Offshore Wind Turbine. *Computation* 9, 71. <https://doi.org/10.3390/computation9060071>
- Jiang, H., Bai, X., Song, G., Luo, M., Ma, X., 2021. Comparing trivariate models for coastal winds and waves accounting for monthly seasonality. *Appl. Ocean Res.* 117, 102959. <https://doi.org/10.1016/j.apor.2021.102959>
- Kim, M.H., 1999. Hydrodynamics of Offshore Structures, in: *Developments in Offshore Engineering*. Elsevier, pp. 336–381. <https://doi.org/10.1016/B978-088415380-1/50027-3>
- Kraus, D., Czado, C., 2017. Growing simplified vine copula trees: improving Di{\ss}mann’s algorithm.
- Li, D.-Q., Zhang, L., Tang, X.-S., Zhou, W., Li, J.-H., Zhou, C.-B., Phoon, K.-K., 2015. Bivariate distribution of shear strength parameters using copulas and its impact on geotechnical system reliability. *Comput. Geotech.* 68, 184–195. <https://doi.org/10.1016/j.compgeo.2015.04.002>
- Li, X., Zhang, W., 2020. Long-term assessment of a floating offshore wind turbine under environmental conditions with multivariate dependence structures. *Renew. Energy* 147, 764–775. <https://doi.org/10.1016/j.renene.2019.09.076>
- Lian, J.J., Xu, K., Ma, C., 2013. Joint impact of rainfall and tidal level on flood risk in a coastal city with a complex river network: a case study of Fuzhou City, China. *Hydrol. Earth Syst. Sci.* 17, 679–689. <https://doi.org/10.5194/hess-17-679-2013>
- Liebscher, E., 2008. Construction of asymmetric multivariate copulas. *J. Multivar. Anal.* 99, 2234–2250. <https://doi.org/10.1016/j.jmva.2008.02.025>
- Lin-ye, J., García-León, M., Gràcia, V., Ortego, M.I., Lionello, P., Sánchez-Arcilla, A., 2017. Multivariate statistical modelling of future marine storms. *Appl. Ocean Res.* 65, 192–205. <https://doi.org/10.1016/j.apor.2017.04.009>
- Lin, Y., Dong, S., 2019. Wave energy assessment based on trivariate distribution of significant wave height, mean period and direction. *Appl. Ocean Res.* 87, 47–63. <https://doi.org/10.1016/j.apor.2019.03.017>
- Lü, T.-J., Tang, X.-S., Li, D.-Q., Qi, X.-H., 2020. Modelling multivariate distribution of multiple soil parameters using vine copula model. *Comput. Geotech.* 118, 103340. <https://doi.org/10.1016/j.compgeo.2019.103340>
- Ma, P., Zhang, Y., 2022. Modelling asymmetrically dependent multivariate ocean data using

- truncated copulas. *Ocean Eng.* 244, 110226. <https://doi.org/10.1016/j.oceaneng.2021.110226>
- Mackay, E., Johanning, L., 2018. A generalised equivalent storm model for long-term statistics of ocean waves. *Coast. Eng.* 140, 411–428. <https://doi.org/10.1016/j.coastaleng.2018.06.001>
- Mazas, F., 2019. Extreme events: a framework for assessing natural hazards. *Nat. Hazards* 98, 823–848. <https://doi.org/10.1007/s11069-019-03581-9>
- Montes-Iturrizaga, R., Heredia-Zavoni, E., 2016. Multivariate environmental contours using C-vine copulas. *Ocean Eng.* 118, 68–82. <https://doi.org/10.1016/j.oceaneng.2016.03.011>
- Nagler, T., Krüger, D., Min, A., 2022. Stationary vine copula models for multivariate time series. *J. Econom.* 227, 305–324. <https://doi.org/10.1016/j.jeconom.2021.11.015>
- Nelsen, R.B., 2006. *An introduction to copulas*, 2nd ed. Springer.
- Petrov, V., Guedes Soares, C., Gotovac, H., 2013. Prediction of extreme significant wave heights using maximum entropy. *Coast. Eng.* 74, 1–10. <https://doi.org/10.1016/j.coastaleng.2012.11.009>
- Qian, J., Dong, Y., 2022. Surrogate-assisted seismic performance assessment incorporating vine copula captured dependence. *Eng. Struct.* 257, 114073. <https://doi.org/10.1016/j.engstruct.2022.114073>
- Ramadhani, A., Khan, F., Colbourne, B., Ahmed, S., Taleb-Berrouane, M., 2022. Resilience assessment of offshore structures subjected to ice load considering complex dependencies. *Reliab. Eng. Syst. Saf.* 222, 108421. <https://doi.org/10.1016/j.ress.2022.108421>
- Ramadhani, A., Khan, F., Colbourne, B., Ahmed, S., Taleb-Berrouane, M., 2021. Environmental load estimation for offshore structures considering parametric dependencies. *Saf. Extrem. Environ.* <https://doi.org/10.1007/s42797-021-00028-y>
- Sadegh, M., Ragno, E., AghaKouchak, A., 2017. Multivariate C opula A analysis toolbox (MvCAT): Describing dependence and underlying uncertainty using a Bayesian framework. *Water Resour. Res.* 53, 5166–5183. <https://doi.org/10.1002/2016WR020242>
- Salleh, N., Yusof, F., Yusop, Z., 2016. Bivariate copulas functions for flood frequency analysis. p. 060007. <https://doi.org/10.1063/1.4954612>
- Salvadori, G., De Michele, C., 2010. Multivariate multiparameter extreme value models and return periods: A copula approach. *Water Resour. Res.* 46, 2009WR009040. <https://doi.org/10.1029/2009WR009040>
- Sandvik, E., Lønnum, O.J.J., Asbjørnslett, B.E., 2019. Stochastic bivariate time series models of waves in the North Sea and their application in simulation-based design. *Appl. Ocean Res.* 82, 283–295. <https://doi.org/10.1016/j.apor.2018.11.010>
- Shooter, R., Ross, E., Ribal, A., Young, I.R., Jonathan, P., 2022. Multivariate spatial conditional extremes for extreme ocean environments. *Ocean Eng.* 247, 110647.

<https://doi.org/10.1016/j.oceaneng.2022.110647>

- Taleb-Berrouane, M., Khan, F., Hawboldt, K., 2021. Corrosion risk assessment using adaptive bow-tie (ABT) analysis. *Reliab. Eng. Syst. Saf.* 214, 107731. <https://doi.org/10.1016/j.ress.2021.107731>
- Taleb-berrouane, M., Khan, F., Hawboldt, K., Eckert, R., Skovhus, T.L., 2018. Model for microbiologically influenced corrosion potential assessment for the oil and gas industry and gas industry. *Corros. Eng. Sci. Technol.* 53, 378–392. <https://doi.org/10.1080/1478422X.2018.1483221>
- Taleb-Berrouane, M., Khan, F., Kamil, M.Z., 2019. Dynamic RAMS analysis using advanced probabilistic approach. *Chem. Eng. Trans.* 77. <https://doi.org/10.3303/CET1977041>
- Taleb-Berrouane, M., Sterrahmane, A., Mehdaoui, D., Lounis., Z., 2017. Emergency Response Plan Assessment Using Bayesian Belief Networks, in: 3rd Workshop and Symposium on Safety and Integrity Management of Operations in Harsh Environments (C-RISE3). St John's NL.
- Taleb Berrouane, M., 2020. Dynamic corrosion risk assessment in the oil and gas production and processing facility.
- Tang, X.-S., Wang, M.-X., Li, D.-Q., 2020. Modelling multivariate cross-correlated geotechnical random fields using vine copulas for slope reliability analysis. *Comput. Geotech.* 127, 103784. <https://doi.org/10.1016/j.compgeo.2020.103784>
- Tao, Y., Wang, Y., Wang, D., Ni, L., Wu, J., 2021. A C-vine copula framework to predict daily water temperature in the Yangtze River. *J. Hydrol.* 598, 126430. <https://doi.org/10.1016/j.jhydrol.2021.126430>
- Wang, F., Li, H., 2019. A non-parametric copula approach to dependence modelling of shear strength parameters and its implications for geotechnical reliability under incomplete probability information. *Comput. Geotech.* 116, 103185. <https://doi.org/10.1016/j.compgeo.2019.103185>
- Wei, K., Shen, Z., Ti, Z., Qin, S., 2021. Trivariate joint probability model of typhoon-induced wind, wave and their time lag based on the numerical simulation of historical typhoons. *Stoch. Environ. Res. Risk Assess.* 35, 325–344. <https://doi.org/10.1007/s00477-020-01922-w>
- Wu, X.Z., 2015. Modelling dependence structures of soil shear strength data with bivariate copulas and applications to geotechnical reliability analysis. *Soils Found.* 55, 1243–1258. <https://doi.org/10.1016/j.sandf.2015.09.023>
- Xu, Q., Fan, Z., Jia, W., Jiang, C., 2020. Fault detection of wind turbines via multivariate process monitoring based on vine copulas. *Renew. Energy* 161, 939–955. <https://doi.org/10.1016/j.renene.2020.06.091>
- Xu, Z.-X., Zhou, X.-P., 2018. Three-dimensional reliability analysis of seismic slopes using the copula-based sampling method. *Eng. Geol.* 242, 81–91. <https://doi.org/10.1016/j.enggeo.2018.05.020>

- Yang, R., Khan, F., Taleb-Berrouane, M., Kong, D., 2020. A time-dependent probabilistic model for fire accident analysis. *Fire Saf. J.* 111. <https://doi.org/10.1016/j.firesaf.2019.102891>
- Yang, X., Qian, J., 2019. Joint occurrence probability analysis of typhoon-induced storm surges and rainstorms using trivariate Archimedean copulas. *Ocean Eng.* 171, 533–539. <https://doi.org/10.1016/j.oceaneng.2018.11.039>
- Yazdi, M., Khan, F., Abbassi, R., Quddus, N., 2022. Resilience assessment of a subsea pipeline using dynamic Bayesian network. *J. Pipeline Sci. Eng.* 100053. <https://doi.org/10.1016/j.jpse.2022.100053>
- Yu. Shmal, G., A. Nadein, V., A. Makhutov, N., A. Truskov, P., I. Osipov, V., 2020. Hybrid Modelling of Offshore Platforms' Stress-Deformed and Limit States Taking into Account Probabilistic Parameters, in: *Probability, Combinatorics and Control*. IntechOpen. <https://doi.org/10.5772/intechopen.88894>
- Zhang, S., Chen, C., Zhang, Q., Zhang, D., Zhang, F., 2015. Wave Loads Computation for Offshore Floating Hose Based on Partially Immersed Cylinder Model of Improved Morison Formula. *Open Pet. Eng. J.* 8, 130–137. <https://doi.org/10.2174/1874834101508010130>
- Zhang, S., Yan, Y., Wang, P., Xu, Z., Yan, X., 2019. Assessment of the offshore wind turbine support structure integrity and management of multivariate hybrid probability frameworks. *Energy Convers. Manag.* 180, 1085–1108. <https://doi.org/10.1016/j.enconman.2018.11.010>
- Zhang, Y., Beer, M., Quek, S.T., 2015. Long-term performance assessment and design of offshore structures. *Comput. Struct.* 154, 101–115. <https://doi.org/10.1016/j.compstruc.2015.02.029>
- Zhang, Y., Gomes, A.T., Beer, M., Neumann, I., Nackenhorst, U., Kim, C.-W., 2019. Modelling asymmetric dependences among multivariate soil data for the geotechnical analysis – The asymmetric copula approach. *Soils Found.* 59, 1960–1979. <https://doi.org/10.1016/j.sandf.2019.09.001>
- Zhang, Y., Kim, C.-W., Beer, M., Dai, H., Soares, C.G., 2018. Modelling multivariate ocean data using asymmetric copulas. *Coast. Eng.* 135, 91–111. <https://doi.org/10.1016/j.coastaleng.2018.01.008>
- Zhao, Y., Dong, S., 2020. A multi-load joint distribution model to estimate environmental design parameters for floating structures. *Ocean Eng.* 217, 107818. <https://doi.org/10.1016/j.oceaneng.2020.107818>
- Zhao, Y., Liao, Z., Dong, S., 2021. Estimation of characteristic extreme response for mooring system in a complex ocean environment. *Ocean Eng.* 225, 108809. <https://doi.org/10.1016/j.oceaneng.2021.108809>

Appendix 5A

Table 5A.1 shows the condition where each wave theory is applicable.

Table 5A.1. The application of wave theories

Condition	Wave Theory
$\frac{d}{L} \geq 0.2, \frac{H}{L} \leq 0.2$	Airy wave theory
$0.1 < \frac{d}{L} < 0.2, \frac{H}{L} \geq 0.2$	Stokes wave theory
$0.04 < \frac{d}{L} < 0.1$	Solitary wave theory

where, d is water depth, L is wavelength, and H is wave height.

4. Airy Wave Theory

In this theory, water particle velocity and acceleration in the horizontal direction can be estimated by (Kim, 1999; S. Zhang et al., 2015)

$$\left. \begin{aligned} u_x &= \frac{Hgk}{2\omega} \frac{\cosh(k(z+d))}{\cosh(kd)} \cos(kx - \omega t) \\ \dot{u}_x &= \frac{2\pi^2 H}{T^2} \frac{\cosh(k(z+d))}{\sinh(kd)} \sin(kx - \omega t) \end{aligned} \right\} \quad (5A.1)$$

g = standard gravity

H = wave height

k = wave number that is calculated using this equation

$$k = \frac{2\pi}{L} \quad (5A.2)$$

While in the vertical direction

$$\left. \begin{aligned} u_z &= \frac{Hgk}{2\omega} \frac{\sinh(k(z+d))}{\cosh(kd)} \sin(kx - \omega t) \\ \dot{u}_z &= -\frac{2\pi^2 H}{T^2} \frac{\sinh(k(z+d))}{\sinh(kd)} \cos(kx - \omega t) \end{aligned} \right\} \quad (5A.3)$$

5. Stokes Wave Theory

The horizontal water particle velocity and acceleration should satisfy this following equation

$$\left. \begin{aligned} u_x &= \frac{H\pi \cosh(k(z+d))}{T \sinh(kd)} \cos(kx - \omega t) + \frac{3}{4} \left(\frac{H\pi}{T} \right) \left(\frac{H\pi}{L} \right) \frac{\cosh(2k(z+d))}{\sinh^4(kd)} \cos 2(kx - \omega t) \\ \dot{u}_x &= 2 \left(\frac{\pi^2 H}{T^2} \right) \frac{\cosh(k(z+d))}{\sinh(kd)} \sin(kx - \omega t) + 3 \left(\frac{H\pi^2}{T^2} \right) \left(\frac{H\pi}{L} \right) \frac{\cosh(2k(z+d))}{\sinh^4(kd)} \sin 2(kx - \omega t) \end{aligned} \right\} \quad (A4)$$

While equation 5A.5 is used to estimate water particle velocity and acceleration in the vertical direction

$$\left. \begin{aligned} u_z &= \frac{H\pi \sinh(k(z+d))}{T \sinh(kd)} \sin(kx - \omega t) + \frac{3}{4} \left(\frac{H\pi}{T} \right) \left(\frac{H\pi}{L} \right) \frac{\sinh(2k(z+d))}{\sinh^4(kd)} \sin 2(kx - \omega t) \\ \dot{u}_z &= -2 \left(\frac{\pi^2 H}{T^2} \right) \frac{\sinh(k(z+d))}{\sinh(kd)} \cos(kx - \omega t) - 3 \left(\frac{H\pi^2}{T^2} \right) \left(\frac{H\pi}{L} \right) \frac{\sinh(2k(z+d))}{\sinh^4(kd)} \cos 2(kx - \omega t) \end{aligned} \right\} \quad (A5)$$

6. Solitary Wave Theory

Water particle velocity and acceleration can be approached by Equation 5A.6

$$\left. \begin{aligned} u &= \frac{CN \left[1 + \cos \left(M \left[\frac{z+d}{d} \right] \right) \cdot \cos \left(M \frac{x}{d} \right) \right]}{\left\{ \cos \left(M \left[\frac{z+d}{d} \right] \right) + \cosh \left(M \frac{x}{d} \right) \right\}^2} \\ \dot{u} &= \frac{CN \left[\sin \left(M \left[\frac{z+d}{d} \right] \right) \cdot \sinh \left(M \frac{x}{d} \right) \right]}{\left\{ \cos \left(M \left[\frac{z+d}{d} \right] \right) + \cosh \left(M \frac{x}{d} \right) \right\}^2} \end{aligned} \right\} \quad (5A.6)$$

Where M,N are functions of H/d and

C is speed of solitary wave that can be estimated using

$$C = \sqrt{2g(H + d)} \quad (5A.7)$$

CHAPTER 6

A COPULA-BASED PROBABILISTIC MODEL TO ASSESS THE RESILIENCE OF OFFSHORE STRUCTURES SUBJECTED TO MULTIPLE ENVIRONMENTAL LOADS

Preface

A version of this chapter has been completed and is ready for journal submission. As the primary author, I work with my co-authors: Dr. Faisal Khan, Dr. Salim Ahmed, Dr. Bruce Colbourne, and Dr. Mohammed Taleb-Berrouane. I conducted a literature review and developed the conceptual framework for developing a resilience assessment methodology considering multiple environmental loads. I prepared the first manuscript draft and revised the manuscript based on the co-authors' and reviewers' feedback. Co-author Dr. Faisal Khan assisted in the idea formulation, development of the concept, and methodology design, reviewed and edited the manuscript draft, and acted as the corresponding author for the manuscript. Co-authors Dr. Salim Ahmed, Dr. Bruce Colbourne, and Dr. Mohammed Taleb-Berrouane provided valuable support and input in reviewing and revising the manuscript draft. These co-authors also assisted in validating, reviewing, and correcting the model and results.

Abstract

Offshore structures are expected to perform safely in specific marine environments. These structures are periodically subjected to extreme natural hazards and the complexity of the marine environment requires a robust and reliable model to capture dependent relationships among environmental variables. Past studies have emphasized linearity and symmetric assumptions to define the relationships between environmental variables. Resilience of offshore structures has been investigated in the past, but the proposed models were not robust enough. The present study introduces C-vine Copulas to model multivariate environmental variables, considering both symmetric and asymmetric dependence structures. The results reveal that symmetric and asymmetric copula functions can define environmental variables in higher dimensions than previously used. Comparison to other methods: independent and multivariate Gaussian analysis also confirms that C-vine copulas better represent marine environmental data. This work uses example loads calculated using the C-vine Copula model to assess an offshore structure's response and resilience. Resilience is quantified considering absorptive, adaptive, and restorative capacities. The study concludes that the proposed model serves as a good tool for offshore structure design.

Keywords: Resilience assessment; vine copulas; absorptive capacity, offshore structure

6.1 Introduction

Natural hazards such as hurricanes, earthquakes, tsunamis, and storms significantly impact offshore structures. Hurricane Katrina destroyed 44 offshore oil and gas facilities and damaged another 21 (Cruz and Krausmann, 2008). Hurricane Rita destroyed 69 offshore facilities while damaging another 32 installations (Cruz and Krausmann, 2008). Hurricanes Gustav and Ike, destroyed 60 offshore platforms and damaged 31 facilities (Kaiser and Yu, 2010). Offshore

structures such as fixed platforms, and Floating Production, Storage, and Offloading systems (FPSO) are designed for those extreme environmental conditions. Offshore structures are exposed to marine environmental variables (Zhao and Dong, 2020) and degradation processes (Taleb-Berrouane et al., 2021) during their design life. Thus, it is crucial to understand and identify the combined effects of marine environmental variables on offshore structures in order to better understand risks caused by extreme marine events.

Marine environmental variables possess significant uncertainties. Identifying the dependence structures between the environmental variables is a challenge during their modelling. These variables generally show some level of interdependency, and predictions and models can be improved if these relationships can be captured. Although the probability of extreme marine events is very low, the consequences can be severe (Deyab et al., 2018; Shooter et al., 2022). A robust and accurate multivariate model is necessary to capture all dependence structures between environmental variables (Ma and Zhang, 2022; Sadegh et al., 2017). A combination of environmental variables acting on a structure can cause more severe consequences than that predicted by estimating each load effect individually (Zhang et al., 2018). Thus, the common assumption of linear dependence or even independence among environmental variables is not considered the best approach (Fazeres-Ferradosa et al., 2018; Wei et al., 2021). Codes and standards such as DNV-RP-C203, API-RP-2FPS, and API-RP-2A-WSD specify requirements to consider the combined effects of wind, wave, and current on an offshore structure while performing risk assessment (Ma and Zhang, 2022). A multivariate joint probability distribution of marine environmental variables should be constructed to meet this requirement.

Copula functions have attracted attention in various research disciplines, as a means to deal with modelling joint probability distributions between correlated variables. Several past studies that

focus on modelling natural hazards on structures are available. Copula functions are shown to be powerful in modelling the effects of natural hazards on infrastructures, both offshore (De Michele et al., 2007; Dong et al., 2017; Ramadhani et al., 2021; Salvadori and De Michele, 2010; Y. Zhang et al., 2015; Zhang et al., 2018) and onshore (Desilver, 2020; Fang et al., 2020). However, an extreme marine event may involve more than two variables with a complex dependence structure. Copulas used in past studies do not capture complex dependence in higher dimensions (Li and Zhang, 2020; N. Xu et al., 2020). Currently available standards such as ISO-19901, DNVGL-RP-C205, DNVGL-RP-C203, and DNVGL-RP-210 do not provide guidance on modelling the multivariate joint probability distribution of marine environmental variables (Zhang et al., 2019).

Several previous contributions are focused on multivariate statistical analysis of marine environmental variables in higher dimensions. The most commonly used methods to construct multivariate models are the maximum entropy and multivariate Gaussian models (Agarwal et al., 2022; Dong et al., 2015; Mackay and Johanning, 2018; Petrov et al., 2013; Shooter et al., 2022). These models were found to be a good fit for marine environmental data. However, linear dependence and a specific marginal distribution such as Gaussian or Extreme values are assumed. These commonly used methods cannot consider more complex dependence structures between environmental variables. Marine environmental variables usually show nonlinear dependence and may show asymmetric structures. Thus, a more flexible method is needed. As previously stated, Copulas have been proven to be flexible in modelling multivariate variables, but to date the application of copula models has been focused on bivariate cases. To use copula models in the higher dimensions, the vine copula is introduced. Bedford and Cooke (2002) introduced vine copula as the decomposition function of a joint distribution into a series of bivariate copulas. Vine copulas were first becoming popular in financial mathematics. However, recently they have

attracted much attention in engineering applications. Vine copulas can deal with complex dependence structures and tail dependence between variables. In geotechnical analysis, vine copulas have been used to model the multivariate distributions of soil parameters (Lü et al., 2020; Qian and Dong, 2022; Tang et al., 2020; Xu and Zhou, 2018).

Based on these studies, vine copulas could provide better results for the reliability-based design of geotechnical structures. Vine copulas also provided a more flexible way to model the cross-correlation of soil parameters. The dependence of multivariate hydrological design was modelled using vine copulas (Jiang et al., 2019). Vine copulas were also used to model the dependence structure between flood characteristics (Tosunoglu et al., 2020). The parameters needed to construct a rainfall model were also successfully generated using vine copulas (Pham et al., 2018). In a similar field, vine copulas were used to construct environmental contours based on the multivariate model of marine environmental parameters such as wave height, wave period, and wind speed. (Amini et al., 2021; Dong et al., 2022; Heredia-Zavoni and Montes-Iturrizaga, 2019; Wei et al., 2021; Q. Xu et al., 2020). These works show that vine copulas are more flexible than alternative methods, based on a graphical model of the investigated variables. Vine copulas also resulted in a better way to construct multivariate models from the decomposition of pair copulas (Bedford et al., 2016). However, in the above mentioned works the multivariate copula models were constructed based on the Archimedean copula family. This copula family is best suited for model variables that show symmetric dependence. However most environmental variables show an asymmetric dependence structure (Zhang et al., 2018). To overcome the limitations of past works, this chapter investigates symmetric and asymmetric copulas to model multivariate environmental variables in higher dimensions.

To further investigate the influence of the copula-based model on the prediction of marine environmental loads, the performance of an offshore structure is assessed subjected to the total environmental load. A structure's performance can be evaluated by assessing the reliability of the structure. To maintain their operability, offshore structures are required to function at a high structural reliability level to withstand any undesirable events that can cause catastrophic consequences. Resilience is thus a metric that can help organizations better design and plan their offshore safety regime. Resilience is defined as a system's ability to withstand undesirable events and recover from them (Vanem, 2016; Zarei et al., 2021). There have been several past studies on the assessment of the resilience of engineering systems. Most resilience assessments that involved natural hazards focused on their impacts on bridges, houses, or commercial buildings (Cai et al., 2021; Cheng et al., 2021; Stochino et al., 2019; Q. Xu et al., 2020). In the process industry, pipeline systems' resilience against microbiologically-influenced corrosion using Petri-nets was assessed (Kamil et al., 2021; Taleb-Berrouane et al., 2020; Taleb Berrouane, 2020). In the power and energy field, a resilience model for a nuclear power plant was proposed. A resilience framework in the nuclear industry was also studied to analyze micro incidents during power plant operations. For wind power plants, a resilience index was developed as a diagnostic tool to assess potential hazards (Afgan and Cvetinovic, 2010). A novel resilience analysis of wind turbines was also proposed to optimize decisions on asset integrity management (Qin and Faber, 2019). The resilience performance of a wind energy park was evaluated to identify priority in the ranking of decision alternatives. Another probabilistic framework for offshore wind farm resilience modelling was developed (Liu et al., 2022). The model demonstrated the significance of prevailing uncertainties in the context of asset integrity management. Resilience is also popular in the field of transportation. The resilience of maritime transport systems was investigated based on the

minimum residual optimization model (Dui et al., 2021). A framework to assess marine LNG offloading systems was also developed based on the Infrastructure Resilience-oriented Modelling Language (IRML) (Hu et al., 2021). For railway systems, a hybrid knowledge-based and data-driven approach was proposed to quantify resilience (Yin et al., 2022). The model was able to demonstrate the quantitative relationship between railway system resilience and different types of events. Resilience of railway networks against simultaneous multiple disruptions was also assessed by combining infrastructure restoration and transport management (Bešinović et al., 2022). The proposed model was able to help decision-makers quantify the impacts of multiple disruptions. Despite the vast body of application of resilience quantification in various fields, studies on the resilience of structures subjected to correlated multivariate environmental variables have not been reported in the open literature.

The present study presents multivariate vine copula models for environmental load estimation for offshore structures. Symmetric and asymmetric copula functions used within the vine copula structure are compared to identify the best-fitted functions in multivariate analysis. Thus, this chapter aims to contribute to; 1.) investigation and construction of multivariate environmental models in higher dimension using vine copulas considering both symmetric and asymmetric dependence structures, and 2.) the assessment of an offshore structure's resilience in terms of reliability, subjected to a total environmental load, modelled using vine copulas.

The remainder of this chapter is organized as follows. Section 6.2 presents the methodology and the basic theories used in the research. The application of vine copula to model the multivariate environmental variables is discussed in Section 6.3. Results and discussions from the estimation of total environmental load to the assessment of the structure's resilience are presented in Section 6.4. The concluding remarks of this chapter are presented in Section 6.5.

6.2 Methodologies

The methodology used to assess the resilience of an offshore structure subject to the total environmental load is illustrated in Fig. 6.1. Correlated environmental parameters are generated using vine copula functions. Resilience is evaluated in terms of the reliability of the structure. Basic theories and methodologies used to perform the proposed research framework are detailed in the next sections.

6.2.1 Copula theory

Copula functions are used to model complex dependencies between environmental variables. Marginal distribution from each variable is “coupled” or “joined” to construct the multivariate models. Copula theories were first introduced in Sklar’s Theorem (Nelsen, 2006). Let H be the n -dimensional distribution function with marginal distributions $F_1, F_2, F_3, \dots, F_n$, then there is a copula, C , such that

$$H(x_1, x_2, \dots, x_n) = C(F_1(x_1), F_2(x_2), \dots, F_n(x_n)) \quad (6.1)$$

Based on Sklar’s theorem, copula functions are very flexible in modelling complex dependencies between environmental variables. Copula functions do not rely on the character of the univariate marginal distributions of the investigated variables. Environmental variables in the original domain are transformed into a cumulative distribution function that follows the uniform distribution function (Zhang et al., 2018). Thus, the domain and range for an n -dimensional copula function can be approached as $C: [0,1]^n \rightarrow [0,1]$.

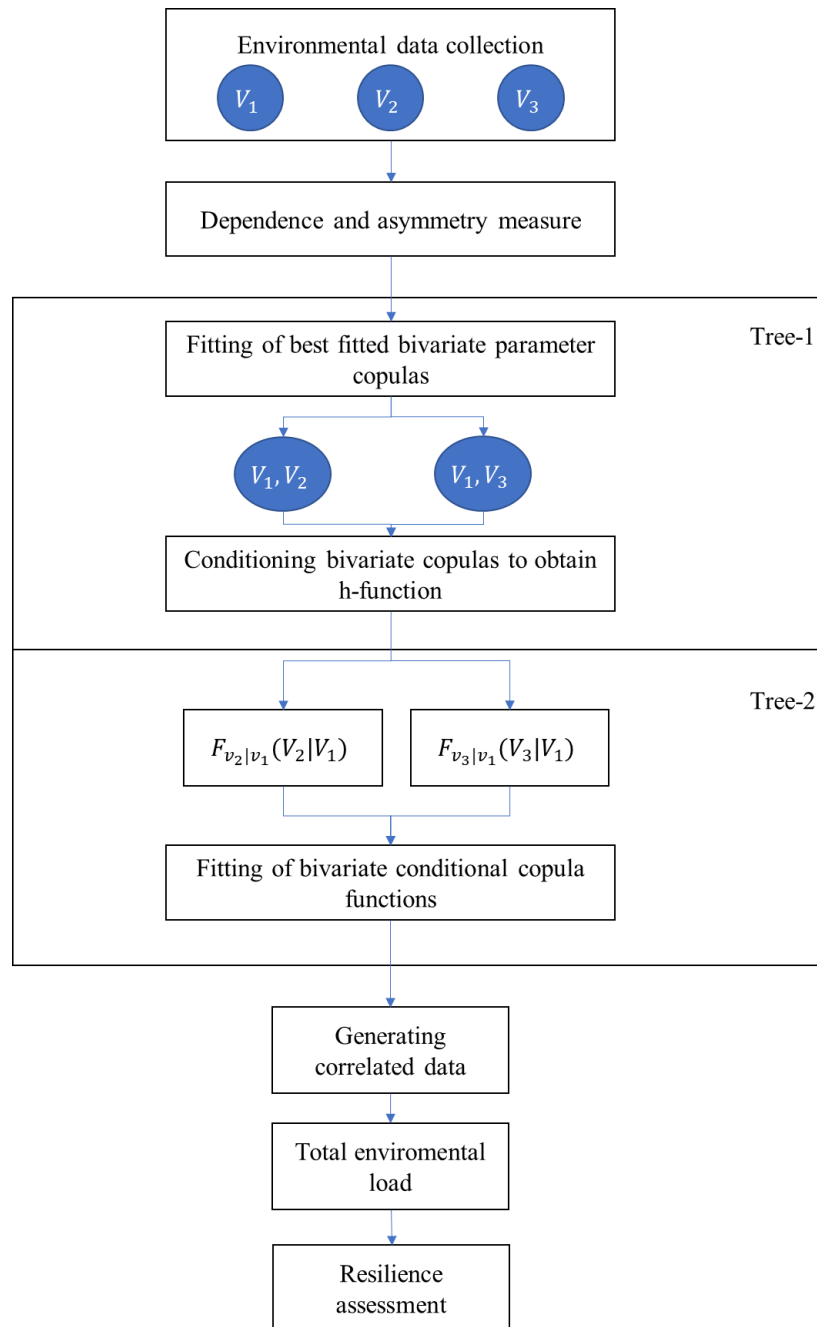


Fig. 6.1. Research framework to quantify structure's resilience subjected to the total environmental load modelled using vine copulas

Due to this flexibility, copula functions are useful for modelling environmental variables with complex dependence structures. Detailed investigation of the application of copula functions to

model a bivariate case of environmental variables can be found in (Ramadhani et al., 2022, 2021). In this chapter, multivariate models of environmental variables are constructed. There are two dependence structures considered in this chapter: symmetric and asymmetric. Copula functions from the Archimedean family are selected to model symmetric dependence structures. Three common copulas from the Archimedean family along with their parameters are presented in Table 6.1

Table 6.1. Common Archimedean copulas with their parameters

Copula	$C_\gamma(u_1, u_2)$	Generating function $\phi_\gamma(t)$	Interval
Clayton	$(u_1^{-\gamma} + u_2^{-\gamma} - 1)^{-\frac{1}{\gamma}}$	$\frac{\gamma}{\gamma + 2}$	$(1, \infty)$
Gumbel	$\exp\left\{-\left[(-\ln u_1)^\gamma + (-\ln u_2)^\gamma\right]^{\frac{1}{\gamma}}\right\}$	$1 - \frac{1}{\gamma}$	$[1, \infty)$
Frank	$\frac{-1}{\gamma} \ln\left(1 + \frac{(e^{-u_1\gamma} - 1)(e^{-u_2\gamma} - 1)}{e^{-\gamma} - 1}\right)$	$1 - \frac{4}{\gamma}(1 - D_1(\gamma))$ Where $D_1(\gamma) = \frac{1}{\gamma} \int_0^\infty \frac{t dt}{\exp(t) - 1}$	$(-\infty, \infty)$

In addition to symmetric dependence, asymmetric dependence is also considered, as most marine environmental variables show this type of dependence (Zhang et al., 2018). There are multiple ways to construct asymmetric copulas. In this chapter, asymmetric copulas are constructed using the product rule, as illustrated in previous studies. The construction of asymmetric copulas using this rule was judged to be the best to model marine environmental variables and considered more practical for a complex engineering system (Y. Zhang et al., 2019; Zhang et al., 2018). This rule was defined through the following theorem (Liebscher, 2008)

Let C_1, \dots, C_k : are copulas. Let $g_{ji}: [0,1] \rightarrow [0,1]$ for $j = 1, \dots, k, i = 1, \dots, d$ be functions with the property that each of them is strictly increasing or identically equal to 1.

Then the general equation to construct asymmetric copulas by using the product rule is defined by

$$\bar{c}(u_1, \dots, u_d) = \prod_{j=1}^k C_j(g_{j_1}(u_1), \dots, g_{j_d}(u_d)) \quad \text{for } u_i \in [0,1] \quad (6.2)$$

To satisfy the assumptions of the theorem, the function g_{ji} should have the following properties

- a) $g_{ji}(1) = 1$ and $g_{ji}(0) = 0$,
- b) g_{ji} is continuous on $(0,1]$,
- c) If there are at least two functions g_{j_1i}, g_{j_2i} with $1 \leq j_1, j_2 \leq k$ which are not identically equal to 1, then $g_{ji}(x) > x$ holds for $x \in (0,1), j = 1, \dots, k$

The function g_{ji} plays a significant role in constructing symmetric copulas into asymmetric copulas. Type-1 individual function g_{ji} , is used, where

$$(I) g_{ji}(v) = v^{\theta_{ji}} \text{ for } j = 1, \dots, k, \text{ where } \theta_{ji} \in [0,1] \text{ and } \sum_{j=1}^k \theta_{ji} = 1 \quad (6.3)$$

Archimedean copulas are used as the basis copula functions to construct asymmetric copulas.

Vine copula theories are introduced in the next section to construct the multivariate models for the selected environmental variables.

6.2.2 Modelling dependence structures using vine copulas

In this chapter, vine copula based multivariate models of the environmental variables are investigated. Vine copulas are known to model multiple random variables considering complex dependence structures (Heredia-Zavoni and Montes-Iturrizaga, 2019; Lü et al., 2020; Montes-Iturrizaga and Heredia-Zavoni, 2016). The main idea of a vine copula is to decompose a joint probability distribution function of multivariate random variables into a product of their univariate distributions, unconditional and conditional pairs. Let X_1, X_2, \dots, X_n denote random variable with their joint probability density function (PDF) $f(x_1, x_2, \dots, x_n)$. This PDF is then decomposed into

$$f(x_1, x_2, \dots, x_n) = f_n(x_n) \cdot f(x_{n-1} \vee x_n) \cdot f(x_{n-2} \vee x_{n-1}, x_n) \dots f(x_1 \vee x_2, \dots, x_n) \quad (6.4)$$

Where the conditional PDF can be expressed by (Tang et al., 2020)

$$f(x \vee v) = c(F(x \vee v_{-m}), F(v_m \vee v_{-m}); \theta_{x, v_m \vee v_{-m}}) f(x \vee v_{-m}) \quad (6.5)$$

Where $c(\cdot, \cdot; \theta)$ is the bivariate copula density function, v_m is an arbitrarily selected component from vector \mathbf{v} , and v_{-m} is the vector \mathbf{v} excluding v_m .

The conditional cumulative distribution function (CDF) can then be expressed as

$$F(x \vee v) = \frac{\partial C(F(x \vee v_{-m}), F(v_m \vee v_{-m}); \theta_{x, v_m \vee v_{-m}})}{\partial F(v_m \vee v_{-m})} \quad (6.6)$$

This partial derivative of the copula function is also called the h-function, $h(F(x \vee v_{-m}), F(v_m \vee v_{-m}); \theta_{x, v_m \vee v_{-m}})$.

A graphical model is usually used to help with modelling complexity when using a vine copula. Vine copulas are often used to model dependence structures among variables in a high-dimensional distribution (Aas et al., 2009; Czado, 2019). A d-dimensional vine copula is a pair-copula with

$d(d-1)/2$ unconditional and conditional bivariate copulas. A set of linked trees also defines the structure of vine copulas T_1, T_2, \dots, T_{d-1} that meets these following criteria (Kraus and Czado, 2017)

1. $T_1 = (V_1, E_1)$ is Tree 1 with nodes $V_1 = \{1, 2, \dots, d\}$ and edges E_1 .
2. For $m = 2, \dots, d - 1$, tree T_m has nodes $V_m = E_{m-1}$ and edges E_m .
3. For $m = 2, \dots, d - 1$, two nodes of T_m can be linked by an edge if these nodes have a shared node with the corresponding edges of T_{m-1} .

There are two common graphical models used to represent vine copulas. Canonical vine (C-vine) and Drawable vine (D-vine) copulas. The main difference lies in the characteristic of nodes in the two types of regular vine. In the C-vine, each node has a unique node connected to other nodes, while in D-vine, each node is only connected to one or two other nodes. The illustration of the C-vine and D-vine models can be seen in Fig. 6.2 as follows

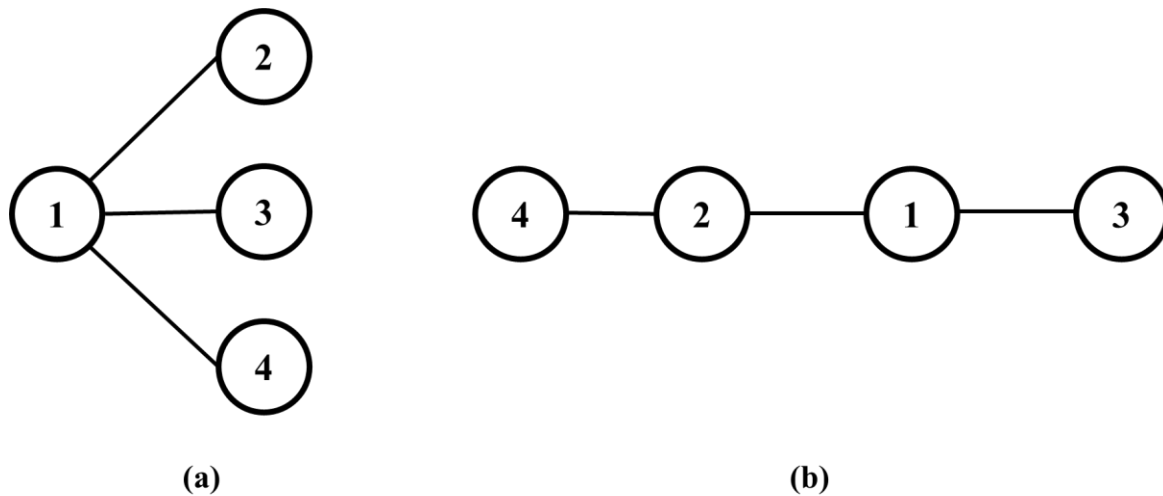


Fig. 6.2. Graphical model for (a) C-vine, and (b) D-vine Copulas

Generally, a joint PDF of d -dimensional random variables can be decomposed using a C-vine copula that satisfies (Czado, 2019)

$$f(x_1, \dots, x_d) = \left[\prod_{j=1}^{d-1} \prod_{i=1}^{d-j} c_{j,j+i;1,\dots,j-1} \right] \times \left[\prod_{k=1}^d f_k(x_k) \right] \quad (6.7)$$

While decomposing a joint PDF of d-dimensional random variables using a D-vine can be expressed using the equation below (Czado, 2019)

$$f(x_1, \dots, x_d) = \left[\prod_{j=1}^{d-1} \prod_{i=1}^{d-j} c_{i,(i+j);(i+1),\dots,(i+j-1)} \right] \times \left[\prod_{k=1}^d f_k(x_k) \right] \quad (6.8)$$

C-vine copulas are found to be more suitable for modelling the marine environmental variables where there is usually one dominating factor among the environmental variables (Bedford et al., 2016; Dong et al., 2022; Nagler et al., 2022). This chapter uses C-vine copulas to model three selected environmental variables: wind speed, wave height, and current velocity. The steps to construct C-vine copulas for three variables are:

1. Determine the marginal PDF of each variable.
2. Identify the best-fit bivariate copula for Tree 1
 - a) Original data are transformed into the copula domain

$$U_i = \frac{R_i}{n+1} = \frac{n\hat{F}_i(X_i)}{n+1} \quad (6.9)$$

where n is the number of observations and $\hat{F}_i(t)$ is the empirical cumulative function

defined as $\hat{F}_i(t) = \frac{1}{n} \sum_{i=1}^n 1(X_i \leq t)$.

- b) Copula parameter estimation is performed using Maximum Log-likelihood Estimation (MLE). The log-likelihood function $L(\theta)$ of a copula function can be expressed as (Lü et al., 2020)

$$L(\theta) = \sum_{i=1}^N \ln c(u_1, u_2; \theta) \quad (6.10)$$

The estimated θ using MLE can be obtained by maximizing $L(\theta)$ (Lü et al., 2020)

$$\hat{\theta} = \operatorname{argmax} L(\theta) \quad (6.11)$$

- c) Select the best-fit copula using AIC scores. (Lü et al., 2020)

$$AIC = -2L(\hat{\theta}) + 2k = -2 \sum_{i=1}^N \ln c(u_{1i}, u_{2i}; \hat{\theta}) \quad (6.12)$$

Where k is the unknown parameter estimated using MLE, the lowest AIC score indicates the best-fit copula.

3. Identify the best-fit bivariate copula for the next tree (Tree 2)

Tree 2 consists of $f(x_2, x_3 \vee x_1) = C_{2,3 \vee 1}(F_{2 \vee 1}(x_2 \vee x_1), F_{3 \vee 1}(x_3 \vee x_1); \theta)$

- a) Data $\{F_2(x_{2i}), F_1(x_{1i}), i = 1, 2, \dots, N\}$ are transformed into data $\{F_{2\vee 1}(x_{2i} \vee x_{1i}), i = 1, 2, \dots, N\}$ using h function (a partial derivative of bivariate copula with respect to the given variable), where (Lü et al., 2020)

$$h(u_2 \vee u_1; \theta) = \frac{\partial C(u_1, u_2; \theta)}{\partial u_1} \quad (6.13)$$

$$\text{So, } F_{2\vee 1}(x_{2i} \vee x_{1i}) = h_{1,2}(F_2(x_{2i}), F_1(x_{1i}); \theta), \text{ for } i = 1, 2, \dots, N$$

- b) Data $\{F_3(x_{3i}), F_1(x_{1i}), i = 1, 2, \dots, N\}$ are also transformed to data $\{F_{3\vee 1}(x_{3i} \vee x_{1i}), i = 1, 2, \dots, N\}$ using the h function, resulting in $F_{3\vee 1}(x_{3i} \vee x_{1i}) = h_{1,3}(F_3(x_{3i}), F_1(x_{1i}); \theta), \text{ for } i = 1, 2, \dots, N$
- c) Based on $\{F_{2\vee 1}(x_{2i} \vee x_{1i}), F_{3\vee 1}(x_{3i} \vee x_{1i})\}$, select the best-fit copula for $C_{2,3|1}$.

4. Perform the same procedure if there are more trees
5. Obtain the joint PDF. For trivariate analysis, the joint PDF will be decomposed as follows

$$f(x_1, x_2, x_3) = f(x_1) \cdot f(x_2) \cdot f(x_3) \cdot C_{1,2}\{F(x_1), F(x_2)\} \cdot C_{1,3}\{F(x_1), F(x_3)\} \cdot C_{2,3\vee 1}\{F(x_2 \vee x_1), F(x_3 \vee x_1)\}$$

Random sampling is then performed to generate the simulated samples from the constructed probability distribution function (PDF) $f_{1,2,\dots,n}(y_1, y_2, \dots, y_n)$. Let (y_1, y_2, \dots, y_n) be a simulated data sample from $f_{1,2,\dots,n}(y_1, y_2, \dots, y_n)$ and (r_1, r_2, \dots, r_n) is a sample independent standard, uniform on $[0,1]$. A Rosenblatt transformation is then used to generate (y_1, y_2, \dots, y_n) based on (r_1, r_2, \dots, r_n) (Lü et al., 2020):

- 1) Solving y_1 . Let $r_1 = F_1(y_1)$. Then, $y_1 = F_1^{-1}(r_1)$ is obtained.

- 2) Solving y_2 . Let $r_2 = F_{2v1}(y_2|y_1) = h_{2,1}(F_2(y_2), F_1(y_1); \theta)$. Then, $y_2 = F_2^{-1}(h_{2v1}^{-1}(r_2, F_1(y_1); \theta))$ is obtained.
- 3) Solving y_3 . Let $r_3 = F_{3v1,2}(y_3|y_1, y_2) = h_{3,1v2}(F_{3v2}(y_3|y_2), F_{1v2}(y_1|y_2); \theta) = h_{3,1v2}(h_{3v2}(F_3(y_3), F_2(y_2); \theta), h_{1v2}(F_1(y_1), F_2(y_2); \theta); \theta)$. Then, $y_3 = F_3^{-1}(h_{3,2}^{-1}(h_{3,1v2}^{-1}(r_3, h_{1,2}(F_1(y_1), F_2(y_2); \theta); \theta), F_2(y_2); \theta))$ is obtained.

Finally, environmental data for a certain return period can be obtained using the conditional correlation model that has been constructed using the best fitted vine copula models. The conditional probability distribution is written as follows (Liu and Zhang, 2016)

$$F(y_1, z_1 | X = x_1) = C(V \leq v_1, W \leq w_1 | U = u_1) = \frac{\partial C(u_1, v_1, w_1)}{\partial u_1} \quad (6.14)$$

And the conditional return period based on a copula function can be estimated using

$$T(y_1, z_1 | X = x_1) = \frac{1}{1 - F(y_1, z_1 | X = x_1)} = \frac{1}{1 - \frac{\partial C(u_1, v_1, w_1)}{\partial u_1}} \quad (6.15)$$

Thus, based on the selected return periods, two environmental variables can be generated based on the dominating environmental variable. The estimation of these environmental variables is based on the best fitted vine copulas. The estimated environmental variables are then used as the input to assess reliability and resilience of the structures.

6.2.3 Resilience assessment

There are various ways of defining resilience. In general, the word resilience is derived from the Latin word “resilire” which means “to bounce back”(Hosseini et al., 2016). It is similarly defined as the capability of a system to withstand undesirable events and be able to recover (Sarwar et al.,

2018; Yodo and Wang, 2016). A more general practical definition states that resilience is the ability of a system to prepare for, and adapt to, any undesirable events and to withstand and recover from these events (Aven, 2011; Ayyub, 2015). From this definition, the resilience of a process system is the ability to cope with disruptive events and avoid failures (Taleb-Berrouane and Khan, 2019). There are many frameworks to assess the resilience of a system. In this chapter, resilience is assessed based on three main capacities: absorptive capacity, adaptive capacity, and restorative capacity (Yarveisy et al., 2020). Absorptive capacity is the capability of a system to deal with a given stress through adaptive mechanisms. Adaptive capacity is the effect of control actions that will make the performance of a system steady and allow the restoration process to a new state. Restorative capacity is the necessary action to bring the system back to the previous or new operational states.

A general equation to quantify resilience can be seen in the following equation (Ayyub, 2015; Bonstrom and Corotis, 2016)

$$Resilience(R) = \int_{T_0}^{T_R} \frac{Q(t)}{T_R} dt \quad (6.16)$$

Where $Q(t)$ is the system's performance, T_0 is the time when the disruptive event starts to occur, and T_{RE} is the time to complete restoration of system performance. To assess the resilience of an offshore structure, the performance of the system can be investigated using the reliability of the offshore structures as the measure of performance. Thus, a simple and robust approach was developed to assess resilience in term of reliability (Yarveisy et al., 2020)

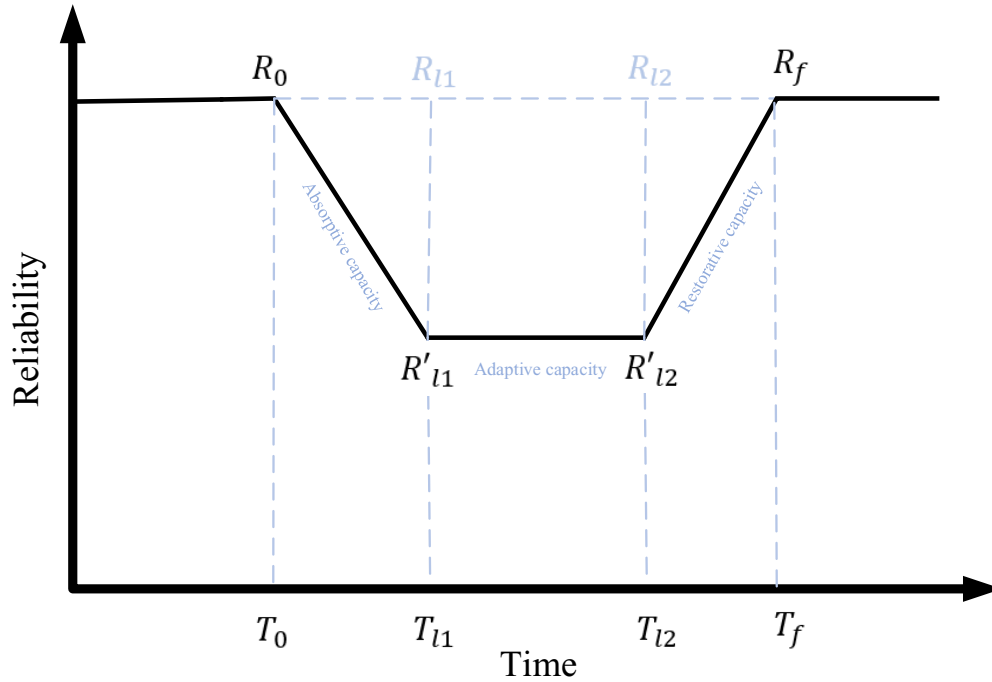


Fig. 6.3. Resilience metric in terms of reliability

Fig. 6.3 shows R_0 (initial reliability) and R_f (final reliability) at their respective times T_0 and T_f . R'_{l1} and R'_{l2} represent the disrupted state reliability at times T_{l1} and T_{l2} . While, reliability levels in the absence of disruption are denoted by R_{l1} and R_{l2} . Yarveisy et al. (2020) developed the equation to quantify resilience as follows

$$Resilience = Ab + Ad * Res - Ab * Ad * Res \quad (6.17)$$

Where,

- a. The Absorptive Capacity (Ab): the ratio of residual reliability to the initial reliability at the time of the disruptive event (Bougofa et al., 2021; Taleb-Berrouane et al., 2019). It can be estimated as (Yarveisy et al., 2020)

$$Ab = \left(\frac{R'_{l1}}{R_0}\right) * \left(1 + \left(\frac{R_0 - R_{l1}}{R_0}\right)\right) \quad (6.18)$$

- b. The Adaptive Capacity (Ad): the ratio of operation duration in the disrupted state to the total period from disruption to a new stable state condition.

$$Ad = 1 - \left(\frac{T_{l2} - T_{l1}}{T_f - T_0}\right) \quad (6.19)$$

- c. The Restorative Capacity (Res): the slope of the recovery and can be estimated using

$$Res = \frac{\arctan \left[\frac{R'_f - R'_{l2}}{\left(\frac{T_f - T_{l2}}{T_f - T_0}\right)} \right]}{90} * \left(\frac{R'_f}{R_f}\right) * \left(\frac{T_{l2} - T_0}{T_f - T_0}\right) \quad (6.20)$$

In this chapter, reliability of the structure is assumed to follow a Poisson process (Rózsás and Mogyorósi, 2017). The probability of n number of loads occurring during time, t, can be estimated as

$$P_n(t) = \frac{(\alpha t)^n e^{(-\alpha t)}}{n!}, n = 0,1,2, \dots \quad (6.21)$$

Where α is the mean number of loads per unit of time. The reliability can be calculated using the following equation (Ebeling, 2004)

$$R(t) = e^{-(1-R)\alpha t} \quad (6.22)$$

Static reliability (R) can be estimated using a limit state assuming random stress and constant strength for the structure (Ebeling, 2004; Li and Zhang, 2020; Wei et al., 2015).

$$g = Resistance - Stress \quad (6.23)$$

Where, Resilience is the product of the yield strength and the projected area, while stress is taken as the base shear force calculated from the total environmental loads (Nizamani, 2014). The

reliability is then calculated using the First Order Reliability Method (FORM). The calculation of the total environmental loads can be seen in Appendix 6A.

6.3 Marine environmental data modelling

Environmental parameters considered in this study are wave height, wind speed, and current velocity. These three parameters are mentioned on API 2A-WSD as they have a specific type of relationship that should be considered (American Petroleum Institute, 2002). The mouth of Placentia Bay in the province of Newfoundland and Labrador was selected as an example location from which to collect the environmental data, largely because the data was readily available. Ocean data for this location was obtained from the Smart Atlantic website (ERDDAP, 2022). The data used in this chapter were recorded hourly between January 1st 2013 and December 31st.

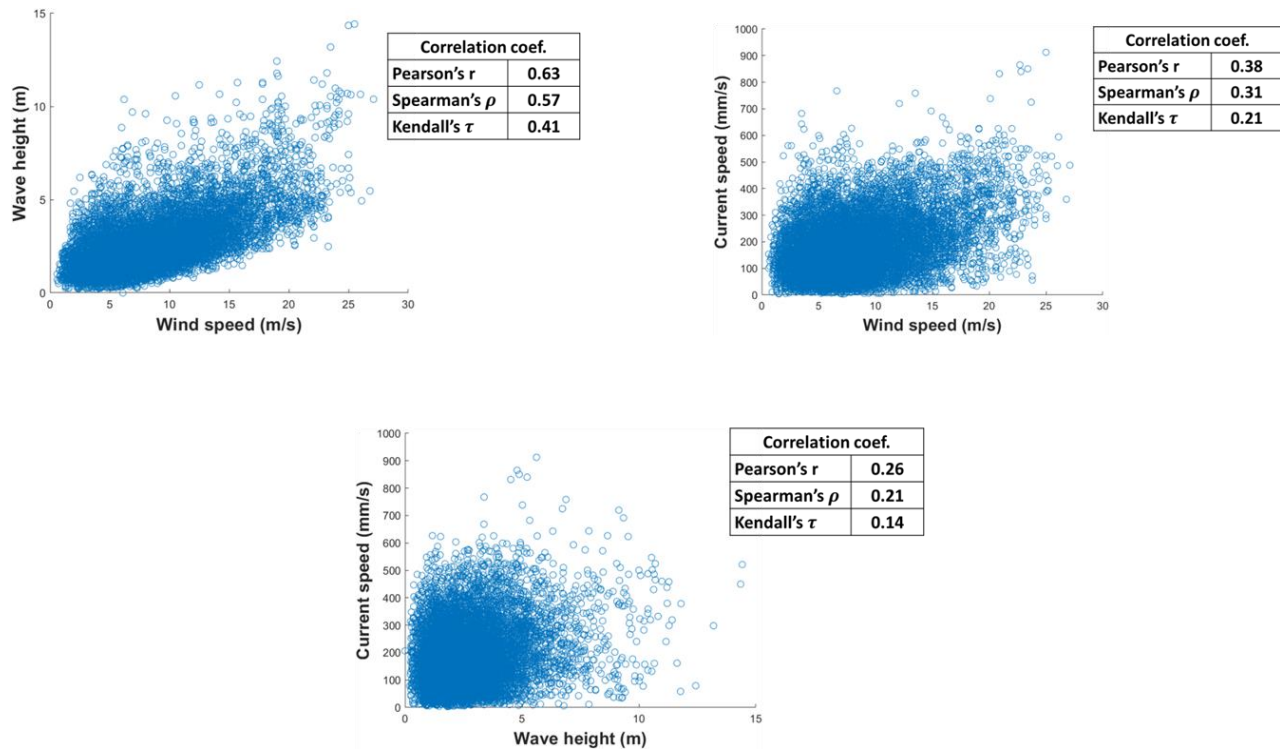


Fig. 6.4. Scatter plots for all environmental variable pairs

Table 6.2. Correlation coefficient (Kendall's tau) between environmental variables

	Wind speed	Wave height	Current velocity
Wind speed	1	0.41	0.21
Wave height		1	0.14
Current velocity			1

Table 6.3. Asymmetry measure between environmental variables

	Wind speed	Wave height	Current velocity
Wind speed	0	0.01	0.26
Wave height		0	0.25
Current velocity			0

Fig. 6.4 shows that each pair of environmental variables has a positive correlation. The Kendall's tau correlation coefficient for each pair is also presented in Table 6.2. From this table, wind speed and wave height show a strong correlation, while all current velocity pairs with other variables show weak correlations. Despite this weak correlation, the asymmetry level for current velocity pairs is higher than the wind speed and wave height pair data, as seen in Table 6.3. In this case, asymmetry copulas play important roles in modelling this dependence structure, as mentioned in previous studies (Ramadhani et al., 2022, 2021).

Marginal distribution for each environmental variable was first identified. The Akaike Information Criterion (AIC) was used to select the best-fitted distribution among all possible marginal distributions considered in this chapter. Table 6.4 shows the AIC values for all distributions, while Table 6.5 shows the statistical parameters for the best-fitted distribution for each environmental variable.

Table 6.4 AIC values for all environmental variables

	Weibull	Normal	Lognormal	Rayleigh	Extreme Value	Exponential	Gamma
Wind speed	71,585	73,506	71,732	71,599	71,315	79,637	71,158*
Wave height	Inf	46,720	Inf	43,219	41,831	49,104	41043*
Current velocity	152,585	155,372	153,767	153,023	152,765	157,689	152,502*

*Indicates the best-fit marginal distribution

Table 6.5 Statistical parameters for the best fitted marginal distribution

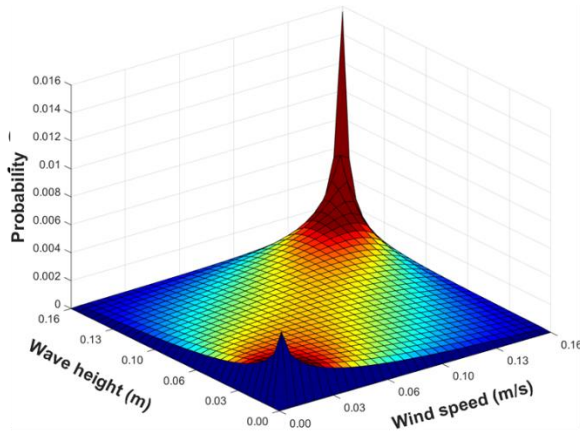
	Mean	Standard Deviation	Shape Parameter	Scale Parameter
Wind speed	8.39	4.34	3.71	2.26
Wave height	2.53	1.52	2.79	0.91
Current velocity	179.93	108.05	2.63	68.41

The smallest value of AIC indicates the best distribution model for the data set. The Gamma distribution is best fitted to all environmental variables. Kolmogorov-Smirnov (KS) tests were carried out to examine the goodness of fit of gamma distribution for all environmental variables. The test statistic values from the KS test for wind, wave, and current data are 0.0125, 0.0059, and 0.012, respectively. These statistics show that the fitted distribution is valid (fail to reject the null hypothesis) at a significance level of 5% (critical value for KS-test is 0.0135) for each environmental variable.

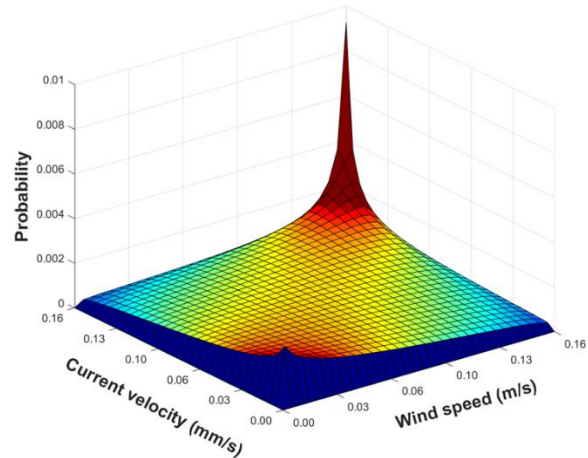
After identifying the marginal distribution for each environmental variable, vine copulas were used to model the complex dependence structure of the marine environmental variables. Two types of dependence structures were selected: symmetric and asymmetric dependence. The Archimedean copula family was selected to model the symmetric dependence structure. For the asymmetric dependence, asymmetric copulas constructed using the product rule were utilized.

For the symmetric dependence structure, Clayton copulas, Gumbel copulas, and Frank copulas were compared to identify which copula is best fitted in each edge of the dependence structure.

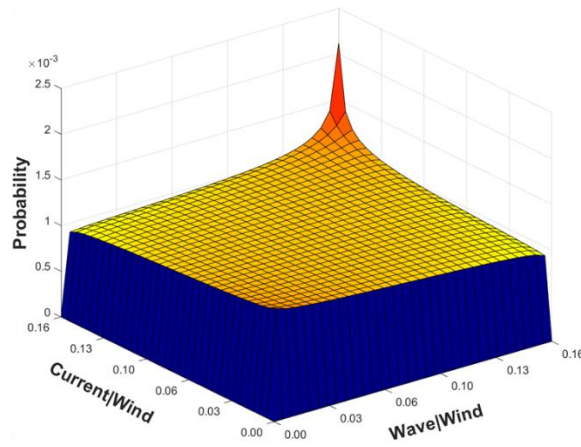
Table 6.6 shows the best-fitted copula function for each edge and its parameter.



(a)



(b)



(c)

Fig. 6.5. Probability distribution functions for (a) wind and wave data in Tree 1 (Table 6.6), (b) wind and current data in Tree 1, and (c) conditional environmental data in Tree 2 (Table 6.6) using symmetric copulas

Table 6.6 Best fitted symmetric copulas and their parameters for each edge

Tree	Edge	Copula	Copula Parameter	$L(\theta)$ ($\times 10^5$)	AIC ($\times 10^5$)
1	X_1, X_2	Clayton	$\gamma = 1.0049$	-3.3290	6.6581
		Gumbel	$\gamma = 1.6352$	-3.3127	6.6255*
		Frank	$\gamma = 4.2656$	-3.3168	6.6337
	X_1, X_3	Clayton	$\gamma = 1.0007$	-3.3527	6.7054
		Gumbel	$\gamma = 1.2598$	-3.3327	6.6655*
		Frank	$\gamma = 1.9706$	-3.3350	6.6701
2	$X_2, X_3 \vee X_1$	Clayton	$\gamma = 1.0137$	-3.3721	6.7443
		Gumbel	$\gamma = 1.0261$	-3.3412	6.6824*
		Frank	$\gamma = -0.0658$	-3.3415	6.6829

*Lowest AIC score indicates the best-fit copula

The Gumbel copula is best fitted to all environmental variable pairs on all the edges of the symmetric dependence structure. Their probability distribution functions are shown in Fig. 6.5.

For the asymmetric dependence structure, the best-fitted copula functions for each edge and their parameters are shown in Table 6.7

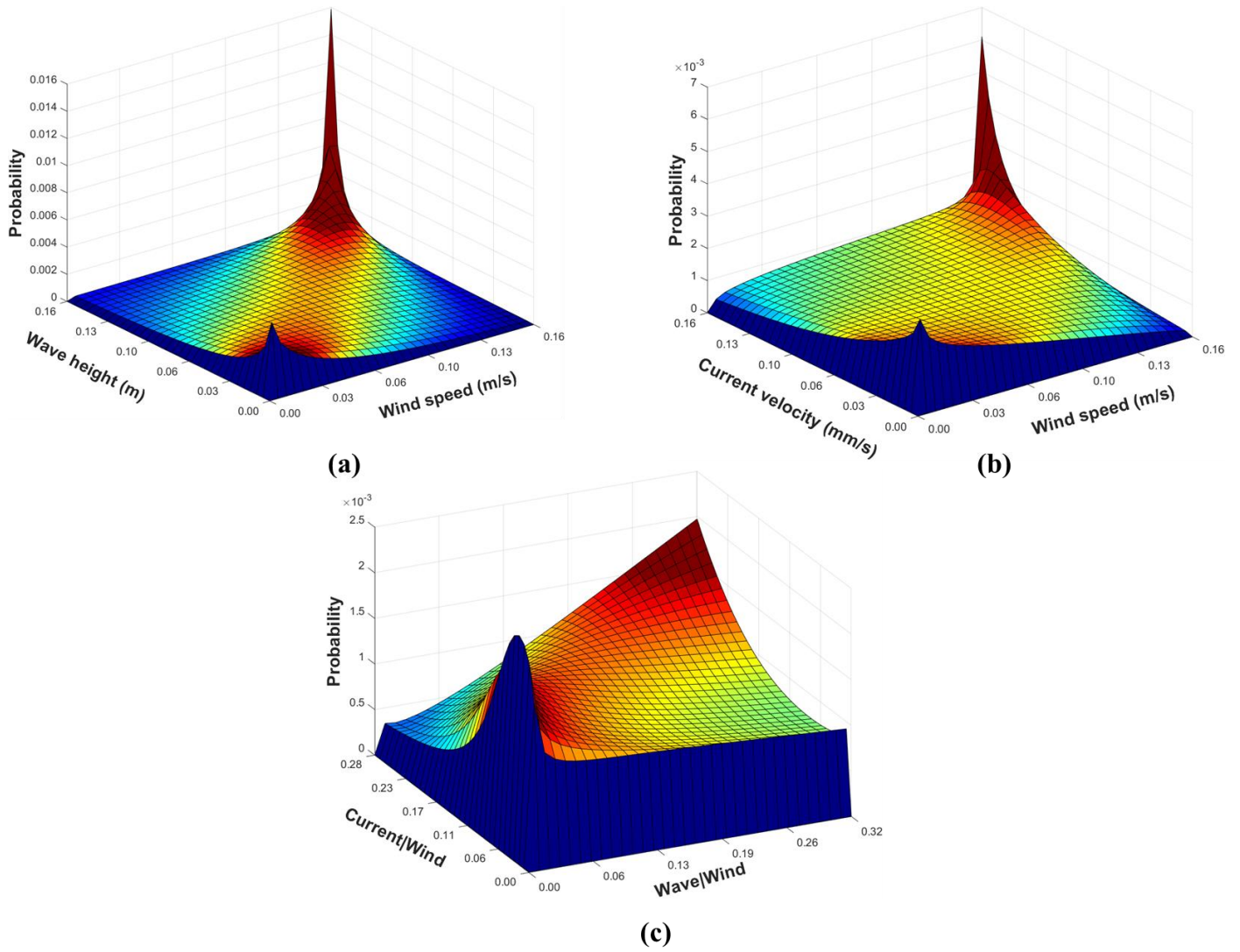


Fig. 6.6. Probability distribution functions for (a) wind and wave data in Tree 1 (Table 6.7), (b) wind and current data in Tree 1 (Table 6.7), and (c) conditional environmental data in Tree 2 (Table 6.7) using asymmetric copulas

Table 6.7 Best fitted asymmetric copulas and their parameters for each edge

Tree	Edge	Copula	Copula Parameter	$L(\theta)$ ($\times 10^5$)	AIC ($\times 10^5$)
1	X_1, X_2	Clayton- Gumbel Type-	$\gamma_1 = 1.8116$ $\gamma_2 = 18.2143$ $\theta_{11} = 0.9857, \theta_{12} = 0.8602$	-2.7257	5.4516

		1	$\theta_{21} = 0.0143, \theta_{22} = 0.1398$		
		Clayton-Frank Type-1	$\gamma_1 = 5.3741$ $\gamma_2 = 7.1045$ $\theta_{11} = 0.1006, \theta_{12} = 0.5423$ $\theta_{21} = 0.8994, \theta_{22} = 0.4577$	-2.7289	5.4580
		Gumbel-Frank Type-1	$\gamma_1 = 1.8264$ $\gamma_2 = -17.5023$ $\theta_{11} = 0.9977, \theta_{12} = 0.8076$ $\theta_{21} = 0.0023, \theta_{22} = 0.1924$	-2.7254	5.4510*
	X_1, X_3	Clayton- Gumbel Type- 1	$\gamma_1 = 1.6183$ $\gamma_2 = 1.9838$ $\theta_{11} = 0.8663, \theta_{12} = 0.2116$ $\theta_{21} = 0.1337, \theta_{22} = 0.7884$	-2.7477	5.4955*
		Clayton-Frank Type-1	$\gamma_1 = 16.0542$ $\gamma_2 = 2.0700$ $\theta_{11} = 0.4564, \theta_{12} = 0.0796$ $\theta_{21} = 0.5436, \theta_{22} = 0.9204$	-2.7488	5.4977
		Gumbel-Frank Type-1	$\gamma_1 = 1.2644$ $\gamma_2 = 11.9340$ $\theta_{11} = 0.1888, \theta_{12} = 0.8256$ $\theta_{21} = 0.8112, \theta_{22} = 0.1744$	-2.7478	5.4957
2	$X_2, X_3 \vee X_1$	Clayton- Gumbel Type- 1	$\gamma_1 = 1.0042$ $\gamma_2 = 2.0115$ $\theta_{11} = 0.8642, \theta_{12} = 0.9537$ $\theta_{21} = 0.1358, \theta_{22} = 0.0463$	-2.2482	4.4966
		Clayton-Frank Type-1	$\gamma_1 = 3.4989$ $\gamma_2 = -3.5458$ $\theta_{11} = 0.3334, \theta_{12} = 0.9039$ $\theta_{21} = 0.6666, \theta_{22} = 0.0961$	-2.2359	4.4719*
		Gumbel-Frank Type-1	$\gamma_1 = 18.7478$ $\gamma_2 = 1.0101$ $\theta_{11} = 0.0013, \theta_{12} = 0.0123$ $\theta_{21} = 0.9987, \theta_{22} = 0.9877$	-2.2374	4.4750

*Lowest AIC score indicates the best-fit copula.

The Gumbel-Frank copula is best fitted to pair wind and wave data in the first tree. In contrast, the Clayton-Gumbel copula is best fitted to model wind and current data, and the Clayton-Frank copula is best fitted for the conditional probability in the second tree. Their probability distribution functions are shown in Fig. 6.6.

6.4 Result and Discussion

6.4.1 Copula models verification

Distribution fitting and error value calculations are carried out to see if the vine copula models fit the marine environmental data. The real data are compared to the best-fitted copula in each edge for both asymmetric and symmetric dependence structures.

From Fig. 6.7, C-vine copulas are fitted to model the multivariate data. Both asymmetric and symmetric copulas are able to model multivariate environmental variables in all trees. In this case, the wind speed was selected as the dominating factor. Wind speed influences both wave height and current velocity. The results in Fig. 6.7 also agree with the findings from other studies. The joint probability distribution constructed using the vine copula is fitted to model the multivariate distribution of ocean environmental parameters (Bai et al., 2021). Lin and Dong (2019) mentioned that a proposed joint multivariate model using vine copulas could represent the wave climate very well. From these findings, the application of vine copulas in marine environmental analysis can deal with any types of dependence between variables in a higher dimension. However, Fig. 6.7 indicates that symmetric copulas performed slightly better in modelling the conditional distribution in the second tree. This is also a result of over-parameterization in using asymmetric copulas that may cause the conditional distribution of environmental variables to not best fit the real data.

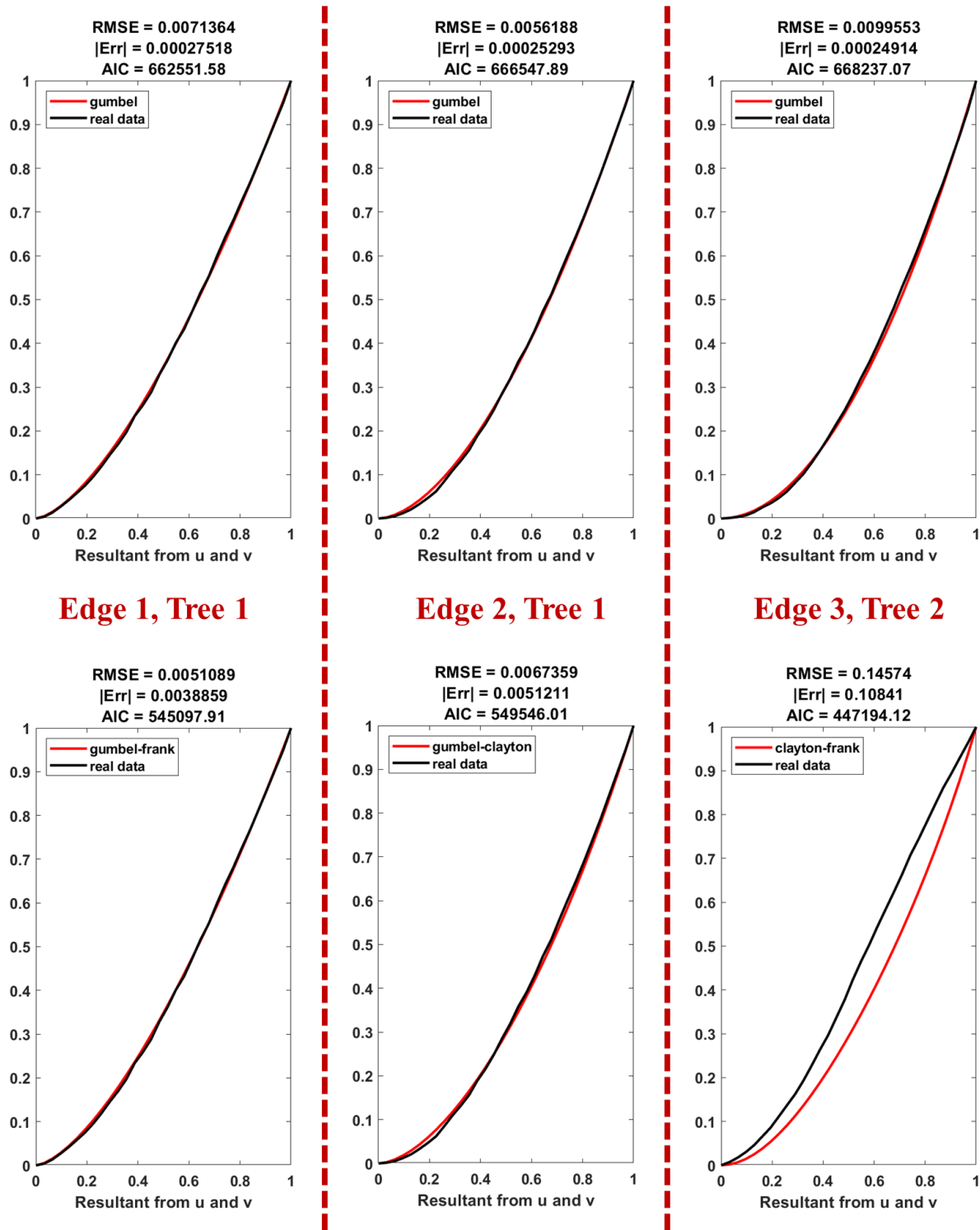


Fig. 6.7. Distribution fitting and error value calculations for all edges using the best fitted symmetric copulas (top), and asymmetric copulas (bottom)

6.4.2 The estimation of the total environmental load

After fitting the marine environmental variables to the asymmetric and symmetric copulas for all edges, a set of random data is generated using the best-fitted copulas. A simulation is then carried out to estimate the total environmental load acting on an offshore structure. In addition to the copula functions, two other common methods are used to compare the results. An independent case generates random data using marginal distributions for each environmental variable. At the same time, a multi-Gaussian method is selected to illustrate the most common multivariate model.

To illustrate the comparison of total environmental load estimated using different models, a simple case study is used. A steel XL monopile structure with a diameter of 9.5m and the immersed part of the pile at 100m is selected (Whitlock, 2022). The wind force is calculated at the reference height of 10m above the mean sea level with a drag coefficient of 0.7 (Det Norske Veritas, 2011). In order to calculate wave load, inertia and drag coefficients are set to be 2 and 1, respectively (Bai and Bai, 2005). Theories used to estimate the total environmental load are detailed in Appendix 6A.

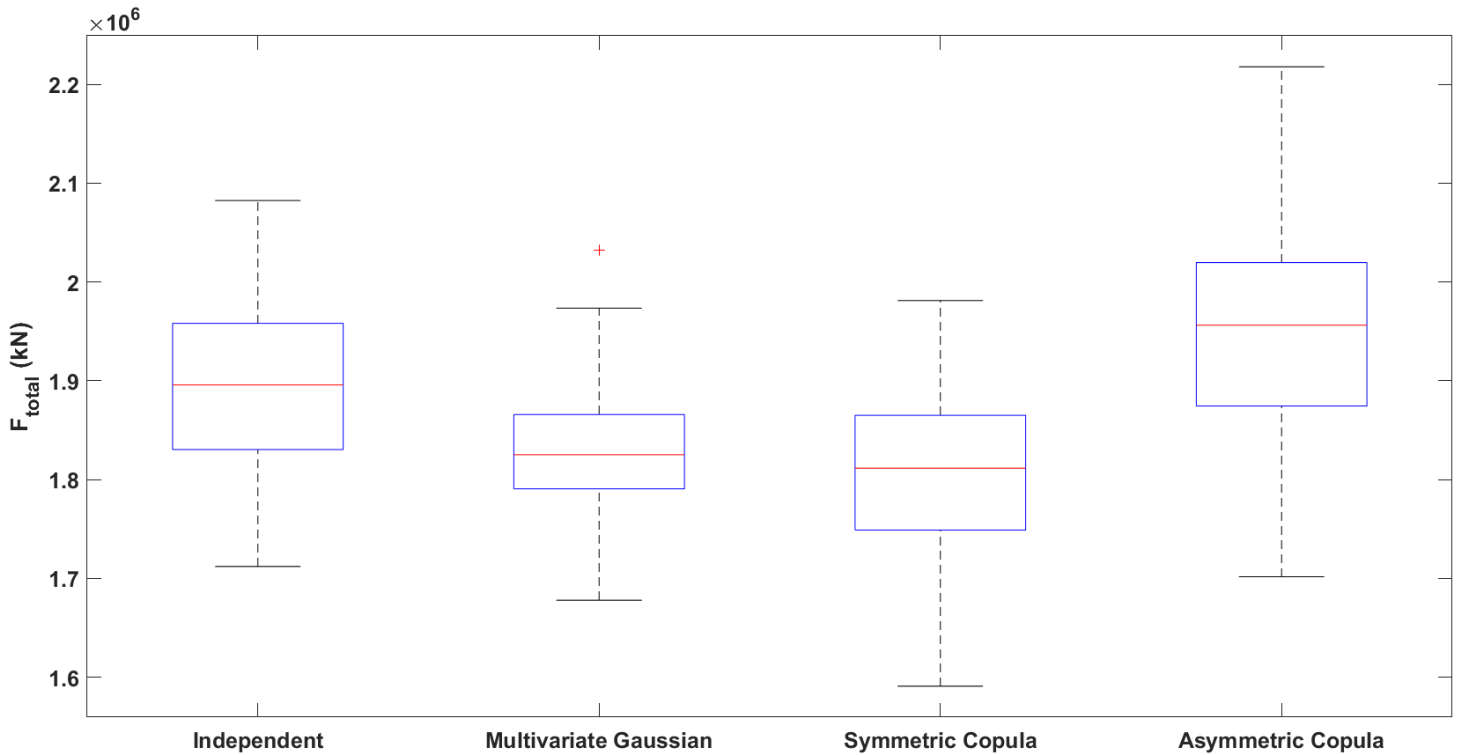


Fig. 6.8. Boxplots for the estimated total environmental loads predicted using the simulated environmental data

Fig. 6.8 shows that the total environmental loads estimated using generated random data from four different methods do not differ significantly. The multivariate Gaussian model produced a lower median total environmental load compared to the independent model. In contrast, C-vine copulas showed different trends. The estimated total environmental loads modelled using symmetric copulas resulted in a lower median load compared to both independent and multivariate Gaussian models. On the other hand, asymmetric copulas produced higher total environmental load compared to the other models. Although the total environmental loads are not significantly different, random data generated using symmetric and asymmetric copulas are able to accommodate tail dependence which is usually the characteristic of marine environmental variables. In the second tree of the C-vine structure used to model the environmental variables, the

Gumbel distribution is best fitted for the symmetric model, while the Clayton-Frank Type-I is best for the asymmetric model.

Gumbel copulas have strong high-value dependencies. Thus, from Fig. 6.8, it can be seen that more data were generated in the higher values tail. The median value of the total environmental load generated using asymmetric copulas is close to the independent models. However, asymmetric copulas still consider the tail dependencies and were able to generate an asymmetric dependence structure compared to the independent model. In addition to this, Table 6.8 shows error values of the real data fitted to the independent and multivariate Gaussian model. It can be seen that the error values are much higher compared to the symmetric and asymmetric values presented in Fig. 6.8. However, the estimated total environmental loads do not differ significantly, and C-vine copulas using both asymmetric and symmetric copulas are best fitted to model the multivariate environmental variables. Both copula models are able to capture the real dependence structure of environmental variables. Failure to capture these dependence structures will lead to misinterpretation of the real dependence type of environmental variables (Zhang et al., 2018). (Jiang et al., 2021) also point out that the proposed multivariate model using vine copulas results in more realistic values by considering the complex dependence structure between environmental variables. Thus, from this study, and supported by other research, vine copulas provide more flexible and appropriate models for the multivariate distribution of environmental variables when compared to the other common methods used in practice.

Table 6.8 Error values for Independent and Multivariate Gaussian method

	RMSE	Mean Absolute Error
Independent method	0.2380	0.1630
Multivariate Gaussian method	0.2351	0.1600

The results obtained from this estimation of total environmental load is used in the next section to assess the reliability and resilience of an offshore structure.

6.4.3 Structural reliability evaluation

After fitting the environmental data to the asymmetric and symmetric C-vine copulas, the reliability of the structure is assessed using this loading information. As mentioned in the previous section, for simplicity, static reliability (R) can be estimated using a limit state assuming random stress and constant strength for the structure. The stress considered in this chapter is the total environmental load. In comparison, the resistance is taken as the product between the yield strength and the area of the pile. Yield strength is assumed to be 450 MPa. Table 6.9 shows the reliability index (β) of the structure estimated using the generated environmental load data from both asymmetric and symmetric data. From this table, the reliability index obtained from two different dependence structures showed similar results. The probability of failure of the structure is in the order of 10^{-6} . This shows that the offshore structure can withstand the random environmental load modelled using symmetric and asymmetric copulas. It was also found that wave height has the highest sensitivity value compared to the other two environmental variables. Thus, the total environmental load largely depends on the wave height. This result also validates a finding that 90% of the total environmental load acting on offshore structures comes from the wave loads (Henry et al., 2019).

Table 6.9 Static reliability calculations using environmental variables data modelled with asymmetric and symmetric C-vine copulas

Copulas	Variables	Generated Data	Reliability Index	Failure Probability	Sensitivity
Asymmetric	Wind (m/s)	8.46	4.63	1.78×10^{-6}	42.50%
	Wave (m)	2.56			90.52%

	Current (mm/s)	180.41			0.01%
Symmetric	Wind (m/s)	8.26			42.50%
	Wave (m)	2.73	4.59	2.18×10^{-6}	90.52%
	Current (mm/s)	155.87			0.01%

In order to assess the reliability of the structure with respect to the selected return periods, wind speed is selected as the dominating factor. This variable is then used to estimate the value of the other environmental variables with different return periods. Table 6.10 provides the summary of the estimation. These values are then used to estimate the reliability of the structure.

Table 6.10 Estimated wave height (m) and current velocity (mm/s) in various return periods (years)

T (years)	Wind speed (m/s) (dominating factor)	Wave height (m)		Current velocity (mm/s)	
		Asymmetric	Symmetric	Asymmetric	Symmetric
10	8.59	7.75	7.91	587.59	562.95
25	11.35	8.69	8.05	643.59	573.91
50	15.95	10.55	8.95	764.86	647.64
75	20.56	11.03	11.03	834.01	683.25
100	25.16	14.41	14.36	837.56	840.53

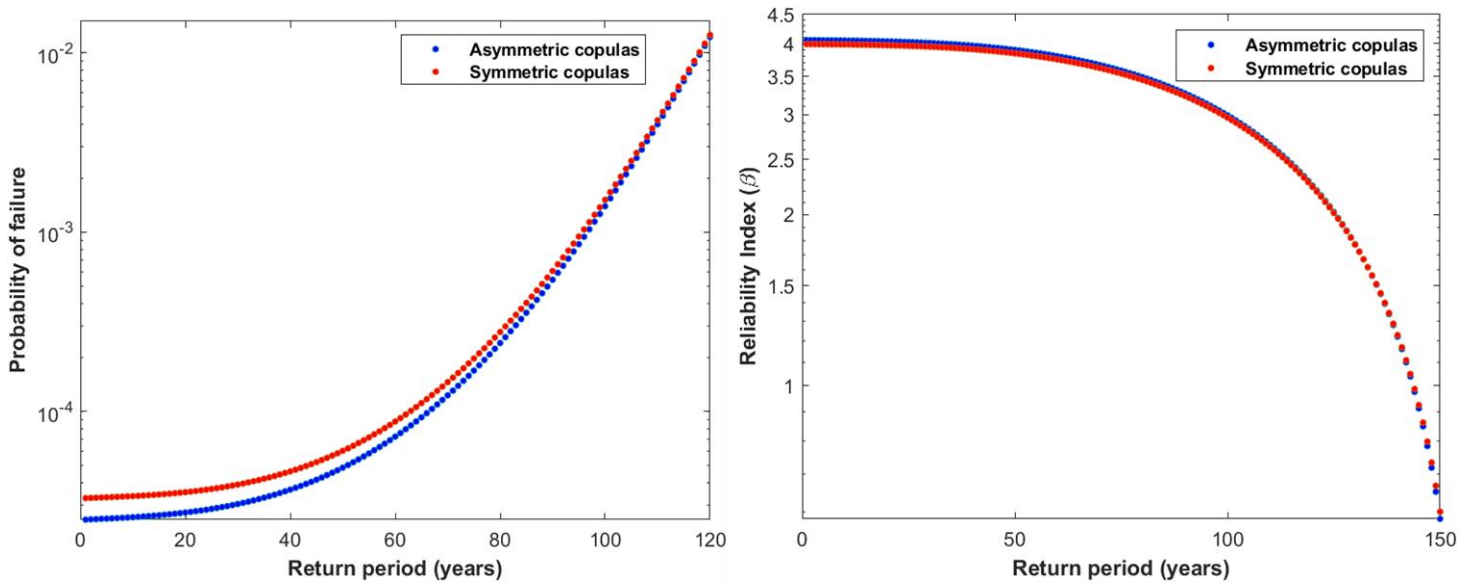
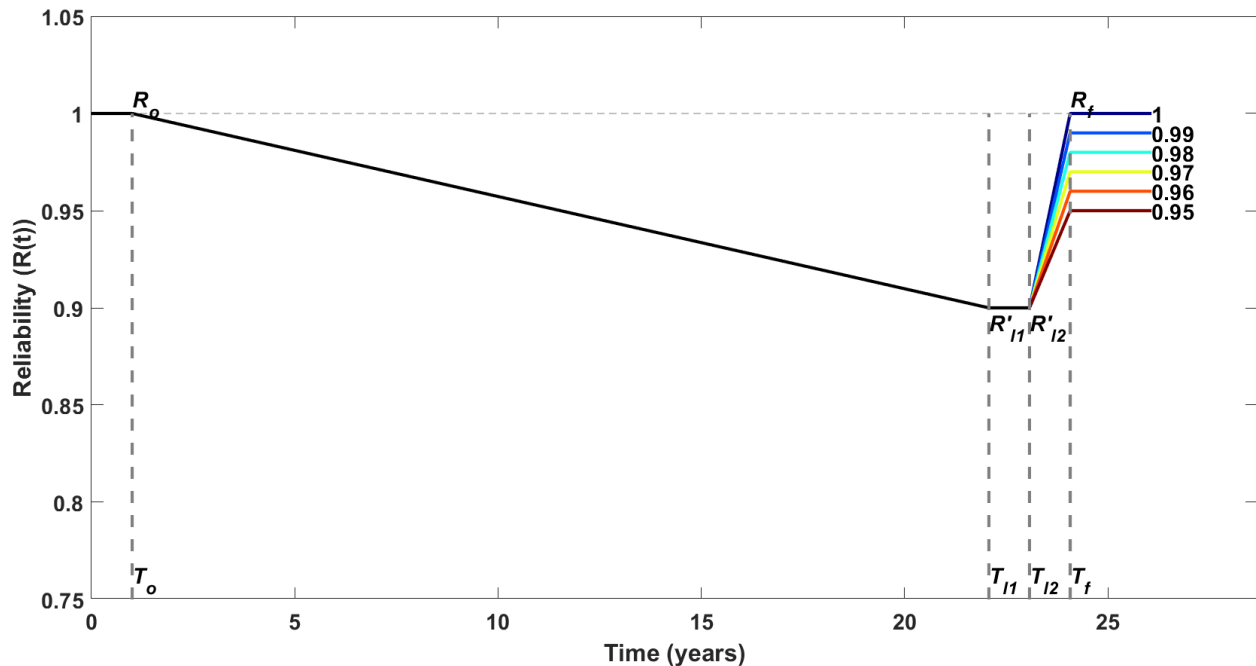


Fig. 6.9. Probability of failure (left) and reliability index (right) in various return periods considering both asymmetric and symmetric C-vine copulas

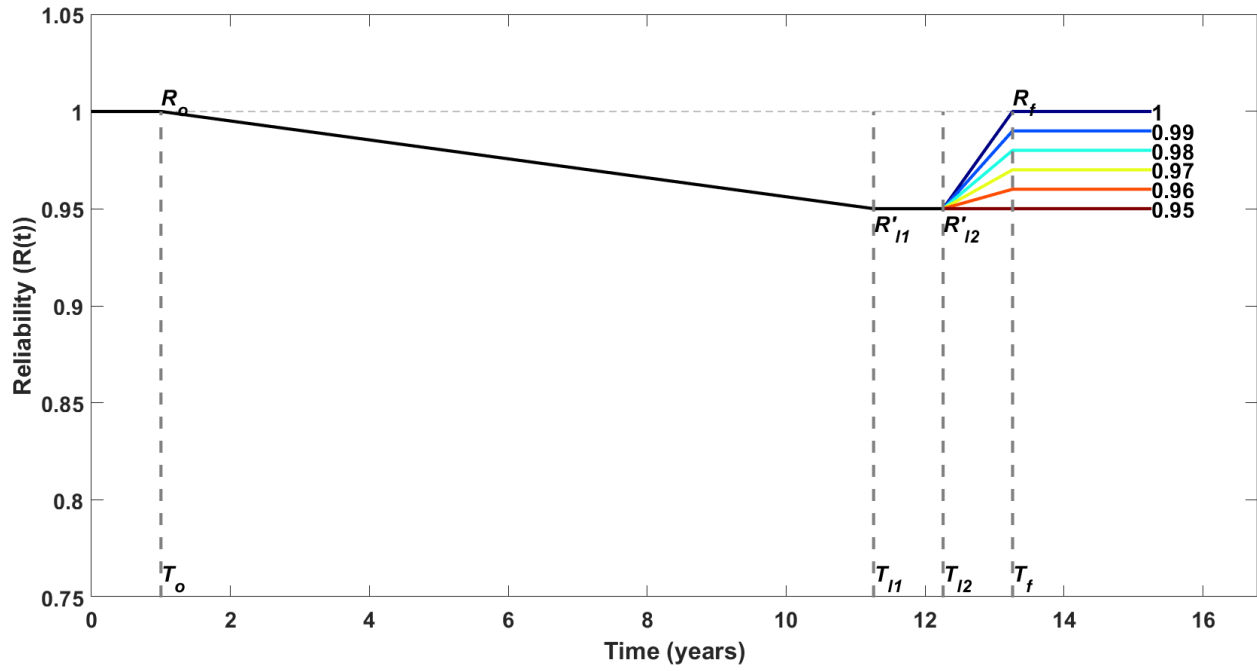
Fig. 6.9 shows the probability of failure and reliability index of the offshore structure subjected to the total environmental load. Environmental data used to estimate the probability of failure are modelled using symmetric and asymmetric copulas. Wind speed data is the dominating factor to estimate the correlated data of the other two environmental variables in various return periods. The figure indicates the same trend as Fig 8, where symmetric and asymmetric C-vine results do not differ significantly. The reliability index shows that symmetric C-vine copulas resulted in a slightly lower reliability index due to higher probability of failure than the asymmetric C-vine copula model. Since the estimations of the probability of failure between symmetric and asymmetric C-vine copula show the same trend, results obtained using symmetric C-vine copulas are used to estimate the resilience of offshore structures in the next section. Symmetric C-vine copulas are selected as they are best fitted to all edges in the dependence structure of the environmental variables.

6.4.4 Resilience assessment

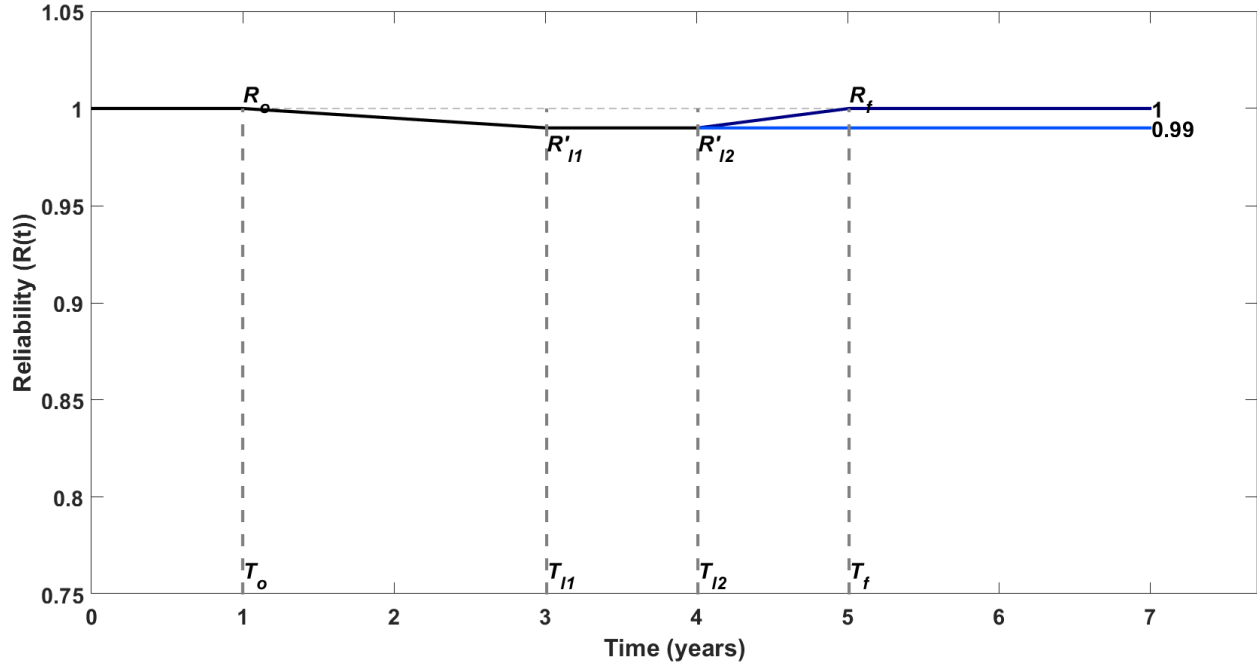
In this chapter, resilience is assessed in terms of the reliability of the offshore structure. The correlated random environmental data used to estimate resilience are derived from the 100-year return period modeled using C-vine copulas. Several scenarios are developed to assess the resilience of the example offshore structure subjected to the derived multivariate marine environmental loads. Initial reliability R_0 is set to be 1, assuming there are no extreme marine events during the first year. Three reliability values are selected at a disrupted steady state: 0.99, 0.95, and 0.90. Ideal recovered reliability, R_f , is set to be equal to the initial reliability. Different new post-recovery reliability states (R'_f) are selected to simulate their effects on the estimated resilience assessment. For recovery period, $T_f - T_{l2}$, the completion of this overall mitigation process is assumed to take approximately 1 year (Tolentino and Ruiz, 2013). A resilience curve for the reliability level at three different disrupted steady states is shown in Fig. 6.10.



(a)



(b)



(c)

Fig. 6.10. Resilience curves with Reliability at disrupted steady state (a) 0.99, (b) 0.95, (c) 0.90 and varied post-recovery reliability states

Table 6.11 Estimated resilience with varied capacities and post-recovery states

No	R'_{l1}	R'_f	Ab	Ad	Res	Resilience
1.	0.9900	1.0000	0.9950	0.7510	0.013	0.9950
2.		0.9900			0.012	0.9949
3.	0.9500	1.0000	0.9550	0.9190	0.013	0.9550
4.		0.9900			0.012	0.9549
5.		0.9800			0.011	0.9548
6.		0.9700			0.011	0.9548
7.		0.9600			0.009	0.9547
8.	0.9000	1.0000	0.9050	0.9570	0.013	0.9055
9.		0.9900			0.012	0.9055
10.		0.9800			0.011	0.9054
11.		0.9700			0.011	0.9053
12.		0.9600			0.009	0.9053
13.		0.9500			0.008	0.9052

Fig. 6.10 shows different scenarios used to assess the resilience of the offshore structure. The reliability of the structure is restored to better new steady states, R'_f , or at least the same level as their R'_{l1} for scenarios 0.95 and 0.99. From Table 6.11, the value of resilience is not significantly different from the value of reliability at the disrupted steady state R'_{l1} and the value of the absorptive capacity. This shows that the resilience metric used in this chapter most significantly depends on the value of absorptive capacity.

Table 6.12 Resilience assessment with respect to different recovery times ($T_f - T_{l2}$)

No	R'_{l1}	$T_f - T_{l2}$ (years)	Ab	Ad	Res	Resilience
1.	0.9000	2.0000	0.9045	0.9585	0.0045	0.9053

2.		3.0000	0.9045	0.9601		0.9051
3.		4.0000	0.9045	0.9616		0.9050
4.		5.0000	0.9045	0.9631		0.9049
5.	0.9500	2.0000	0.9547	0.9246	0.0012	0.9549
6.		3.0000	0.9547	0.9299		0.9548
7.		4.0000	0.9546	0.9345		0.9548
8.		5.0000	0.9545	0.9385		0.9547
9.	0.9900	2.0000	0.9949	0.8004	0.0001	0.9950
10.		3.0000	0.9949	0.8336		0.9950
11.		4.0000	0.9948	0.8573		0.9949
12.		5.0000	0.9948	0.8752		0.9949

Table 6.13 Resilience with different periods of stable disrupted operation

No.	R'_{t1}	R'_f	$T_{t2} - T_{t1}$ (year)	Ad	Resilience
1.	0.9900	1.0000	2.0000	0.6008	0.9950
2.			4.0000	0.4294	0.9950
3.			6.0000	0.3341	0.9949
1.	0.9500	1.0000	2.0000	0.8492	0.9550
2.			4.0000	0.7379	0.9549
3.			6.0000	0.6524	0.9548
1.	0.900	1.0000	2.0000	0.9169	0.9056
2.			4.0000	0.8466	0.9055
3.			6.0000	0.7863	0.9055

Table 6.12 shows that with various recovery times for different reliability levels at the disrupted steady state, the value of resilience remains essentially equal to its absorptive capacity. Eq. 6.17 shows that restorative capacity depends on both absorptive and adaptive capacity. Another comparison is then illustrated according to various periods during stable disrupted operation, $T_{t2} -$

T_{l1} . Table 6.13 shows that the adaptive capacity is reduced when the period of disrupted operation is expanded. However, this extension has no impact on the assessment of resilience. This also validates Eq. 6.17, because adaptive capacity also depends on absorptive capacity. Thus, absorptive capacity is the only independent resilience capacity in the applied metric. This absorptive capacity refers to the inherent design of the system or structure to withstand extreme marine events. This capacity is determined by the offshore structure's safety design and physical characteristics. If we suppose reliability at a disrupted steady state can be maintained close to the initial reliability, then the ability of the system to withstand the disruptive events and restore its functions will be higher too. Higher absorptive capacity means less effort and resources needed to carry out restoration attempts on the structure. This finding agrees with previous studies assessing the resilience of a system with the same metric (Ramadhani et al., 2022; Yarveisy et al., 2020).

Table 6.14 Allowable number of extreme events with different environmental variables data for various return periods

Return period (years)	α	T_{l2} (years)
100	3	23.072
75	9	25.414
50	55	25.9457

Finally, a typical offshore structure's life is usually 20 to 30 years, with some exceptions for minimal production platforms with a 10-year design lives (Wahab et al., 2020). Table 6.14 shows the allowable number of extreme marine events for different environmental return periods. This shows that the structure can only withstand three 100-year environmental events in order to survive for the specified design life. If the return period is reduced, the number of extreme events allowed to impact the structure increases. This is because lower return period data will result in a

smaller probability of failure. Thus, selecting return period data is essential to predict the maximum number of extreme events allowed to impact the structure. This can also be valuable input for decision makers to specify a high resilience metric.

6.5 Conclusion

The proposed methodology is built on vine copulas to construct a multivariate joint distribution of marine environmental variables in higher dimensions. The correlation and the degree of asymmetry between environmental variables are first investigated. Then, trivariate models for environmental variables with wind speed as the dominating factor are constructed using C-vine copula models. Asymmetric and symmetric copulas are selected as the building blocks. Environmental data are finally generated using the best-fitted copulas in each edge and compared to other common multivariate methods. The total environmental loads estimated using all methods show similar values, with symmetric C-vine copulas and asymmetric C-vine copulas resulting in the lowest and highest median of total environmental load, respectively. Error-values estimated for all methods show that both symmetric and asymmetric C-vine copulas fit better to the environmental data compared to the other two methods. Symmetric C-vine copulas provide lower error in the second tree of the dependence structure than asymmetric C-vine copulas. This shows that symmetric C-vine copulas fit better to model the multivariate environmental variables.

Furthermore, identifying wind speed as the dominating variable made it possible to derive and generate correlated data of the other two variables. These data are then used to evaluate the reliability of the structure subjected to the total environmental loads. The results show that the reliability index using symmetric C-vine copulas resulted in a slightly lower reliability index due to a higher probability of failure than the asymmetric C-vine copula model. This reliability value is then used to estimate the resilience of the offshore structure.

Resilience is quantified based on a reliability assessment of the structure subjected to total environmental loads. Quantification of resilience is mainly found to be dependent on the absorptive capacity. This is the only capacity in the resilience metric that is independent. Absorptive capacity is the critical indicator in a system. A higher level of residual reliability will result in a better ability to withstand undesirable events and restore functionality. This capacity is translated into the inherent physical characteristic of the structure that enables it to withstand disruptive events. Thus, system design plays an essential role in achieving a high resilience metric.

The main challenge in the resilience quantification in this study is the quality of the environmental data collected. Future work will focus on integrating advanced modelling tools such as neural networks to enhance the data processing and analysis

Conflict of Interest

The authors declare that they have no known competing financial interests or personal relationships that could have appeared to influence the work reported in this chapter.

Acknowledgements

The authors would like to express their gratitude to the financial assistance provided by the Natural Science and Engineering Council of Canada (NSERC) and the Canada Research Chair (CRC) Tier I Program in Offshore Safety and Risk Engineering.

References

- Aas, K., Czado, C., Frigessi, A., Bakken, H., 2009. Pair-copula constructions of multiple dependence. *Insur. Math. Econ.* 44, 182–198. <https://doi.org/10.1016/j.insmatheco.2007.02.001>
- Afgan, N., Cvetinovic, D., 2010. Wind power plant resilience. *Therm. Sci.* 14, 533–540. <https://doi.org/10.2298/TSCI1002533A>

- Agarwal, G., Tu, W., Sun, Y., Kong, L., 2022. Flexible quantile contour estimation for multivariate functional data: Beyond convexity. *Comput. Stat. Data Anal.* 168, 107400. <https://doi.org/10.1016/j.csda.2021.107400>
- American Petroleum Institute, 2002. Recommended Practice for Planning, Designing and Constructing Fixed Offshore Platforms - Working Stress Design. Washington, D.C.
- Amini, A., Abdollahi, A., Hariri-Ardebili, M.A., Lall, U., 2021. Copula-based reliability and sensitivity analysis of aging dams: Adaptive Kriging and polynomial chaos Kriging methods. *Appl. Soft Comput.* 109, 107524. <https://doi.org/10.1016/j.asoc.2021.107524>
- Aven, T., 2011. On Some Recent Definitions and Analysis Frameworks for Risk, Vulnerability, and Resilience. *Risk Anal.* 31, 515–522. <https://doi.org/10.1111/j.1539-6924.2010.01528.x>
- Ayyub, B.M., 2015. Practical Resilience Metrics for Planning, Design, and Decision Making. *ASCE-ASME J. Risk Uncertain. Eng. Syst. Part A Civ. Eng.* 1, 04015008. <https://doi.org/10.1061/AJRUA6.0000826>
- Bai, X., Jiang, H., Huang, X., Song, G., Ma, X., 2021. 3-Dimensional direct sampling-based environmental contours using a semi-parametric joint probability model. *Appl. Ocean Res.* 112, 102710. <https://doi.org/10.1016/j.apor.2021.102710>
- Bai, Y., Bai, Q., 2005. *Subsea Pipelines and Risers*. Elsevier BV: Amsterdam.
- Bedford, T., Cooke, R.M., 2002. Vines--a new graphical model for dependent random variables. *Ann. Stat.* 30. <https://doi.org/10.1214/aos/1031689016>
- Bedford, T., Daneshkhah, A., Wilson, K.J., 2016. Approximate Uncertainty Modelling in Risk Analysis with Vine Copulas. *Risk Anal.* 36, 792–815. <https://doi.org/10.1111/risa.12471>
- Bešinović, N., Ferrari Nassar, R., Szymula, C., 2022. Resilience assessment of railway networks: Combining infrastructure restoration and transport management. *Reliab. Eng. Syst. Saf.* 224, 108538. <https://doi.org/10.1016/j.res.2022.108538>
- Bonstrom, H., Corotis, R.B., 2016. First-Order Reliability Approach to Quantify and Improve Building Portfolio Resilience. *J. Struct. Eng.* 142. [https://doi.org/10.1061/\(ASCE\)ST.1943-541X.0001213](https://doi.org/10.1061/(ASCE)ST.1943-541X.0001213)
- Bougofa, M., Taleb-Berrouane, M., Bouafia, A., Baziz, A., Kharzi, R., Bellaouar, A., 2021. Dynamic availability analysis using dynamic Bayesian and evidential networks. *Process Saf. Environ. Prot.* 153, 486–499. <https://doi.org/10.1016/j.psep.2021.07.003>
- Cai, B., Zhang, Y., Wang, H., Liu, Y., Ji, R., Gao, C., Kong, X., Liu, J., 2021. Resilience evaluation methodology of engineering systems with dynamic-Bayesian-network-based degradation and maintenance. *Reliab. Eng. Syst. Saf.* 209, 107464. <https://doi.org/10.1016/j.res.2021.107464>
- Cheng, Y., Elsayed, E.A., Chen, X., 2021. Random Multi Hazard Resilience Modelling of Engineered Systems and Critical Infrastructure. *Reliab. Eng. Syst. Saf.* 209, 107453. <https://doi.org/10.1016/j.res.2021.107453>

- Cruz, A.M., Krausmann, E., 2008. Damage to offshore oil and gas facilities following hurricanes Katrina and Rita: An overview. *J. Loss Prev. Process Ind.* 21, 620–626. <https://doi.org/10.1016/j.jlp.2008.04.008>
- Czado, C., 2019. *Analyzing Dependent Data with Vine Copulas*, Lecture Notes in Statistics. Springer International Publishing, Cham. <https://doi.org/10.1007/978-3-030-13785-4>
- De Michele, C., Salvadori, G., Passoni, G., Vezzoli, R., 2007. A multivariate model of sea storms using copulas. *Coast. Eng.* 54, 734–751. <https://doi.org/10.1016/j.coastaleng.2007.05.007>
- Desilver, D., 2020. Renewable energy is growing fast, but fossil fuels still dominate [WWW Document]. URL <https://www.pewresearch.org/fact-tank/2020/01/15/renewable-energy-is-growing-fast-in-the-u-s-but-fossil-fuels-still-dominate/>
- Det Norske Veritas, 2011. *Modelling and analysis of marine operations. Recommended Practice: DNV-RP-H103.*
- Deyab, S.M., Taleb-berrouane, M., Khan, F., Yang, M., 2018. Failure analysis of the offshore process component considering causation dependence. *Process Saf. Environ. Prot.* 1, 220–232. <https://doi.org/10.1016/j.psep.2017.10.010>
- Dong, S., Chen, C., Tao, S., 2017. Joint probability design of marine environmental elements for wind turbines. *Int. J. Hydrogen Energy* 42, 18595–18601. <https://doi.org/10.1016/j.ijhydene.2017.04.154>
- Dong, S., Tao, S., Li, X., Soares, C.G., 2015. Trivariate maximum entropy distribution of significant wave height, wind speed and relative direction. *Renew. Energy* 78, 538–549. <https://doi.org/10.1016/j.renene.2015.01.027>
- Dong, W., Sun, H., Tan, J., Li, Z., Zhang, J., Yang, H., 2022. Regional wind power probabilistic forecasting based on an improved kernel density estimation, regular vine copulas, and ensemble learning. *Energy* 238, 122045. <https://doi.org/10.1016/j.energy.2021.122045>
- Dui, H., Zheng, X., Wu, S., 2021. Resilience analysis of maritime transportation systems based on importance measures. *Reliab. Eng. Syst. Saf.* 209, 107461. <https://doi.org/10.1016/j.res.2021.107461>
- Ebeling, C.E., 2004. *An introduction to reliability and maintainability engineering.* McGraw-Hill Education.
- ERDDAP, 2022. Mouth of Placentia Bay Buoy [WWW Document]. URL https://www.smartatlantic.ca/erddap/tabledap/SMA_MouthofPlacentiaBayBuoy.html (accessed 8.28.21).
- Fang, G., Pan, R., Hong, Y., 2020. Copula-based reliability analysis of degrading systems with dependent failures. *Reliab. Eng. Syst. Saf.* 193, 106618. <https://doi.org/10.1016/j.res.2019.106618>
- Fazeres-Ferradosa, T., Taveira-Pinto, F., Vanem, E., Reis, M.T., Neves, L. das, 2018. Asymmetric copula-based distribution models for met-ocean data in offshore wind engineering

- applications. *Wind Eng.* 42, 304–334. <https://doi.org/10.1177/0309524X18777323>
- Henry, Z., Jusoh, I., Ayob, A., 2019. Structural Integrity Analysis of Fixed Offshore Jacket Structures. *J. Mek.* 40.
- Heredia-Zavoni, E., Montes-Iturrizaga, R., 2019. Modelling directional environmental contours using three dimensional vine copulas. *Ocean Eng.* 187, 106102. <https://doi.org/10.1016/j.oceaneng.2019.06.007>
- Hosseini, S., Barker, K., Ramirez-Marquez, J., 2016. A review of definitions and measures of system resilience. *Reliab. Eng. Syst. Saf.* 145, 47–61. <https://doi.org/https://doi.org/10.1016/j.res.2015.08.006>
- Hu, J., Khan, F., Zhang, L., 2021. Dynamic resilience assessment of the Marine LNG offloading system. *Reliab. Eng. Syst. Saf.* 208, 107368. <https://doi.org/10.1016/j.res.2020.107368>
- Jacomet, A., Khosravifardshirazi, A., Sahafnejad-Mohammadi, I., Dibaj, M., Javadi, A.A., Akrami, M., 2021. Analysing the Influential Parameters on the Monopile Foundation of an Offshore Wind Turbine. *Computation* 9, 71. <https://doi.org/10.3390/computation9060071>
- Jiang, C., Xiong, L., Yan, L., Dong, J., Xu, C.-Y., 2019. Multivariate hydrologic design methods under nonstationary conditions and application to engineering practice. *Hydrol. Earth Syst. Sci.* 23, 1683–1704. <https://doi.org/10.5194/hess-23-1683-2019>
- Jiang, H., Bai, X., Song, G., Luo, M., Ma, X., 2021. Comparing trivariate models for coastal winds and waves accounting for monthly seasonality. *Appl. Ocean Res.* 117, 102959. <https://doi.org/10.1016/j.apor.2021.102959>
- Kaiser, M.J., Yu, Y., 2010. The impact of Hurricanes Gustav and Ike on offshore oil and gas production in the Gulf of Mexico. *Appl. Energy* 87, 284–297. <https://doi.org/10.1016/j.apenergy.2009.07.014>
- Kamil, M.Z., Taleb-Berrouane, M., Khan, F., Amyotte, P., 2021. Data-driven operational failure likelihood model for microbiologically influenced corrosion. *Process Saf. Environ. Prot.* 153, 472–485. <https://doi.org/10.1016/j.psep.2021.07.040>
- Kim, M.H., 1999. Hydrodynamics of Offshore Structures, in: *Developments in Offshore Engineering*. Elsevier, pp. 336–381. <https://doi.org/10.1016/B978-088415380-1/50027-3>
- Kraus, D., Czado, C., 2017. Growing simplified vine copula trees: improving Di{\ss}mann’s algorithm.
- Li, X., Zhang, W., 2020. Long-term assessment of a floating offshore wind turbine under environmental conditions with multivariate dependence structures. *Renew. Energy* 147, 764–775. <https://doi.org/10.1016/j.renene.2019.09.076>
- Liebscher, E., 2008. Construction of asymmetric multivariate copulas. *J. Multivar. Anal.* 99, 2234–2250. <https://doi.org/10.1016/j.jmva.2008.02.025>
- Lin, Y., Dong, S., 2019. Wave energy assessment based on trivariate distribution of significant

- wave height, mean period and direction. *Appl. Ocean Res.* 87, 47–63. <https://doi.org/10.1016/j.apor.2019.03.017>
- Liu, M., Qin, J., Lu, D.-G., Zhang, W.-H., Zhu, J.-S., Faber, M.H., 2022. Towards resilience of offshore wind farms: A framework and application to asset integrity management. *Appl. Energy* 322, 119429. <https://doi.org/10.1016/j.apenergy.2022.119429>
- Liu, X., Zhang, Q., 2016. Analysis of the return period and correlation between the reservoir-induced seismic frequency and the water level based on a copula: A case study of the Three Gorges reservoir in China. *Phys. Earth Planet. Inter.* 260, 32–43. <https://doi.org/10.1016/j.pepi.2016.09.001>
- Lü, T.-J., Tang, X.-S., Li, D.-Q., Qi, X.-H., 2020. Modelling multivariate distribution of multiple soil parameters using vine copula model. *Comput. Geotech.* 118, 103340. <https://doi.org/10.1016/j.compgeo.2019.103340>
- Ma, P., Zhang, Y., 2022. Modelling asymmetrically dependent multivariate ocean data using truncated copulas. *Ocean Eng.* 244, 110226. <https://doi.org/10.1016/j.oceaneng.2021.110226>
- Mackay, E., Johanning, L., 2018. A generalised equivalent storm model for long-term statistics of ocean waves. *Coast. Eng.* 140, 411–428. <https://doi.org/10.1016/j.coastaleng.2018.06.001>
- Montes-Iturrizaga, R., Heredia-Zavoni, E., 2016. Multivariate environmental contours using C-vine copulas. *Ocean Eng.* 118, 68–82. <https://doi.org/10.1016/j.oceaneng.2016.03.011>
- Nagler, T., Krüger, D., Min, A., 2022. Stationary vine copula models for multivariate time series. *J. Econom.* 227, 305–324. <https://doi.org/10.1016/j.jeconom.2021.11.015>
- Nelsen, R.B., 2006. *An introduction to copulas*, 2nd ed. Springer.
- Nizamani, Z., 2014. *Environmental load factors and system strength evaluation of offshore jacket platforms*, 4th ed. Springer International Publishing Switzerland 2015.
- Petrov, V., Guedes Soares, C., Gotovac, H., 2013. Prediction of extreme significant wave heights using maximum entropy. *Coast. Eng.* 74, 1–10. <https://doi.org/10.1016/j.coastaleng.2012.11.009>
- Pham, M.T., Vernieuwe, H., De Baets, B., Verhoest, N.E.C., 2018. A coupled stochastic rainfall–evapotranspiration model for hydrological impact analysis. *Hydrol. Earth Syst. Sci.* 22, 1263–1283. <https://doi.org/10.5194/hess-22-1263-2018>
- Qian, J., Dong, Y., 2022. Surrogate-assisted seismic performance assessment incorporating vine copula captured dependence. *Eng. Struct.* 257, 114073. <https://doi.org/10.1016/j.engstruct.2022.114073>
- Qin, J., Faber, M.H., 2019. Resilience Informed Integrity Management of Wind Turbine Parks. *Energies* 12, 2729. <https://doi.org/10.3390/en12142729>
- Ramadhani, A., Khan, F., Colbourne, B., Ahmed, S., Taleb-Berrouane, M., 2022. Resilience assessment of offshore structures subjected to ice load considering complex dependencies.

- Reliab. Eng. Syst. Saf. 222, 108421. <https://doi.org/10.1016/j.ress.2022.108421>
- Ramadhani, A., Khan, F., Colbourne, B., Ahmed, S., Taleb-Berrouane, M., 2021. Environmental load estimation for offshore structures considering parametric dependencies. Saf. Extrem. Environ. <https://doi.org/10.1007/s42797-021-00028-y>
- Rózsás, Á., Mogyorósi, Z., 2017. The effect of copulas on time-variant reliability involving time-continuous stochastic processes. Struct. Saf. 66, 94–105. <https://doi.org/10.1016/j.strusafe.2017.02.004>
- Sadegh, M., Ragno, E., AghaKouchak, A., 2017. Multivariate C copula A analysis toolbox (MvCAT): Describing dependence and underlying uncertainty using a B bayesian framework. Water Resour. Res. 53, 5166–5183. <https://doi.org/10.1002/2016WR020242>
- Salvadori, G., De Michele, C., 2010. Multivariate multiparameter extreme value models and return periods: A copula approach. Water Resour. Res. 46, 2009WR009040. <https://doi.org/10.1029/2009WR009040>
- Sarwar, A., Khan, F., Abimbola, M., James, L., 2018. Resilience Analysis of a Remote Offshore Oil and Gas Facility for a Potential Hydrocarbon Release. Risk Anal. 38, 1601–1617. <https://doi.org/10.1111/risa.12974>
- Shooter, R., Ross, E., Ribal, A., Young, I.R., Jonathan, P., 2022. Multivariate spatial conditional extremes for extreme ocean environments. Ocean Eng. 247, 110647. <https://doi.org/10.1016/j.oceaneng.2022.110647>
- Stochino, F., Bedon, C., Sagaseta, J., Honfi, D., 2019. Robustness and Resilience of Structures under Extreme Loads. Adv. Civ. Eng. 2019, 1–14. <https://doi.org/10.1155/2019/4291703>
- Taleb-Berrouane, M., Khan, F., 2019. Dynamic Resilience Modelling of Process Systems. Chem. Eng. Trans. 77, 313–318. <https://doi.org/https://doi.org/10.3303/CET1977053>
- Taleb-Berrouane, M., Khan, F., Amyotte, P., 2020. Bayesian Stochastic Petri Nets (BSPN) - A new modelling tool for dynamic safety and reliability analysis. Reliab. Eng. Syst. Saf. 193. <https://doi.org/10.1016/j.ress.2019.106587>
- Taleb-Berrouane, M., Khan, F., Hawboldt, K., 2021. Corrosion risk assessment using adaptive bow-tie (ABT) analysis. Reliab. Eng. Syst. Saf. 214, 107731. <https://doi.org/10.1016/j.ress.2021.107731>
- Taleb-Berrouane, M., Khan, F., Kamil, M.Z., 2019. Dynamic RAMS Analysis Using Advanced Probabilistic Approach. Chem. Eng. Trans. 77, 241–246. <https://doi.org/https://doi.org/10.3303/CET1977041>
- Taleb Berrouane, M., 2020. Dynamic corrosion risk assessment in the oil and gas production and processing facility (Doctoral dissertation, Memorial University of Newfoundland).
- Tang, X.-S., Wang, M.-X., Li, D.-Q., 2020. Modelling multivariate cross-correlated geotechnical random fields using vine copulas for slope reliability analysis. Comput. Geotech. 127,

103784. <https://doi.org/10.1016/j.compgeo.2020.103784>

- Tolentino, D., Ruiz, S.E., 2013. Time Intervals for Maintenance of Offshore Structures Based on Multiobjective Optimization. *Math. Probl. Eng.* 2013, 1–15. <https://doi.org/10.1155/2013/125856>
- Tosunoglu, F., Gürbüz, F., İspirli, M.N., 2020. Multivariate modelling of flood characteristics using Vine copulas. *Environ. Earth Sci.* 79, 459. <https://doi.org/10.1007/s12665-020-09199-6>
- Vanem, E., 2016. Joint statistical models for significant wave height and wave period in a changing climate. *Mar. Struct.* 49, 180–205. <https://doi.org/10.1016/j.marstruc.2016.06.001>
- Wahab, M.M.A., Kurian, V.J., Liew, M.S., Kim, D.K., 2020. Condition Assessment Techniques for Aged Fixed-Type Offshore Platforms Considering Decommissioning: a Historical Review. *J. Mar. Sci. Appl.* 19, 584–614. <https://doi.org/10.1007/s11804-020-00181-z>
- Wei, K., Arwade, S.R., Myers, A.T., Hallowell, S., Hajjar, J.F., Hines, E.M., 2015. Performance Levels and Fragility for Offshore Wind Turbine Support Structures during Extreme Events, in: *Structures Congress 2015*. American Society of Civil Engineers, Reston, VA, pp. 1891–1902. <https://doi.org/10.1061/9780784479117.163>
- Wei, K., Shen, Z., Ti, Z., Qin, S., 2021. Trivariate joint probability model of typhoon-induced wind, wave and their time lag based on the numerical simulation of historical typhoons. *Stoch. Environ. Res. Risk Assess.* 35, 325–344. <https://doi.org/10.1007/s00477-020-01922-w>
- Whitlock, R., 2022. DEME Group completes monopile installation at Arcadis Ost 1 offshore wind farm [WWW Document]. URL <https://www.renewableenergymagazine.com/wind/deme-group-completes-monopile-installation-at-arcadis-20220726> (accessed 8.6.22).
- Xu, N., Yuan, S., Liu, X., Ma, Y., Shi, W., Zhang, D., 2020. Risk assessment of sea ice disasters on fixed jacket platforms in Liaodong Bay. *Nat. Hazards Earth Syst. Sci.* 20, 1107–1121. <https://doi.org/10.5194/nhess-20-1107-2020>
- Xu, Q., Fan, Z., Jia, W., Jiang, C., 2020. Fault detection of wind turbines via multivariate process monitoring based on vine copulas. *Renew. Energy* 161, 939–955. <https://doi.org/10.1016/j.renene.2020.06.091>
- Xu, Z.-X., Zhou, X.-P., 2018. Three-dimensional reliability analysis of seismic slopes using the copula-based sampling method. *Eng. Geol.* 242, 81–91. <https://doi.org/10.1016/j.enggeo.2018.05.020>
- Yarveysy, R., Gao, C., Khan, F., 2020. A simple yet robust resilience assessment metrics. *Reliab. Eng. Syst. Saf.* 197, 106810. <https://doi.org/10.1016/j.ress.2020.106810>
- Yin, J., Ren, X., Liu, R., Tang, T., Su, S., 2022. Quantitative analysis for resilience-based urban rail systems: A hybrid knowledge-based and data-driven approach. *Reliab. Eng. Syst. Saf.* 219, 108183. <https://doi.org/10.1016/j.ress.2021.108183>
- Yodo, N., Wang, P., 2016. Resilience Modelling and Quantification for Engineered Systems Using

Bayesian Networks. *J. Mech. Des.* 138. <https://doi.org/10.1115/1.4032399>

- Yu. Shmal, G., A. Nadein, V., A. Makhutov, N., A. Truskov, P., I. Osipov, V., 2020. Hybrid Modelling of Offshore Platforms' Stress-Deformed and Limit States Taking into Account Probabilistic Parameters, in: *Probability, Combinatorics and Control*. IntechOpen. <https://doi.org/10.5772/intechopen.88894>
- Zarei, E., Ramavandi, B., Darabi, A.H., Omidvar, M., 2021. A framework for resilience assessment in process systems using a fuzzy hybrid MCDM model. *J. Loss Prev. Process Ind.* 69, 104375. <https://doi.org/10.1016/j.jlp.2020.104375>
- Zhang, S., Chen, C., Zhang, Q., Zhang, D., Zhang, F., 2015. Wave Loads Computation for Offshore Floating Hose Based on Partially Immersed Cylinder Model of Improved Morison Formula. *Open Pet. Eng. J.* 8, 130–137. <https://doi.org/10.2174/1874834101508010130>
- Zhang, S., Yan, Y., Wang, P., Xu, Z., Yan, X., 2019. Assessment of the offshore wind turbine support structure integrity and management of multivariate hybrid probability frameworks. *Energy Convers. Manag.* 180, 1085–1108. <https://doi.org/10.1016/j.enconman.2018.11.010>
- Zhang, Y., Beer, M., Quek, S.T., 2015. Long-term performance assessment and design of offshore structures. *Comput. Struct.* 154, 101–115. <https://doi.org/10.1016/j.compstruc.2015.02.029>
- Zhang, Y., Gomes, A.T., Beer, M., Neumann, I., Nackenhorst, U., Kim, C.-W., 2019. Reliability analysis with consideration of asymmetrically dependent variables: Discussion and application to geotechnical examples. *Reliab. Eng. Syst. Saf.* 185, 261–277. <https://doi.org/10.1016/j.res.2018.12.025>
- Zhang, Y., Kim, C.-W., Beer, M., Dai, H., Soares, C.G., 2018. Modelling multivariate ocean data using asymmetric copulas. *Coast. Eng.* 135, 91–111. <https://doi.org/10.1016/j.coastaleng.2018.01.008>
- Zhao, Y., Dong, S., 2020. A multi-load joint distribution model to estimate environmental design parameters for floating structures. *Ocean Eng.* 217, 107818. <https://doi.org/10.1016/j.oceaneng.2020.107818>

Appendix 6A

The total environmental load acting on a structure is estimated using

$$F_{Tot} = \sum \psi_i F_i \quad (6A.1)$$

where, ψ_i are the factors for load combination (Yu. Shmal et al., 2020). Three environmental loads considered here are wind, wave, and current loads.

The wind force on a structural member or surface acting normal to the member axis is calculated using (Jacomet et al., 2021)

$$F_{wind} = CqA\sin \alpha \quad (6A.2)$$

where

C = shape coefficient

q = basic wind pressure or suction

A = projected area of the member normal to the direction of the wind velocity

α = angle between wind direction and the member axis

Basic wind pressure can be estimated using (Jacomet et al., 2021)

$$q = \frac{1}{2} \rho_a U_z^2 \quad (6A.3)$$

where, ρ_a is the mass density of air and U_z is the wind velocity profile estimated using the following equation (Jacomet et al., 2021)

$$U_z = U_{z_0} \left(\frac{z}{z_0} \right)^{1/7} \quad (6A.4)$$

where,

U_{z_0} = mean velocity at a reference height

z_0 = reference height

z = height above mean sea level

The total wave force for a suitably slender structure, or element of a structure, is then estimated using Morison's equation (Jacomet et al., 2021; Zhang et al., 2015)

$$F_{T_{wave}} = F_I + F_D \quad (6A.5)$$

$$F_{T_{wave}} = C_M \rho V \dot{u} + \frac{1}{2} C_D \rho A |u| u \quad (6A.6)$$

where,

C_M and C_D are inertia and drag coefficient, respectively

ρ = water density

V = volume of the body

A = reference area

u = water wave particle velocity

\dot{u} = water wave particle acceleration

When calculating wave force on an offshore structure, it is also important to select the most appropriate wave theory. Water wave particle velocity and acceleration are calculated using these wave theories. Wave theories considered in this chapter are as follows

Table A1 shows the condition where each wave theory is applicable.

Table A1. Application of wave theories

Condition	Wave Theory
$\frac{d}{L} \geq 0.2, \frac{H}{L} \leq 0.2$	Airy wave theory
$0.1 < \frac{d}{L} < 0.2, \frac{H}{L} \geq 0.2$	Stokes wave theory
$0.04 < \frac{d}{L} < 0.1$	Solitary wave theory

where, d is water depth, L is wavelength, and H is wave height.

1. Airy Wave Theory

In this theory, water particle velocity and acceleration in the horizontal direction can be estimated by (Kim, 1999; S. Zhang et al., 2015)

$$\begin{aligned}
u_x &= \frac{Hgk \cosh(k(z+d))}{2\omega \cosh(kd)} \cos(kx - \omega t) \\
\dot{u}_x &= \frac{2\pi^2 H \cosh(k(z+d))}{T^2 \sinh(kd)} \sin(kx - \omega t)
\end{aligned}
\tag{6A.7}$$

g = standard gravity

H = wave height

k = wave number that is calculated using this equation

$$k = \frac{2\pi}{L} \tag{6A.8}$$

While in the vertical direction

$$\begin{aligned}
u_z &= \frac{Hgk \sinh(k(z+d))}{2\omega \cosh(kd)} \sin(kx - \omega t) \\
\dot{u}_z &= -\frac{2\pi^2 H \sinh(k(z+d))}{T^2 \sinh(kd)} \cos(kx - \omega t)
\end{aligned}
\tag{6A.9}$$

2. Stokes Wave Theory

The horizontal water particle velocity and acceleration should satisfy this following equation

$$\begin{aligned}
u_x &= \frac{H\pi \cosh(k(z+d))}{T \sinh(kd)} \cos(kx - \omega t) + \frac{3}{4} \left(\frac{H\pi}{T}\right) \left(\frac{H\pi}{L}\right) \frac{\cosh(2k(z+d))}{\sinh^4(kd)} \cos 2(kx - \omega t) \\
\dot{u}_x &= 2 \left(\frac{\pi^2 H}{T^2}\right) \frac{\cosh(k(z+d))}{\sinh(kd)} \sin(kx - \omega t) + 3 \left(\frac{H\pi^2}{T^2}\right) \left(\frac{H\pi}{L}\right) \frac{\cosh(2k(z+d))}{\sinh^4(kd)} \sin 2(kx - \omega t)
\end{aligned}
\tag{6A.10}$$

While equation A11 is used to estimate water particle velocity and acceleration in the vertical direction

$$\begin{aligned}
u_z &= \frac{H\pi}{T} \frac{\sinh(k(z+d))}{\sinh(kd)} \sin(kx - \omega t) + \frac{3}{4} \left(\frac{H\pi}{T}\right) \left(\frac{H\pi}{L}\right) \frac{\sinh(2k(z+d))}{\sinh^4(kd)} \sin 2(kx - \omega t) \\
\dot{u}_z &= -2 \left(\frac{\pi^2 H}{T^2}\right) \frac{\sinh(k(z+d))}{\sinh(kd)} \cos(kx - \omega t) - 3 \left(\frac{H\pi^2}{T^2}\right) \left(\frac{H\pi}{L}\right) \frac{\sinh(2k(z+d))}{\sinh^4(kd)} \cos 2(kx - \omega t)
\end{aligned}
\tag{6A.11}$$

3. Solitary Wave Theory

Water particle velocity and acceleration can be approached by Equation A12

$$\begin{aligned}
u &= \frac{CN[1 + \cos(M[\frac{z+d}{d}]) \cdot \cos(M\frac{x}{d})]}{\{\cos(M[\frac{z+d}{d}]) + \cosh(M\frac{x}{d})\}^2} \\
\dot{u} &= \frac{CN[\sin(M[\frac{z+d}{d}]) \cdot \sinh(M\frac{x}{d})]}{\{\cos(M[\frac{z+d}{d}]) + \cosh(M\frac{x}{d})\}^2}
\end{aligned}
\tag{6A.12}$$

Where M,N are functions of H/d and

C is speed of solitary wave that can be estimated using

$$c = \sqrt{2g(H + d)}
\tag{6A.13}$$

Current loads are also commonly taken into consideration in designing offshore structures and are estimated using (Yu. Shmal et al., 2020)

$$F_{Current} = \frac{1}{2} C_D \rho A U |U|
\tag{6A.14}$$

where,

C_D = drag coefficient

ρ = water density

U = current velocity

A = reference cross-sectional area

CHAPTER 7

SUMMARY, CONCLUSIONS, AND RECOMMENDATIONS

7.1 Summary

The current research focuses on modelling environmental variables to estimate the total environmental loads acting on offshore structures. This research also assesses offshore structures' performance in terms of resilience when subjected to environmental loads. After an extensive literature review, the existing knowledge gaps are identified. The dependence among the investigated variables was identified as a topic requiring research attention. Copula functions are used to address the identified challenges in dealing with variable dependencies. The copula-based probabilistic models developed here are compared with the existing methods and results suggest that the copula-based approach is better suited to model the correlated marine environmental variables considering both symmetric and asymmetric dependence structures.

The first two technical chapters focus on developing bivariate models using copula functions. In addition to standard copula family models, asymmetric copulas are studied to provide a more comprehensive understanding of dependence structure among environmental variables. The correlated environmental data generated from symmetric and asymmetric copula functions estimate the total environmental loads acting on an offshore structure. These data are then used to assess the performance of the offshore structure in terms of resilience. The proposed methodology provides a robust and flexible approach to assess the resilience of a structure subjected to correlated marine environmental loads for the bivariate case.

The other two technical chapters investigate further the development of multivariate models in higher dimensions. Vine copulas are used to model this phenomenon. The modeled data estimate the total environmental loads on an offshore structure. These environmental loads are then used as input to assess the resilience of offshore structures.

The use of copula theories is the highlight of this thesis. Novel methodologies are proposed to estimate the total environmental loads and a structure's resilience for both bivariate and multivariate cases. In addition, asymmetric copulas are used extensively to model all possible dependence structures of marine environmental variables. From this thesis, asymmetric dependence between environmental variables is found to be always present. The application of asymmetric copulas to perform multivariate analysis for offshore structures provide a better approach to capturing all possible dependency levels that ocean parameter data might have.

7.2 Conclusions

The work detailed in this thesis demonstrates that the original premise of the study has been proven. Copula functions can better model complex and marginal dependencies between environmental variables in models of loading on offshore structures. This is particularly valuable for harsh environments, in which the dependencies between variables are expected to be more influential. Furthermore, the work of developing and evaluating a methodology has provided methods and algorithms that make the use of copula functions and the incorporation of complex dependencies in environmental variables readily achievable in engineering practice. These are the main achievements of this study. Contributing achievements arising from the individual stages of the research are listed below.

7.2.1 Development of bivariate copula models to estimate the total environmental loads

This study analyses and interprets the influence of several copula functions used to estimate environmental loads on an offshore structure. The Gumbel and Clayton-Gumbel type-1 Copula functions, in comparison to the conventional joint distribution function techniques, were found to offer lower RMSE values and a higher probability of occurrence. The generated data set had a comparatively low asymmetry measurement and was scattered symmetrically in the copula domain. A symmetric copula—in this case, the Gumbel copula—was thus best matched to the data set to assess the environmental load. The use of asymmetric copulas in multivariate analysis for offshore structures is advantageous in capturing all potential dependence structures that marine environmental variables might have.

7.2.2 Development of a novel methodology to assess resilience considering a parametric dependence

This study presents a reliable method for quantifying resilience. A simple demonstration is presented to assess the capacities of offshore structures subjected to iceberg load. Both ice parameters and meteorological factors influence the iceberg collision force. From the meteorological standpoint, waves and wind load determine the drift velocity of the iceberg. It is concluded that marine environmental variables are interdependent and exhibit an asymmetric dependence structure. Thus, the Gumbel-Frank Type-I is best fitted to model the dependence between the environmental variables. Resilience is quantified based on a reliability assessment of the structure subjected to the iceberg load. Quantification of resilience was mainly found to be dependent on absorptive capacity. It is critical in a system as a higher level of residual reliability will result in a better ability to withstand disruptive events and restore functionality. This capacity is the inherent physical characteristic of the structure that enables it to withstand disruptive events.

7.2.3 Development of multivariate models to estimate total environmental loads using vine copulas

This study presents a vine copula-based framework to estimate the total environmental load in a higher dimension. Joint distributions for trivariate analysis are constructed using the c-vine models. Building blocks are constructed using both symmetric and asymmetric copulas. The independent load case and multi-Gaussian distribution function were compared with the other known methods. Estimating the total environmental load depended on the copula function fitted in the final edge of the tree. It is concluded that vine copulas are well suited to model multivariate environmental variables and provide more realistic models of interdependent environmental effects. The C-vine models constructed using asymmetric copulas as the building blocks provide a lower estimation of the total environmental load than the calculation of each environmental variable individually. The error results obtained from c-vine using asymmetric copula are also lower than those obtained from the multi-Gaussian distribution function. This study provides a new perspective on applying vine copulas to model marine environmental variables with complex dependency structures in higher dimensions. The result from this study is also potentially valuable for further probabilistic structural analysis of offshore structures.

7.2.4 Development of a novel methodology to assess resilience subjected to multiple environmental loads

This study presents a proposed methodology built on vine copulas to construct a multivariate joint distribution of marine environmental variables in higher dimensions. Asymmetric and symmetric copulas are selected as the building blocks to construct the C-vine copula models. Environmental data are generated using the best-fitted copulas in each edge and compared to other common multivariate methods. Error values estimated for all methods show that symmetric and asymmetric C-vine copulas fit better to the environmental data. Symmetric C-vine copulas provide a lower

error in the second tree of the dependence structure than asymmetric C-vine copulas. This shows that symmetric C-vine copulas fit better to model the multivariate environmental variables using the collected data set. These correlated data are then used to evaluate the reliability of the structure subjected to the total environmental loads. The results show that the symmetric C-vine copula's reliability index resulted in a slightly lower reliability index due to a higher probability of failure than the asymmetric C-vine copula model. Resilience quantified based on a reliability assessment of the structure subjected to total environmental loads shows a similar result. Quantification of resilience is mainly found to be dependent on absorptive capacity. Thus, absorptive capacity is the critical indicator in a system.

7.3 Recommendations

This thesis introduces the concept of copula theories to model the joint distribution of marine environmental variables for both bivariate and multivariate cases. The copula models are used to generate correlated environmental variables as inputs to assess the resilience of offshore structures subjected to environmental loads. However, the scope of the current research can be improved by adopting the following recommendations.

7.3.1 The use of a large met-ocean data set

The results obtained in this thesis depend mainly on the quality of the selected environmental data. Using a large met-ocean data set will help improve the reliability of the environmental load estimation for offshore structures.

7.3.2 Development of a multivariate model for risk analysis of offshore structures

This thesis assumes a simplified offshore structure to estimate the total environmental loads and assess the structure's resilience. Future works should be able to capture the overall risk profile of

offshore structures subjected to all types of loads. The consideration of parametric dependence should be highlighted. The fluid-structure interactions should also be captured better in future works to assess better the overall performance of offshore structures operating in harsh environments.

7.3.3 Development of resilience assessment methodology considering managerial aspects

In this thesis, resilience assessment largely depends on the acceptable level of reliability in the disrupted state. Identifying this acceptable level will require involvement from all organizational stakeholders to provide more reasonable and realistic assumptions. Future work should involve managerial aspects in quantifying the resilience of an offshore structure

7.3.4 Development of more advanced modelling tools using neural networks

In this thesis, applying copula theories can better capture the dependence structure of marine environmental variables. More advanced modelling tools, such as neural networks, will help enhance data processing and analysis for future work.